Synthesis, self-assembly and controlled drug delivery of novel thermo-responsive and amphiphilic block copolymers based on polylactide, polyacrylamide and poly(oligo(ethylene glycol) methacrylate)

Yanfei Hu

Collège Doctoral du Languedoc-Roussillon

THÈSE

Pour obtenir le grade de

Docteur

Délivré par **Université de Montpellier**

Préparée au sein de l'école doctorale Sciences Chimiques et Biologiques pour la Santé

Et de l'unité de recherche UMR CNRS 5247

Spécialité : Chimie et Physico-chimie des Polymères

Présentée par

Yanfei Hu

Synthèse, auto-assemblage et libération contrôlée de principes actifs de nouveaux copolymères à blocs thermo-sensibleset amphiphiles à base de polylactide, de polyacrylamide et de poly(oligo(éthylène glycol) méthacrylate)

Soutenue le 8 avril 2015 devant le jury composé de

Mr Didier GIGMES, Directeur de recherche, Aix-Marseille Université	Rapporteur
Mr Christophe MINGOTAUD, Directeur de recherche, Université Paul Sabatier	Rapporteur
Mme Catherine LADAVIERE, Chargé de recherche, Université de Lyon 1	Examinateur
Mr André DERATANI, Directeur de recherche, Université de Montpellier	Examinateur
Mr Suming LI, Directeur de recherche, Université de Montpellier	Directeur de thèse
Mr Vincent DARCOS, Ingénieur d'étude, Université de Montpellier	Co-encadrant

UNIVERSITE MONTPELLIER

Table of contents

Résumé

Dans les dernières décennies, les polymères sensibles aux stimulants ont attiré une grande attention en raison de leur potentiel pour la libération ciblée de principes actifs, en particulier pour la libération ciblée d'anti-tumoraux. Le support idéal de principes actifs devrait être thermo-sensible au tissu tumoral où la température est d'environ 42 °C, c'est-à-dire bien supérieure à la température corporelle. Parmi les divers polymères thermo-sensibles, le poly(*N*-isopropylacrylamide) (PNIPAAm) est considéré comme le "standard d'or" parce qu'il est biocompatible et présente une température critique inférieure de solution (LCST) autour de 32 °C qui est relativement insensible aux changements environnementaux. Variation du pH, de la concentration ou de l'environnement chimique n'influence que légèrement la LCST du PNIPAAm. De plus, l'introduction d'un comonomère hydrophile de type méthacrylamide, comme le *N*,*N*-diméthylacrylamide (DMAAm), permet d'augmenter et d'ajuster précisément la LCST des copolymères obtenus. Néanmoins, ces copolymères thermo-sensibles ne peuvent pas s'auto-assembler en nano-agrégats tels que des micelles capables d'encapsuler des principes actifs.

Poly(L-lactide) (PLLA) est un polyester biodégradable et biocompatible largement utilisé pour des applications biomédicales et pharmaceutiques telles que les implants chirurgicaux, les supports en ingénierie tissulaire et des supports de principes actifs. Les copolymères à blocs de PNIPAAm et de PLLA combinent la thermo-sensibilité et l'hydrophilie du PNIPAAm avec la dégradabilité et l'hydrophobie du PLLA. En outre, des micelles "intelligentes" peuvent être obtenues par auto-assemblage des copolymères amphiphiles PLLA/PNIPAAm ou PLLA/P(NIPAAm-*co*-DMAAm) en milieu aqueux. Cependant, les copolymères préparés en utilisant des méthodes de synthèse traditionnelles présentent généralement des structures macromoléculaires mal définies conduisant à une large transition de phase autour de la LCST, ce qui n'est pas bénéfique pour les applications pharmaceutiques, notamment comme

support pour la libération ciblée des anti-tumoraux.

D'autre part, les polyméthacrylates thermo-sensibles contenant de courtes chaînes pendantes d'oligo(éthylène glycol) ont été récemment proposés comme une alternative au PNIPAAm. Ces analogues de PEG présentent des propriétés remarquables comme l'hydrophilie, la biocompatibilité et la thermo-sensibilité, et sont considérées comme une nouvelle génération de biomatériaux "intelligents". La valeur de LCST peut être contrôlée dans une gamme de température allant de l'ambiante à 90 °C en utilisant des comonomères oligo(éthylène glycol) méthacrylate (OEGMA) de longueurs de chaîne différentes entre 2 et 9. Les copolymères thermo-sensibles et amphiphiles dérivés des blocs P(OEGMA) et PLLA sont capables de s'auto-assembler dans un milieu aqueux pour donner des micelles "intelligentes" comme dans le cas des copolymères PLLA/PNIPAAm ou PLLA/P(NIPAAm-*co*-DMAAm). Néanmoins, au mieux de notre connaissance, les propriétés d'encapsulation et de libération de principes actifs des copolymères de PLLA et d'analogues de PEG n'ont pas été étudiées en détail jusqu'à présent.

Dans ce travail de thèse, une étude détaillée est réalisée sur la synthèse, la caractérisation, l'auto-assemblage et la libération de principes actifs des copolymères à base de PLLA et P(NIPAAm-*co*-DMAAm) et à base de PLLA et d'analogues de PEG. Les copolymères triblocs possèdent le même bloc central PLLA et deux blocs hydrophiles latéraux. La composition des blocs hydrophiles est modifiée en utilisant différents rapports de NIPAAm/DMAAm ou de comonomères OEGMA de façon à ajuster la LCST des copolymères. Les copolymères obtenus présentent une structure de chaînes bien définie et une faible dispersité des masses molaires. Les micelles obtenues par auto-assemblage présentent une très faible CMC, une taille en dessous de 100 nm et une libération de principes actifs thermo-sensible, ce qui est très prometteur pour la libération ciblée des anti-tumoraux. Le contenu principal de cette thèse est présenté ci-dessous:

1) Une série de copolymères triblocs thermo-sensibles PNIPAAm-*b*-PLLA-*b*-PNIPAAm est synthétisée par la polymérisation radicalaire par transfert d'atomes (ATRP) du NIPAAm en présence d'un macro-amorceur de PLLA possédant une degré de polymérisation en unité acide lactique de 40. La polymérisation est réalisée en utilisant un complexe CuCl/tris(2-diméthylaminoéthyl) amine (Me_6TREN) comme catalyseur à 25 °C dans un mélange DMF/eau (50/50 v/v) pendant 30 minutes. La masse molaire des copolymères obtenus varie entre 18000 à 38000 $g.mol^{-1}$, et la dispersité entre 1,10 et 1,28. Les suivies cinétiques de $\ln([M]_0/[M])$ *vs*. $t^{2/3}$ présentent une relation linéaire pendant les 10 premières minutes pour un rapport NIPAAm/macro-amorceur de 100, et pendant les 30 premières minutes pour un rapport NIPAAm/macro-amorceur de 200 et 300, ce qui indique que la concentration d'espèces actives reste constante durant la période indiquée.

Les micelles sont formées par auto-assemblage de copolymères dans un milieu aqueux à température ambiante. La structure cœur-couronne des micelles est confirmée par la spectroscopie RMN ^1H dans deux solvants différents ($CDCl_3$ et D_2O). La concentration micellaire critique (CMC) déterminée par la spectroscopie de fluorescence se trouve dans la gamme de 0,0077 à 0,016 mg mL^{-1}. Les copolymères présentent une LCST entre 32,1 et 32,8 °C obtenue par des mesures de transmittance UV-Vis. Les micelles sont sous forme sphériques avec un diamètre moyen compris entre 31,4 et 83,3 nm déterminé par la TEM et la DLS. La taille des micelles augmente avec la longueur des blocs hydrophiles de PNIPAAm parce que ceux-ci sont étendus dans l'eau en dessous de la LCST. Les micelles présentent différents comportements thermo-sensibles en fonction de la concentration. A forte concentration (3,0 mg ml^{-1}), l'agrégation des micelles se produit lorsque la température est élevée au-dessus de la LCST, conduisant à l'augmentation de la taille de micelles. En revanche, à faible concentration (0,2 mg ml^{-1}), une diminution de la taille de micelles est observée à cause de l'effondrement de blocs de PNIPAAm au-dessus de la LCST.

2) Dans cette seconde partie, des copolymères triblocs thermo-sensibles P(NIPAAm-*co*-DMAAm)-*b*-PLLA-*b*-P(NIPAAm-*co*-DMAAm) sont synthétisés par l'ATRP du NIPAAm et du DMAAm en utilisant le même macro-amorceur PLLA que précédemment. La polymérisation est réalisée dans les mêmes conditions que dans le cas des copolymères PNIPAAm-*b*-PLLA-*b*-PNIPAAm. Le DMAAm est incorporé dans les chaînes de copolymère en tant que comonomère plus hydrophile afin de réguler et d'augmenter la LCST. Le rapport NIPAAm/DMAAm varie de 100/0 à 66/24. Les copolymères obtenus présentent une structure de chaînes bien définie avec des masses molaires M_n allant de 23600 à 27000 g mol^{-1} et de faibles dispersités ($Đ$ = 1.10 à 1.18).

Des micelles de taille entre 37 et 54 nm avec une distribution étroite sont obtenues par auto-assemblage de copolymères en milieu aqueux. Des valeurs très faibles de CMC sont obtenues, allant de 0,010 à 0,015 mg ml^{-1}. La LCST augmente linéairement de 32,2 à 39,1 °C avec l'augmentation de la proportion en monomère DMAAm de 0 à 24 % dans la partie hydrophile. La présence de motifs DMAAm dans les copolymères conduit à une transition de phase extrêmement étroite ($\Delta T < 0,5$ °C) par rapport aux copolymères PNIPAAm-*b*-PLLA-*b*-PNIPAAm ($\Delta T = 2,8$ °C). Des changements réversibles de taille des micelles sont observés avec une variation de température à travers la LCST. En fait, lorsque les motifs DMAAm sont introduits, les chaînes de P(NIPAAm-*co*-DMAAm) deviennent plus hydrophiles par rapport à celles de PNIPAAm. Ainsi, la LCST augmente avec la transition de phase plus étroite.

L'amphotéricine B (AmpB), un principe actif faiblement hydrosoluble pour le traitement de mycose systémique, est utilisée comme modèle afin d'évaluer le potentiel de copolymères pour la libération de principes actifs. L'AmpB est encapsulée dans les micelles en utilisant la méthode de dialyse avec une efficacité d'encapsulation au-dessus de 59 %. Les tests de libération *in vitro* sont effectués à 37 ou 38 ° C dans l'eau en utilisant un copolymère ayant une LCST de 37,8 °C. Une libération initiale brutale est observée dans tous les cas. La vitesse de libération à

38 °C est beaucoup plus rapide que celle à 37 °C, ce qui suggère que les micelles de copolymères triblocs P(NIPAAm-*co*-DMAAm)-*b*-PLLA-*b*-P(NIPAAm-*co*-DMAAm) pourraient permettre une libération thermo-sensible de principes actifs après administration *in vivo*.

La cytotoxicité des copolymères est évaluée par le test MTT après incubation avec les myocytes cardiaques de souris (MCM) et les fibroblastes embryonnaires de souris (MEF). Les valeurs de densité optique (OD) sur le substrat polymère sont légèrement supérieures à celles de la solution de culture comme témoin négatif, et bien supérieures à celles de solution de phénol comme témoin positif. Les valeurs de taux de croissance relative (RGR) des copolymères sont bien au-dessus de 100 % pendant 4 jours d'incubation avec les cellules MCF et MEF, correspondant à un niveau de cytotoxicité de 0. En outre, l'adhésion et la prolifération de cellules sont observées sur le substrat polymère. Les cellules présentent des formes broche, polygone ou ovale, et le pseudopode de cellules s'étend vers l'extérieur. Ainsi, le test MTT et l'observation de la morphologie des cellules indiquent que les copolymères P(NIPAAm-*co*-DMAAm)-*b*-PLLA-*b*-P(NIPAAm-*co*-DMAAm) présentent une très bonne cytocompatibilité.

3) La troisième partie de thèse porte sur une étude approfondie sur les propriétés d'encapsulation et de libération de principes actifs des copolymères triblocs thermo-sensibles P(NIPAAm-*co*-DMAAm)-*b*-PLLA-*b*-(NIPAAm-*co*-DMAAm). Quatre copolymères sont d'abord synthétisés par l'ATRP comme décrit précédemment. Le rapport NIPAAm/DMAAm varie de 68,2/31,8 à 60,6/39,4, et la masse molaire de 18000 à 26000 g mol^{-1} avec une faible dispersité ($Đ$ = 1,1). Les copolymères présentent une très faible CMC qui augmente légèrement de 0,0113 à 0,0144 mg mL^{-1} avec l'augmentation de la teneur en DMAAm de 31,8 à 39,4 mol% dans les blocs hydrophiles P(NIPAAm-*co*-DMAAm). Parallèlement, la LCST des copolymères augmente de 44,7 °C à 49,4 °C dans de l'eau et diminue d'environ 3.5 °C dans le tampon phosphate salin (PBS). D'autre part, la taille des micelles augmente

légèrement de 36,7 à 44,1 nm avec une teneur croissante en DMAAm. Le potentiel zêta de micelles varie dans la gamme de -12,4 à -18,7 mV, en accord avec la structure de micelles ayant les blocs PLLA dans le cœur et P(NIPAAm-*co*-DMAAm) dans la couronne. Un copolymère avec une LCST de 42,1 °C dans le PBS est sélectionné pour une étude approfondie de libération de principes actifs.

Un principe actif anticancéreux, la curcumine, est encapsulé dans les micelles de copolymère à l'aide de la méthode dite "évaporation de solvant/hydratation de membrane". Des charges en curcumine jusqu'à 20,4% sont obtenues avec une excellente efficacité d'encapsulation (> 94%). La LCST diminue de 42,1 °C pour les micelles seules dans le PBS à 38,0, 37,8 et 37,5°C avec une charge en curcumine de 6,0, 12,1 et 20,4%, respectivement. La transition de phase reste très étroite (<0,5 °C) dans tous les cas. D'autre part, la taille augmente de 38,6 nm pour les micelles seules à 47,5, 53,7 et 88,2 nm pour les micelles avec une charge en curcumine de 6,0, 12,1 et 20,4 %, respectivement, ce qui indique que l'incorporation de curcumine conduit à de plus grandes tailles de micelles. En outre, le potentiel zêta dans l'eau augmente de -12,4 mV pour micelles seules jusqu'à -18,1 mV pour 20,4% de charge. Des valeurs de potentiel zêta inférieures sont obtenues dans le PBS en raison de l'effet d'écran ionique et agrégation de micelles. Toutes les solutions micellaires restent homogènes et transparentes sur plus d'un mois, ceci étant dû à la charge négative en surface de smicelles.

Des études de libération de principes actifs sont effectuées dans des conditions *in vitro* à 37 et 40 °C, c'est-à-dire en dessous ou au-dessus de la LCST des micelles chargées. Une libération initiale brutale est observée dans tous les cas, suivie d'une libération plus lente. La vitesse de libération à 40 °C est plus rapide que celle à 37 °C en raison de la libération thermo-sensible au-dessus de la LCST. D'autre part, les micelles faiblement chargées présentent une vitesse de libération plus élevée que celles à plus forte charge. Ce résultat pourrait être attribué à l'effet de la solubilité. La théorie de Peppas est appliquée pour décrire les comportements de libération. Les résultats

indiquent un mécanisme de libération contrôlée par une combinaison de diffusion et de dégradation. Par ailleurs, les tests de cytotoxicité *in vitro* utilisant les cellules fibrosarcome murin (L929) et lungcarcinoma humaine (A549) confirment une très bonne cytocompatibilité des copolymères.

4) Dans la dernière partie de thèse, des copolymères triblocs en peigne P(MEO_2MA-*co*-OEGMA)-*b*-PLLA-*b*-P(MEO_2MA-*co*-OEGMA) sont synthétisés par ATRP des comonomères MEO_2MA et OEGMA (M_n = 475) en utilisant le même macro-amorceur Br-PLLA-Br dans des conditions similaires. Les copolymères obtenus présentent une structure de chaînes bien définie avec des masses molaires M_n variant de 27100 à 9800 g mol^{-1} et une dispersité d'environ 1,40. Le rapport MEO_2MA/OEGMA dans les blocs hydrophiles varie de 79/21 à 42/58.

Des micelles thermo-sensibles sont obtenues par auto-assemblage des copolymères dans un milieu aqueux. La CMC des copolymères augmente légèrement de 0,0113 à 0,0130 mg ml^{-1} avec l'augmentation de la teneur en monomère OEGMA de 21 à 58 mol% grâce à son plus grande hydrophilie par rapport à MEO_2MA. La LCST des micelles dans l'eau augmente de 36,4 à 56,7 °C avec la teneur en monomère OEGMA passant de 21% à 43%. Les données ne sont pas disponibles pour les copolymères avec des teneurs en OEGMA plus élevées, ceci étant dû à l'évaporation rapide de l'eau au-dessus de 60 °C. La présence de sel diminue de manière significative la LCST des copolymères. Une diminution de près de 17 °C est observée lorsque l'on compare les valeurs de LCST dans le PBS et dans l'eau, ce qui suggère un effet de déshydratation très fort des ions phosphate. La taille des micelles augmente de 20,7 à 102,5 nm avec la teneur en OEGMA passant de 21% à 58%. D'autre part, le potentiel zêta de micelles est compris entre -0,77 et -1,99 mV, ce qui implique une charge de surface presque neutre.

La curcumine est encapsulée dans les micelles en utilisant la méthode "évaporation de solvant/hydratation de membrane" avec une efficacité d'encapsulation de plus de 90%.

La taille des micelles diminue de 102,2 nm pour micelles seules à 37,6 nm avec 10,8% de charge en curcumine, et la LCST diminue de 45,1 °C à 38,3 °C. Parallèlement, le potentiel zêta augmente de -1,99 jusqu'à -44,9 mV. Ces résultats indiquent que la charge en curcumine influence fortement la procédure d'auto-assemblage. Les copolymères triblocs sont supposés s'auto-assembler en micelles avec un cœur PLA, une mésophase PMA et une couronne hydrophile PEG. L'encapsulation de la curcumine dans le cœur et dans la mésophase est susceptible de conduire à une diminution de la taille et de la LCST des micelles, et une augmentation du potentiel zêta.

La libération *in vitro* de curcumine est réalisée dans le PBS (pH = 7,4) à 37 °C et 41 °C, c'est-à-dire en dessous ou au-dessus de la LCST, respectivement. Une libération initiale brutale est observée dans tous les cas, suivie d'une libération plus lente. 81,8 et 92,6% de libération sont observés pour les micelles avec 5,9% de charge en curcumine après 14 jours à 37 et 41 °C, respectivement. Une libération plus faible est obtenue pour les micelles avec 10,8% de charge. La libération totale atteint 59,5 et 75,9 % à 37 et 41 °C dans la même période, respectivement. Par conséquent, la libération de curcumine n'est pas seulement dépendante de la transition de phase à la LCST, mais aussi de la charge en curcumine car la solubilité est un facteur limitant.

En résumé, deux séries de copolymères triblocs thermo-sensibles, à savoir PLA/P(NIPAAm-*co*-DMAAm) et PLA/P(MEO_2MA-*co*-OEGMA) sont synthétisées avec succès par combinaison de la ROP et l'ATRP. Les copolymères amphiphiles obtenus présentent des propriétés intéressantes d'auto-assemblage, une LCST ajustable autour de la température du corps et une excellente cytocompatiblity. La forte teneur en principe actif, l'excellente efficacité d'encapsulation, et la libération thermo-sensible indiquent que ces copolymères sont prometteurs pour l'administration ciblée de principes actifs anticancéreux.

Abstract

In the past decades, stimuli-responsive polymers have drawn great attention due to their potential for targeted drug delivery, especially for targeted delivery of anti-tumor drugs. The ideal drug carrier should be thermo-responsive to the tumor tissue where the temperature is ~42 ^{o}C, *i.e.* higher than the body temperature. Among the various thermo-responsive polymers, poly(*N*-isopropyl acrylamide) (PNIPAAm) is considered as the "gold standard" as it is biocompatible and exhibits a lower critical solution temperature (LCST) around 32 ^{o}C which is relatively insensitive to environmental changes. Variation of pH, concentration or chemical environment only slightly affects the LCST of PNIPAAm. In contrast, introduction of an acrylamide comonomer, *N, N*-dimethyl acrylamide (DMAAm) allows to increase and precisely adjust the LCST of the resulting copolymers. Nevertheless, these thermo-responsive copolymers cannot self-assemble into nanocarriers such as micelles capable of encapsulating drugs.

Poly(L-lactide) (PLLA) is a biodegradable and biocompatible polyester widely used in biomedical and pharmaceutical applications such as surgical implants, tissue engineering scaffolds and drug carriers. Block copolymers based on PNIPAAm and PLLA combine the thermo-sensitivity and hydrophilicity of PNIPAAm and the degradability and hydrophobicity of PLLA. Moreover, "smart" micelles can be obtained by self-assembly of amphiphilic PLLA/PNIPAAm or PLLA/P(NIPAAm-*co*-DMAAm) copolymers in aqueous medium. However, copolymers prepared using traditional synthetic methods generally exhibit poorly defined macromolecular structures with broad phase transition around the LCST, which is not beneficial for pharmaceutical applications as carrier for targeted drug delivery.

On the other hand, thermo-responsive polymethacrylates containing short oligo(ethylene glycol) side chains have been recently proposed as an alternative to PNIPAAm or P(NIPAAm-*co*-DMAAm). These PEG analogues exhibit outstanding properties such as hydrophilicity, biocompatibility and thermo-sensitivity, and are

regarded as a new generation of “smart” biomaterials. The LCST can be adjusted from the room temperature up to 90 °C by using oligo(ethylene glycol) methacrylate (OEGMA) comonomers of different chain lengths ranging from 2 to 9. Thermo-responsive and amphiphilic copolymers derived from OEGMA and PLLA are able to self-assemble in aqueous medium to yield “smart” micelles as in the case of PLLA/PNIPAAm or PLLA/P(NIPAAm-*co*-DMAAm) copolymers. Nevertheless, to the best of our knowledge, the drug encapsulation and drug release properties of PLLA/PEG analogues in physiological conditions have not been investigated in detail, so far.

In this work, a detailed investigation is performed on the synthesis, characterization, self-assembly and drug release behavior of PLLA/P(NIPAAm-*co*-DMAAm) and PLLA/PEG analogues. The triblock copolymers possess the same PLLA central block and two lateral hydrophilic blocks. The composition of hydrophilic blocks is varied using different NIPAAm/DMAAm ratios or OEGMA comonomers so as to adjust the LCST of the copolymers. The obtained copolymers exhibit well-defined structure and narrow molecular weight dispersity. Self-assembled micelles present very low CMC, size below 100 nm and thermo-responsive drug release behavior, which is most promising for targeted delivery of antitumor drugs. The main contents of this thesis are shown in the following:

1) A series of thermo-responsive PNIPAAm-*b*-PLLA-*b*-PNIPAAm triblock copolymers were successfully prepared by atom transfer radical polymerization (ATRP) of NIPAAm in the presence of a α, ω-Br-PLLA-Br macroinitiator with a block length of 40. The reaction was realized using a CuCl/tris(2-dimethylaminoethyl) amine (Me_6TREN) complex as catalyst at 25 ^{o}C in a DMF/water (50/50 v/v) mixture for 30 min. The molecular weight of the resulting copolymers ranges from 18000 to 38000 g mol^{-1}, and the dispersity from 1.10 to 1.28. Kinetic plots of $\ln([M]_0/[M])$ against $t^{2/3}$ exhibit a linear relationship during the first 10 min for NIPAAm/macroinitiator ratio of 100, and during the first 30 min for

NIPAAm/macroinitiator ratios of 200 and 300, indicating that the concentration of active species remain constant at the initial stage.

Micelles are formed by self-assembly *o*f copolymers in aqueous medium at room temperature. Core-shell structure micellization of the copolymers was confirmed by ^{1}H NMR spectroscopy in two different solvents ($CDCl_3$ and D_2O). The critical micelle concentration (CMC) determined by fluorescence spectroscopy is in the range of 0.0077-0.016 mg mL^{-1}. The copolymer micelles exhibit a lower critical temperature (LCST) between 32.1 and 32.8 ^oC obtained from UV-Vis transmittance measurements. The micelles are spherical in shape with a mean diameter between 31.4 and 83.3 nm, as determined by TEM and DLS. The size of micelles increases with increasing the length of hydrophilic PNIPAAm blocks since they are extended in water below the LCST. The micelles exhibit different thermo-responsive behaviors as a function of the concentration. At high concentration (3.0 mg mL^{-1}), aggregation of micelles occurs when the temperature is raised above the LCST, leading to micelle size increase. In contrast, at low concentration (0.2 mg mL^{-1}), a decrease of micelle size is detected because of the collapse of PNIPAAm blocks above the LCST.

2) In this second part, thermo-responsive P(NIPAAm-*co*-DMAAm)-*b*-PLLA-*b*-P(NIPAAm-*co*-DMAAm) triblock copolymers were synthesized by ATRP of NIPAAm and DMAAm using the same α, ω-Br-PLLA-Br macroinitiator. The polymerization was realized under the same conditions as in the case of PNIPAAm-*b*-PLLA-*b*-PNIPAAm copolymers. DMAAm was incorporated in copolymer chains as a more hydrophilic comonomer in order to tune the LCST. The NIPAAm/DMAAm ratio ranges from 100/0 to 66/24. The resulting copolymers present well defined chain structures with M_n ranging from 23600 to 27000 g mol^{-1} and low dispersity ($Đ$=1.10-1.18).

Nano-size micelles (37 to 54 nm) with narrow distribution were obtained by self-assembly of copolymers in aqueous medium. Very low CMC values were obtained,

ranging from 0.010 to 0.015 mg mL^{-1}. The LCST linearly increases from 32.2 to 39.1 ^{o}C with increasing the DMAAm content from 0 to 24 % in the hydrophilic part. The presence of DMAAm units in the copolymers leads to extremely narrow phase transition (ΔT<0.5 ^{o}C), as compared to PNIPAAm-*b*-PLLA-*b*-PNIPAAm copolymers (ΔT=2.8 ^{o}C). Reversible micelle size changes are observed with temperature variation across the LCST. In fact, when randomly distributed DMAAm is introduced, the P(NIPAAm-*co*-DMAAm) chains become more hydrophilic as compared to PNIPAAm. Thus the LCST phase transition shifts to higher temperature and becomes sharper.

Amphotericin B (AmpB), a poorly water-soluble drug for the treatment of systemic mycosis, was used as a model drug to evaluate the potential of copolymers for drug delivery. AmpB was encapsulated in micelles using dialysis method with drug loading efficiency above 59 %. *In vitro* drug release was performed at 37 or 38 °C in water using a copolymer with a LCST of 37.8 °C. An initial burst release is observed in all cases. The release rate at 38 °C is much faster than that at 37 °C, suggesting that P(NIPAAm-*co*-DMAAm)-*b*-PLLA-*b*-P(NIPAAm-*co*-DMAAm) triblock copolymer micelles could achieve thermo-responsive release after *in vivo* administration.

The cytotoxicity of copolymers was evaluated by MTT assay after incubation with mouse cardiac myocytes (MCM) and mouse embryonic fibroblasts (MEF). The values of optical density (OD) on polymer substrate are slightly higher than those in the culture solution as the negative control, and much higher than those in phenol as the positive control. The relative growth rate (RGR) values of the copolymer are well above 100 % during 4 days incubation with MCF and MEF cells, corresponding to a cytotoxicity level of 0. Moreover, cell adhesion and proliferation are observed on the copolymer substrate. Cells exhibit spindle, polygon or oval shapes, and the pseudopodium of cells stretches out. Thus, MTT assay and cell morphology observation indicate that P(NIPAAm-*co*-DMAAm)-*b*-PLLA-*b*-P(NIPAAm-*co*-DMAAm) copolymers presents outstanding cytocompatibility.

3) The third part deals with a detailed investigation of the drug encapsulation and drug release properties of thermo-responsive P(NIPAAm-*co*-DMAAm)-*b*-PLLA-*b*-P(NIPAAm-*co*-DMAAm) triblock copolymers. Four copolymers were first synthesized by ATRP as described previously. The NIPAAm/DMAAm ratio varies from 68.2/31.8 to 60.6/39.4, and the molecular weight from 18000 to 26000 g mol^{-1} with narrow dispersity ($Đ$ = 1.1). The copolymers exhibit very low CMC which slightly increases from 0.0113 to 0.0144 mg mL^{-1} while the DMAAm content increases from 31.8 to 39.4 mol% in the hydrophilic P(NIPAAm-*co*-DMAAm) blocks. Meanwhile, the LCST of copolymers increases from 44.7 °C to 49.4 °C in water and decreases by *ca.*3.5 °C in phosphate buffered saline (PBS). On the other hand, the micelle size slightly increases from 36.7 to 44.1 nm with increasing DMAAm content. The zeta-potential of micelles varies in the -12.4 to -18.7 mV range, in agreement with the structure of micelles having PLLA block in the core and P(NIPAAm-*co*-DMAAm) blocks at the corona. A copolymer with a LCST of 42.1 °C in PBS was selected for detailed drug release studies.

An anticancer drug, curcumin, was encapsulated in the core of micelles using solvent evaporation/membrane hydration method. High drug loading up to 20.4 % is achieved with high loading efficiency (>94 %). The LCST decreases from 42.1 °C for blank micelles in PBS to 38.0, 37.8 and 37.5 ^{o}C with drug loading of 6.0, 12.1 and 20.4 %, respectively. The phase transition intervals remain very sharp (<0.5 ^{o}C) in all cases. On the other hand, the micelle size increases from 38.6 nm for blank micelles to 47.5, 53.7 and 88.2 nm with drug loading of 6.0, 12.1 and 20.4 %, respectively, indicating that curcumin incorporation leads to larger micelles. Moreover, the zeta potential in water decreases from -12.4 mV for blank micelles up to -18.1 mV for 20.4 % drug loading. Higher zeta potential values are obtained in PBS due to the ionic screening effect and aggregation of micelles. All micelles remain homogeneously transparent over 1 month due to the negative surface charge.

Drug release studies were performed under *in vitro* conditions at 37 and 40 °C, *i.e.* below or above the LCST of drug loaded micelles. Initial burst release is observed in all cases, followed by a slower release. The release rate is higher at 40 °C than that at 37 °C due to thermo-responsive release above the LCST. On the other hand, micelles with lower drug loading exhibit higher release rate than those with higher drug loading. This finding could be assigned to the solubility effect. Peppas' theory is applied to describe the release behaviors. The results indicate a combination of diffusion and degradation controlled release. Moreover, the *in vitro* cytotoxicity tests using murine fibrosarcoma (L929) and human lungcarcinoma (A549) cells confirm the good cytocompatibility of the copolymers.

4) In the last part of the work, thermo-responsive comb-like P(MEO_2MA-*co*-OEGMA)-*b*-PLLA-*b*-P(MEO_2MA-*co*-OEGMA) triblock copolymers were synthesized by ATRP of MEO_2MA and OEGMA (M_n = 300 g mol^{-1}) comonomers using the same α, ω-Br-PLLA-Br macroinitiator under similar conditions. The resulting copolymers present well defined chain structures with M_n varying from 27100 to 9800 g mol^{-1} and dispersity of *c.a* 1.40. The MEO_2MA/OEGMA ratio in the hydrophilic blocks varies from 79/21 to 42/58.

Thermo-responsive micelles are obtained by self-assembly of copolymers in aqueous medium. The CMC of copolymers slightly increases from 0.0113 to 0.0130 mg mL^{-1} with increasing the OEGMA content from 21 to 58 % due to its higher hydrophilicity. The LCST of micelles in water increases from 36.4 to 56.7 ^oC with the content of OEGMA increasing from 21 % to 43 %. Data are not available for copolymers with higher OEGMA contents due to fast evaporation of water above 60 ^oC. The presence of salt significantly decreases the LCST of copolymers. A decrease of nearly 17 ^oC is observed when comparing the LCST values in PBS and in water, suggesting the strong dehydration effect of phosphate ions. The micelle size increases from 20.7 to 102.5 nm with the content of OEGMA increasing from 21 % to 58 %. On the other

hand, the zeta potential of micelles ranges from -0.77 to -1.99 mV, which implies a nearly neutral surface charge.

Curcumin is encapsulated in micelles by using solvent evaporation/membrane hydration method with loading efficiency above 90 %. The micelle size decreases from 102.2 nm for blank micelles to 37.6 nm with 10.8 % drug loading, and the LCST decreases from 45.1 °C to 38.3 ^{o}C. Interestingly, the zeta potential decreases from -1.99 up to -44.9 mV. These findings indicate that drug loading strongly affects the self-assembly procedure. Triblock copolymers are assumed to self-assemble in micelles with a PLA core, a PMA mesophase and a hydrophilic corona. Curcumin encapsulation in the core and in the mesophase could lead to decrease of micelle size and LCST and increase of zeta potential.

In vitro drug release is performed in pH 7.4 PBS at 37 °C and 41 ^{o}C, *i.e.* below or above the LCST, respectively. An initial fast release from micelles is observed in all cases, followed by slower release. 81.8 % and 92.6 % release is observed for micelles with 5.9 % drug loading after 14 days at 37 ^{o}C and 41 ^{o}C, respectively. Slower release is obtained for micelles with 10.8 % drug loading. The total release reaches 59.5 % and 75.9 % at 37 ^{o}C and 41 ^{o}C in the same period, respectively. Therefore, drug release is not only dependent on the phase transition across the LCST, but also on the drug loading because the solubility of curcumin is a limiting factor.

Therefore, two series of thermo-responsive triblock copolymers, *i.e.* PLA/P(NIPAAm-*co*-DMAAm) and PLA/P(MEO_2MA-*co*-OEGMA) are successfully synthesized by combination of ROP and ATRP. The resulting amphiphilic copolymers present interesting self-assembling properties, variable LCST, and outstanding cytocompatiblity. The high drug content and encapsulation efficiency, and thermo-responsive drug release behavior indicate that these copolymers are promising candidate for targeted delivery of anticancer drugs.

List of Tables

List of Schemes

List of Figures

Abbreviation List

A

A549: Lungcarcinoma cell

AIBN: Azobisisobutyronitrile

AmpB: Amphotericin B

ATRP: Atom transfer radical polymerization

B

BPO: Benzoyl peroxide

Bpy: Bipyridine

Br-PCL-Br: α, ω-Bromopropionyl poly(ε-caprolactone)

Br-PLLA-Br: α, ω-Bromopropionyl poly(L-lactide)

C

CaH_2: Calcium hydride

CLSM: Confocal laser scanning microscopy

CMC: Critical micellar concentration

CMT: Critical micelle temperature

CuCl: Copper (I) chloride

D

DDS: Drug delivery systems

DTBz: Dithiobenzoate

DL: Drug loading

D-LA: D-lactide

DLS: Dynamic laser scattering

DMAAm: *N, N*-dimethylacrylamide

DMEM: Dulbecco's Modified Eagle's Meduim

DMF: *N, N*-dimethyformamide

DMSO: Dimethyl sulfoxide

DOSY NMR: Diffusion-ordered NMR

E

EDTA:

EE: Encapsulation efficiency

EPR: Enhanced permeability and retention

F

FDA: Food and Drug Administration

H

^{1}H NMR: Proton Nuclear Magnetic Resonance

HepG2: Human hepatocellular carcinoma cell line

HMTETA: Hexamethyltriethylenetetramine

HO-PLLA-OH: α,ω-Hydroxy Poly(L-lactide)

I

ICP-MS: Inductively coupled plasma-mass spectrometey

L

L929: Murine fibrosarcoma

L-LA: L-lactide

LCST: Lower critical solution temperature

M

Mal: Maleimide

MCM: Mouse cardiac myocytes

MEF: Mouse embryonic fibroblasts

MEO_2MA: 2-(2-Methoxyethoxy) ethyl methacrylate

Me_6TREN: Tris(2-dimethylaminoethyl) amine

mPEG-*b*-PCL: Poly(ethylene glycol)-*b*-poly(ε-caprolactone)

MTT: 3-(4, 5-Dimethylthiazol-2-yl)-2,5-diphenyltetrazolium bromide

MWCO: Molecular weight cut off

N

NMP: Nitroxide mediated polymerization

O

OD: Optical density

OEGMA: Oligo(ethylene glycol) methacrylate

P

PDLA: Poly(D-lactide)

PEG (or PEO): Poly(ethylene glycol)

PLA: Polylactide

PLGA-*b*-PEG-*b*-PLGA :

Poly(D,L-lactide-*co*-glycolide)-*b*-poly(ethyleneglycol)-*b*-poly(D,L-lactide-*co*-glycolide)

PLGA-*b*-POEGMA:

Poly(lactide-co-glycolide)-*b*-poly(oligo(ethyleneglycol) methacrylate)

PLLA: Poly(L-lactide)

PMA: Polymethacrylate

PMEOMA: Poly(2-methoxy ethyl) methacrylate

PMDETA: Pentamethyldiethylenetriamine

PNIPAAm: Poly(*N*-isopropylacrylamide)

P(NIPAAm-*co*-DMAAm)-*b*-PLGA:

Poly(*N*-isopropylacrylamide-*co*-*N,N*-dimethylacrylamide)-*b*-poly(D,L-lactide-*co*-glycolide)

PNIPAAm-*b*-PLLA-*b*-PNIPAAm:

Poly(*N*-isopropylacrylamide)-*b*-poly(*L*-lactide)-*b*-poly(*N*-isopropylacylamide)

P(NIPAAm-*co*-DMAAm)-*b*-PLLA-*b*-P(NIPAAm-*co*-DMAAm):

Poly(*N*-isopropylacrymine-*co*-*N,N*-dimethylacrylamine)-*b*-poly(L-lactide)-*b*-poly(*N*-isopropylacrymine-*co*-*N,N*-dimethylacrylamine)

P(NIPAAm-co-DMAAm)-*b*-PCL:

Poly(*N*-isopropylacrylamide-*co*-*N,N*-dimethylacrylamide-*b*-ε-caprolactone)

PNIPAAm-*b*-PS:

Poly(*N*-isopropylacrylamide)-*b*-polystylene

PNIPAAm-*b*-PMMA:

Poly(*N*-isopropylacrylamide)-*b*-poly(methyl methylacrylate)

PNIPAAm-*b*-PtBA: Poly(*N*-isopropylacrylamide)-*b*-poly(tert-butyl acrylate)

PSMA: Prostate specific membrane antigen

PTMC-*b*-PGA: Poly(trimethylene carbonate)-*b*-poly(L-glutamic acid)

R

RAFT: Reversible addition-fragmentation chain transfer

RES: Reticuloendothelial system

RGR: Relative growth ratio

ROP: ring-opening polymerization

S

SEC: Size exclusion chromatography

SG1: *N*-tert-butyl-*N*-(1-diethylphosphono-2, 2-dimethylpropyl) nitroxide

$Sn(Oct)_2$: Tin(II)2-ethylhexanoate

T

TEM: Transmission electron microscopy

THF: Tetrahydrofuran

WHO: World Health Organization

Z

ZP: Zeta potential

Symbol List

Đ: Molecular weight dispersity

D: Diffusion coefficients of the solutes

D_0 : The translational diffusion coefficient at finite dilution

G : Relaxation frequency

h : The viscosity of the medium

k_B*:* Boltzmann constant

M_n*:* Molecular weight

q: Wave vector

R_H: Apparent equivalent hydrodynamic radius

T: Temperature

t: Time

ΔT: Phase transition interval

General introduction

Vectors prepared from amphiphilic block copolymers have been widely investigated for pharmaceutical applications such as gene or cancer therapy. Among them, nanocarrier has drawn great attention due to the passive enhanced permeability and retention effect (EPR). Polymer micelles with small size (<200 nm) and low critical micelle concentration (CMC) exhibit outstanding stability, high drug loading and loading efficiency, and targeted drug delivery by EPR, which makes them promising candidate as nanocarrier of anticancer drugs. However, most of the reported micelles are not stimuli-responsive.

The aim of this work is to develop novel triblock copolymer micelles as nanocarrier which combines both the passive targeting by EPR and active targeting by thermo-responsiveness.

The first chapter of the thesis is a bibliography which provides an overview on the state of the art in this domain. Nanocarriers including liposomes, polymersomes, nanoparticles and polymeric micelles are introduced. Then, amphiphilic polylactide/poly(ethylene glycol) (PLA/PEG) block copolymers are discussed as the most studied bioresorbable and biocompatible micelles for controlled drug delivery. The principle of thermo-responsive polymeric micelles was presented. Two different families of thermo-responsive (co)polymers, polyacrylamide and poly(oligo(ethylene glycol) methacrylate) or PEG analogues, as well as their amphiphilic block copolymers with PLA, are then introduced, including the synthesis, self-assembly and drug release properties.

The second chapter focuses on the synthesis, characterization and self-assembly of poly(*N*-isopropylacrylamide)-*b*-poly(L-lactide)-*b*-poly(*N*-isopropylacrylamide) (PNIPAAm-*b*-PLLA-*b*-PNIPAAm) triblock copolymers. Herein, for the first time, we

report the synthesis of triblock copolymers by by ATRP of NIPAAm using a Br-PLLA-Br macroinitiator. Kinetic studies are realized to illustrate the relationship between the molecular weight and NIPAAm/macroinitiator ratio. Self-assembly properties of copolymers and phase transition across the lower critical solution temperature (LCST) are determined by CMC, DLS, TEM and UV transmittance measurements.

In the third chapter, an acrylamide comonomer, *N, N*-dimethylacrylamide (DMAAm) is introduced to increase and precisely adjust the LCST of the resulting P(NIPAAm-*co*-DMAAm)-*b*-PLLA-*b*-P(NIPAAm-*co*-DMAAm) triblock copolymers. The copolymers are successfully synthesized under the same conditions and fully characterized. Self-assembly and phase transition of copolymers are studied. Preliminary drug release is realized in water using Amphotericin B as a model. The cytotoxicity of copolymers is evaluated by MTT assay after incubation with mouse cardiac myocytes (MCM) and mouse embryonic fibroblasts (MEF).

The fourth chapter deals with the properties and *in vitro* drug release behavior of drug loaded micelles. Curcumin, an anticancer drug, is loaded in P(NIPAAm-*co*-DMAAm)-*b*-PLLA-*b*-P(NIPAAm-*co*-DMAAm) triblock copolymer micelles by solvent evaporation/membrane rehydration method. The properties such as drug loading, loading efficiency and the effect of drug loading on the LCST, size and morphology are investigated. *In vitro* drug release is performed at temperatures below or above LCST. Peppas' theory is applied to describe the drug release behavior. The cytotoxicity is further evaluated using murine fibrosarcoma (L929) and human lung carcinoma cell (A549) cells to confirm the good cytocompatibility of the copolymers.

The fifth chapter describes the synthesis, micellization and *in vitro* drug release from P(MEO_2MA-*co*-OEGMA)-*b*-PLLA-*b*-P(MEO_2MA-*co*-OEGMA) triblock copolymers. The copolymers are synthesized by ATRP using the same macroinitiator and catalyst system as in the case of PLA/PNIPAm copolymers. Micellization is performed in

aqueous medium and confirmed by CMC, DLS and TEM measurements. *In vitro* drug release is performed in pH 7.4 PBS at 37 °C (below the LCST) and 41 ^{o}C (above the LCST). The effects of temperature and drug loading on the drug release are discussed.

Chapter 1 Bibliography

1.1 “Magic bullet” for cancer therapy

Cancer is nowadays a leading cause of death in the word. The World Health Organization (WHO) reported the approximately 14 million new cases and 8.2 million cancer related deaths in 2012 [1]. The number of new cases is expected to rise by about 70 % over the next two decades. For efficient cancer therapy, it is of key importance to improve our knowledge of cancer physiopathology, to discover new anti-cancer drugs and to develop novel biomedical technologies. Currently, the cancer therapy has become a multidisciplinary challenge requiring close collaboration among clinicians, biological and materials scientists, and biomedical engineers.

The concept of “magic bullet” that hits its target without damaging healthy issues proposed by the Nobel laureate Paul Ehrlich in 1906 turned to reality for cancer treatment and serious infectious diseases [2]. The challenge of the targeting is triple: (i) to find the drug that effectively treats this disease, (ii) to find how to carry the drug, and (iii) to find the proper target for a particular disease.

In the past decade, “magic bullet” from nanotechnology has been considered as one of the most challenging innovations in pharmacology, and is now widely used in prevention, diagnosis and therapy of cancer [3-6]. Nanocarriers have been exploited to protect the drug, to optimize its targeting, to limit its accumulation in healthy organs, to reduce its potential toxicity and to control its release [7].

1.1.1 Passive and active targeting in cancer therapy

The specific tumor targeting requires better profiles of pharmacokinetics and pharmacodynamics, controlled and sustained release of drugs, improved specificity, increased internalization and intracellular delivery and, more importantly, lower

systemic toxicity [8]. As shown in Figure 1.1, one can distinguish two kinds of tumor targeting, *i.e.* passive targeting and active targeting. Drug carriers with size ranging from 10 to 200 nm can reach tumor passively through the leaky vasculature surrounding the tumors by the enhanced permeability and retention (EPR) effect. In contrast, ligands grafted at the surface of drug carriers allow active targeting by binding to the receptors over expressed by cancer cells or angiogenic endothelial cells, followed by drug release in tumor [9]. However, the active targeting process cannot be separated from the passive one because it occurs only after passive accumulation in tumors [10].

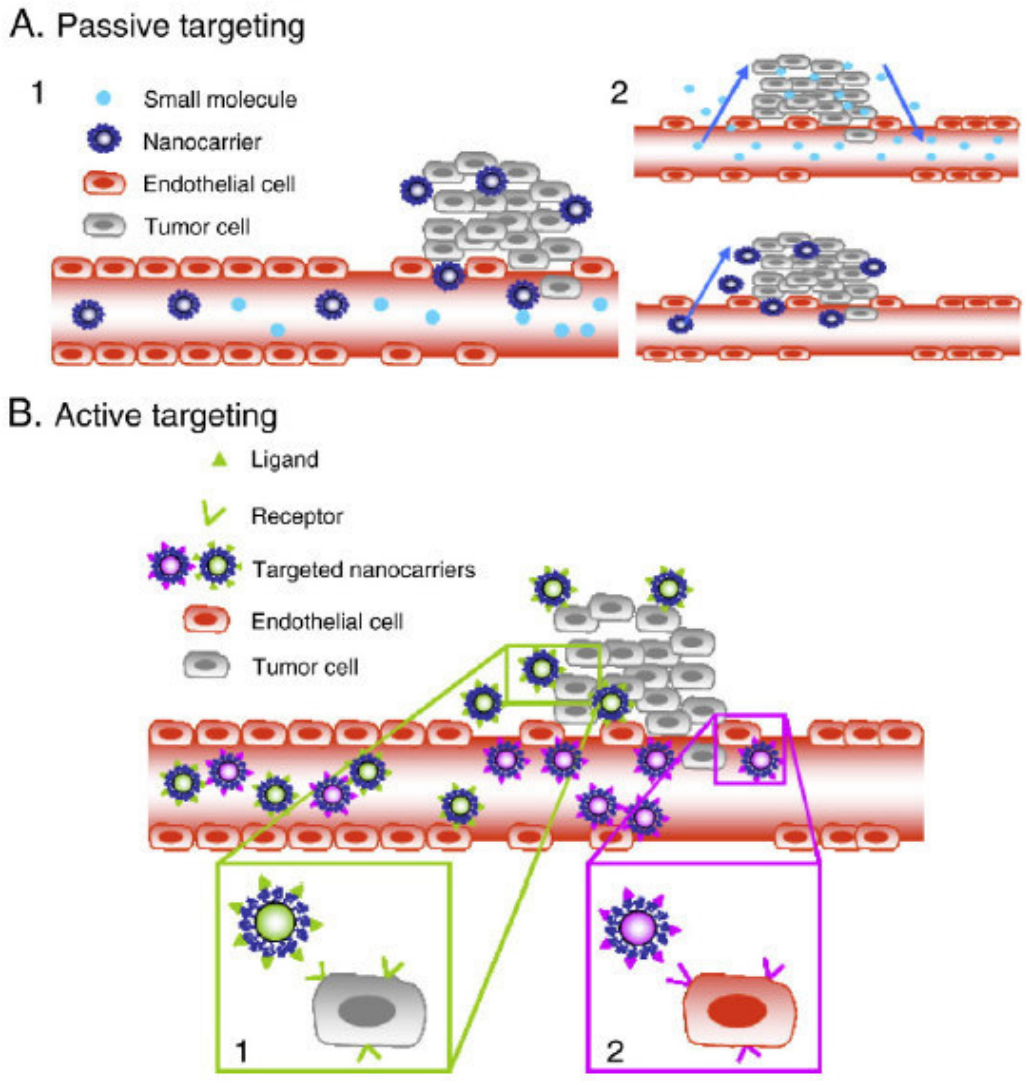

Figure 1.1 Passive targeting (A) and active targeting (B) of nanocarriers. From ref. [9].

Indeed, all nanocarriers use the "passive targeting" EPR effect as a guiding principle [11]. As shown in Figure 1.1A, nanocarriers reach tumors selectively through the leaky vasculature surrounding the tumors. Small drug molecules (unencapsulated by a polymeric matrix) diffuse freely in and out the tumor blood vessels because of their small size. Thus their effective concentration in the tumor decreases rapidly. In contrast, drug-loaded nanocarriers cannot diffuse back into the blood stream because of their large size (10-200 nm), thus resulting in progressive accumulation by the EPR effect, which has become the "gold standard" in cancer-targeting drug designing.

The EPR effect is applicable for almost all rapidly growing solid tumors [12]. Indeed, it can be observed in almost all human cancers with the exception of hypovascular tumors such as prostate cancer or pancreatic cancer [13]. The EPR effect will be optimal if nanocarriers can circulate for a long period of time. Very high local concentration of drug-loaded nanocarriers can be achieved at the tumor site, for instance 10–50 times higher than in normal tissue within 1–2 days [14].

1.1.2 Polymeric delivery system

Because of the specific characteristics of the tumor microenvironment and tumor angiogenesis, it is possible to design drug delivery systems that specifically deliver anti-cancer drugs to tumors. However, most of the conventional therapeutic agents have poor pharmacokinetic profiles and are distributed nonspecifically in the body leading to systemic toxicity associated with serious side effects.

In the past decades, polymeric delivery system has been widely exploited for various biomedical and pharmaceutical applications [15]. Early in 1970s, Yolles *et al.* proposed the concept of polymeric delivery system which is expected to deliver the right amount of active agent at the right time to the right site [16, 17]. From then on, polymeric delivery system has attracted more and more attention [18, 19]. Controlled release systems are expected to deliver the drug into the systemic circulation at a

predetermined rate, while targeted delivery systems should release medications at or near the targeted site. The advantage of targeted delivery is that high local concentration of drug can be achieved. The drug is predominantly delivered to the tumor rather than distributed throughout the whole body.

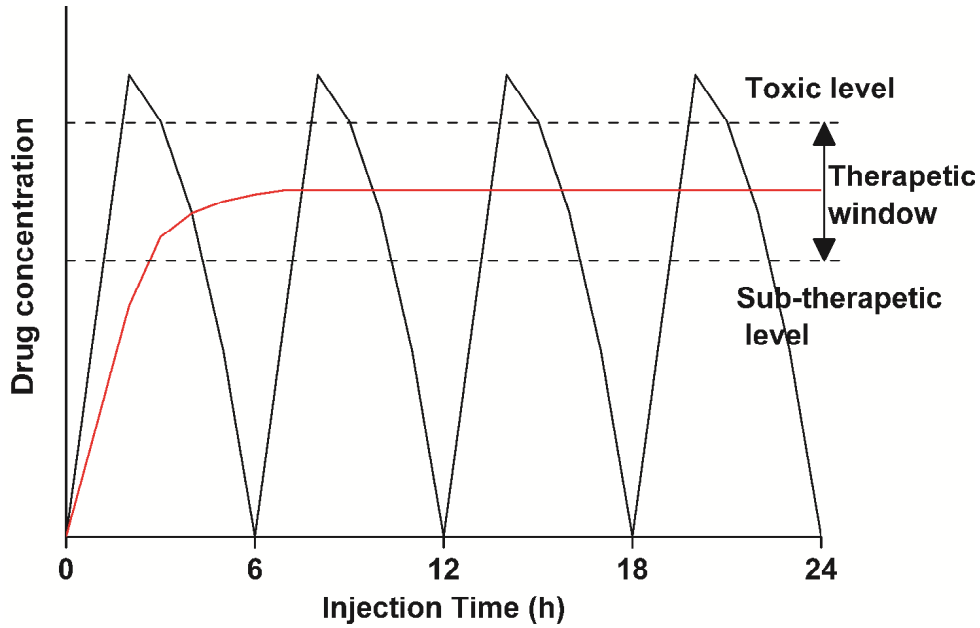

Figure 1.2 Drug concentrations at site of therapeutic action after delivery as a conventional injection (black) and as a temporal controlled release system (red). From ref. [20] with modification.

Indeed, drugs usually have an optimum concentration range within which maximum benefit is achieved. Concentrations above or below this range are ether toxic or exhibit no therapeutic effect [20]. Controlled release over an extended duration is highly beneficial for drugs that are rapidly metabolized and eliminated from the body after administration. As shown in Figure 1.2, the concentration of drug at the site of activity after release from conventional administration (4 injections administered at 6 hourly intervals) is compared with that after release from a controlled release system. In the case of conventional drug release, the drug concentration strongly fluctuates during the 24 h period, and only a portion of the treatment period is in the therapeutic window. With the controlled release system, in contrast, the drug concentration is within the therapeutic window for almost 24 h. Controlled drug release could provide

a significant improvement in clinic therapy. A temporally controlled release system would ensure that the maximum possible benefit is derived from the drug.

Consequently, polymeric delivery systems could allow to deliver the drugs *in vivo* with the following benefits: 1) maintenance of optimum therapeutic drug concentration in the blood with minimum fluctuation; 2) predictable and reproducible release rate for extended duration; 3) prolongation of activity period for short half-life drugs; 4) elimination or decrease of side effects, frequent dosing and wastage of drug; and 5) optimized therapy and improved patient compliance.

1.1.3 Thermo-responsive targeted drug delivery

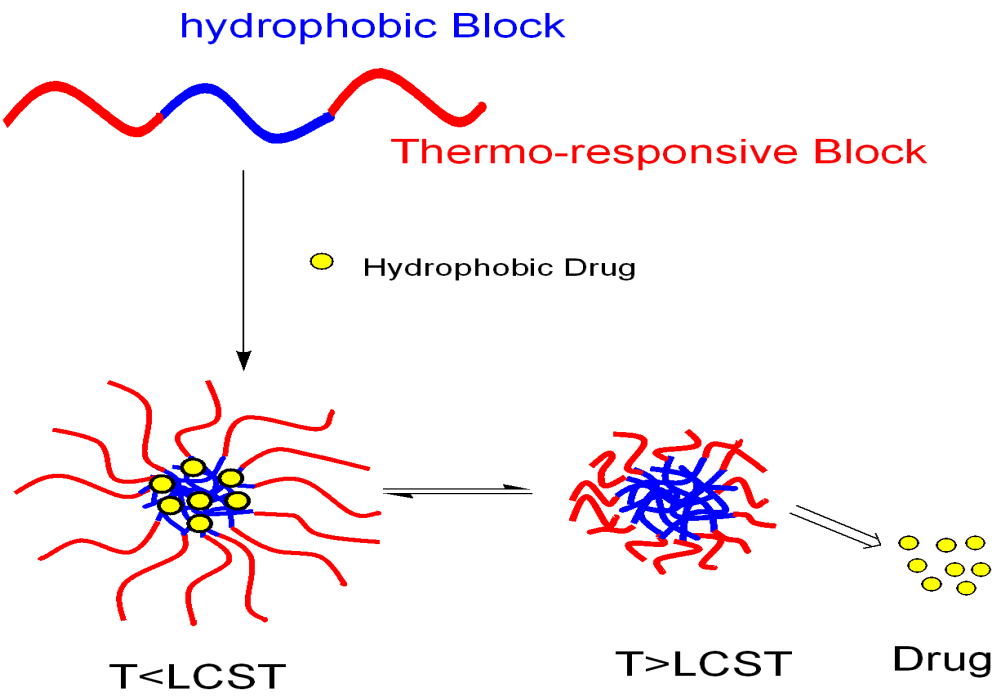

Scheme 1.1 Drug release from thermo-responsive polymeric micelles.

A new targeting strategy consists in developing "activable" or "activated" nanocarriers due to the fast cancer cell metabolism. It is well known that different from normal tissues, tumor has higher temperature (~42 ^{o}C) and lower pH (~5.3) due to fast cell metabolism [21]. Recently, "smart" polymers which are responsive to stimuli such as pH, acid and heat have also drawn great attention as drug delivery

systems [4, 22-29]. Thus, active target-specific delivery of drugs from these systems to various sites in the body can be achieved to improve the therapeutic therapy, meanwhile minimizing undesired side-effects.

Temperature is the most widely used stimulus in environmentally responsive polymeric drug delivery systems. The change of temperature is not only relatively easy to control, but also easily applicable both *in vitro* and *in vivo*. Therefore, temperature-responsive nanocarriers have been largely developed [30, 31]. These polymers generally exhibit a lower critical solution temperature (LCST) above which phase separation occurs. As shown in Scheme 1.1, micelles can be obtained by self-assembly of amphiphilic and thermo-responsive block copolymers below the LCST, encapsulating a hydrophobic drug in the core of micelles. With increasing the temperature above the LCST, the hydrophilic shell composed of thermo-responsive blocks becomes hydrophobic and collapsed, and the micelles shrink or aggregate, leading to faster drug release.

1.2 Nanocarrier

Various nanocarriers have been investigated for controlled or targeted drug delivery. Figure 1.3 shows the various families of nanocarrier from 1 nm to 1 μm, including branched polymers, micelles, liposomes, polymersomes, nanoparticles and micelles.

The size limit strongly depends on the target. Nanocarriers below 400 nm are more suitable for accumulation in most tumors depending on cut-off size of vascular pores. The lower limit is determined by the sieving coefficients for the glomerular capillary wall in the kidney to avoid rapid renal filtration (that clears particles below 10 nm such as branched polymers). Among the various systems, nanocarriers with sizes between 10 and 200 nm are most promising candidate for targeted drug delivery because they can avoid being cleared by the reticuloendothelial system (RES) or mechanically filtered through the spleen and liver, and are small enough to efficiently

accumulate in tumors by the EPR effect.

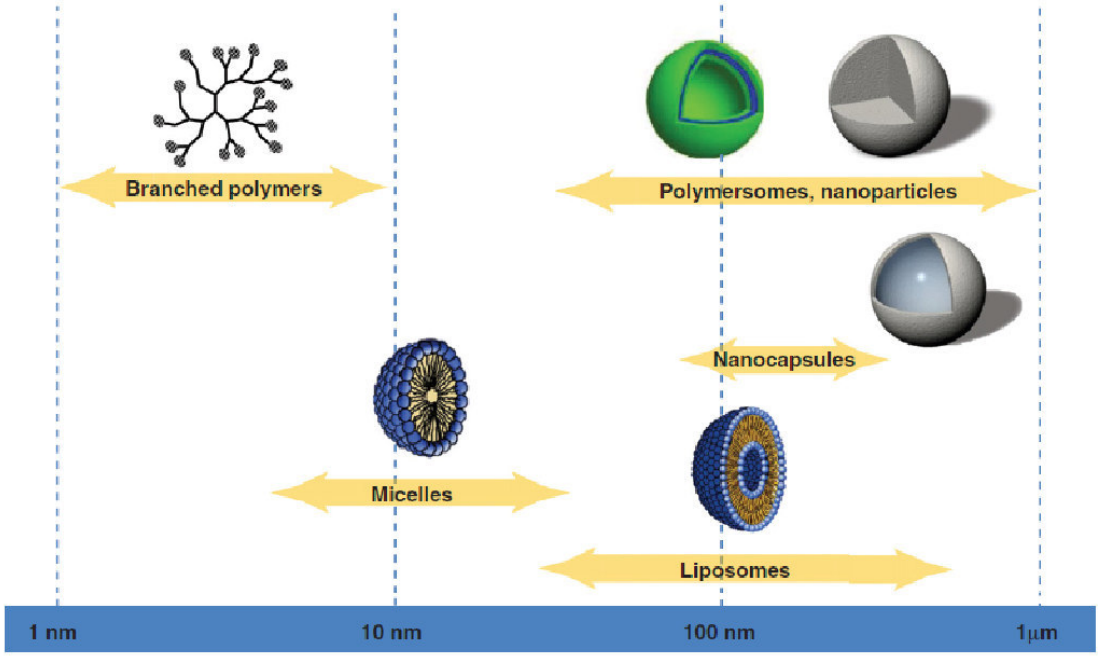

Figure 1.3 Different families of nanocarrier for drug delivery. From ref. [7] with modification.

1.2.1 Liposome

The first liposome was reported by Gregoriadis *et al*. in 1974 [32]. Liposomes are defined as spherical lipid vesicles composed of amphiphilic phospholipids with a bilayer membrane structure, and constitute an excellent tool for the understanding of biological events such as cell adhesion, signal transduction or endocytosis. The closed bilayers are formed by protecting the hydrophobic groups from the aqueous environment which is in contact with the hydrophilic head group [3]. The polar character of the liposomal core enables polar drug molecules to be encapsulated, while lipophilic molecules are solubilized within the bilayer according to their affinity towards phospholipids. Channel proteins can be incorporated without loss of activity within the hydrophobic domain of vesicle bilayers, acting as a size-selective filter only allowing passive diffusion of small solutes such as ions, nutrients and antibiotics.

Drugs that are encapsulated in a nanocage functionalized with channel proteins are

effectively protected from premature degradation by proteolytic enzymes. Drug molecules are able to diffuse through the channel, driven by the concentration difference between the interior and the exterior of the nanocage. Depending upon the size and number of bilayers, liposomes can be divided in three categories: multilamellar vesicles, large unilamellar vesicles, and small unilamellar vesicles. On the other hand, liposomes can also be classified in five types in terms of composition and mechanism of intracellular delivery, *i.e.* conventional liposomes, pH-sensitive liposomes, cationic liposomes, immune-liposomes, and long-circulating liposomes [33].

Liposomes can be prepared by using film casting and hydration method. Materials are first dissolved in a solvent to yield a homogenous solution, and then a thin film is obtained by using a rotary evaporator. Subsequently, the film is hydrated by addition of water. Water permeation in the thin film driven by hydration forces allows to form bilayers, and finally yields vesicles upon separation from the recipient's surface.

Liposomes have been investigated for the delivery of vaccine, toxoids, gene, anticancer, and anti-HIV drugs [33-37]. However, although liposome technology was discovered over 40 years ago, liposome-based drug formulations have rarely entered the stage of clinical applications. The major drawback of liposomes is their low mechanical stability and high leakiness, mainly due to their small membrane thickness (3–5 nm). Other factors such as limited versatility of chemical structures, poor batch-to-batch reproducibility, difficulties in sterilization, large size (up to 400 nm) and low drug loading also contribute to restrain the development of liposomes as drug carrier [7, 38].

Recently, modification of liposome by PEG has been successfully developed [36]. Doxil® (Sequus Pharmaceuticals, Menlo Park, California), the first FDA-approved nano-drug (1995), is a long-acting PEGylated liposomal formulation of doxorubicin.

It alters dramatically the pharmacokinetic properties of doxorubicin with prolonged drug circulation time, escaping from the RES, high loading of doxorubicin and targeted release at the tumor due to the EPR effect [39, 40].

1.2.2 Polymersome

In the past decade, polymersomes (also referred to as polymeric vesicles) have attracted growing interest based on their intriguing aggregation phenomena, cell and virus-mimicking dimensions and functions, as well as tremendous potential applications in medicine, pharmacy, and biotechnology [41, 42]. Unlike liposomes self-assembled from low molecular weight lipids, polymersomes are in general prepared from macromolecular amphiphiles of various architectures including amphiphilic diblock, triblock, graft as well as dendritic copolymers [43-45].

The preparation methods of polymersomes are generally classified into two groups: solvent-switching and film hydration. Solvent-switching techniques have been widely used in the preparation of polymeric vesicles (and also for other morphologies) as most amphiphilic block copolymers are not directly soluble in water. Initially the amphiphilic copolymer is dissolved in a common organic solvent for both blocks and then water is added gradually to the copolymer solution. The hydrophobic blocks tend to associate together in the polar environment to form a bilayer, whereas the hydrophilic blocks are solvated to form the corona which colloidally stabilizes the vesicle. Film hydration technique is the same as that used for liposomes preparation mentioned above, involving film casting and hydration to induce self-assembly and polymersome formation.

Polymersomes and liposomes present similar architectures. Both are nano- to micrometer-sized capsules with a bilayered membrane enclosing an aqueous compartment. They are able to encapsulate hydrophilic molecules within the aqueous core and also hydrophobic molecules within the membrane. Moreover, because

polymersomes are composed of block copolymers instead of small molecules, they present lower permeability and higher mechanical stability, and their architecture is more tunable as compared to liposomes [7].

Polymersome is one of the most interesting drug delivery systems because of multi drug loading capacity, membrane robustness and stealth properties [46, 47]. Some authors have studied polymersomes for targeted drug delivery [48]. Two anticancer drugs, paclitaxel and doxorubicin have been encapsulated in polymersomes for cancer therapy as reported by Ahmed *et al*. [49]. The drugs are loaded into polymersomes by a pH-gradient method established for liposomes. A single systemic injection of the dual drug combination shows a higher maximum tolerated dose than the free drug cocktail and shrinks tumors more effectively and more sustainably than free drug: 50 % smaller tumors are observed at 5 days with polymersomes. Drug accumulation within tumors was also observed, showing the potential of multi-drug delivery by polymersomes for clinical applications.

However, the major drawback of polymersome delivery systems is the long encapsulation procedure (up to weeks). Recently, Lecommandoux *et al*. proposed a convenient and reproducible nanoprecipitation method to obtain stable and pH-inducible poly(trimethylene carbonate)-*b*-poly(L-glutamic acid) (PTMC-*b*-PGA) polymersomes loaded with a remarkably high content of doxorubicin (47 %, w/w %) at pH 10.5 [42, 50]. Doxorubicin and polymer are dissolved in dimethyl sulfoxide (DMSO). Then an aqueous phase is quickly added to the organic phase under stirring. Excess drug and DMSO are removed by dialysis against a buffer solution. After neutralization, an aqueous dispersion of drug-loaded vesicles is obtained which remains stable for a prolonged period of time (at least 6 months) without vesicle disruption or drug precipitation.

Furthermore, to prevent premature drug leakage, Lecommandoux *et al*. reported the

preparation of polymeric vesosomes, that is, polymersomes in polymersomes [51]. Vesosomes present controlled permeability by encapsulating nano-size polymersomes inside larger polymersomes. A double-membrane diffusion barrier effect was demonstrated since the observed *in vitro* release rate of doxorubicin from vesosomes was twice slower than that from polymersomes.

In principle, drug release from polymersomes is governed by the diffusion of drug through the membrane. According to the diffusion-interface theory, the driving force is the concentration gradient of drug between the polymersome and the surrounding medium [52]. When drug molecules diffuse from the core of polymersomes to the surrounding medium, the release rate is a function of the square root of time. The size distribution of polymersomes also influences the overall release rate [53]. Based on theoretical approaches, polymersomes suitable for the delivery of specific drugs can be designed and the release kinetics predicted. Nevertheless, in many cases, the control for drug release cannot be adjusted to the desired level because the properties of polymersomes cannot be varied to a large extent due to lack of versatility for the composition of block copolymers [54].

Recently, to achieve targeted drug delivery, significant efforts have been devoted to develop "smart" polymersomes which are responsive to pH, heat, light as well as magnetic field [28, 55-66]. Stimuli-responsive polymersomes have emerged as novel programmable delivery systems allowing to readily modulate the release of encapsulated contents by the stimulus. Stimuli-responsive release could significantly enhance the therapeutic efficacy and minimize the side effects. It is also feasible to form and disassemble polymersomes in water simply by applying an appropriate stimulus. Lecommandoux *et al*. reported biologically active polymersomes from polypeptide block copolymers prepared by "click chemistry" [67-69]. Hybrid polymer/lipid vesicles were also developed when the content of lipids was below 20 mol %, in which lipids are randomly distributed in the polymer-rich membrane [70,

71].

1.2.3 Nanoparticle

Nanoparticles include both nanospheres and nanocapsules in solid state, either amorphous or crystalline. They are able to absorb or encapsulate a drug, thus protecting it against chemical and enzymatic degradation [18]. Nanoparticles as drug carrier can be obtained from both biodegradable polymers and non-biodegradable ones [3, 72, 73]. Recently, biodegradable polymeric nanoparticles have attracted great attention in view of their applications in controlled and targeted delivery of drugs [11, 74-76].

Polymeric nanoparticles can be prepared from emulsion or precipitation method. Formation of hollow structures, named nanocapsules, can also be achieved. Their size is generally between 10 and 1000 nm and strongly depends on the preparation method. The solid nature of nanoparticles confers great stability and controlled drug release rate. Nanoparticles with size ranging from 10 to 200 nm can preferentially concentrate in tumor by virtue of the EPR effect as mentioned above. In addition, multiple drug loadings can be achieved within nanoparticles [7].

Moreover, surface PEGylated nanoparticles also have been developed to provide excellent pharmacokinetic control, and are suitable for the entrapment and delivery of a wide range of therapeutic agents [77-79]. PEGylated nanoparticles allow to reduce the immunogenicity, and to limit the phagocytosis of nanoparticles by the RES, thus resulting in increased blood concentration of drug in organs such as the brain, intestines, and kidneys.

Nanoparticles are matrix systems in which the drug is physically and uniformly dispersed. Drug release kinetics can be adjusted by careful selection of polymers or polymer blends. Thus, drug release from nanoparticles generally occurs either by

diffusion or by matrix degradation or both.

1.2.4 Polymeric micelle

In the past decades, self-assembly of amphiphilic block copolymers in aqueous solutions into various micellar structures has been extensively investigated. Bader *et al*. first proposed micelles as potential drug carrier in 1984 [80]. Since then, micelles attracted more and more interest for controlled release of drugs due to their numerous advantages including reduced side effects of drugs, targeted drug delivery, and prolonged blood circulation time [81-86]. Drug encapsulation can be simply realized by physical mixing, which is attractive as compared to chemical conjugate [85, 87].

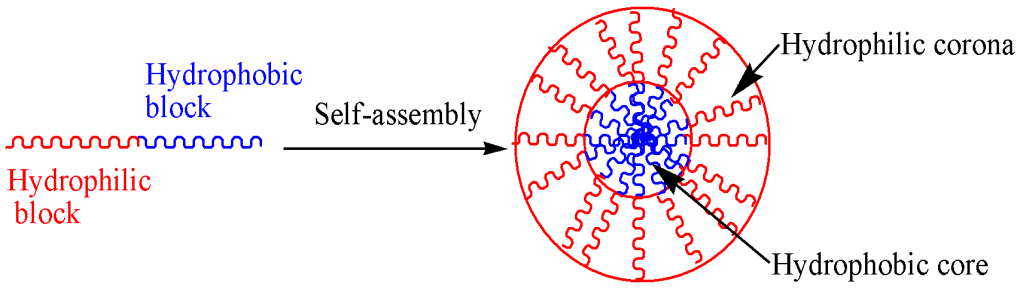

Scheme 1.2 Self-assembly micelles from amphiphilic block copolymer.

In an aqueous medium, polymeric micelles generally present a core-corona structure driven by hydrophobic interactions above the critical micellar concentration (CMC) as shown in Scheme 1.2 [88]. The hydrophobic inner core allows encapsulation of hydrophobic drugs by physical entrapment, whereas the hydrophilic shell acts as a stabilizing/interacting corona [89]. Micelles are thus used to encapsulate drugs with poor water solubility [90, 91]. Compared to polymersome systems, micelles have advantages such as simple preparation and efficient drug loading.

Polymeric micelles can be prepared by using different methods: direct dissolution, dialysis, nanoprecipitation (solvent-switching), and solution casting/membrane hydration. Direct dissolution involves simply dissolving a water soluble amphiphilic

copolymer in an aqueous medium. Dialysis consists in dialyzing a copolymer solution against water. Nanoprecipitation and membrane hydration methods are the same as those used for the preparation of polymersomes mentioned above. Yang *et al*. compared micelles prepared by direct dissolution and dialysis methods [92, 93]. Similar drug loading and encapsulated efficiency were obtained for both methods. Micelles by direct dissolution method present major advantages such as easy formulation and absence of toxic organic solvents, which shows great potential as carrier of hydrophobic drugs.

Polymeric micelles generally have small sizes (*i.e.* <200 nm) with narrow distribution, which allows them to escape from non-specific uptake by the RES cells and to achieve long circulation in the blood stream [81, 87, 94]. Drug molecules can be incorporated by means of chemical, physical or electrostatic interactions, depending on their physicochemical properties. Amphiphilic block copolymers are attractive for drug delivery applications since their chemical composition, molecular weight and block lengths can be easily changed, which allows control of the size and morphology of micelles. Polymeric micelles can target tumor sites by passive as well as active targeting mechanisms. In fact, the inherent properties of micelles including size in the nano range, stability in plasma, long circulation *in vivo*, and the pathological characteristics of tumor allow them to target the tumor site by the EPR effect [88, 95-101].

Recently, growing interest has been paid to amphiphilic block copolymer micelles as novel carrier for drug targeting [84, 91, 102-104]. The distribution of drug loaded polymeric micelles in the body is mainly determined by their size and surface properties, and less affected by the properties of drug embedded in the inner core of micelles. In this regard, the size and surface properties of polymeric micelles have crucial importance in achieving controllable drug delivery with efficacy [84, 105]. Prolonged *in vivo* circulation time and adequate retention of drug within the carrier

are prerequisites to successful drug targeting [106]. Thermo-responsive and pH polymeric micelles have also been developed to achieve targeted drug release at the tumor site [29, 103, 107, 108].

1.3 Amphiphilic copolymers for uses as nanocarrier

1.3.1 PLA/PEG block copolymers

1.3.1.1 Polylactide

From a theoretical point of view, micelles prepared from biodegradable polymers would be more beneficial in applications since no accumulation of polymers occurs after drug release. As a biodegradable polymer, polylactide (PLA) has been extensively investigated as controlled drug release systems for biomedical and pharmaceutical applications [72, 109, 110]. PLA presents outstanding biocompatibility and variable biodegradability. The final degradation product, lactic acid, is a metabolite and can be easily eliminated from the human body *via* the Kreb's cycle.

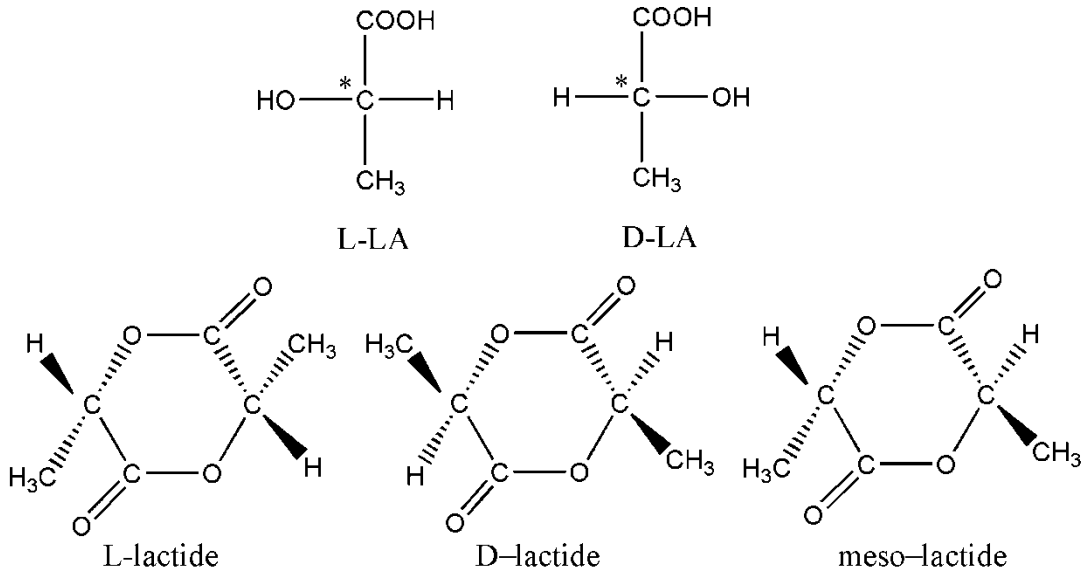

Scheme 1.3 Chemical structures of lactic acid enantiomers, and lactide diastereoisomers.

It should be noted that lactic acid is chiral molecule due to the presence of an asymmetric carbon atom, and thus exists in the form of L-lactic and D-lactic acid enantiomers. Similarly, the cyclic diester of lactic acid, lactide, exists in the form of three kinds of diastereoisomers, *i.e.* L-lactide, D-lactide and meso-lactide. In the case of LA-containing polymer chains, chirality of LA units provides a worthwide means to adjust the physical-chemical, biological and mechanical characteristics of polymers. The structure of various enantiomers and diastereoisomers of lactic acid and lactide is shown in Scheme 1.3.

Consequently, PLA exists in the form of poly(L-lactide) (PLLA), poly(D-lactide) (PDLA), and various stereocopolymers. In 1987, Ikada *et al.* first reported that physical interaction between PLLA and PDLA, namely stereocomplexation, strongly affects the crystallization behavior, thermal resistance, mechanical properties as well as the hydrolytic resistance of PLA based materials [111]. These improvements are due to the stronger interaction between L-LA and D-LA sequences. Novel stereocomplexation-induced micelles and hydrogels have been reported in the case of PLA/PEG block copolymers [86, 93, 112-114].

1.3.1.2 Poly(ethylene glycol)

Poly(ethylene glycol) (PEG), also as known as poly(ethylene oxide) (PEO) depending on the synthetic conditions, is a linear polyether terminated with hydroxyl end groups. PEG has been approved by the US Food and Drug Administration (FDA), and is probably the most widely applied synthetic polymer in the domains of biotechnology, pharmacology, and medicine [15, 100]. PEG is a cheap, neutral, water soluble and biocompatible polymer with good hydrolytic resistance. PEG generally has narrow molecular weight distributions which are readily accessible by anionic polymerization of ethylene oxide. The water solubility of PEG results from the strong tendency to form hydrogen bonds with water via -O- groups. The hydrophilic character with surface-wetting properties is especially important for the prevention of protein

adsorption and the blood compatibility in biomedical applications.

"Stealth" effect is a key property of PEG, which allows avoiding a fast recognition by the immune system followed by rapid clearance from the body. Chemical attachment of PEG to the drug of choice is a process called PEGylation [110]. The concept of PEGylation was first introduced by Davis *et al.* in 1970s [77]. Unexpected finding by PEGylation was observed, including improved pharmacokinetic and pharmacodynamic properties of polypeptide drugs due to increased water solubility, reduced renal clearance and toxicity. PEGylation reduces kidney clearance simply by making the molecules larger as the kidneys filter substances according to their size.

Studies of PEG in solution revealed that ethylene oxide subunit is tightly associated with two or three water molecules. This binding of water molecules makes PEGylated compounds function as though they are five to ten times larger compared to a soluble protein of similar molecular weight, as confirmed by size exclusion chromatography and gel electrophoresis [78, 115]. When attached to hydrophobic drugs or carriers, PEG provides them with good physical and thermal stability, preventing or reducing aggregation of drugs in storage and *in vivo* as a result of the steric hindrance. Therefore, PEG with associated water molecules behaves like a shield to protect the attached drug from enzymatic degradation, rapid renal clearance and interactions with cell surface proteins, thereby limiting adverse immunological effects.

PEGylated drugs are also more stable over a range of pH and temperature changes as compared to their unPEGylated counterparts. Consequently, PEGylation confers to drugs a number of clinical benefits, such as sustained blood levels that enhance the drug efficacy, fewer adverse reactions, longer shelf life and improved patient convenience [116]. The ability of PEGylation to influence the pharmacokinetic properties of drugs and drug carriers is widely utilized in pharmaceutics [77, 78, 117]. In fact, all polymer based stealth drug delivery systems that have been brought to the

market up to now contain PEGylated compounds and no other synthetic polymer has yet gained this statue [100].

1.3.1.3 PLA/PEG copolymers

PLA is highly hydrophobic, which considerably restricts its applications as a biomaterial. Thus, PLA/PEG block copolymers have drawn great attention since they combine the properties of both blocks, including the degradability and bioresorbability of PLA, hydrophilicity and renal filterability of PEG, and biocompatibility of both. Moreover, PEG chains present at the surface of biomaterials or drug carriers are particularly efficient for preventing the absorption of proteins and the adhesion of cells due to steric repulsion effects [118].

The synthesis of PLA can be realized either by ring-opening polymerization (ROP) of lactide or by polycondensation of lactic acid. The difference is that the former generally yields polymers with high molecular weights, whereas the latter results in low molecular weight oligomers. The synthesis of PLA/PEG block copolymers is usually realized by ROP of lactide in the presence of mono- or dihydroxyl PEG (Scheme 1.4). Various di- or triblock copolymers can be obtained with different PLA block lengths and chirality, and PEG block lengths.

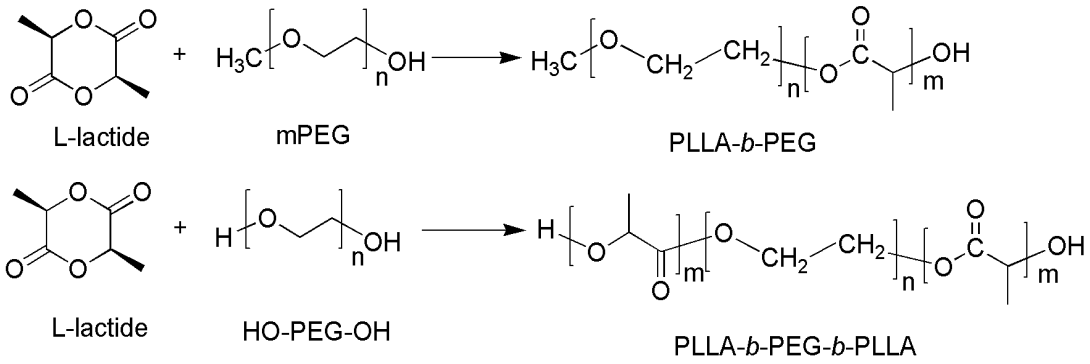

Scheme 1.4 Synthesis of PLA/PEG block copolymers by ring opening polymerization.

In the past decades, PLA/PEG copolymer micelles have been largely investigated as drug carrier [44, 119-121]. Anti-tumor drugs such as paclitaxel, beta-lapachone and doxorubicin have been loaded in PLA/PEG micelles [110, 122-124]. Currently, the most advanced micellar formulations encapsulating hydrophobic drugs such as doxorubicin and paclitaxel have already entered the market in India (Nanoxel®) and South Korea (Genexol-PM®) [104, 125]. Most recently, the first "active" docetaxel encapsulated PLA/PEG micelles (BIND-014®) with tumor target prostate specific membrane antigen (PSMA) has been approved in USA for the treatment of solid tumors and metastatic cancers [126]. The micelles present major advantages such as decreased side effects, better pharmacological profiles, and improved drug tolerance over the current clinical formulations.

Nevertheless, PEG/PLA micelles are not responsive to environment changes. In fact, many bioactive agents used in pharmacotherapy exhibit side effects that may affects the drug efficacy. For instance, compounds used for cancer therapy can kill not only cancer cells, but also normal cells in the body, which results in undesired side effects [87]. The EPR effect is considered as passive targeting method. Drug targeting could be further enhanced by introducing a polymeric matrix which is responsive to variation of temperature [127, 128].

1.3.2 Thermo-responsive PLA/PNIPAAm copolymers

1.3.2.1 Poly(*N*-isopropylacrylamide)

Poly(*N*-isopropylacrylamide) (PNIPAAm) is the most studied thermo-responsive polymer with a LCST at 32 ^{o}C where it exhibits a sharp phase transition from hydrophilic coils to hydrophobic globules [129]. Hydrogen bonding is formed between amide groups and water molecules in PNIPAAm solutions under the LCST. In contrast, the alkyl backbone and isopropyl groups present a competitive hydrophobic effect [129]. The phase transition, as shown in Scheme 1.5, is attributed

to the entropic gain since water molecules associated to the amide groups are released to the aqueous phase when the temperature increases above the LCST [130, 131].

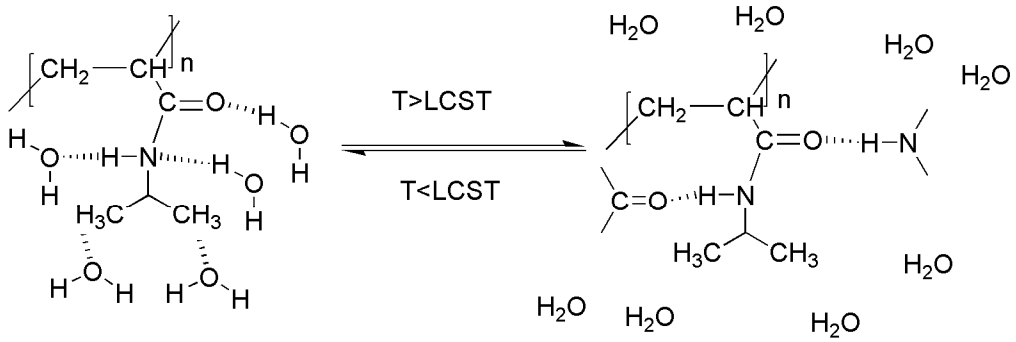

Scheme 1.5 Phase transition of PNIPAAm chains in response to temperature changes. From Ref. [131] with modification.

As suggested by Cho *et al.,* the phase transition of PNIPAAm across the LCST involves at least three phenomena: (i) rearrangement of bound water around either hydrophobic isopropyl or hydrophilic amide groups of PNIPAAm, (ii) intermolecular and intramolecular hydrogen bonding between the amide groups, and (iii) association of hydrophobic groups in PNIPAAm mainchains [132]. When increasing the temperature above the LCST, polymer-polymer interactions are thermo-dynamically favored as compared to polymer-water interactions. Water molecules around the hydrophilic groups also are released to the medium. The intermolecular and intramolecular interactions between PNIPAAm chains include not only hydrophobic association of the hydrophobic groups, but also hydrogen bonding between the amide groups. PNIPAAm chains thus become dehydrated globules in the form of a suspension.

In Ono's work, the number of water molecules per NIPAAm unit in homogeneous solution was determined to be 11 exactly below the LCST, employing the high-frequency dielectric relaxation technique [132]. Thus, PNIPAAm is regarded as a "golden standard" thermo-responsive polymer due to the fact that its LCST is relatively insensitive to physical and chemical environment [27]. Slight variations of

pH, concentration or chemical environment only affect the LCST of PNIPAAm by a few degrees [129].

PNIPAAm homopolymer was initially synthesized by free radical polymerization. It can be functionalized by reaction with chain transfer agents having functional acid, hydroxyl or amino groups [129]. Introduction of functional end groups could allow to improve the properties of polymers including thermo-sensitivity, pH sensitivity or fine tuning of the LCST. However, the molecular weight and dispersity of polymers were not controlled.

The atom transfer radical polymerization (ATRP) of NIPAAm was first reported by Masci *et al.* [133] using CuCl/tris(2-dimethylaminoethyl) amine (Me_6TREN) as a catalytic system. The polymerization was carried out in a DMF/water (50:50 v/v) solvent mixture at 20 ^{o}C. Kinetic studies showed that the reaction was of first order up to 92 % conversion at 35 minutes. Molecular weights up to 22000 and low dispersities ($Đ$ =1.19) were obtained. In addition, block copolymer of dimethylacrylamide (DMAAm) and NIPAAm was obtained by successive ATRP. Later, Ye *et al.* reported well controlled ATRP of NIPAAm using the same catalyst system in various aqueous solvent mixtures at room temperature and at 0 ^{o}C [134].

Generally, the ATRP in aqueous medium is fast and hardly controllable, which leads to polymers of relatively low molecular weights with broad molecular weight distributions. The lack of control could be attributed to the occurrence of side reactions. In particular, hydrolysis of the deactivator leads to faster polymerization and eventually loss of control. However, the ATRP of NIPAAm can be well controlled due to the high stability of the catalyst complex CuCl/Me_6TREN in water at low temperature (<50 ^{o}C).

Further modification of PNIPAAm by combination of controlled radical polymerization and click chemistry has also been investigated. Ooi *et al.* and Boere *et*

al. reported hydrogels with peptide based on PNIPAAm by combination of reversible addition-fragmentation chain transfer (RAFT) polymerization and click chemistry [135, 136]. De *et al*. reported block copolymers of NIPAAm and DMAAm by RAFT polymerization [137]. A biological ligand, folic acid, was then clicked on the copolymer chain ends. Pan *et al*. synthesized miktoarm star-shaped PNIPAAm-DNA by click chemistry [138]. The modification of PNIPAAm based polymers with target ligand and DNA could provide active targeting properties for anticancer applications.

1.3.2.2 PLA/PNIPAAm copolymers

PNIPAAm based polymers could be used for controlled delivery of anticancer drugs or DNA [139-146]. However, these polymers are hydrophilic and non degradable, which limits their potential applications as drug carrier. Block copolymers based on PNIPAAm and PLA combine both the thermo-sensitivity and hydrophilicity of PNIPAAm and the degradability and hydrophobicity of PLA [147-149]. Increasing the temperature above the LCST could result in collapse of micelles and burst-like release of encapsulated drug. Thus, targeted drug delivery could be achieved by using thermo-sensitive and partially degradable micelles prepared from PLA/PNIPAAm copolymers.

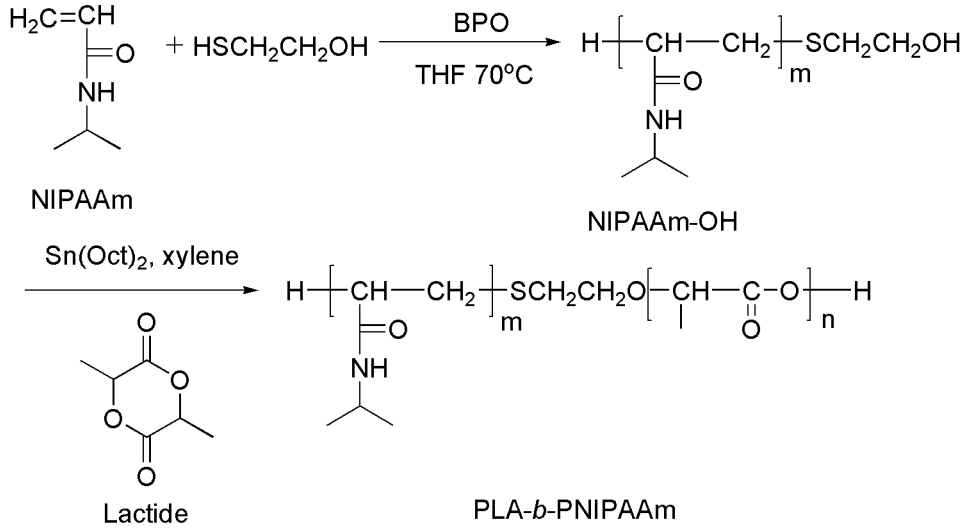

Scheme 1.6 Synthesis of PLA-*b*-PNIPAAm diblock copolymers by free radical polymerization and ring-opening polymerization.

In the past decades, most PLA/PNIPAAm block copolymers were prepared by combination of free radical polymerization and ring-opening polymerization (Scheme 1.6) [146-150]. First, hydroxyl-terminated PNIPAAm-OH was obtained by free radical polymerization of NIPAAm initiated by benzoyl peroxide (BPO), using 2-hydroxyethanethiol as chain transfer agent. Then, PNIPAAm-OH is used to initiate lactide polymerization using tin(II)2-ethylhexanoate ($Sn(Oct)_2$) as catalyst. However, the obtained copolymers have poorly controlled molecular weight with large dispersity ($Đ$>2), which leads to a broad phase transition at the LCST. Moreover, only PLA-*b*-PNIPAAm diblock copolymers could be obtained by this method.

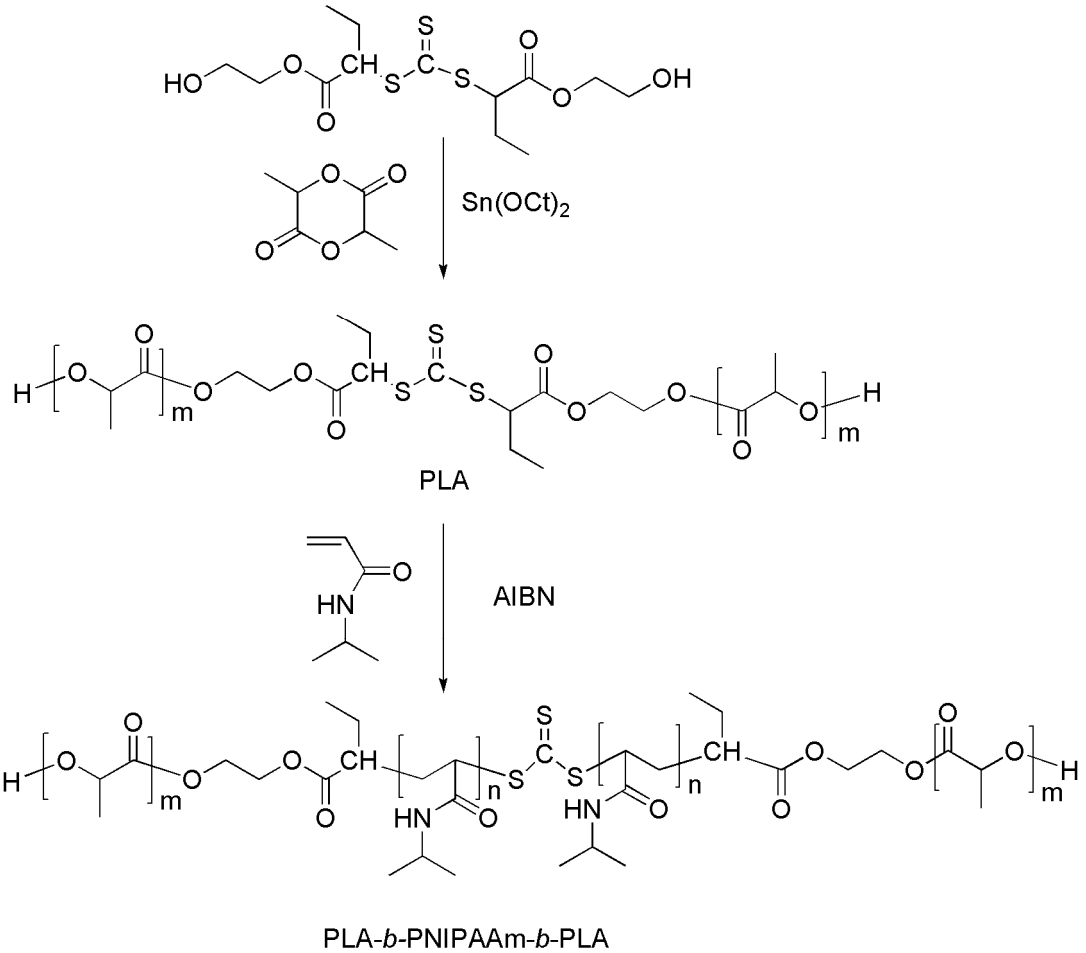

Scheme 1.7 Synthesis of PLA-*b*-PNIPAAm-*b*-PLA triblock copolymers by combination of ROP and RAFT polymerization. From Ref. [198].

Recently, living polymerization such as RAFT polymerization is also used to prepare PLA/PNIPAAm diblock or triblock copolymers [151, 152]. Hales *et al*. reported the synthsesis of PLA-*b*-PNIPAAm diblock copolymers by combination of ROP and RAFT polymerization. Well-defined architectures with narrow dispersities ($Đ < 1.54$) were obtained. [152]. You *et al*. reported the synthesis of PLA-*b*-PNIPAAm-*b*-PLA triblock copolymers using a similar route [198]. As shown in Scheme 1.7, PLA was first prepared from ROP of lactide initiated by a RAFT agent with hydroxyl end groups, using $Sn(Oct)_2$ as catalyst in toluene at 110 ^oC. Then RAFT reaction of NIPAAm was realized in THF at 100 ^oC using azobisisobutyronitrile (AIBN) as catalyst. Narrow molecular weight dispersity of 1.2 to 1.3 was obtained. Unfortunately, no data are available about the LCST of the obtained copolymers.

Thermo-responsive polymeric micelles are supposed to be soluble in blood stream and become insoluble after accumulation in a tumor with higher temperature due to fast metabolism [21]. Therefore, this property could be exploited for targeted delivery of anti-tumor drugs. In order to increase the LCST, another hydrophilic acrylamide comonomer, DMAAm was introduced in PNIPAAm chains [106, 153-156]. Akimoto *et al.* synthesized well-defined P(NIPAAm-*co*-DMAAm)-*b*-PLA diblock copolymers by combination of RAFT polymerization and ROP [157]. The terminal dithiobenzoate (DTBz) groups were reduced to thiol groups and reacted with maleimide (Mal). In aqueous medium, the resulting copolymers formed surface-functionalized thermo-responsive micelles, hydrophobic DTBz-surface micelles demonstrating a significant lower LCST at 30.7 °C while Mal-surface micelles has a higher LCST at 40.0 °C. Temperature induced intracellular uptake of micelles was also studied by Akimoto *et al*. [158, 159]. Improved micelle uptake was observed above the LCST probably due to the enhanced interactions between the cell membrane and micelles through dehydration of the micelle corona.

Thermo-responsive release of doxorubicin from P(NIPAAm-*co*-DMAAm)-*b*-PLA has been investigated by Kohori *et al*. [160]. No cytotoxicity of micelles was observed at 37 or 42.5 °C. Enhanced interactions between micelles and cells above the LCST seem to increase the incorporation rate of drug loaded micelles into cells. Liu *et al.* reported *in vitro* release of doxorubicin from poly(*N*-isopropylacrylamide-*co*-*N,N*-dimethylacrylamide)-*b*-poly(D,L-lactide -*co*-glycolide) [P(NIPAAm-*co*-DMAAm)-*b*-PLGA] micelles. Confocal laser scanning microscopy revealed that free drug molecules enter cell nuclei very fast, and that drug loaded micelles accumulate mostly in cytoplasm after endocytosis. At a temperature above the LCST, more drug molecules release from the micelles and enter the nuclei as compared to the case below the LCST. Drug loaded micelles exhibit greater cytotoxicity at a temperature above the LCST due to the collapse of micelles. Later, Li *et al*. reported similar maleimide end-functional P(NIPAAm-*co*-DMAAm)-*b*-PLA and poly(*N*-isopropylacrylamide-*co*-*N,N*-dimethylacrylamide-*b*-ε-caprolactone) (P(NIPAAm-co-DMAAm)-*b*-PCL) copolymers with LCST of 39 and 40.5 ^{o}C, respectively [108]. Doxorubicin was also used as model to investigate the drug release behavior. Comparing with the normal physiological conditions (pH=7.4, 37 ^{o}C), drug release and hydrophobic core degradation were obviously enhanced under simulated tumor tissue conditions (pH=5.3, T=40 ^{o}C). Both flow cytometry and fluorescent microscopy showed that doxorubicin released from micelles is about 4 times higher than that by the commercial formulation Taxotere®. *In vitro* cytotoxicity assay against N-87 cancer cell and confocal laser scanning microscopy (CLSM) also confirmed enhanced drug efficiency. However, the drug loading is quite low (<5 %). Besides, whether the drug release is controlled by thermo-responsive phase transition or degradation is uncertain. In fact, PLA shows faster degradation at pH=5.3 and 40 °C than at pH=7.4 and 37 °C.

1.3.3 Thermo-responsive copolymers from PLA/PEG analogues

1.3.3.1 PEG analogues

Recently, thermo-responsive polymers containing short oligo(ethylene glycol) side chains of different chain lengths were proposed as an attractive alternative to PNIPAAm [161-167]. These PEG analogues exhibit not only the properties such as hydrophilicity and biocompatibility, but also thermo-sensitivity. They are regarded as a new generation of "smart" biocompatible materials. Zhou *et al*. reported microgels based on oligo(ethylene glycol) methacrylate (OEGMA) for drug delivery applications. The microgels are nontoxic and released drug molecules remain active to kill cancer cells [168].

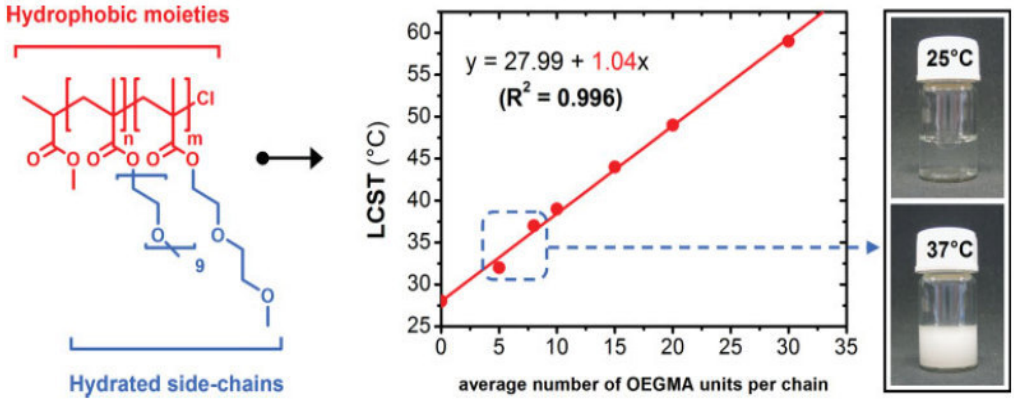

Figure 1.4 Lower critical solution temperature (LCST) of PEG analogues as a function of the content of OEGMA units per chain. From ref. [170].

PEG macromonomers, *i.e*. molecules composed of a polymerizable moiety connected to a short OEG chain were firstly reported by Neugebauer in 1980s [169]. Novel macromolecular architectures with PEG side chains were obtained. The significant advantage of PEG macromomomers is the possibility to access high molecular weight PEG based copolymers using mild conditions. Random copolymers of

2-(2-methoxyethoxy) ethyl methacrylate (MEO_2MA) and OEGMA (M_n=475) exhibit a LCST value between 26 and 90 °C, which could be precisely adjusted by varying the comonomer composition (Figure 1.4) [170]. For example, LCST values of either 32.8 °C (comparable to the standard LCST of PNIPAAm), 37.8 °C (body temperature) or 39–40.8 °C (fever temperatures) were obtained in pure water for copolymers possessing in average 5, 8, or 10% of OEGMA units, respectively.

The solubility of PEG analogues is dependent on the number of repeat units of PEG side chains. These non linear PEG analogues could be insoluble in water, or soluble up to 100 °C. Poly(2-methoxy ethyl) methacrylate (PMEOMA) with only 1 EO unit is not soluble in water at room temperature. PEG analogues with side chain length between 2 and 10 exhibit a LCST in aqueous solution. As the length increases, polymers derived from MEO_2MA, MEO_3MA and OEGMA (5 to 9 units) showed a LCST at 26, 52 and 60-90 °C, respectively [161, 171].

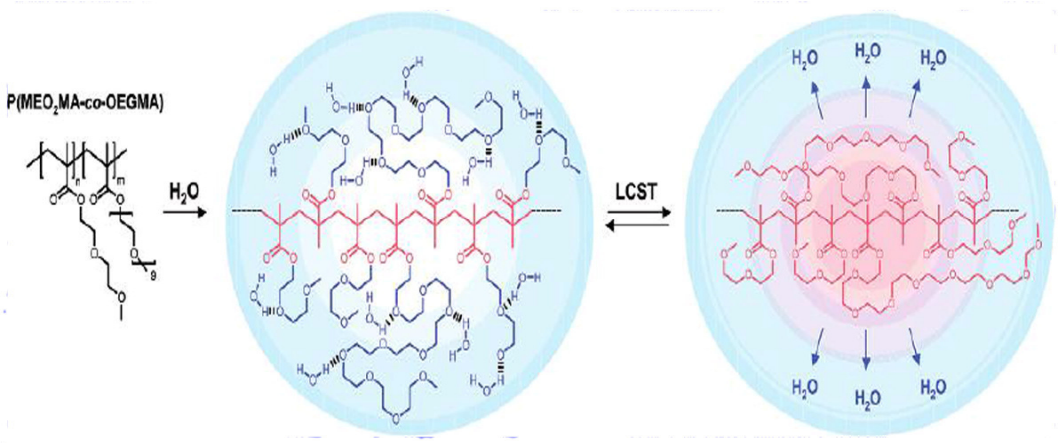

Scheme 1.8 Phase transition mechanism of PEG analogues in aqueous medium. From ref. [172].

In fact, similar to PNIPAAm, the phase transition is also related to the balance between hydrophilic and hydrophobic moieties in the macromolecular structures. As shown in Scheme 1.8, hydrogen bonding between the ether oxygen of PEG and surrounding water molecules is the driving force for the solubilization of PEG analogues at room temperature [172-174]. This solubilizing effect is counterbalanced

by the hydrophobicity of the apolar polymethacrylate (PMA) backbone.

The phase transition of PEG analogues is nearly reversible, whereas PNIPAAm exhibits a significant hysteresis (Figure 1.5) [175]. PNIPAAm shows a sharp phase transition when heated, and a broad hysteresis is observed at the cooling process. In fact, PNIPAAm chains become dehydrated globules above the LCST, where intramolecular and intermolecular hydrogen bonding is formed between the amide groups [176]. During the cooling process, the rehydration of PNIPAAm is hindered by hydrogen bonding, leading to a broad hysteresis. In the case of PEG analogues, polymer-polymer interactions in the globules are Van Der Waals forces which are weaker than hydrogen bonding, thus leading to a reversible phase transition behavior at the cooling cycle.

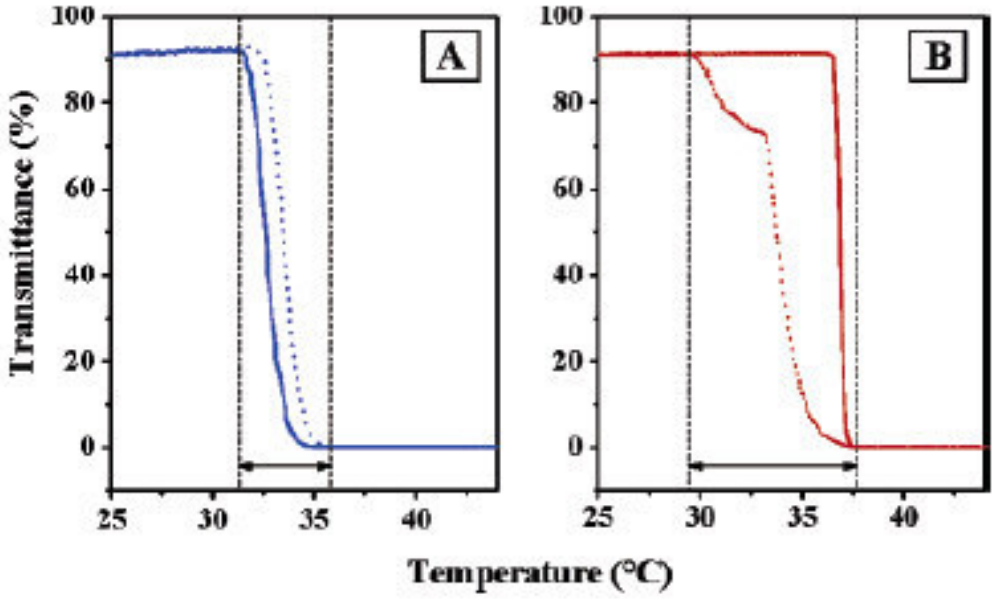

Figure 1.5 Plots of transmittance as a function of temperature of (A) P(MEO_2MA-*co*-OEGMA) containing 5 mol % of OEGMA, and (B) PNIPAAm in water at 3 mg mL^{-1} (solid line: heating, dashed line: cooling). From ref. [175].

Lutz *et al*. investigated the cytotoxicity of non linear PEG analogues in comparison with a commercial linear PEG (M_n = 20, 000) [170]. Figure 1.6 shows the metabolic cell viability measured for human hepatocellular carcinoma (HepG2) cell lines after

incubation at 37.8 ^{o}C in the presence of PEG and P(MEO_2MA-*co*-OEGMA) containing 10, 30 and 100 mol % of OEGMA. In all cases, *in vitro* cell assay demonstrates excellent cell viability, thus showing that PEG analogues are apparently not cytotoxic as linear PEG.

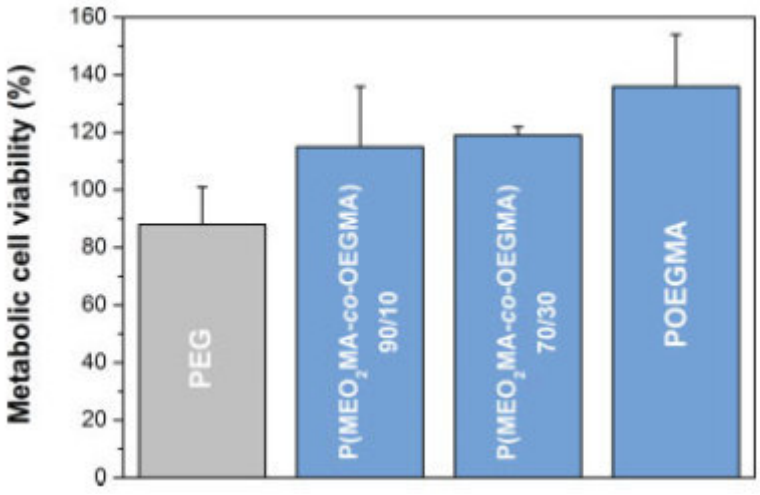

Figure 1.6 Metabolic cell viability measured for human hepatocellular carcinoma (HepG2) cell lines incubated at 37.8 ^{o}C in the presence of PEG and P(MEO_2MA-*co*-OEGMA)of various compositions. From ref. [170].

Free radical polymerization is the most versatile method for the synthesis of non-liner PEG analogues [169]. The resulting polymers could be promising for biomedical applications as they are principally composed of biocompatible OEG segments. However, the polymers prepared from radical polymerization are characterized by high dispersity with poorly controlled molecular weight and architecture.

Han *et al.* reported homopolymers and copolymers of MEO_2MA and MEO_3MA synthesized by living anionic polymerization [161]. The obtained polymers have narrow molecular weight distribution ($Đ$<1.1). The LCST tends to decrease with increasing the M_n of polymers. In addition, polymers with higher molecular weights exhibit sharper phase transition at the LCST, suggesting that longer polymer chains easily forms the intermolecular and intramolecular aggregation at lower temperature, which results in faster phase separation.

PEG analogues have also been synthesized by RAFT polymerization in aqueous medium [171, 177, 178]. Linear first order kinetics are obtained for both POEGMA and P(MEO_2MA–*co*-OEGMA) with well-defined chain structures and dispersity below 1.3. Nitroxide mediated polymerization (NMP) was initially considered to be unsuitable for polymerization of MEO_2MA or OEGMA due to the occurrence of irreversible termination reactions [179]. Recently, Nicolas *et al*. developed a very simple and efficient method to synthesize PEG analogues by NMP using *N*-tert-butyl-*N*-(1-diethylphosphono-2,2-dimethylpropyl) nitroxide (SG1) as transfer agent in the presence of a small amount of acrylonitrile [180]. The authors also reported the synthesis of degradable and comb-like PEG-based copolymers by nitroxide-mediated radical ROP [181]. The limitation of NMP of MEO_2MA or OEGMA has been solved by adding a small amount of an appropriate comonomer (acrylonitrile, <10 mol%), which leads to a dramatic decrease of the average activation−deactivation equilibrium rate constant and allows high monomer conversions to obtain well-defined MEO_2MA and OEGMA homopolymers and copolymers ($Đ$<1.4).

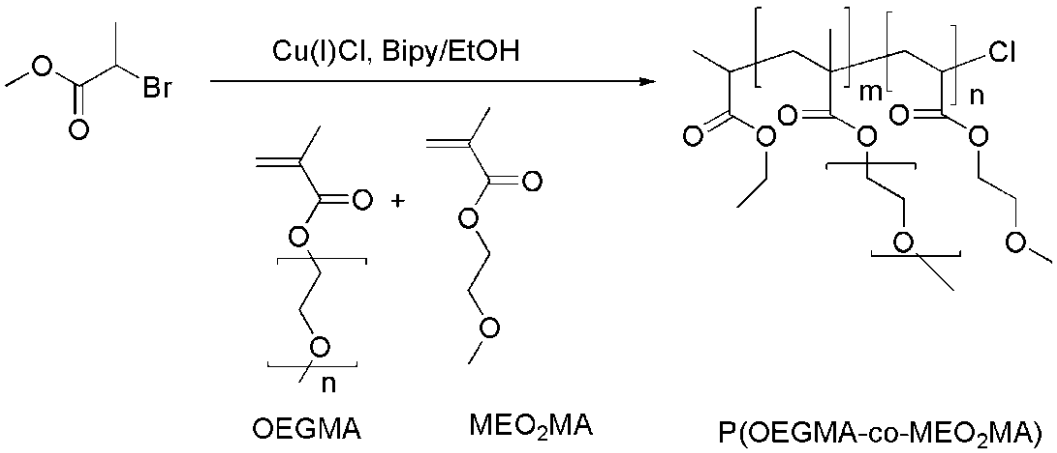

Scheme 1.9 Synthesis of PEG analogues by ATRP of OEGMA and MEO_2MA. From ref. [172].

The ATRP of OEGMA (DP_{OEG}=7 or 8) was first reported by Wang *et al*. in aqueous medium at room temperature [182, 183]. The resulting polymers have narrow

molecular weight distribution. Matyjaszewski *et al*. investigated the successive ATRP of MEO_2MA and MEO_3MA in toluene or anisole solution [184, 185]. Recently, Lutz *et al.* obtained well-defined thermo-responsive P(MEO_2MA-*co*-OEGMA) copolymers by ATRP in pure ethanol at 60 ^oC (Scheme 1.9) [170, 186, 187].

PEG analogues could be further modified by "click chemistry" (Scheme 1.10) [188, 189]. Well-defined POEGMA synthesized by ATRP could be post-functionalized via copper catalyzed 1, 3-dipolar cycloaddition. In fact, the bromine chain-ends of POEGMA can be transformed into azide groups and subsequently reacts with alkynes. For example, click chemistry can be used for the reaction of POEGMA with functional biopolymers such as oligopeptides [190]. In addition, target molecules such as folic acid could also be clicked on POEGMA using this method [191, 192].

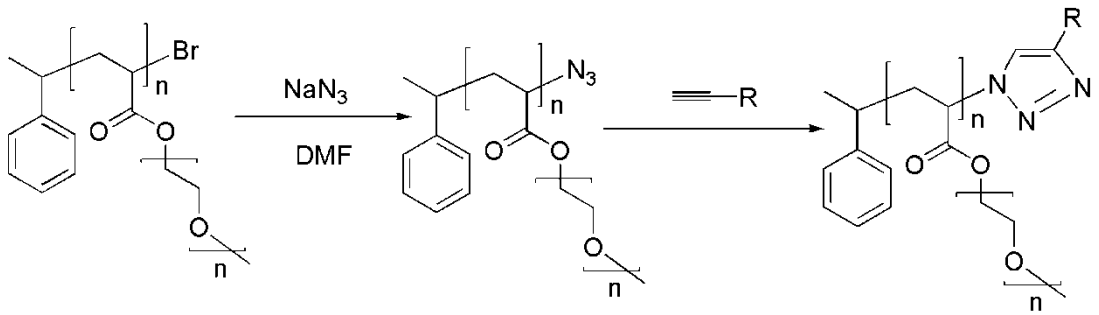

Scheme 1.10 Strategy for the functionalization of well-defined POEGMA using click chemistry. From ref. [193].

1.3.3.2 PLA/PEG analogues block copolymer

Although the hydrophilic/hydrophobic balance exists in the case of PEG analogues, whether the polymers can induce aggregation such as micelles in water still remains controversial. Ito *et al*. reported that PEG analogues generally adopt a compact coil conformation in water. Fluorimetry studies suggest micelle formation of PEG analogues in water due to weak hydrophobic interactions [193-195].

In the case of P(OEGMA-*co*-MEO_2MA) copolymers, the bimodal Dynamic laser

scattering (DLS) intensity distribution indicated coexistence of free polymer coils of 3.7 nm and larger aggregates of 150 nm (Figure 1.7). However, the latter are indeed a negligible minority, *i.e.* less than 0.01 % of the overall volume distribution (Figure 1.7B). These findings confirm that the conformation of P(OEGMA-*co*-MEO_2MA) is predominantly random coil in water. Hence, hydrophobic blocks should be introduced in PEG analogue chains so as to obtain amphiphilic copolymers for applications in the field of drug delivery.

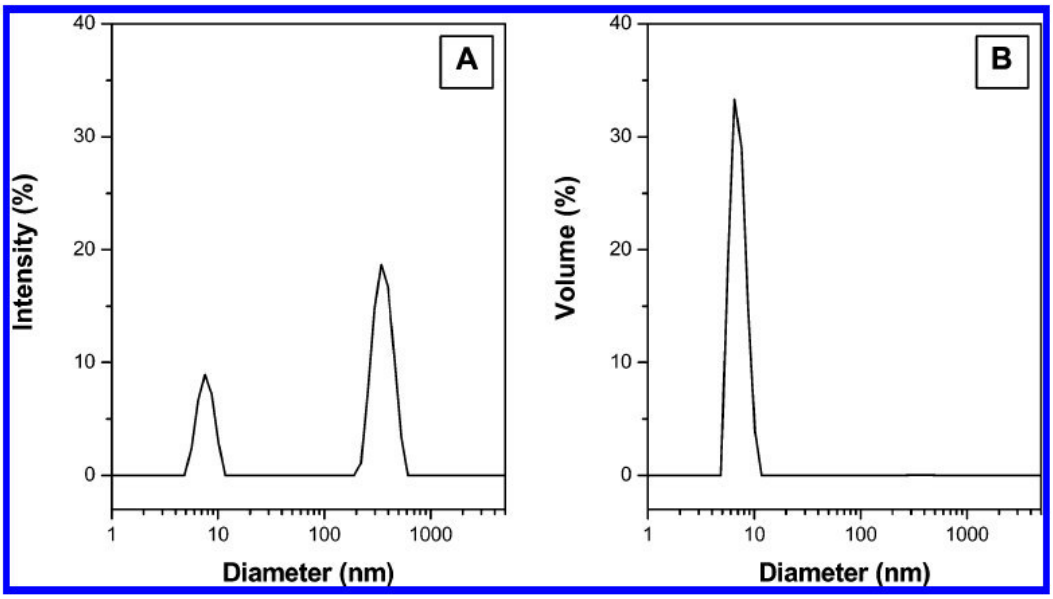

Figure 1.7 Intensity size distribution (A) and volume size distribution (B) of P(MEO_2MA-*co*-OEGMA) determined by DLS at room temperature at 3 mg mL^{-1} in aqueous solution. From ref. [172].

Saeed prepared PLGA-*b*-OEGMA copolymers by combining ROP and RAFT polymerization [196]. The resulting copolymers self-assembled to form micelles able to encapsulate carboxyfluorescein and fluorescein isothiocyanate as model of hydrophobic drugs. Selected copolymer micelles were incubated with 3T3 fibroblasts as a model cell line, and were rapidly taken up as indicated by fluorescence microscopy assays. Later on, Luzon *et al.* obtained POEGMA-*b*-PCL-*b*-POEGMA triblock copolymers by ATRP, using α,ω-bromopropionyl Br-PCL-Br as macroinitiator [197]. The CMC and critical micelle temperature (CMT) were

determined. Self-assembly is temperature and concentration dependent. Decrease of the CMT is observed as the concentration increases. The same synthetic route was adopted by Bakkour *et al*. for the synthesis of POEGMA-*b*-PLLA-*b*-POEGMA triblock copolymers [198]. The self-assembly and drug encapsulation potential of the copolymers were reported. Most recently, Fenyves *et al*. synthesized amphiphilic bottlebrush block copolymers containing PLA and PEG side chains using a grafting-from method, and studied their self-assembly in aqueous medium [199]. Spherical, cylindrical micelles as well as bilayer structures were observed. However, the copolymers shown above exhibit very high LCST (>80 °C) and no drug release was reported.

1.4 Summary and work plan

PLA/PEG amphiphilic copolymer micelles have been widely studied for biomedical applications due to the passive targeted drug delivery by the EPR effect. However, these micelles present no active stimuli response to environmental changes. The ideal intelligent drug carrier should be stimuli responsive to the tumor so as to improve the drug efficacy. It is well known that fast metabolism of tumor cells after mutation makes the tumor issue very different from normal tissues with higher temperature (~42 ^{o}C), lower pH (pH~5.3) and anomalistic vessel (intercellular gap junction= 300-700 nm) [15, 200]. Therefore, novel thermo-responsive micelles based on PNIPAAm or PEG analogues have drawn much attention for active targeted delivery of anti-tumor drugs. However, only PLA-*b*-PNIPAAm diblock copolymers were obtained from combination of ROP and radical polymerization, and few PLA-*b*-PNIPAAm-*b*-PLA triblock copolymers were prepared from combination of ROP and RAFT polymerization. Moreover, the LCST of these copolymers could not be precisely controlled around the body temperature, which limits the potential applications in targeted drug delivery.

Herein, in this work, PNIPAAm-*b*-PLLA-*b*-PNIPAAm triblock copolymers are first prepared by combination of ROP and ATRP, using a Br-PLLA-Br macroinitiator. Then, a comonomer, DMAAm, is introduced to copolymer chains in order to increase and precisely adjust the LCST of the resulting P(NIPAAm-co-DMAAm)-*b*-PLLA-*b*-P(NIPAAm-*co*-DMAAm) copolymers. The physico-chemical properties of the various copolymers and self-assembly behavior are fully characterized by NMR, SEC, UV, DLS and TEM, *etc*. An anticancer drug, curcumin, is used as model drug to monitor the drug encapsulation and release properties of micelles under physiological conditions.

In the case of thermo-responsive PLA/PEG analogues reported in literature, the LCST is much higher than the body temperature. Moreover, to the best of our knowledge, no drug release data are available for these micelles. In this contribution, P(OEGMA-*co*-MEO_2MA)-*b*-PLLA-*b*-P(OEGMA-*co*-MEO_2MA) triblock copolymers are prepared by combination of ROP and ATRP, using the same Br-PLLA-Br macroinitiator. The self-assembly and drug release properties are also investigated. Thus, this work should allow to evaluate the potential of two different thermo-responsive systems for targeted delivery of anti-tumor drugs.

1.5 References

[1] B. W. Stewart, C. P. Wild, World Cancer Report 2014 IARC Nonserial Publication (2014).
[2] P. Ehrlich, The collected papers of paul Ehrlich. pergamon, London (1960).
[3] S. K. Sahoo, V. Labhasetwar, Nanotech approaches to drug delivery and imaging. Drug Discov. Today 8 (2003) 1112-1120.
[4] P. Couvreur, C. Vauthier, Nanotechnology: Intelligent design to treat complex disease. Pharm. Res. 23 (2006) 1417-1450.
[5] D. Peer, J. M. Karp, S. Hong, O. C. FaroKhzad, R. Margalit, R. Langer, Nanocarriers as an emerging platform for cancer therapy. Nat. Nanotechnol. 2 (2007) 751-760.
[6] M. Sun, X. Su, B. Y. Ding, X. L. He, X. J. Liu, A. H. Yu, H. X. Lou, G. X. Zhai, Advances in nanotechnology-based delivery systems for curcumin. Nanomedicine 7 (2012) 1085-1100.
[7] M. Beija, R. Salvayre, N. Lauth-de Viguerie, J. D. Marty, Colloidal systems for drug delivery: from design to therapy. Trends Biotechnol. 30 (2012) 485-496.

[8] N. Bertrand, J. Wu, X. Y. Xu, N. Kamaly, O. C. Farokhzad, Cancer nanotechnology: The impact of passive and active targeting in the era of modern cancer biology. Adv. Drug Deliv. Rev. 66 (2014) 2-25.
[9] F. Danhier, O. Feron, V. Prat, To exploit the tumor microenvironment: Passive and active tumor targeting of nanocarriers for anti-cancer drug delivery. J. Controlled Release 148 (2010) 135-146.
[10] H. Hillaireau, P. Couvreur, Nanocarriers' entry into the cell: relevance to drug delivery. Cell. Mol. Life Sci. 66(17) (2009) 2873-2896.
[11] B. Haley, E. Frenkel, Nanoparticles for drug delivery in cancer treatment. Urol. Oncol.-Semin. Orig. Investig. 26(1) (2008) 57-64.
[12] H. Maeda, G. Y. Bharate, J. Daruwalla, Polymeric drugs for efficient tumor-targeted drug delivery based on EPR-effect. Eur. J. Pharm. Biopharm. 71 (2009) 409-419.
[13] H. Maeda, T. Sawa, T. Konno, Mechanism of tumor-targeted delivery of macromolecular drugs, including the EPR effect in solid tumor and clinical overview of the prototype polymeric drug SMANCS. J. Controlled Release 74 (2001) 47-61.
[14] A. K. Iyer, G. Khaled, J. Fang, H. Maeda, Exploiting the enhanced permeability and retention effect for tumor targeting. Drug Disco. Today 11 (2006) 812-818.
[15] R. Duncan, The dawning era of polymer therapeutics. Nat Rev Drug Discov. 2 (2003) 347-360.
[16] J. H. Woodland, S. Yolles, Long-acting delivery systems For Narcotic Antagonists.1. J. Med. Chem. 16(8) (1973) 897-901.
[17] S. Yolles, T. D. Leafe, J.H. Woodland, F. J. Meyer, Long-acting delivery systems For Narcotic Antagonists 2. Release rates of naltrexone from poly(lactic acid) Composites. J. Pharm. Sci. 64 (1975) 348-349.
[18] T. M. Allen, P. R. Cullis, Drug delivery systems: Entering the mainstream. Science 303 (2004) 1818-1822.
[19] R. Langer, Drug delivery and targeting. Nature 392 (1998) 5-10.
[20] K. E. Uhrich, S. M. Cannizzaro, R. S. Langer, K. M. Shakesheff, Polymeric Systems for Controlled Drug Release. Chem. Rev.99 (1999) 3181-3198.
[21] A. Chilkoti, M. R. Dreher, D. E. Meyer, D. Raucher, Targeted drug delivery by thermally responsive polymers. Adv. Drug Deliv. Rev. 54 (2002) 613-630.
[22] A. K. Bajpai, S. K. Shukla, S. Bhanu, S. Kankane, Responsive polymers in controlled drug delivery. Prog. Polym. Sci. 33 (2008) 1088-1118.
[23] S. Ganta, H. Devalapally, A. Shahiwala, M. Amiji, A review of stimuli-responsive nanocarriers for drug and gene delivery. J. Control. Release 126 (2008) 187-204.
[24] V. P. Torchilin, Multifunctional nanocarriers. Adv. Drug Deliv. Rev. 58 (2006) 1532-1555.
[25] D. Schmaljohann, Thermo- and pH-responsive polymers in drug delivery. Adv. Drug Deliv. Rev. 58 (2006) 1655-1670.
[26] C. D. H. Alarcon, S. Pennadam, C. Alexander, Stimuli responsive polymers for biomedical applications. Chem. Soc. Rev. 34 (2005) 276-285.
[27] E. S. Gil, S. M. Hudson, Stimuli-reponsive polymers and their bioconjugates. Prog. Polym. Sci. 29((2004) 1173-1222.
[28] F. H. Meng, Z. Y. Zhong, J. Feijen, Stimuli-Responsive Polymersomes for Programmed

Drug Delivery. Biomacromolecules 10 (2009) 197-209.
[29] N. Rapoport, Physical stimuli-responsive polymeric micelles for anti-cancer drug delivery. Prog. Polym. Sci. 32 (2007) 962-990.
[30] D. Roy, W. L. A. Brooks, B. S. Sumerlin, New directions in thermoresponsive polymers. Chem. Soc. Rev. 42 (2013) 7214-7243.
[31] I. S. Kim, Y. I. Jeong, C. S. Cho, S. H. Kim, Thermo-responsive self-assembled polymeric micelles for drug delivery in vitro. Inter.l J. Pharm. 205 (2000) 165-172.
[32] G, Gregoria, E. J. Wills, C. P. Swain, A. S. Tavill, Drug carrier potential of liposomes in cancer chemotherap. Lancet 1 (1974) 1313-1316.
[33] W. E. Bawarski, E. Chidlowsky, D. J. Bharali, S. A. Mousa, Emerging nanopharmaceuticals. Nanomed. Nanotechnol. Biol. Med. 4 (2008) 273-282.
[34] A. Bochot, E. Fattal, Liposomes for intravitreal drug delivery: A state of the art. J. Controlled Release 161 (2012) 628-634.
[35] D. J. Bharali, S. A. Mousa, Emerging nanomedicines for early cancer detection and improved treatment: Current perspective and future promise. Pharmacol. Ther. 128(2) (2010) 324-335.
[36] T. Lammers, F. Kiessling, W. E. Hennink, G. Storm, Nanotheranostics and Image-Guided Drug Delivery: Current Concepts and Future Directions. Molecular Pharmaceutics 7(6) (2010) 1899-1912.
[37] R. B. Campbell, D. Fukumura, E. B. Brown, L. M. Mazzola, Y. Izumi, R. K. Jain, V. P. Torchilin, L. L. Munn, Cationic charge determines the distribution of liposomes between the vascular and extravascular compartments of tumors. Cancer Res. 62 (2002) 6831-6836.
[38] B. Mishra, B. B. Patel, S. Tiwari, Colloidal nanocarriers: a review on formulation technology, types and applications toward targeted drug delivery. Nanomedicine: Nanotechnology, Biology and Medicine 6 (2009) 9-24.
[39] S. Unezaki, K. Maruyama, O. Ishida, A. Suginaka, J. Hosoda, M. Iwatsuru, Enhanced tumor targeting and improved antitumor activity of doxorubicin by long-circulating liposomes containing amphipathic poly(ethylene glycol). Inter. J. Pharm. 126 (1995) 41-48.
[40] T. Daemen, J. Regts, M. Meesters, M. T. TenKate, I. BakkerWoudenberg, G. L. Scherphof, Toxicity of doxorubicin entrapped within long-circulating liposomes. J. Controlled Release 44 (1997) 1-9.
[41] C. J. F. Rijcken, O. Soga, W. E. Hennink, C. F. van Nostrum, Triggered destabilisation of polymeric micelles and vesicles by changing polymers polarity: An attractive tool for drug delivery. J. Controlled Release 120 (2007) 131-148.
[42] K. K. Upadhyay, A. N. Bhatt, A. K. Mishra, B. S. Dwarakanath, S. Jain, C. Schatz, J. F. Le Meins, A. Farooque, G. Chandraiah, A. K. Jain, A. Misra, S. Lecommandoux, The intracellular drug delivery and anti tumor activity of doxorubicin loaded poly(gamma-benzyl L-glutamate)-*b*-hyaluronan polymersomes. Biomaterials 31 (2010) 2882-2892.
[43] D. E. Discher, A. Eisenberg, Polymer vesicles. Science 297 (2002) 967-973.
[44] F. Ahmed, D. E. Discher, Self-porating polymersomes of PEG-PLA and PEG-PCL: hydrolysis-triggered controlled release vesicles. J. Controlled Release 96 (2004) 37-53.
[45] K. Kita-Tokarczyk, J. Grumelard, T. Haefele, W. Meier, Block copolymer vesicles using concepts from polymer chemistry to mimic biomembranes. Polymer 46 (2005) 3540-3563.
[46] M. Massignani, H. Lomas, G. Battaglia, Modern Techniques for Nano- and

Microreactors/-Reactions, Springer-Verlag Berlin, Berlin,Vol. 229, (2010) pp. 115-154.
[47] R. P. Brinkhuis, F. Rutjes, J. C. M. van Hest, Polymeric vesicles in biomedical applications. Polym. Chem. 2 (2011) 1449-1462.
[48] S. L. Li, B. Byrne, J. Welsh, A. F. Palmer, Self-assembled poly(butadiene)-*b*-poly(ethylene oxide) polymersomes as paclitaxel carriers. Biotechnol. Prog. 23 (2007) 278-285.
[49] F. Ahmed, R. I. Pakunlu, A. Brannan, F. Bates, T. Minko, D. E. Discher, Biodegradable polymersomes loaded with both paclitaxel and doxorubicin permeate and shrink tumors, inducing apoptosis in proportion to accumulated drug. J. Controlled Release 116 (2006) 150-158.
[50] C. Sanson, C. Schatz, J. F. Le Meins, A. Soum, J. Thevenot, E. Garanger, S. Lecommandoux, A simple method to achieve high doxorubicin loading in biodegradable polymersomes. J. Controlled Release 147 (2010) 428-435.
[51] M. Marguet, L. Edembe, S. Lecommandoux, Polymersomes in Polymersomes: Multiple Loading and Permeability Control. Angew. Chem.-Int. Edit. 51(5) (2012) 1173-1176.
[52] D. M. Saylor, C. S. Kim, D. V. Patwardhan, J. A. Warren, Diffuse-interface theory for structure formation and release behavior in controlled drug release systems. Acta Biomaterialia 3 (2007) 851-864.
[53] J. S. Lee, J. Feijen, Polymersomes for drug delivery: Design, formation and characterization. J. Controlled Release 161 (2012) 473-483.
[54] A. Mecke, C. Dittrich, W. Meier, Biomimetic membranes designed from amphiphilic block copolymers. Soft Matter 2 (2006) 751-759.
[55] W. Chen, F. H. Meng, R. Cheng, Z. Y. Zhong, pH-Sensitive degradable polymersomes for triggered release of anticancer drugs: A comparative study with micelles. J. Controlled Release 142 (2010) 40-46.
[56] Y. F. Du, W. Chen, M. Zheng, F. H. Meng, Z.Y. Zhong, pH-sensitive degradable chimaeric polymersomes for the intracellular release of doxorubicin hydrochloride. Biomaterials 33 (2012) 7291-7299.
[57] S. B. Lecommandoux, O. Sandre, F. Checot, J. Rodriguez-Hernandez, R. Perzynski, Magnetic nanocomposite micelles and vesicles. Adv. Mater. 17 (2005) 712-+.
[58] X. Tong, G. Wang, A. Soldera, Y. Zhao, How can azobenzene block copolymer vesicles be dissociated and reformed by light? J. Phys. Chem. B 109 (2005) 20281-20287.
[59] S. H. Qin, Y. Geng, D. E. Discher, S. Yang, Temperature-controlled assembly and release from polymer vesicles of poly(ethylene oxide)-block-poly(*N*-isopropylacrylamide). Adv. Mater. 18 (2006) 2905-2909.
[60] O. Onaca, R. Enea, D. W. Hughes, W. Meier, Stimuli-Responsive Polymersomes as Nanocarriers for Drug and Gene Delivery. Macromol. Biosci. 9 (2009) 129-139.
[61] W. Agut, A. Brulet, C. Schatz, D. Taton, S. Lecommandoux, pH and Temperature Responsive Polymeric Micelles and Polymersomes by Self-Assembly of Poly[2-(dimethylamino)ethyl methacrylate]-*b*-Poly(glutamic acid) Double Hydrophilic Block Copolymers. Langmuir 26 (2010) 10546-10554.
[62] H. De Oliveira, J. Thevenot, S. Lecommandoux, Smart polymersomes for therapy and diagnosis: fast progress toward multifunctional biomimetic nanomedicines. Wiley Interdiscip. Rev.-Nanomed. Nanobiotechnol. 4 (2012) 525-546.

[63] H. Oliveira, E. Perez-Andres, J. Thevenot, O. Sandre, E. Berra, S. Lecommandoux, Magnetic field triggered drug release from polymersomes for cancer therapeutics. J. Controlled Release 169 (2013) 165-170.
[64] L. Pourtau, H. Oliveira, J. Thevenot, Y. L. Wan, A. R. Brisson, O. Sandre, S. Miraux, E. Thiaudiere, S. Lecommandoux, Antibody-Functionalized Magnetic Polymersomes: In vivo Targeting and Imaging of Bone Metastases using High Resolution MRI. Adv. Healthc. Mater. 2 (2013) 1420-1424.
[65] C. Sanson, O. Diou, J. Thevenot, E. Ibarboure, A. Soum, A. Brulet, S. Miraux, E. Thiaudiere, S. Tan, A. Brisson, V. Dupuis, O. Sandre, S. Lecommandoux, Doxorubicin Loaded Magnetic Polymersomes: Theranostic Nanocarriers for MR Imaging and Magneto-Chemotherapy. ACS Nano 5 (2011) 1122-1140.
[66] J. Thevenot, H. de Oliveira, O. Sandre, L. Pourtau, E. Andres, S. Miraux, E. Thiaudiere, E. Berra, S. Lecommandoux, Multifunctional polymersomes for cancer theranostics. J. Controlled Release 172 (2013) E44-E45.
[67] J. Huang, C. Bonduelle, J. Thevenot, S. Lecommandoux, A. Heise, Biologically Active Polymersomes from Amphiphilic Glycopeptides. J. Am. Chem. Soc. 134 (2012) 119-122.
[68] E. Garanger, S. Lecommandoux, Towards Bioactive Nanovehicles Based on Protein Polymers. Angew. Chem.-Int. Edit. 51 (2012) 3060-3062.
[69] M. Marguet, O. Sandre, S. Lecommandoux, Polymersomes in "Gelly" Polymersomes: Toward Structural Cell Mimicry. Langmuir 28 (2012) 2035-2043.
[70] M. Chemin, P. M. Brun, S. Lecommandoux, O. Sandre, J. F. Le Meins, Hybrid polymer/lipid vesicles: fine control of the lipid and polymer distribution in the binary membrane. Soft Matter 8 (2012) 2867-2874.
[71] J. F. Le Meins, C. Schatz, S. Lecommandoux, O. Sandre, Hybrid polymer/lipid vesicles: state of the art and future perspectives. Mater. Today 16 (2014) 397-402.
[72] A. Kumari, S. K. Yadav, S. C. Yadav, Biodegradable polymeric nanoparticles based drug delivery systems. Colloid Surf. B-Biointerfaces 75 (2010) 1-18.
[73] P. Anand, H.B. Nair, B. Sung, A.B. Kunnumakkara, V.R. Yadav, R.R. Tekmal, B.B. Aggarwal, Design of curcumin-loaded PLGA nanoparticles formulation with enhanced cellular uptake, and increased bioactivity in vitro and superior bioavailability in vivo. Biochem. Pharma. 79 (2009) 330-338.
[74] P. Couvreur, Nanoparticles in drug delivery: Past, present and future. Adv. Drug Deliv. Rev. 65 (2012) 21-23.
[75] S. Parveen, R. Misra, S.K. Sahoo, Nanoparticles: a boon to drug delivery, therapeutics, diagnostics and imaging. Nanomed.: Nanotech., Biology and Medicine 8 (2011) 147-166.
[76] H. D. Tang, C. J. Murphy, B. Zhang, Y. Q. Shen, M. H. Sui, E. A. Van Kirk, X. W. Feng, W. J. Murdoch, Amphiphilic curcumin conjugate-forming nanoparticles as anticancer prodrug and drug carriers: in vitro and in vivo effects. Nanomedicine 5 (2010) 855-865.
[77] J. M. Harris, R. B. Chess, Effect of pegylation on pharmaceuticals. Nat. Rev. Drug Discov. 2 (2003) 214-221.
[78] G. Molineux, Pegylation: engineering improved pharmaceuticals for enhanced therapy. Cancer Treat. Rev. 28 (2002) 13-16.
[79] A. H. Faraji, P. Wipf, Nanoparticles in cellular drug delivery. Bioorg. Med. Chem. 17 (2009) 2950-2962.

[80] H. Bader, H. Ringsdorf, B. Schmidt, Watersoluble polymer medicine. Angew. Makromol. Chem. 123 (1984) 457-485.
[81] G. S. Kwon, K. Kataoka, Block-copolymer micelles as long-circulating drug vesicles. Adv. Drug Deliv. Rev. 16 (1995) 295-309.
[82] M. C. Jones, J. C. Leroux, Polymeric micelles - a new generation of colloidal drug carriers. Eur. J. Pharm. Biopharm. 48 (1999) 101-111.
[83] K. Letchford, H. Burt, A review of the formation and classification of amphiphilic block copolymer nanoparticulate structures: micelles, nanospheres, nanocapsules and polymersomes. Eur. J. Pharm. Biopharm. 65 (2007) 259-269.
[84] K. Kataoka, A. Harada, Y. Nagasaki, Block copolymer micelles for drug delivery: design, characterization and biological significance. Adv. Drug Deliv. Rev. 47 (2001) 113-131.
[85] M. L. Adams, A. Lavasanifar, G. S. Kwon, Amphiphilic block copolymers for drug delivery. Journal of Pharmaceutical Sciences 92 (2003) 1343-1355.
[86] B. Jeong, Y. H. Bae, D. S. Lee, S. W. Kim, Biodegradable block copolymers as injectable drug-delivery systems. Nature 388 (1997) 860-862.
[87] A. Rosler, G. W. M. Vandermeulen, H. A. Klok, Advanced drug delivery devices via self-assembly of amphiphilic block copolymers. Adv. Drug Deliv. Rev. 53 (2001) 95-108.
[88] G. Gaucher, M. H. Dufresne, V. P. Sant, N. Kang, D. Maysinger, J. C. Leroux, Block copolymer micelles: preparation, characterization and application in drug delivery. J. Controlled Release 109 (2005) 169-188.
[89] C. O. Rangel-Yagui, A. Pessoa, L. C. Tavares, Micellar solubilization of drugs. J. Pharm. Pharm. Sci. 8 (2005) 147-163.
[90] Y. Tian, S. R. Mao, Amphiphilic polymeric micelles as the nanocarrier for peroral delivery of poorly soluble anticancer drugs. Expert Opin. Drug Deliv. 9 (2012) 687-700.
[91] Y. Yu, X. L. Zhang, L. Y. Qiu, The anti-tumor efficacy of curcumin when delivered by size/charge-changing multistage polymeric micelles based on amphiphilic poly(beta-amino ester) derivates. Biomaterials 35 (2014) 3467-3479.
[92] L. Yang, X. H. Wu, F. Liu, Y. R. Duan, S. M. Li, Novel Biodegradable Polylactide/poly(ethylene glycol) Micelles Prepared by Direct Dissolution Method for Controlled Delivery of Anticancer Drugs. Pharm. Res. 26 (2009) 2332-2342.
[93] L. Yang, X. Qi, P. Liu, A. El Ghzaoui, S. M. Li, Aggregation behavior of self-assembling polylactide/poly(ethylene glycol) micelles for sustained drug delivery. Inter. J. Pharm. 394 (2010) 43-49.
[94] U. Kedar, P. Phutane, S. Shidhaye, V. Kadam, Advances in polymeric micelles for drug delivery and tumor targeting. Nanomed.: Nanotech., Biology and Medicine 6 (2010) 714-729.
[95] Y. Yan, G. K. Such, A. P. R. Johnston, J. P. Best, F. Caruso, Engineering Particles for Therapeutic Delivery: Prospects and Challenges. ACS Nano 6 (2012) 3663-3669.
[96] C. Oerlemans, W. Bult, M. Bos, G. Storm, J. F. Nijsen, W. Hennink, Polymeric Micelles in Anticancer Therapy: Targeting, Imaging and Triggered Release. Pharm. Res. 27 (2010) 2569-2589.
[97] I. Hevus, A. Modgil, J. Daniels, A. Kohut, C. Sun, S. Stafslien, A. Voronov, Invertible Micellar Polymer Assemblies for Delivery of Poorly Water-Soluble Drugs. Biomacromolecules 13 (2012) 2537-2545.
[98] K. Letchford, R. Liggins, H. Burt, Pharmaceutics, preformulation and drug delivery.

Journal of Pharmaceutical Sciences 97 (2008) 1179-1190.
[99] H. Maeda, J. Wu, T. Sawa, Y. Matsumura, K. Hori, Tumor vascular permeability and the EPR effect in macromolecular therapeutics: a review. J. Controlled Release 65 (2000) 271-284.
[100] K. Knop, R. Hoogenboom, D. Fischer, U. S. Schubert, Poly(ethylene glycol) in Drug Delivery: Pros and Cons as Well as Potential Alternatives. Angew. Chem.-Int. Edit. 49 (2010) 6288-6308.
[101] L. Liu, L. Sun, Q. Wu, W. Guo, L. Li, Y. Chen, Y. Li, C. Gong, Z. Qian, Y. Wei, Curcumin loaded polymeric micelles inhibit breast tumor growth and spontaneous pulmonary metastasis. Inter. J. of Pharm. 443 (2013) 175-182.
[102] R. L. Yang, S. A. Zhang, D. L. Kong, X. L. Gao, Y. J. Zhao, Z. Wang, Biodegradable Polymer-Curcumin Conjugate Micelles Enhance the Loading and Delivery of Low-Potency Curcumin. Pharm. Res. 29 (2012) 3512-3525.
[103]V. A. Sethuraman, M. C. Lee, Y. H. Bae, A biodegradable pH-sensitive micelle system for targeting acidic solid tumors. Pharm. Res. 25 (2008) 657-666.
[104] C. Deng, Y. Jiang, R. Cheng, F. Meng, Z. Zhong, Biodegradable polymeric micelles for targeted and controlled anticancer drug delivery: Promises, progress and prospects. Nano Today 7 (2012) 467-480.
[105] J. Nicolas, S. Mura, D. Brambilla, N. Mackiewicz, P. Couvreur, Design, functionalization strategies and biomedical applications of targeted biodegradable/biocompatible polymer-based nanocarriers for drug delivery. Chem. Soc. Rev. 42 (2013) 1147-1235.
[106] S. Q. Liu, N. Wiradharma, S. J. Gao, Y. W. Tong, Y. Y. Yang, Bio-functional micelles self-assembled from a folate-conjugated block copolymer for targeted intracellular delivery of anticancer drugs. Biomaterials 28 (2007) 1423-1433.
[107] J. Z. Du, R. K. O'Reilly, Advances and challenges in smart and functional polymer vesicles. Soft Matter 5 (2009) 3544-3561.
[108] W. Li, J. F. Li, J. Gao, B. H. Li, Y. Xia, Y. C. Meng, Y. S. Yu, H. W. Chen, J. X. Dai, H. Wang, Y. J. Guo, The fine-tuning of thermosensitive and degradable polymer micelles for enhancing intracellular uptake and drug release in tumors. Biomaterials 32 (2011) 3832-3844.
[109] A. C. Albertsson, I. Varma, Degradable Aliphatic Polyesters, Vol. 157, Springer Berlin Heidelberg, 2002, pp. 1-40.
[110] G. S. He, L. L. Ma, J. Pan, S. Venkatraman, ABA and BAB type triblock copolymers of PEG and PLA: A comparative study of drug release properties and"stealth particle characteristics. Inter. J. Pharm.334 (2007) 48-55.
[111] Y. Ikada, K. Jamshidi, H. Tsuji, S. H. Hyon, Stereocomplex formation between enantiomeric poly(lactides). Macromolecules 20 (1987) 904-906.
[112] S. M. Li, M. Vert, Synthesis, characterization, and stereocomplex-induced gelation of block copolymers prepared by ring-opening polymerization of L(D)-lactide in the presence of poly(ethylene glycol). Macromolecules 36 (2003) 8008-8014.
[113] Y. Zhang, X. H. Wu, Y. R Han, F. Mo, Y. Duan, S. M Li, Novel thymopentin release systems prepared from bioresorbable PLA-PEG-PLA hydrogels. Inter. J. Pharm. 386 (2010) 15-22.
[114] L. Yang, A. El Ghzaoui, S. M. Li, In vitro degradation behavior of

poly(lactide)-poly(ethylene glycol) block copolymer micelles in aqueous solution. Inter. J. Pharm. 400 (2010) 96-103.
[115] A. Kozlowski, J. M. Harris, Improvements in protein PEGylation: pegylated interferons for treatment of hepatitis C. J. Controlled Release 72 (2001) 217-224.
[116] A. Kozlowski, S. A. Charles, J. M. Harris, Development of pegylated interferons for the treatment of chronic hepatitis C. Biodrugs 15 (2001) 419-429.
[117] R. Gref, M. Luck, P. Quellec, M. Marchand, E. Dellacherie, S. Harnisch, T. Blunk, R. H. Muller, 'Stealth' corona-core nanoparticles surface modified by polyethylene glycol (PEG): influences of the corona (PEG chain length and surface density) and of the core composition on phagocytic uptake and plasma protein adsorption. Colloid Surf. B-Biointerfaces 18 (2000) 301-313.
[118] S. I. Jeon, J. H. Lee, J. D. Andrade, P. G. Degennes, Protein surface interactions in the presence of polyethylene oxide 1. Simplified theory. J. Colloid Interface Sci. 142 (1991) 149-158.
[119] T. Riley, C. R. Heald, S. Stolnik, M. C. Garnett, L. Illum, S. S. Davis, S. M. King, R. K. Heenan, S. C. Purkiss, R. J. Barlow, P. R. Gellert, C. Washington, Core-shell structure of PLA-PEG nanoparticles used for drug delivery. Langmuir 19 (2003) 8428-8435.
[120] T. Govender, T. Riley, T. Ehtezazi, M. C. Garnett, S. Stolnik, L. Illum, S. S. Davis, Defining the drug incorporation properties of PLA-PEG nanoparticles. Inter. J. Pharm. 199 (2000) 95-110.
[121] T. Riley, S. Stolnik, C. R. Heald, C. D. Xiong, M. C. Garnett, L. Illum, S. S. Davis, S. C. Purkiss, R. J. Barlow, P. R. Gellert, Physicochemical evaluation of nanoparticles assembled from poly(lactic acid)-poly(ethylene glycol) (PLA-PEG) block copolymers as drug delivery vehicles. Langmuir 17 (2001) 3168-3174.
[122] S. S. Venkatraman, P. Jie, F. Min, B. Y. C. Freddy, G. Leong-Huat, Micelle-like nanoparticles of PLA-PEG-PLA triblock copolymer as chemotherapeutic carrier. Inter. J. Pharm. 298 (2005) 219-232.
[123] R. T. Liggins, H. M. Burt, Polyether-polyester diblock copolymers for the preparation of paclitaxel loaded polymeric micelle formulations. Adv. Drug Deliv. Rev. 54 (2002) 191-202.
[124] E. Blanco, E. A. Bey, Y. Dong, B. D. Weinberg, D. M. Sutton, D. A. Boothman, J. M. Gao, beta-Lapachone-containing PEG-PLA polymer micelles as novel nanotherapeutics against NQO1-overexpres sing tumor cells. J. Controlled Release 122 (2007) 365-374.
[125] S. C. Kim, D. W. Kim, Y. H. Shim, J. S. Bang, H. S. Oh, S. W. Kim, M. H. Seo, In vivo evaluation of polymeric micellar paclitaxel formulation: toxicity and efficacy. J. Controlled Release 72 (2001) 191-202.
[126] J. Hrkach, D. Von Hoff, M. M. Ali, E. Andrianova, J. Auer, T. Campbell, D. De Witt, M. Figa, M. Figueiredo, A. Horhota, S. Low, K. McDonnell, E. Peeke, B. Retnarajan, A. Sabnis, E. Schnipper, J. J. Song, Y. H. Song, J. Summa, D. Tompsett, G. Troiano, T. Van Geen Hoven, J. Wright, P. LoRusso, P. W. Kantoff, N. H. Bander, C. Sweeney, O. C. Farokhzad, R. Langer, S. Zale, Preclinical Development and Clinical Translation of a PSMA-Targeted Docetaxel Nanoparticle with a Differentiated Pharmacological Profile. Sci. Transl. Med. 4 (2012) 128-139.
[127] S. Cammas, K. Suzuki, C. Sone, Y. Sakurai, K. Kataoka, T. Okano, Thermo-responsive

polymer nanoparticles with a core-shell micelle structure as site-specific drug carriers. J..Controlled Release 48 (1997) 157-164.
[128] J. Chung, M. Yokoyama, T. Aoyagi, Y. Sakurai, T. Okano, Effect of molecular architecture of hydrophobically modified poly(*N*-isopropylacrylamide) on the formation of thermoresponsive core-shell micellar drug carriers. J. Controlled Release 53 (1998) 119-130.
[129] G. Schild, Poly(*N*-isopropylacrylamide)-experiment, theory and application. Prog. Polym. Sci. (1992) 163-249.
[130] S. Fujishige, K. Kubota, I. Ando, Phase-Transition of Aqueous-Solutions of Poly(*N*-Isopropylacrylamide) and Poly(*N*-isopropylmethacrylamide). J. Phys. Chem. 93 (1989) 3311-3313.
[131] Y. Okada, F. Tanaka, Cooperative Hydration, Chain Collapse, and Flat LCST Behavior in Aqueous Poly(*N*-isopropylacrylamide) Solutions. Macromolecules 38 (2005) 4465-4471.
[132] Y. Ono, T. Shikata, Hydration and Dynamic Behavior of Poly(*N*-isopropylacrylamide)s in Aqueous Solution:A Sharp Phase Transition at the Lower Critical Solution Temperature. J. Am. Chem. Soc. 128 (2006) 10030-10031.
[133] G. Masci, L. Giacomelli, V. Crescenzi, Atom transfer radical polymerization of *N*-isopropylacrylamide. Macromol. Rapid Commun. 25 (2004) 559-564.
[134] J. D. Ye, R. Narain, Water-Assisted Atom Transfer Radical Polymerization of *N*-isopropylacrylamide: Nature of Solvent and Temperature. J. Phys. Chem. B 113 (2009) 676-681.
[135] K. W. M. Boere, B. G. Soliman, D. T. S. Rijkers, W. E. Hennink, T. Vermonden, Thermoresponsive Injectable Hydrogels Cross-Linked by Native Chemical Ligation. Macromolecules 47 (2014) 2430-2438.
[136] H. W. Ooi, K. S. Jack, H. Peng, A. K. Whittaker, "Click" PNIPAAm hydrogels - a comprehensive study of structure and properties. Polym. Chemi. 4 (2013) 4788-4800.
[137] P. De, S. R. Gondi, B. S. Sumerlin, Folate-conjugated thermoresponsive block copolymers: Highly efficient conjugation and solution self-assembly. Biomacromolecules 9 (2008) 1064-1070.
[138] P. J. Pan, M. Fujita, W. Y. Ooi, K. Sudesh, T. Takarada, A. Goto, M. Maeda, Thermoresponsive Micellization and Micellar Stability of Poly(*N*-isopropylacrylamide)-*b*-DNA Diblock and Miktoarm Star Polymers. Langmuir 28 (2012) 14347-14356.
[139] W. Y. Ooi, M. Fujita, P. J. Pan, H. Y. Tang, K. Sudesh, K. Ito, N. Kanayama, T. Takarada, M. Maeda, Structural characterization of nanoparticles from thermoresponsive poly(*N*-isopropylacrylamide)-DNA conjugate. J. Colloid Interface Sci. 374 (2012) 315-320.
[140] A. Wang, C. Tao, Y. Cui, L. Duan, Y. Yang, J. Li, Assembly of environmental sensitive microcapsules of PNIPAAm and alginate acid and their application in drug release. J. Colloid Interface Sci. 332 (2009) 271-279.
[141] Y. Liu, X. Cao, M. Luo, Z. Le, W. Xu, Self-assembled micellar nanoparticles of a novel star copolymer for thermo and pH dual-responsive drug release. J. Colloid Interface Sci. 329 (2009) 244-252.
[142] C. H. Hu, X. Z. Zhang, L. Zhang, X. D. Xu, R. X. Zhuo, Temperature- and pH-sensitive hydrogels to immobilize heparin-modified PEI/DNA complexes for sustained gene delivery. J. Mater. Chem. 19 (2009) 8982-8989.

[143] P. van Rijn, H. Park, K. Ozlem Nazli, N.C. Mougin, A. Boker, Self-Assembly Process of Soft Ferritin-PNIPAAm Conjugate Bionanoparticles at Polar-Apolar Interfaces. Langmuir 29 (2013) 276-284.
[144] N. M. Matsumoto, P. Prabhakaran, L. H. Rome, H. D. Maynard, Smart Vaults: Thermally-Responsive Protein Nanocapsules. ACS Nano 7 (2013) 867-874.
[145] H. Wei, S. X. Cheng, X. Z. Zhang, R.X. Zhuo, Thermo-sensitive polymeric micelles based on poly(*N*-isopropylacrylamide) as drug carriers. Prog. Polym. Sci. 34 (2009) 893-910.
[146] H. Wei, X. Z. Zhang, C. Cheng, S. X. Cheng, R.X. Zhuo, Self-assembled, thermosensitive micelles of a star block copolymer based on PMMA and PNIPAAm for controlled drug delivery. Biomaterials 28 (2007) 99-107.
[147] K. Fukashi, S. Kiyotaka, A. Takao, Y. Masayuki, S. Yasuhisa, O. Teruo, Preparation and characterization of thermally responsive block copolymer micelles comprising poly(*N*-isopropylacrylamide-*b*-DLlactide). J.Controlled Release 55 (1998) 87-98.
[148] J. Qin, Y. S. Jo, J. E. Ihm, D. K. Kim, M. Muhammed, Thermosensitive Nanospheres with a Gold Layer Revealed as Low-Cytotoxic Drug Vehicles. Langmuir 21 (2005) 9346-9351.
[149] M. K. Eri Ayano, Tsutomu Ishihara, Hideko Kanazawa, Teruo Okano, Poly (*N*-isopropylacrylamide)-PLA and PLA blend nanoparticles for temperature-controllable drug release and intracellular uptake. Colloids Surf. B: Biointerfaces 99 (2012) 67-73.
[150] S. Q. Liu, Y. Y. Yang, X. M. Liu, Y. W. Tong, Preparation and Characterization of Temperature-Sensitive Poly(*N*-isopropylacrylamide)-*b*-poly(d,l-lactide) Microspheres for Protein Delivery. Biomacromolecules 4 (2003) 1784-1793.
[151] Y. You, C. Hong, W. Wang, W. Lu, C. Pan, Preparation and Characterization of Thermally Responsive and Biodegradable Block Copolymer Comprised of PNIPAAM and PLA by Combination of ROP and RAFT Methods. Macromolecules 37 (2004) 9761-9767.
[152] M. Hales, C. Barner-Kowollik, T. P. Davis, M. H. Stenzel, Shell-Cross-Linked Vesicles Synthesized from Block Copolymers of Poly(D,L-lactide) and Poly(*N*-isopropylacrylamide) as Thermoresponsive Nanocontainers. Langmuir (20) (2004) 10809-10817.
[153] F. Kohori, K. Sakai, T. Aoyagi, M. Yokoyama, M. Yamato, Y. Sakurai, T. Okano, Control of adriamycin cytotoxic activity using thermally responsive polymeric micelles composed of poly(*N*-isopropylacrylamide-*co*-*N,N*-dimethylacrylamide)-*b*-poly(d,l-lactide). Colloids and Surfaces B: Biointerfaces 16 (1999) 195-205.
[154] S. Q. Liu, Y. W. Tong, Y. Y. Yang, Incorporation and in vitro release of doxorubicin in thermally sensitive micelles made from poly(*N*-isopropylacrylamide-*co*-*N,N*-dimethylacrylamide)-*b*-poly(d,l-lactide-*co*-glycolide) with varying compositions. Biomaterials 26 (2005) 5064-5074.
[155] S. Q. Liu, Y. Y. Yang, X. M. Liu, Y. W. Tong, Preparation and Characterization of Temperature-Sensitive Poly(*N*-isopropylacrylamide)-*b*-poly(d,l-lactide) Microspheres for Protein Delivery. Biomacromolecules 4 (2003) 1784-1793.
[156] S. Q. Liu, Y. W. Tong, Y. Y. Yang, Thermally sensitive micelles self-assembled from poly(*N*-isopropylacrylamide-*co*-*N,N*-dimethylacrylamide)-*b*-poly(D,L-lactide-*co*-glycolide) for controlled delivers of paclitaxel. Mol. Biosyst. 1 (2005) 158-165.
[157] J. Akimoto, M. Nakayama, K. Sakai, T. Okano, Molecular Design of Outermost Surface Functionalized Thermoresponsive Polymeric Micelles with Biodegradable Cores. J. Polym.

Sci. Part a-Polym. Chemi. 46 (2008) 7127-7137.
[158] J. Akimoto, M. Nakayama, K. Sakai, T. Okano, Thermally Controlled Intracellular Uptake System of Polymeric Micelles Possessing Poly(*N*-isopropylacrylamide)-Based Outer Coronas. Mole. Pharm. 7 (2010) 926-935.
[159] J. Akimoto, M. Nakayama, K. Sakai, T. Okano, Temperature-Induced Intracellular Uptake of Thermoresponsive Polymeric Micelles. Biomacromolecules 10 (2009) 1331-1336.
[160] F. Kohori, K. Sakai, T. Aoyagi, M. Yokoyama, M. Yamato, Y. Sakurai, T. Okano, Control of adriamycin cytotoxic activity using thermally responsive polymeric micelles composed of poly(*N*-isopropylacrylamide-*co*-*N,N*-dimethylacrylamide)-*b*-poly(d,l-lactide). Colloids and Surfaces B: Biointerfaces 16 (1999) 195-205.
[161] S. Han, M. Hagiwara, T. Ishizone, Synthesis of Thermally Sensitive Water-Soluble Polymethacrylates by Living Anionic Polymerizations of Oligo(ethylene glycol) Methyl Ether Methacrylates. Macromolecules 36 (2003) 8312-8319.
[162] H. Kitano, T. Hirabayashi, M. Gemmei-Ide, M. Kyogoku, Effect of macrocycles on the temperature-responsiveness of poly[(methoxy diethylene glycol methacrylate)-graft-PEG]. Macromol. Chem. Phys. 205 (2004) 1651-1659.
[163] M. M. Ali, H. D. H. Stover, Well-defined amphiphilic thermosensitive copolymers based on poly(ethylene glycol monomethacrylate) and methyl methacrylate prepared by atom transfer radical polymerization. Macromolecules 37 (2004) 5219-5227.
[164] J. A. Jones, N. Novo, K. Flagler, C.D. Pagnucco, S. Carew, C. Cheong, X. Z. Kong, N. A. D. Burke, H. D. H. Stover, Thermoresponsive copolymers of methacrylic acid and poly(ethylene glycol) methyl ether methacrylate. J. Polym. Sci. Pol. Chem. 43 (2005) 6095-6104.
[165] S. Sugihara, S. Kanaoka, S. Aoshima, Double thermosensitive diblock copolymers of vinyl ethers with pendant oxyethylene groups: Unique physical gelation. Macromolecules 38 (2005) 1919-1927.
[166] D. Zhang, C. Macias, C. Ortiz, Synthesis and solubility of (mono-) end-functionalized poly(2-hydroxyethyl methacrylate-g-ethylene glycol) graft copolymers with varying macromolecular architectures. Macromolecules 38 (2005) 2530-2534.
[167] B. Zhao, D. J. Li, F. J. Hua, D. R. Green, Synthesis of thermosensitive water-soluble polystyrenics with pendant methoxyoligo(ethylene glycol) groups by nitroxide-mediated radical polymerization. Macromolecules 38 (2005) 9509-9517.
[168] T. Zhou, W. Wu, S. Zhou, Engineering oligo(ethylene glycol)-based thermosensitive microgels for drug delivery applications. Polymer 51 (2010) 3926-3933.
[169] D. Neugebauer, Graft copolymers with poly(ethylene oxide) segments. Polym. Int. 56 (2007) 1469-1498.
[170] J. F. Lutz, Polymerization of oligo(ethylene glycol) (meth)acrylates: Toward new generations of smart biocompatible materials. J. Polym. Sci. Part A: Polym. Chemi. 46 (2008) 3459-3470.
[171] M. Mertoglu, S. Garnier, A. Laschewsky, K. Skrabania, J. Storsberg, Stimuli responsive amphiphilic block copolymers for aqueous media synthesised via reversible addition fragmentation chain transfer polymerisation (RAFT). Polymer 46 (2005) 7726-7740.
[172] J. F. Lutz, K. Weichenhan, O. Akdemir, A. Hoth, About the Phase Transitions in Aqueous Solutions of Thermoresponsive Copolymers and Hydrogels Based on

2-(2-methoxyethoxy)ethyl Methacrylate and Oligo(ethylene glycol) Methacrylate. Macromolecules 40 (2007) 2503-2508.
[173] R. Begum, H. Matsuura, Conformational properties of short poly(oxyethylene) chains in water studied by IR spectroscopy. J. Chem. Soc.-Faraday Trans. 93 (1997) 3839-3848.
[174] K. Tasaki, Poly(oxyethylene)-water interactions: A molecular dynamics study. J. Am. Chem. Soc. 118 (1996) 8459-8469.
[175] J. F. Lutz, O. Akdemir, A. Hoth, Point by Point Comparison of Two Thermosensitive Polymers Exhibiting a Similar LCST: Is the Age of Poly(NIPAM) Over? J. Am. Chem. Soc. 128 (2006) 13046-13047.
[176] X. H. Wang, X. P. Qiu, C. Wu, Comparison of the coil-to-globule and the globule-to-coil transitions of a single poly(*N*-isopropylacrylamide) homopolymer chain in water. Macromolecules 31 (1998) 2972-2976.
[177] S. Garnier, A. Laschewsky, Synthesis of new amphiphilic diblock copolymers and their self-assembly in aqueous solution. Macromolecules 38 (2005) 7580-7592.
[178] C. Pietsch, M. W. M. Fijten, H. M. L. Lambermont-Thijs, R. Hoogenboom, U. S. Schubert, Unexpected reactivity for the RAFT copolymerization of oligo(ethylene glycol) methacrylates. J. Polym. Sci. Part A: Polym. Chemi. 47 (2009) 2811-2820.
[179] G. S. Ananchenko, H. Fischer, Decomposition of model alkoxyamines in simple and polymerizing systems. I. 2, 2, 6, 6-tetramethylpiperidinyl-*N*-oxyl-based compounds. J. Polym. Sci. Pol. Chem. 39 (2001) 3604-3621.
[180] M. Chenal, S. Mura, C. Marchal, D. Gigmes, B. Charleux, E. Fattal, P. Couvreur, J. Nicolas, Facile Synthesis of Innocuous Comb-Shaped Polymethacrylates with PEG Side Chains by Nitroxide-Mediated Radical Polymerization in Hydroalcoholic Solutions. Macromolecules 43 (2010) 9291-9303.
[181] V. Delplace, A. Tardy, S. Harrisson, S. Mura, D. Gigmes, Y. Guillaneuf, J. Nicolas, Degradable and Comb-Like PEG-Based Copolymers by Nitroxide-Mediated Radical Ring-Opening Polymerization. Biomacromolecules 14 (2013) 3769-3779.
[182] X. S. Wang, S. F. Lascelles, R. A. Jackson, S. P. Armes, Facile synthesis of well-defined water-soluble polymers via atom transfer radical polymerization in aqueous media at ambient temperature. Chem. Commun. (18) (1999) 1817-1818.
[183] X. S. Wang, S. P. Armes, Facile atom transfer radical polymerization of methoxy-capped oligo(ethylene glycol) methacrylate in aqueous media at ambient temperature. Macromolecules 33 (2000) 6640-6647.
[184] S. I. Yamamoto, J. Pietrasik, K. Matyjaszewski, The effect of structure on the thermoresponsive nature of well-defined poly(oligo(ethylene oxide) methacrylates) synthesized by ATRP. J. Polym. Sci. Part A: Polym. Chemi. 46 (2008) 194-202.
[185] S. Yamamoto, J. Pietrasik, K. Matyjaszewski, ATRP synthesis of thermally responsive molecular brushes from oligo(ethylene oxide) methacrylates. Macromolecules 40 (2007) 9348-9353.
[186] J. F. Lutz, A. Hoth, Preparation of Ideal PEG Analogues with a Tunable Thermosensitivity by Controlled Radical Copolymerization of 2-(2-Methoxyethoxy)ethyl Methacrylate and Oligo(ethylene glycol) Methacrylate. Macromolecules 39 (2006) 893-896.
[187] J. F. Lutz, J. Andrieu, S. uzgun, C. Rudolph, S. Agarwal, Biocompatible, Thermoresponsive, and Biodegradable:Simple Preparation of "All-in-One" Biorelevant

Polymers. Macromolecules 40 (2007) 8540-8543.
[188] J. F. Lutz, H. G. Borner, K. Weichenhan, Combining ATRP and "click" chemistry: a promising platform toward functional biocompatible polymers and polymer bioconjugates. Macromolecules 39 (2006) 6376-6383.
[189] J. F. Lutz, H.G. Borner, K. Weichenhan, Combining atom transfer radical polymerization and click chemistry: A versatile method for the preparation of end-functional polymers. Macromole. Rapid Commun. 26 (2005) 514-518.
[190] Y. Cheng, C. He, C. Xiao, J. Ding, X. Zhuang, X. Chen, Versatile synthesis of temperature-sensitive polypeptides by click grafting of oligo(ethylene glycol). Polym. Chemi. 2 (2011) 2627-2634.
[191] J. F. Lutz, H.G. Borner, Modern trends in polymer bioconjugates design. Prog. Polym. Sci. 33 (2008) 1-39.
[192] S. J. T. Rezaei, M. R. Nabid, H. Niknejad, A. A. Entezami, Folate-decorated thermoresponsive micelles based on star-shaped amphiphilic block copolymers for efficient intracellular release of anticancer drugs. Inter. J. Pharm. 437 (2012) 70-79.
[193] K. Ito, K. Tanaka, H. Tanaka, G. Imai, S. Kawaguchi, S. Itsuno, Poly(ethylene oxide) macromonomers. 7. Micellar polymerization in water. Macromolecules 24 (1991) 2348-2354.
[194] K. Ito, Y. Tomi, S. Kawaguchi, Poly(ethylene oxide) macromonomers. 10. Characterization and solution properties of the regular comb polymers with polystyrene main chains and poly(ethylene oxide) side chains. Macromolecules 25 (1992) 1534-1538.
[195] S. Kawaguchi, A. Yekta, J. Duhamel, M.A. Winnik, K. Ito, Fluorescence Probe Study of Micelle Formation of Poly(ethylene oxide) Macromonomers in Water. The Journal of Physical Chemistry 98 (1994) 7891-7898.
[196] A.O. Saeed, S. Dey, S.M. Howdle, K.J. Thurecht, C. Alexander, One-pot controlled synthesis of biodegradable and biocompatible co-polymer micelles. J. Mater. Chem. 19 (2009) 4529-4535.
[197] M. Luzón, T. Corrales, F. Catalina, V. San Miguel, C. Ballesteros, C. Peinado, Hierarchically organized micellization of thermoresponsive rod-coil copolymers based on poly[oligo(ethylene glycol) methacrylate] and poly(ε-caprolactone). J. Polym. Sci. Part A: Polym. Chemi. 48 (2010) 4909-4921.
[198] Y. Bakkour, V. Darcos, F. Coumes, S. M Li, J. Coudane, Brush-like amphiphilic copolymers based on polylactide and poly(ethylene glycol): Synthesis, self-assembly and evaluation as drug carrier. Polymer 54 (2013) 1746-1754.
[199] R. Fenyves, M. Schmutz, I. J. Horner, F.V. Bright, J. Rzayev, Aqueous Self-Assembly of Giant Bottlebrush Block Copolymer Surfactants as Shape-Tunable Building Blocks. J. Am. Chem. Soc. 136 7762-7770.
[200] T. Yahara, T. Koga, S. Yoshida, S. Nakagawa, H. Deguchi, K. Shirouzu, Relationship Between Microvessel Density and Thermographic Hot Areas in Breast Cancer. Surgery Today 33 (2003) 243-248.

Chapter 2 Synthesis and self-assembling of PNIPAAm-*b*-PLLA-*b*-PNIPAAm thermo-responsive triblock copolymers prepared by combination of ROP and ATRP

Abstract: In this work, novel thermo-responsive poly(*N*-isopropylacrylamide)-*block*-poly(*L*-lactide)-*block*-poly(*N*-isopropylacylamide) (PNIPAAm-*b*-PLLA-*b*-PNIPAAm) triblock copolymers were successfully prepared by ATRP of NIPAAm with Br-PLLA-Br macroinitiator, using a CuCl/tris(2-dimethylaminoethyl) amine (Me_6TREN) complex as catalyst at 25 ^oC in a DMF/water mixture for 30 mins. The molecular weight of the copolymers ranges from 18, 000 to 38, 000 g mol^{-1}, and the dispersity from 1.10 to 1.28. Micelles are formed by self-assembly of copolymers in aqueous medium at room temperature, as evidenced by ^1H NMR, DLS and TEM. Core-shell structure micellization of the triblock copolymers was confirmed by ^1H NMR spectra in two selective solvent environments ($CDCl_3$ and D_2O). The critical micelle concentration determined by fluorescence spectroscopy is in the range of 0.0077-0.016 mg mL^{-1}. The copolymer micelles exhibit a LCST between 32.1 and 32.8 ^oC. The micelles are spherical in shape with a mean diameter between 31 and 83 nm, as determined by TEM and DLS. When the temperature is raised above the LCST, micelle size increases at high copolymer concentrations due to aggregation. In contrast, at low copolymer concentrations, decrease of micelle size is observed due to collapse of PNIPAAm chains.

Keywords: poly(*N*-isopropylacrylamide); poly(L-lactide); ring-opening polymerization; atom transfer radical polymerization; self-assembly; micelle; thermo-responsive.

2.1 Introduction

In the past decade, self-assembling micelles prepared from amphiphilic block copolymers have been widely investigated for their potential applications in the pharmaceutical field as drug carrier [1-4]. These polymeric micelles present a core-shell structure: an inner core able to encapsulate hydrophobic drugs with improved solubility, and a hydrophilic shell that stabilizes the micelles in aqueous solution and inhibits aggregation. Furthermore, they possess a nano-scale size range (*i.e.* <200 nm) with a narrow distribution, and can achieve higher accumulation at the target site through an enhanced permeability and retention effect (EPR effect). Other advantages of micelles include reduced side effects of anticancer drugs, targeted drug delivery, and prolonged blood circulation time, which make them promising as carrier of hydrophobic drugs.

Among the various micellar systems, "smart" micelles derived from stimuli-responsive polymers have drawn great attention in the past years [5, 6]. Thermo-responsive polymers, in particular poly(*N*-isopropylacrylamide) (PNIPAAm), are probably the most promising stimuli-responsive polymers. PNIPAAm shows a lower critical solution temperature (LCST) of about 32 ^{o}C, which is relatively insensitive to slight variation of environmental conditions [7]. Below the LCST, thermo-sensitive polymers exhibit a random coil structure whereas above the LCST, a collapsed globular structure is obtained. With the development of living polymerization during the last decade, novel thermo-sensitive amphiphilic block copolymer micelles involving PNIPAAm, such as poly(*N*-isopropylacrylamide)-*b*-polystylene (PNIPAAm-*b*-PS), poly(*N*-isopropylacrylamide)-*b*-poly(methyl methylacrylate) (PNIPAAm-*b*-PMMA) and poly(*N*-isopropylacrylamide)-*b*-poly(tert-butyl acrylate) PNIPAAm-*b*-PtBA, have been prepared [8-11]. Nevertheless, these polymers are nondegradable, which limits their potential applications as drug carrier.

In this context, the use of polylactide (PLA) appears very interesting for biomedical and pharmaceutical applications such as controlled drug release systems, medical implants and scaffolds in tissue engineering [12-15]. Copolymerization of NIPAAm with lactide allows combining the thermo-sensitivity of PNIPAAm and the degradability of PLA [16-19]. To date, few examples of block copolymers based on PNIPAAm and PLA described in the literature are obtained by ring-opening polymerization (ROP) of lactide initiated by hydroxyl-terminated PNIPAAm precursor [16-20]. The precursor is first obtained by free radical polymerization initiated by benzoyl peroxide (BPO), using 2-hydroxyethanethiol as chain transfer agent. The ROP of lactide is then carried out with tin (II) 2-ethylhexanoate ($Sn(Oct)_2$) as catalyst. The resulting copolymers exhibit poorly controlled molecular weights and large dispersity ($Đ=M_w/M_n$) [16-20]. Besides, only PNIPAAm-*b*-PLA diblock copolymers were obtained using this approach.

To improve the control, living/controlled polymerization, especially reversible addition-fragmentation chain transfer (RAFT), was also used to synthesize PNIPAAm/PLA diblock or triblock as such technique allows to obtain copolymers with well controlled molecular weight and narrow dispersity [21, 22]. Hales *et al.* synthesized PNIPAAm-*b*-PLA diblock copolymers by combination of RAFT and ROP [23]. Shell cross-linked vesicles with sizes above 230nm were prepared from the copolymers. You *et al.* reported the synthesis of a PLA-*b*-PNIPAAm-*b*-PLA triblock copolymer *via* the same route [24]. However, only the LCST of the copolymer was determined. Most recently, Akimoto *et al.* reported P(NIPAAm-*co*-DMAAm)-*b*-PLA diblock micelles prepared by combination of RAFT and ROP [25-27]. The thermo-responsive micelles showed time-dependent intracellular uptake above LCST without exhibiting cytotoxicity.

In this contribution, we report for the first time, to the best of our knowledge, the synthesis of self-assembly of novel PNIPAAm-*b*-PLLA-*b*-PNIPAAm ABA triblock

copolymers prepared by combination of ROP and ATRP. PNIPAAm-*b*-PLLA-*b*-PNIPAAm was prepared by a controlled ATRP process using a poly(L-lactide) as macroinitiator, allowing an excellent control over the molecular weight under mild condition reactions. The kinetics of the polymerization and the self-assembly behavior of the resulting copolymers were investigated.

2.2 Experimental Section

2.2.1 Materials

L-lactide was purchased from PuracBiochem (Goerinchem, The Netherlands). *N*-isopropylacrylamide (NIPAAm), stannous 2-ethylhexanoate ($Sn(Oct)_2$, 1,4-benzenedimethanol, 2-bromopropionyl bromide, triethylamine, tris(2-dimethylaminoethyl)amine (Me_6TREN), copper (I) chloride (CuCl), *N,N*-dimethy formamide (DMF), diethyl ether and methanol were obtained from Sigma-Aldrich (St-Quentin Fallavier, France), and were used without further purification. Dichloromethane and toluene were supplied by Sigma-Aldrich, and were dried over calcium hydride (CaH_2) for 24 hours at room temperature and distilled under reduced pressure. Ultrapure water with a conductivity of 18 MΩ was produced using a Millpore Mill-Q water system.

2.2.2 Characterization

Proton Nuclear Magnetic Resonance (^{1}H NMR) ^{1}H NMR spectra were recorded on a Bruker spectrometer (AMX300) at 300 MHz Chemical shifts were referenced to the peak of residual non-deuterated solvents.

Size Exclusion Chromatography Size exclusion chromatography (SEC) was performed on a Varian 390-LC equipped with a refractive index detector and two ResiPore columns (300×7.5 mm). Measurements were performed at 60 °C at a flow

rate of 1 mL min^{-1}， The eluent was DMF (0.1 *wt*% LiBr). Calibration was realized with PMMA standards.

Fluorescence Spectroscopy The CMC of the copolymers was determined by fluorescence spectroscopy using pyrene as a hydrophobic fluorescent probe. Measurements were carried outon an RF 5302 Shimadzu spectrofluorometer (Japan) equipped with a Xenon light source (UXL-150S, Ushio, Japan). Briefly, an aliquot of pyrene solution (6×10^{-6} M in acetone, 1 mL) was added to different vials, and the solvent was evaporated. Then, 10 mL of aqueous solutions of different concentrations were added to the vials. The final concentration of pyrene in each vial was 6×10^{-7} M. After equilibrating at room temperature overnight, the fluorescence excitation spectra of the solutions were recorded from 300 to 360 nm at an emission wavelength of 394 nm. The emission and excitation slit widths were 3 nm and 5 nm, respectively. The excitation fluorescence values I_{337} and I_{333}, respectively at 337 and 333 nm, were used for subsequent calculations.

Cloud Point The thermo-sensitivity of the copolymers was estimated from transmittance changes with temperature. The measurements were carried out on copolymer solutions at 3.0 mg mL^{-1} at a wavelength of 500 nm, using a Perkin Elmer Lambda 35 UV-Visible spectrometer equipped with a Peltier temperature programmer PTP-1+1. The temperature ramp was 0.1 °C min^{-1}.

Dynamic Light Scattering Dynamic light scattering (DLS) was performed with a Malvern Instrument Nano-ZS equipped with a He-Ne laser (λ = 632.8 nm). Polymer solutions at 1.0 mg mL^{-1} were filtered through a 0.45 μm PTFE microfilter before measurements. The correlation function was analyzed via the general purpose method (NNLS) to obtain the distribution of diffusion coefficients (D) of the solutes. The apparent equivalent hydrodynamic radius (R_H) was determined from the cumulant method using the Stokes-Einstein equation:

$$R_H = \frac{K_B T}{6\pi\eta\Gamma} \quad q^2 = \frac{K_B T}{6\pi\eta D_0}$$

Where k_B is Boltzmann constant, T is the temperature, Γ is the relaxation frequency, q is the wave vector, η is the viscosity of the medium, and D_0 is the translational diffusion coefficient at finite dilution. Mean radius values were obtained from triplicate runs. Standard deviations were evaluated from hydrodynamic radius distribution.

Transmission Electron Microscopy Transmission electron microscopy (TEM) experiments were realized on a JEOL 1200 EXII instrument operating at an acceleration voltage 120 kV. TEM samples were prepared by dropping a polymer solution at 1.0 mg mL^{-1} onto a carbon-coated copper grid, followed by air drying.

2.2.3 Synthesis of HO-PLLA-OH (Run 1, Table 2.1)

The ring-opening polymerization (ROP) of L-lactide was performed in solution using standard Schlenk technique under argon atmosphere. A total of 10 g of L-lactide (69.4 mmol), 281 mg of $Sn(Oct)_2$ (69.4×10^{-2} mmol), 480 mg of 1,4-benzenedimethanol (3.47 mmol), and 20 mL of anhydrous toluene were placed in an oven dried Schlenk tube fitted with a rubber septum. The solution was further degassed by five freeze-pump-thaw cycles, and polymerization proceeded under stirring at 80 °C for 4 hours. After cooling down to room temperature, the mixture was poured in cold diethyl ether. The precipitated polymer was collected by filtration and drying *in vacuo.* Yield (%) =92 %.

^{1}H NMR (300 MHz, $CDCl_3$) [Figure 1A]: δ (ppm) = 7.30 (s, $4H_{Ar}$); 5.11 (m, $1H_a$); 4.33 (m,$1H_c$); 1.52 (d, $3H_b$); 1.44(d, $3H_d$)

$M_{n,\,NMR}$= 3000 g mol^{-1}, $M_{n,\,SEC}$=4300 g mol^{-1}; $Đ$ =1.03

2.2.4 Synthesis of Br-PLLA-Br

In a dried round bottom flask equipped with a drying tube filled with $CaCl_2$, 2 g (0.667 mmol) of HO-PLLA-OH was dissolved in 20 mL of dried dichloromethane with stirring (Run 2, Table 2.1). Then, 0.298 mL (2 mmol) of triethylamine and 0.209 mL (2 mmol) of 2-bromopropionylbromide were added dropwise to the solution in an ice bath. The reaction mixture was then stirred for 72 hours at room temperature. The precipitated by-product (i.e. $Et_3N{\cdot}HBr$) was removed by filtration. The filtrate was washed using 5 % sodium bicarbonate (3 × 30 mL) and then water (3 ×30 mL). The organic phase was dried over anhydrous $MgSO_4$ and filtered. The filtrate was poured in cold methanol. The precipitated polymer was collected by filtration and drying *in vacuo*.

^1H NMR (300 MHz, $CDCl_3$) [Figure 1B] δ (ppm) = 7.29 (S, $4H_{Ar}$), 5.11 (m, $1H_a$), 4.33 (m, $1H_c$+$1H_e$), 1.8 (d, $3H_f$), 1.52 (d, $3H_b$).

$M_{n,\,NMR}$ = 3300 g mol^{-1}, $M_{n,\,SEC}$ = 4700 g mol^{-1}, $Đ$=1.04

2.2.5 Synthesis of PNIPAAm-*b*-PLLA-*b*-PNIPAAm

Triblock copolymers were prepared using a standard Schlenk technique (Run T1, Table 2.1). Typically, 100 mg (0.0304 mmol) of Br-PLA-Br, 344 mg (3.04 mmol) of NIPAAm and 6.0 mg (0.0608 mmol) of CuCl were dissoloved in 1.5 mL DMF, then 0.3 mL of H_2O were introduced into a Schlenk tube. After five freeze-pump-thaw cycles, 16.3 µL (0.0608 mmol) of Me_6TREN was added under argon atmosphere. The reaction was then allowed to proceed under stirring at 25 ^oC for 30 minutes. During the reaction, samples were taken from the solution at preset time intervals for NMR and SEC analyses. After quenching with liquid N_2, the viscous solution was precipitated by addition of diethylether. The crude product was dissolved in 10 mL CH_2Cl_2. The catalyst was removed by passing the dilute solution through an aluminum oxide column. The resulting colorless solution was then concentrated,

followed by precipitation in cold diethylether. The final product was dried under vacuum at room temperature for 24 h.

^{1}H NMR (300 MHz, $CDCl_3$) δ (ppm) = 7.29(S, $4H_{Ar}$), 5.11 (m, $1H_a$), 3.94 (m,$1H_e$), 2.07 (t, $1H_d$), 1.76 (m, $2H_c$), 1.52 (d, $3H_b$), 1.09 (d, 6Hf).

$M_{n,\,NMR}$= 14000 g mol^{-1}, $M_{n,\,SEC}$ = 18000 g mol^{-1}, $Đ$= 1.08

2.3 Results and discussion

2.3.1 Synthesis of PNIPAAm-*b*-PLLA-*b*-PNIPAAm

Amphiphilic and thermo-responsive triblock copolymers, namely PNIPAAm-*b*-PLLA-*b*-PNIPAAm, were prepared in three steps according to the following reaction sequence: (i) synthesis of α, ω-telechelic HO-PLLA-OH by ROP of L-lactide, (ii) modification of HO-PLLA-OH using 2-bromopropionyl bromide to obtain di-2-bromopropionyl-terminated Br-PLLA-Br macroinitiator, and (iii) ATRP of NIPAAm from the Br-PLLA-Br macroinitiator yielding PNIPAAm-*b*-PLLA-*b*-PNIPAAm triblock copolymers.

The synthesis of Br-PLLA-Br macroinitiator was performed according to a procedure previously reported [28]. In the first step, PLLA bearing two hydroxyl end groups (HO-PLLA-OH) was obtained by ROP of L-lactide using $Sn(Oct)_2$ as catalyst and 1,4-dimethanol benzene as initiator. The molecular weight determined by ^{1}H NMR ($M_{n,NMR}$= 3000 g mol^{-1}) (Figure 2.1A) is close to the targeted value (2900 g mol^{-1}), while the M_n determined by SEC ($M_{n,SEC}$= 4400 g mol^{-1}) with PS standards is higher. The polymer exhibits a very low dispersity ($Đ$= 1.03), in agreement with a good control of the reaction.

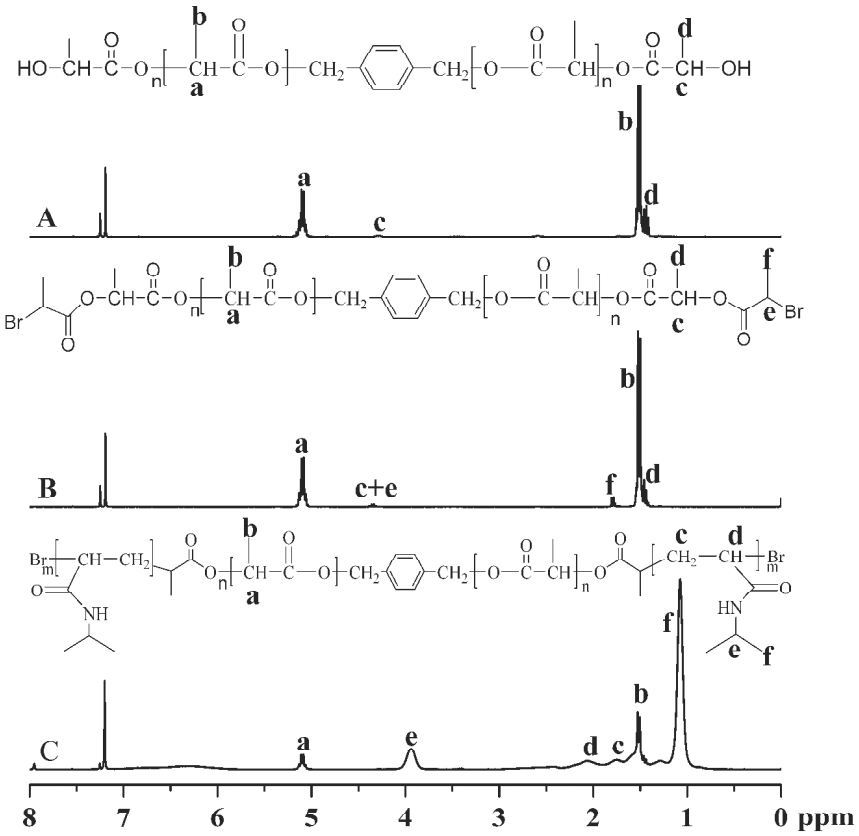

Figure 2.1 ^{1}H NMR spectra of HO-PLLA-OH (A), Br-PLLA-Br (B) and PNIPAAm-*b*-PLA-*b*-PNIPAAm (C) in $CDCl_3$.

In the second step, HO-PLLA-OH reacted with 2-bromopropionyl bromide in the presence of triethylamine, yielding Br-PLLA-Br as ATRP macroinitiator (Scheme 2.1). The attachment of the bromopropionyl group is confirmed by ^{1}H NMR (Figure 2.1B). A doublet appears at 1.8 ppm corresponding to the methyl groups (f) adjacent to the bromine. The transformation of hydroxyl endgroups into corresponding 2-bromopropionyl moiety is almost quantitative (98 %), as determined by comparing the peak area of methyl (f) protons of 2-bromopropionyl at 1.8 ppm with that of the aromatic protons at 7.29 ppm. Br-PLLA-Br shows a slight increase of molecular weight ($M_{n,\,NMR}$= 3300 g mol^{-1}, $M_{n,\,SEC}$ =4700 g mol^{-1}) as determined by SEC and ^{1}H NMR analyses, indicating that no chain cleavage occurred during the esterification reaction. The dispersity of Br-PLLA-Br remains unchanged ($Đ$ = 1.04) as compared to HO-PLLA-OH.

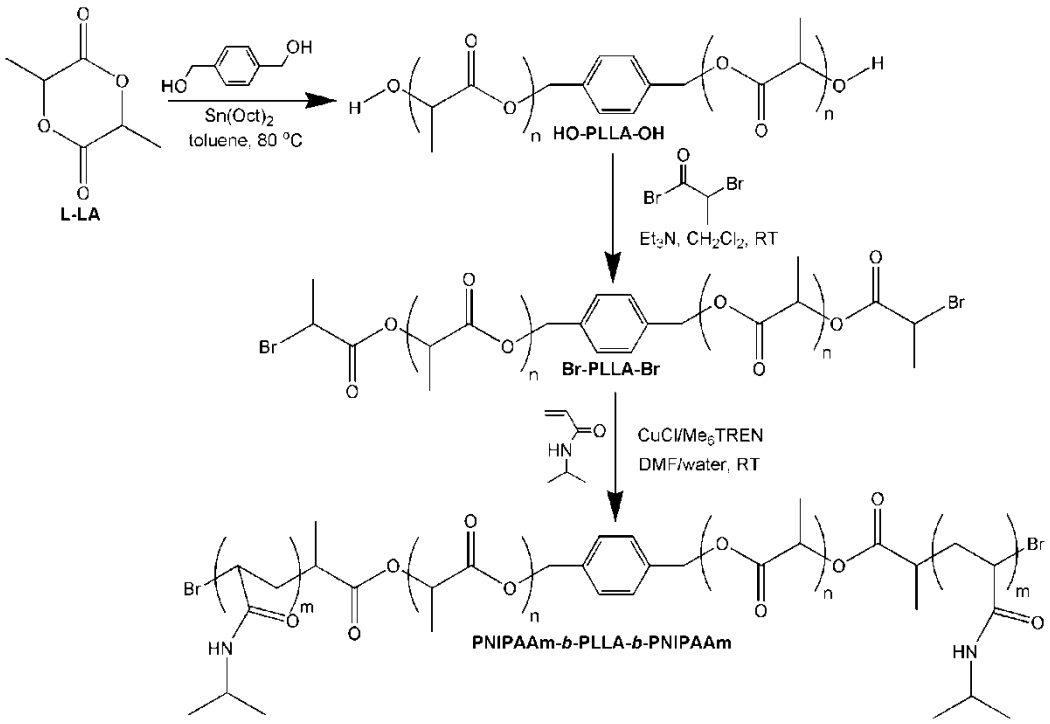

Scheme 2.1 Synthesis of PNIPAAm-*b*-PLLA-*b*-PNIPAAm triblock copolymers via combination of ring-opening polymerization and atom transfer radical polymerization

Table 2.1 Molecular characteristics of PNIPAAm-*b*-PLLA-*b*-PNIPAAm triblock copolymers

Run	$[NIPAAm]_0/[PLLA]_0$	Time (min)	Conversion[a] %	[NIPAAm]/[LA][a]	$M_{n,NMR}$[a] (g mol^{-1})	$M_{n,SEC}$[b] (g mol^{-1})	$Đ$[b]
HO-PLLA-OH	-	-	92	-	3000	4400	1.03
Br-PLLA-Br	-	-	98	-	3300	4700	1.04
T1[a]	100	30	71	2.4	14000	18000	1.08
T2[a]	200	30	58	4.2	22100	26700	1.10
T3[a]	300	30	53	5.4	27500	31500	1.13
T4[a]	300	120	65	6.9	34400	37500	1.28

[a] determined by ^{1}H NMR,

[b] determined by SEC in DMF using PMMA standards for calibration

[c]ATRP of NIPAAm. *Conditions of polymerization:* $[NIPAAm]_0$=1.69 M, T=25 °C, [initiator]/[CuCl]/[Me_6TREN]=1/2/2, solvent mixture DMF/water=5/1.

Finally, the ATRP of NIPAAm initiated by Br-PLLA-Br macroinitiator was successfully performed at 25 °C in a DMF/water mixture using CuCl/Me_6TREN complex as catalyst system. A series of amphiphilic thermo-responsive PNIPAAm-*b*-PLLA-*b*-PNIPAAm triblock copolymers were obtained by varying the

ratio of NIPAAm to PLLA from 100 to 300 equivalents and the reaction time from 30 to 120 min (Run T1-T4, Table 2.1). The molecular weight ranges between 14000 and 35000 g mol^{-1} with narrow dispersity ($Đ$= 1.08-1.28), indicating good control of the reaction. The molecular weights determined by ^{1}H NMR well agree with those obtained by SEC in DMF with PMMA standards.

Loh *et al.* reported the synthesis of poly(*N*-isopropylacrylamide)-*b*-poly(ε-caprolactone)-*b*-poly(*N*-isopropylacrylamide) (PNIPAAm-*b*-PCL-*b*-PNIPAAm) in dioxane using CuBr/HMTETA as catalyst system [29]. No kinetic study was performed, and the copolymer exhibited large dispersity ranging from 1.4 to 1.7. In the case of our PNIPAAm-*b*-PLLA-*b*-PNIPAAm, these conditions led to a poor control of the ATRP polymerization with low kinetics. In this context, ATRP was performed using experimental conditions similar to those described by Masci *et al.*, who first reported controlled polymerization of *N*-isopropylacrylamide using ATRP in DMF/water (1:1) with CuCl/Me_6TREN as catalyst system [30]. More recently, the effect of both solvent and temperature on the ATRP of NIPAAm was investigated by Ye *et al.* [31]. Water was proved to facilitate the reaction in organic-aqueous solvent systems. In this work, a DMF/water mixture with volume ratio of 5/1 was used as reaction solvent. The CuCl/Me_6TREN catalyst system was selected due to its high stability at low temperature which allows achieving a good control on the polymerization [30, 32].

Figure 2.1C shows a typical NMR spectrum of PNIPAAm-*b*-PLLA-*b*-PNIPAAm obtained for run T2 (Table 2.1). The signals at 3.94 and 1.09 ppm are assigned to the protons of PNIPAAm, while those at 5.11 and 1.52 ppm are characteristic of protons from PLLA. The composition and the molecular weight of copolymers were calculated from the integrations of the methine groups of PNIPAAm and PLLA at 3.94 and 5.11 ppm, respectively. Figure 2.2 shows the SEC traces of different triblock copolymers in comparison with Br-PLLA-Br. A shift to higher molecular weight is

detected for the copolymers, indicating successful initiation of the ATRP of NIPAAm by the macroinitiator.

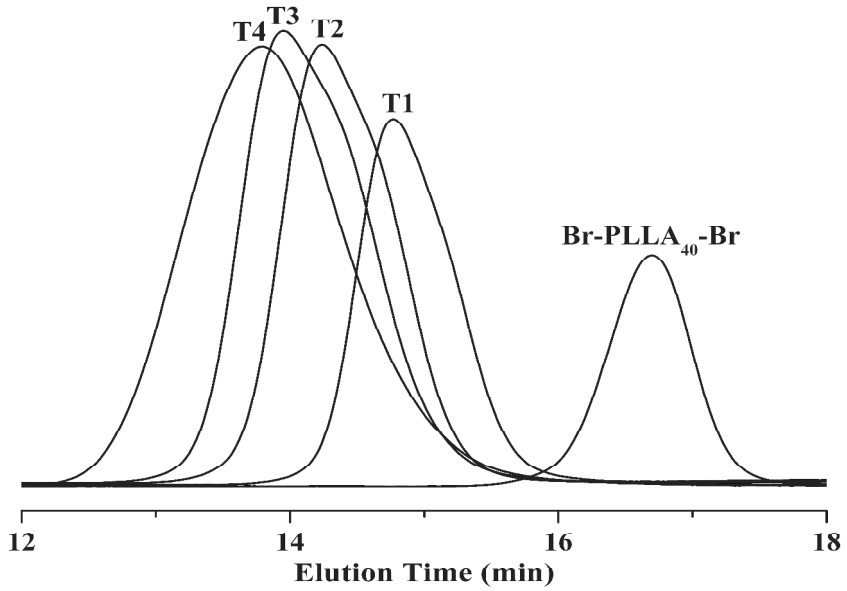

Figure 2.2 SEC chromatograms in DMF of Br-PLLA-Br and copolymers T1, T2, T3 and T4.

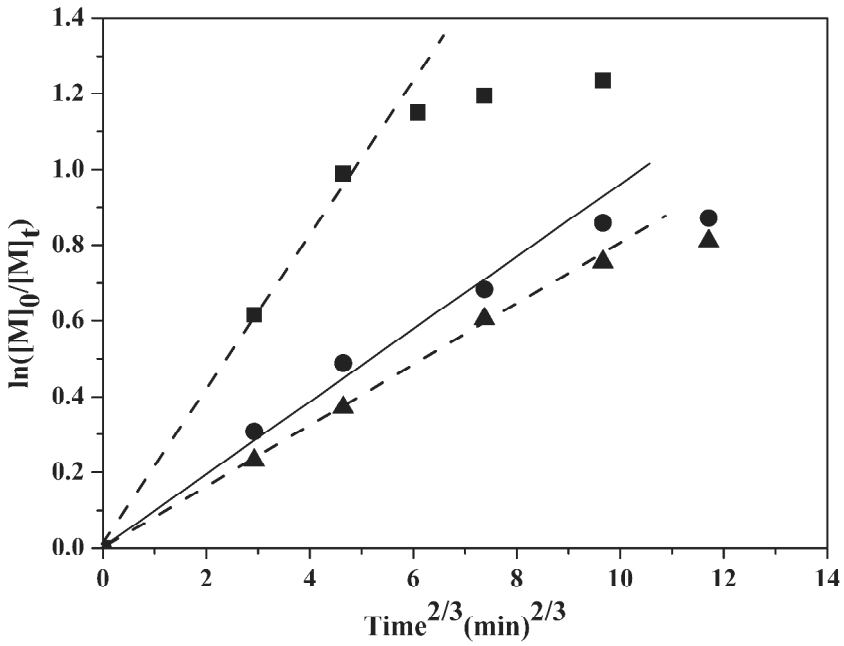

Figure 2.3 Kinetic plots for the polymerization of *N*-isopropylacrylamide in a DMF/water mixture at 25 °C using a PLLA macroinitiator: (■) [NIPAAm]/[Br-PLLA-Br]/[CuCl]/[Me_6TREN]= 100/1/2/2; (●) [NIPAAm]/[Br-PLLA-Br]/[CuCl]/[Me_6TREN]= 200/1/2/2; (▲) [NIPAAm]/[Br-PLLA-Br]/[CuCl]/ [Me6TREN]= 300/1/2/2. $[NIPAAm]_0$ = 1.69 M.

A kinetic study was carried out in order to examine the livingness of the polymerization of NIPAAm. Figure 2.3 shows the kinetic plots for the polymerization of NIPAAm at 25 °C, the ratio of NIPAAm/macroinitiator varying from 100 to 300. The initial concentration of monomer was kept constant in each experiment by adjusting the volume of solvent mixture. Samples were withdrawn from the reaction mixture at 0, 5, 10, 20, 30 and 40 minutes. The plot of $\ln([M]_0/[M]$ against $time^{2/3}$ was introduced to analyze the kinetics, considering the persistent radical effect in the absence of conventional initiation [33-38]. The resulting kinetic plots exhibit a linear relationship during the first 10 minutes for NIPAAm/macroinitiator ratio of 100, and during the first 30 minutes for NIPAAm/macroinitiator ratios of 200 and 300, indicating that the concentration of active species remained relatively constant. The conversion decreases with increasing the ratio of monomer to macroinitator due to decrease in the polymerization rate. On the other hand, the reaction with 100 equivalents of NIPAAm is faster than that with 200 and 300 equivalents because of higher initiator concentration.

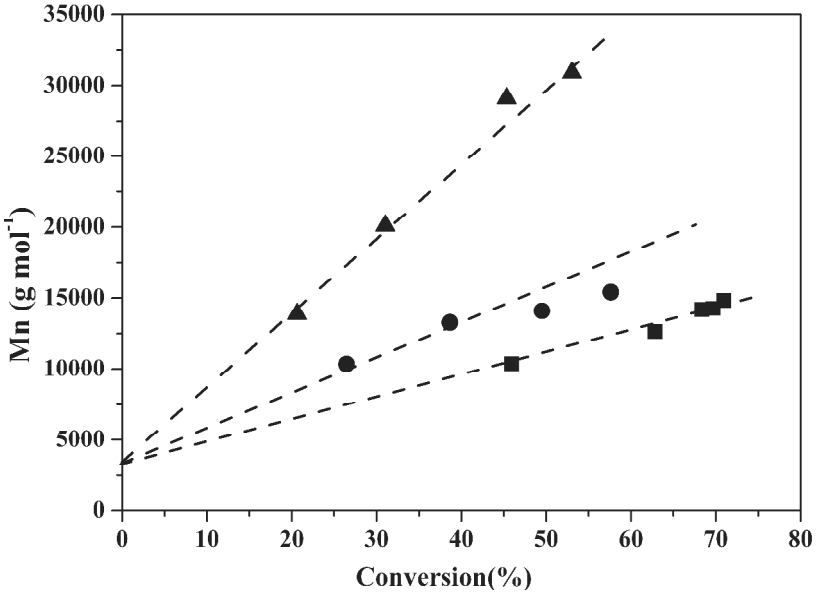

Figure 2.4 M_n *vs* conversion plots of the polymerization of *N*-isopropylacrylamide in DMF/water mixture solution at 25 °C using Br-PLLA-Br macroinitiator**:** (■) [NIPAAm]/[Br-PLLA-Br]/[CuCl] /[Me_6TREN]= 100/1/2/2; (●) [NIPAAm]/[Br-PLLA-Br]/[CuCl]/[Me_6TREN]= 200/1/2/2; (▲) [NIPAAm] /[Br-PLLA-Br]/[CuCl]/[Me_6TREN]= 300/1/2/2.

The evolution of M_n *vs.* conversion is shown in Figure 2.4. The molecular weight linearly increases with conversion, which is indicative of the living character of the reaction. Evolution of SEC traces for the ATRP of NIPAAM (NIPAAm/macroinitiator ratio=100) was followed at different reaction time periods (Figure 2.5). Shift to shorter elution time or higher M_n is noticed in all cases. Therefore, all data suggest a well-controlled ATRP of NIPAAm using a hydrophobic Br-PLLA-Br as macroinitiator to prepare triblock copolymers based on PLA and PNIPAAm.

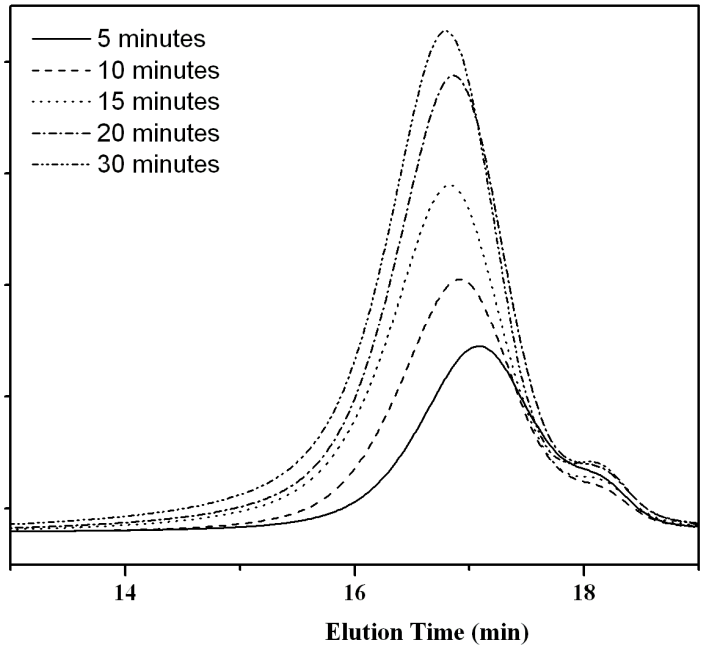

Figure 2.5 SEC traces for the polymerization of *N*-isopropylacrylamide in a DMF/water mixture at 25 °C using a PLLA macroinitiator. [NIPAAm]/[Br-PLLA-Br]/[CuCl]/[Me_6TREN]= 100/1/2/2.

As shown in Figure 2.6, the influence of temperature on the kinetics was also investigated. The $\ln([M]_0/[M]$ *vs.* time$^{2/3}$ plots shows a linear increase at 25 ^oC. On the contrary, the kinetic plot shows much slower reaction rate at 0 ^oC because of the lower reactivity of the catalyst system.

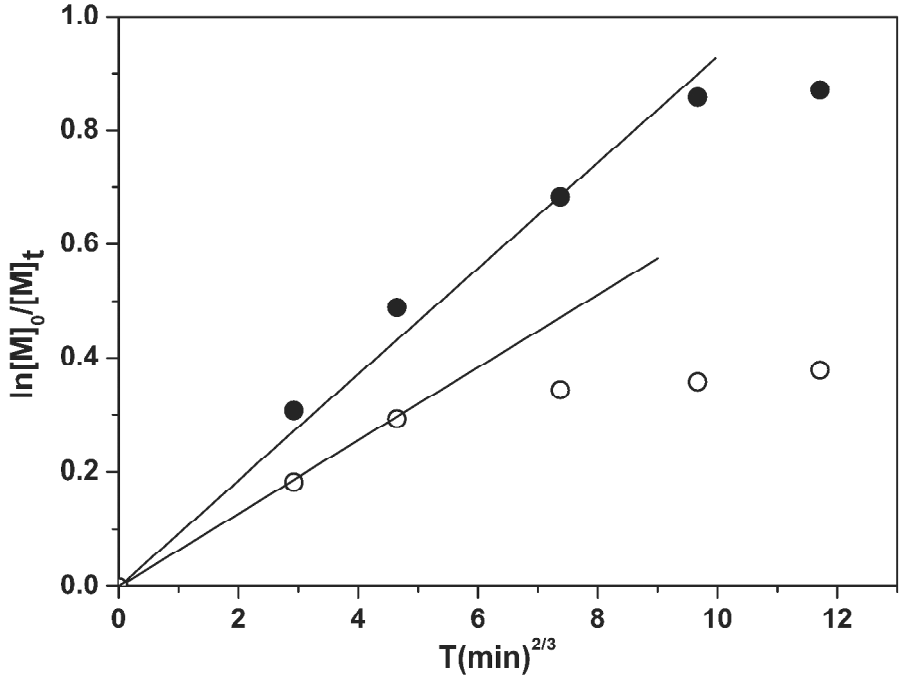

Figure 2.6 The influence of temperature on the kinetics: (●) 25 °C and (○) 0 °C. [NIPAAm]/[Br-PLLA-Br]/[CuCl]/[Me_6TREN]= 200/1/2/2.

2.3.2 Self-assembling of copolymers

Amphiphilic block copolymers are susceptible to self-assemble into various aggregates in aqueous medium, including spherical micelles, anisotropic micelles, filomicelles, nanotubes and so forth. Spherical micelles are the most commonly observed aggregates because of minimum free energy. The hydrophobic parts segregate in the core, while the hydrophilic blocks constitute the shell which interacts with the external environment. The aggregation of core-forming blocks can result in the disappearance of NMR signals [20, 23, 39]. Thus, ^{1}H NMR analysis in selective solvents provides an insight into the self-assembly process of PNIPAAm-*b*-PLA-*b*-PNIPAAm [23].

Figure 2.7 shows the ^{1}H NMR spectra of triblock copolymer T1 in $CDCl_3$ and in deuterated water (D_2O). $CDCl_3$ is a good solvent for PNIPAAm and PLLA, and signals of both blocks are observed. The signals at 3.94 and 1.09 ppm are assigned to the protons of PNIPAAm, while those at 5.11 and 1.52 ppm are characteristic of the

protons from PLLA. On the other hand, D_2O only solubilizes hydrophilic PNIPAAm segments of the copolymer. As a consequence, only signals corresponding to PNIPAAm are detected (Figure 2.7B). Signals belonging to PLLA block disappear due to the limited molecular motion of the moiety in aqueous medium. This finding confirmed the formation of micelles composed of a hydrophobic PLLA core and a hydrophilic PNIPAAm shell.

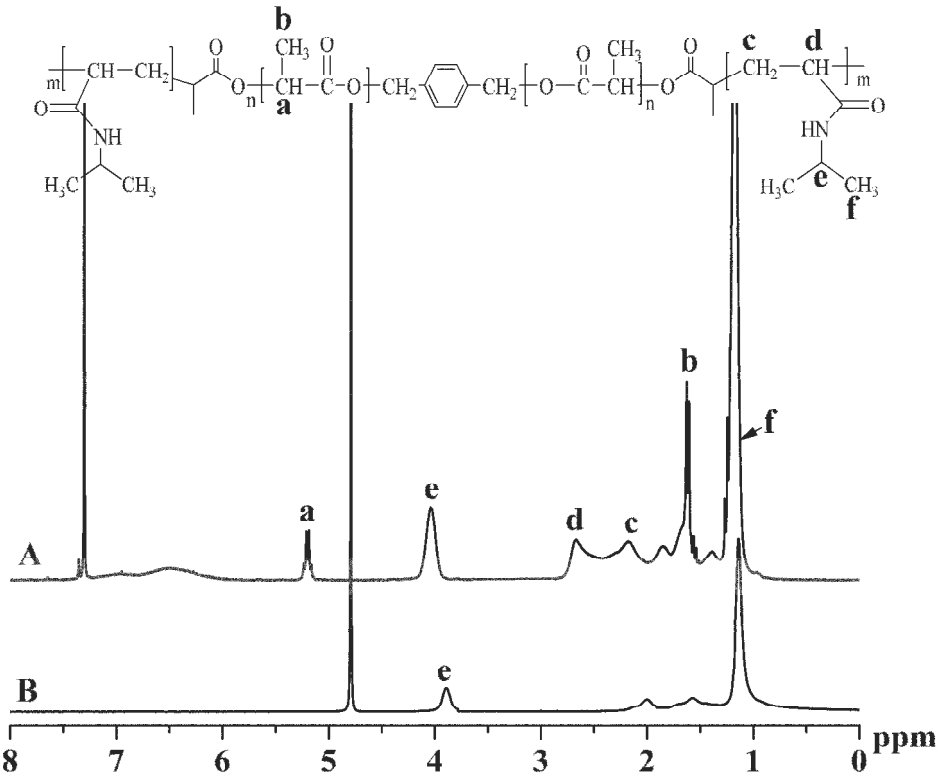

Figure 2.7 ^{1}H NMR spectra of PNIPAAm-*b*-PLLA-*b*-PNIPAAm triblock copolymer T1 in (A) $CDCl_3$ and (B) D_2O.

The critical micellar concentration (CMC) of PNIPAAm-*b*-PLLA-*b*-PNIPAAm copolymers was determined by fluorescence spectroscopy using pyrene as the fluorescent probe [40]. All measurements were performed at room temperature to ensure the solubilization in water of the PNIPAAm moieties. Figure 2.8A shows an overlay of excitation spectra of pyrene (6×10^{-7} M) at different copolymer concentrations. When the copolymer concentration of pyrene containing solutions

increases above the CMC, significant changes are observed on the excitation spectra due to the transfer of free pyrene molecules into the hydrophobic micellar core.

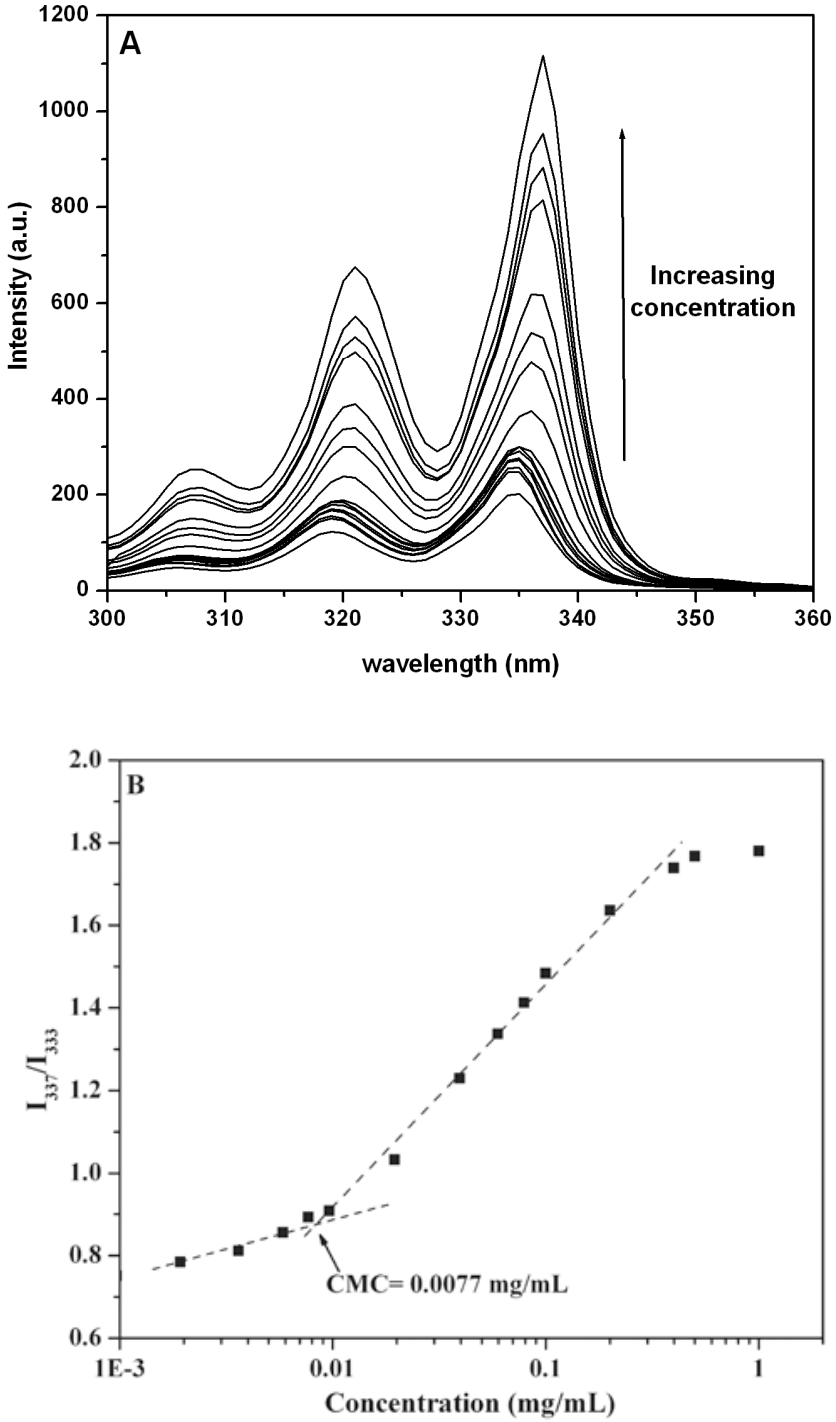

Figure 2.8 Fluorescence excitation spectra (λ_{em}=394 nm) of pyrene (6×10^{-7} M) in aqueous solutions of PNIPAAm-*b*-PLLA-*b*-PNIPAAm triblock copolymer (T1) (A); Plots of the intensity ratios (I_{337}/I_{333} from pyrene excitation spectra) *vs.* the concentration of PNIPAAm-*b*-PLLA-*b*-PNIPAAm copolymer (T1) in water (B).

Figure 2.8B shows the plots of the I_{337}/I_{333} intensity ratio against the copolymer concentration. The intensity ratio exhibits a substantial increase at a particular concentration, indicating the incorporation of pyrene into micelles. The CMC of the different triblock copolymers was obtained from the intersection of the two linear regression lines of the plot. The values range from 0.0077 to 0.016 mg mL^{-1} (Table 2.2), which are much lower than those of PNIPAAm-*b*-PLA diblock copolymers described by Fukashi *et al.* [16]. Copolymers with longer PNIPAAm block exhibits higher CMC due to higher hydrophilicity. In all cases, the very low CMC indicates the strong tendency of triblock copolymers to self-assemble into highly stable micelles in aqueous medium.

2.3.3 Morphology and size distribution of micelles

The size distribution and the morphology of micelles were investigated by DLS and TEM, respectively. Figure 2.9A shows the TEM image of the copolymer T4. Most micelles are spherical in shape with small size (78~120 nm). Few aggregated particles are also detected. A typical DLS graph of T4 micelles at 1 mg mL^{-1} is shown in Figure 2.9B. The average diameter is 83 nm with a dispersity index of 0.167. The observed monomodal size distribution indicates the formation of micelles with relatively similar sizes. Figure 2.9B also shows the plot of the correlation coefficient *versus* the decay time. The observed curve confirms a monomodal size distribution of micelles [10].

The difference between TEM and DLS data could be attributed to the experimental conditions. In fact, DLS determines the hydrodynamic diameter of micelles in aqueous solutions, whereas TEM shows the dehydrated solid state of micelles. Table 2.2 shows the DLS data of all copolymer micelles in water at 25 ^{o}C. The average diameter ranges from 31 to 83 nm with narrow size distribution ($Đ$ = 0.167-0.220), which are smaller than that of PNIPAAm-PCL-PNIPAAm triblock polymer micelles (92-125 nm) reported by Loh *et al.* [29]. The size of micelles increases with

increasing ratio of NIPAAm to LA units. Copolymers with longer PNIPAAm blocks tend to form larger micelle size because hydrophilic PNIPAAm blocks are extended in water below LCST.

Table 2.2 Characterization of PNIPAAm-*b*-PLLA-*b*-PNIPAAm triblock copolymer micelles.

Run	[NIPAAm]/[LA]	*LCST*[a] (°C)	*CMC*[b] (mg mL^{-1})	D_H[c] (nm)	*PDI*[c]
T1	2.4	32.1	0.0077	31	0.210
T2	4.2	32.3	0.0088	64	0.210
T3	5.4	32.4	0.0098	71	0.118
T4	6.9	32.8	0.0160	83	0.167

a) determined from turbidimetry measurements at 3 mg mL^{-1}.

b) determined at 25 °C by fluorescence using pyrene as fluorescent probe.

c) determined at 25 °C by dynamic light scattering at 1 mg mL^{-1}

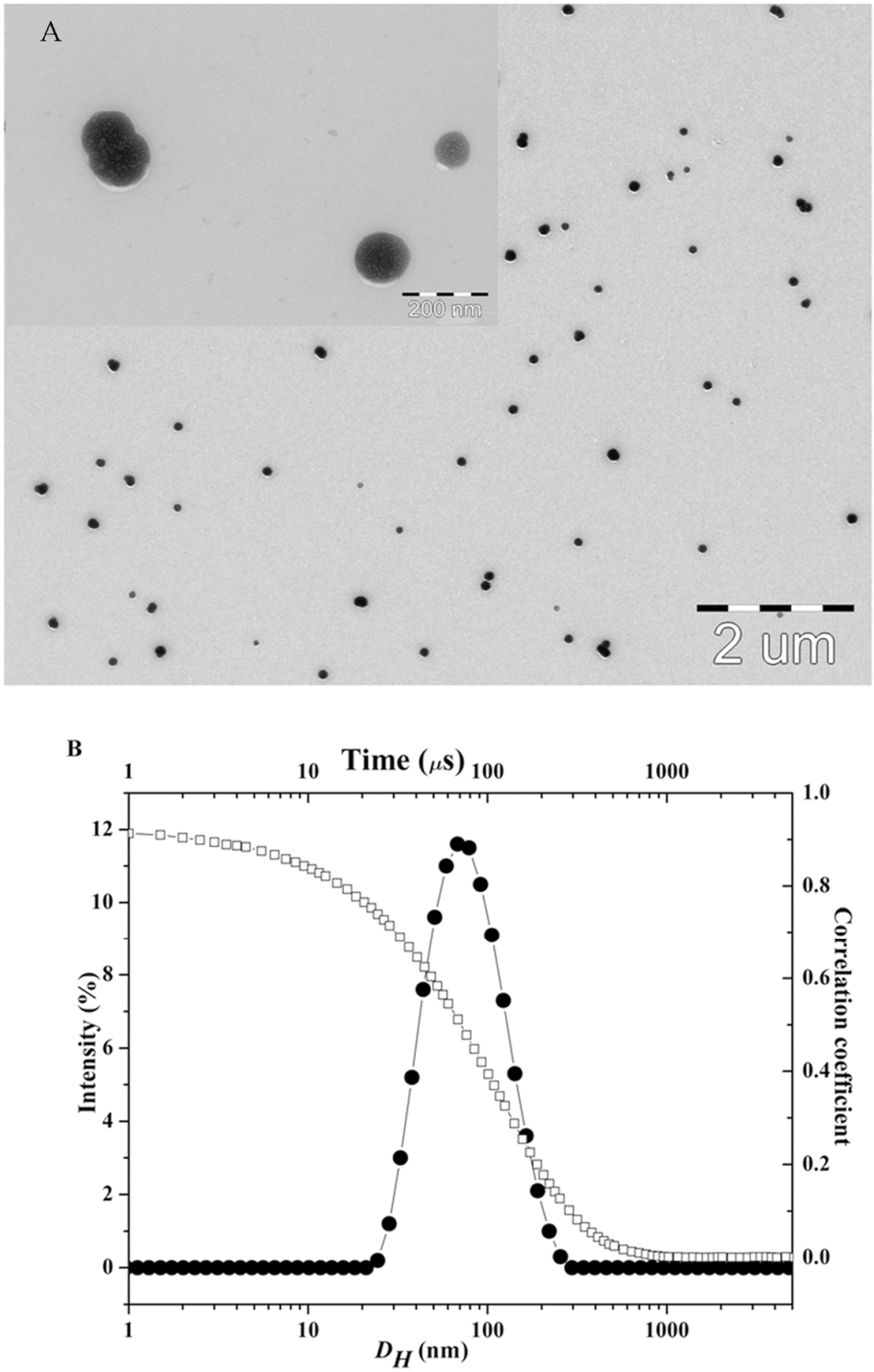

Figure 2.9 TEM (A) and DLS (B) results of self-assembling micelles of copolymer T4 at 1.0 mg mL^{-1}.

2.3.4 Thermo-responsive behavior of micelles

PNIPAAm exhibits a LCST of 32 °C which is relatively insensitive to variation of the environmental conditions. Thermo-responsive polymers become insoluble when the temperature increases above the LCST due to coil to globule transition. This phase transition can be evidenced by light transmission measurements of a micelle solution as a function of temperature.

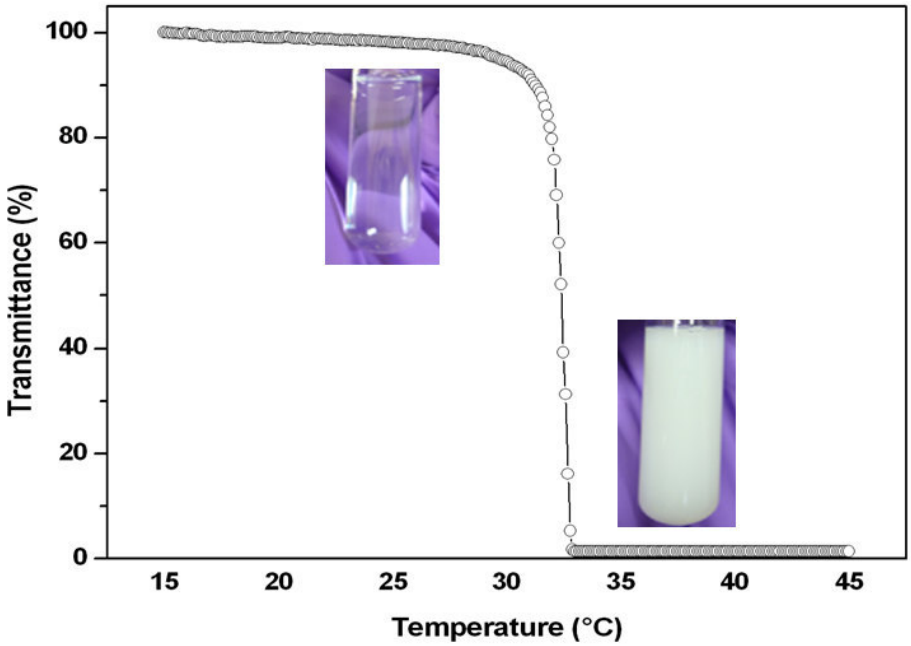

Figure 2.10 Plot of transmittance changes as a function of temperature for aqueous solution (3.0 mg mL^{-1}) of triblock copolymer T2.

Figure 2.10 shows a typical phase transition of copolymer T2 at 3.0 mg mL^{-1}. A sharp light transmittance decrease from 100 to 0 % is observed at 32.3 ^{o}C, which indicates phase transition from a transparent solution to a precipitated suspension. Varying the [NIPAAm]/[LLA] ratio from 2.4 to 6.9, the LCST only slightly increases from 32.1 to 32.8 ^{o}C (Table 2.2). Copolymer T1 exhibits the lowest LCST (32.1 ^{o}C) because of the highest hydrophobic PLLA content. In contrast, copolymer T4 with the highest PNIPAAm content shows the highest LCST at 32.8 ^{o}C. However, the LCST variation is very limited although higher hydrophobic PLLA content favors copolymer precipitation. Actually, the length of PNIPAAm blocks has no substantial effect on

the LCST since the hydrogen-bonding between PNIPAAm chains and neighboring water molecules leads to flat LCST behavior with little block length dependence [40-42]. Similar findings were previously reported in the literature [24].

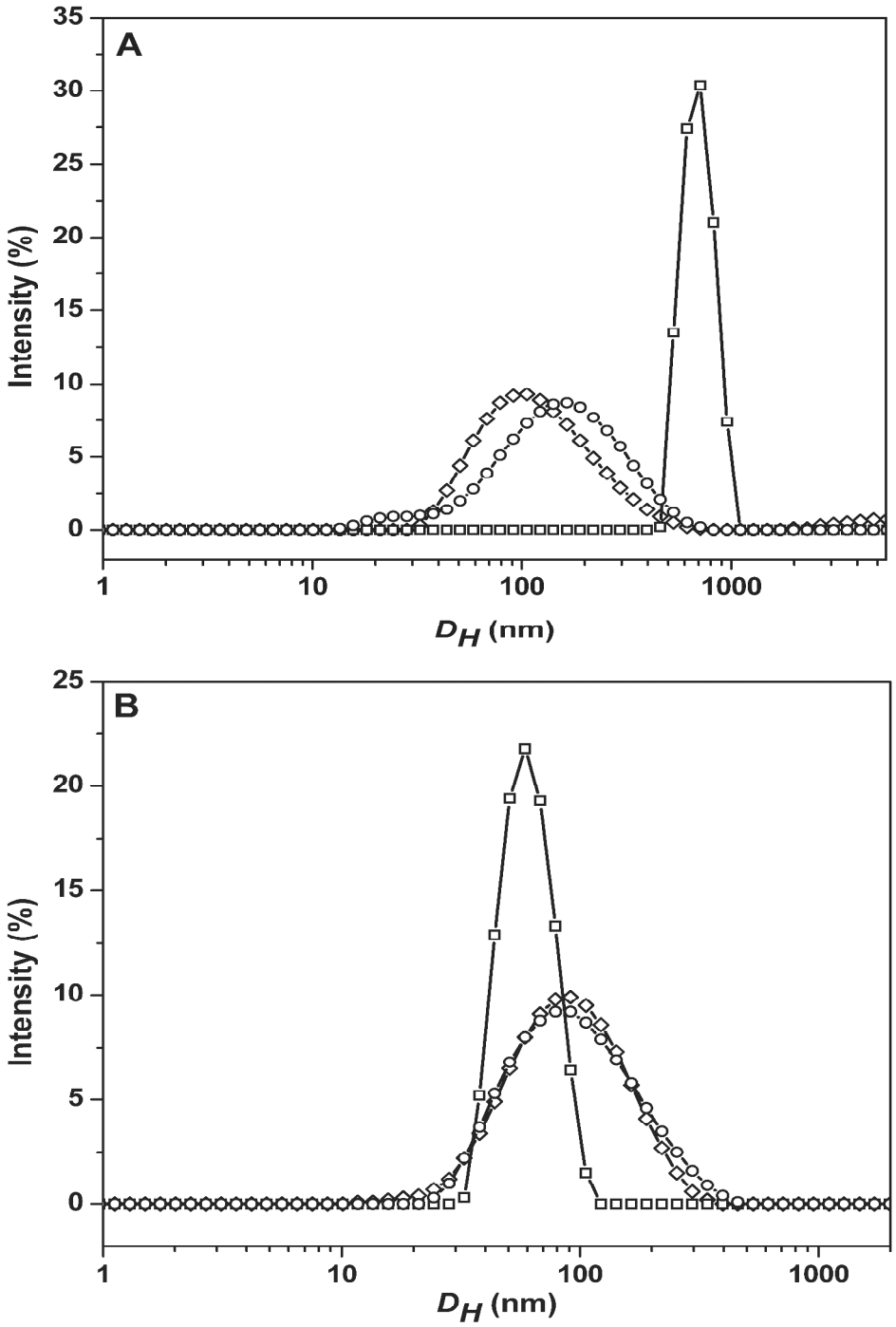

Figure 2.11 Hydrodynamic diameter distributions obtained for micelles of copolymer T2: (A) at a concentration of 3 mg mL^{-1}, and (B) at a concentration of 0.2 mg mL^{-1}. (◇) T= 20 °C, (□) T= 40 °C, (○) T= 20 °C

The thermo-responsive behavior of micelles was illustrated by DLS measurements (Figure 2.11). In the case of high copolymer concentration (3.0 mg mL^{-1}), the size of the micelles increases from 100 nm to 654 nm when the temperature is raised from 20 to 40 ^{o}C (Figure 2.11A). On the contrary, in the case of low concentrations (0.2 mg mL^{-1}), the micelles exhibit a totally different thermo-responsive behavior. The diameter of micelles decreases from 82 nm at 20 ^{o}C to 63 nm at 40 ^{o}C (Figure 2.11B). In both cases, the initial micelle sizes are recovered after cooling the solution down to room temperature.

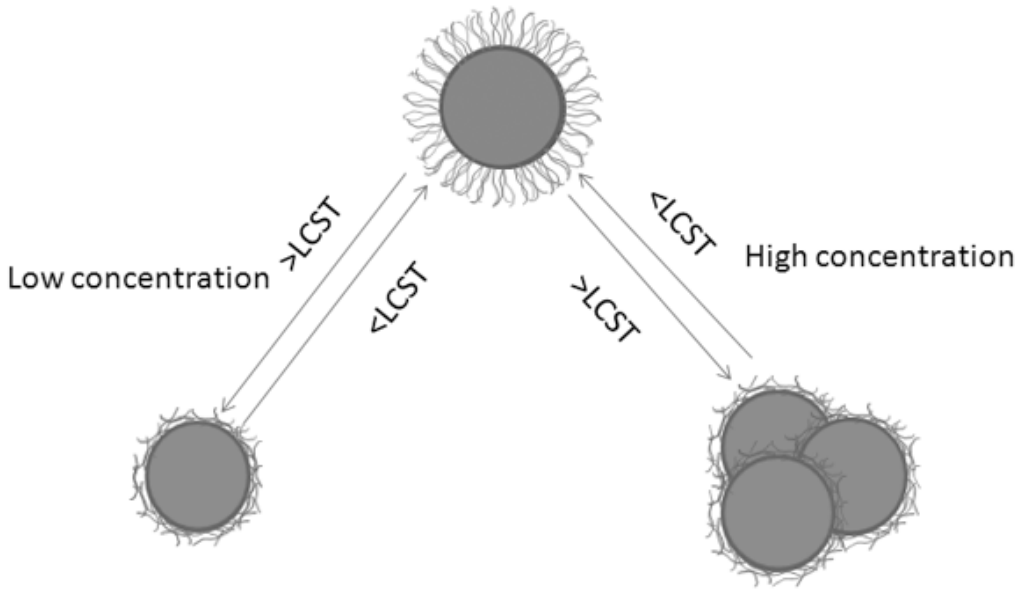

Scheme 2.2 Illustration of the temperature responsive behavior of micelles with varying temperatures across the LCST at low or high concentrations

These findings could be explained as follows (Scheme 2.2). PNIPAAm-*b*-PLLA-*b*-PNIPAAm copolymers form micelles in water at 25 ^{o}C with a hydrophobic PLA core and a hydrophilic PNIPAAm corona. As the temperature increases, PNIPAAm chains become hydrophobic and eventually collapse. Micelles aggregate to form larger particles with increased hydrophobicity of PNIPAAm [6, 7]. On the other hand, at low concentrations, PNIPAAm chains at the outer shell collapse

above the LCST, leading to decrease of micelle size. Micelles are well separated from each other and can hardly aggregate.

Triblock copolymer micelles composed of degradable PLLA core and thermo-responsive PNIPAAm corona exhibit nano-scale sizes and very low CMC values. Once loaded with a hydrophobic drug, the micelles could be easily administered by intravenous injection. With degradation of PLA, the drug would be gradually released and the micelles would dissociate into PNIPAAm chains. It is noteworthy that PNIPAAm with molecular weight below 50000 g mol^{-1} exhibits no toxicity during long-term circulation and can be excreted by glomerular filtration [16, 43, 44]. Therefore, amphiphilic PNIPAAm-*b*-PLLA-*b*-PNIPAAm triblock copolymers appear very promising as carrier of hydrophobic drugs.

2.4 Conclusion

In this work, a series of novel well-defined amphiphilic PNIPAAm-*b*-PLLA-*b*-PNIPAAm triblock copolymers were successfully synthesized by combining ROP and ATRP under mild conditions. The resulting copolymers present well controlled molecular weight and narrow dispersity, and are susceptible to self-assemble into spherical micelles in aqueous medium. The CMC of the copolymers ranges from 0.0077 to 0.016 mg mL^{-1}. The very low CMC values demonstrate the strong tendency of copolymers toward formation of micelles. The LCST of the copolymer is in the range of 32.1-32.8 ^{o}C. Both the CMC and LCST increase with increasing PNIPAAm block length. The size of micelles obtained from DLS ranges from 31 to 83 nm with narrow distributions. The micelles exhibit different thermo-responsive behaviors at high or low concentrations. At high concentrations (3.0 mg mL^{-1}), aggregation of micelles occurs when the temperature is raised above the LCST, leading to micelle size increase. In contrast, at low concentrations (0.2 mg mL^{-1}), a decrease of micellesize is detected because of the collapse of PNIPAAm blocks above the LCST.

Therefore, PNIPAAm-*b*-PLLA-*b*-PNIPAAm triblock copolymer micelles appear very promising for application as drug carrier. Future work is underway to prepare PNIPAAm/PLLA-based triblock copolymers with LSCT above the physiological temperature (37 ^{o}C) by addition of a third comonomer, using similar ROP and ATRP methods.

2.5 References

[1] E. L. Thomas, The ABCs of Self-Assembly. Science 286 (1999) 1307.

[2] Y. Yan, G. K. Such, A. P. R. Johnston, J. P. Best, F. Caruso, Engineering Particles for Therapeutic Delivery: Prospects and Challenges. ACS Nano 6 (2012) 3663-3669.

[3] C. Oerlemans, W. Bult, M. Bos, G. Storm, J.F. Nijsen, W. Hennink, Polymeric Micelles in Anticancer Therapy: Targeting, Imaging and Triggered Release. Pharm. Res. 27 (2010) 2569-2589.

[4] A. L. Monica, L. Adams, G. S. Kwon, Amphiphilic Block Copolymers for Drug Delivery. J. Pharm. Sci. 92 (2003) 1343-1355.

[5] A. K. Bajpai, S. K. Shukla, S. Bhanu, S. Kankane, Responsive polymers in controlled drug delivery. Prog. Polym. Sci. 33. (2008) 1088-1118.

[6] B. Guillerm, V. Darcos, V. Lapinte, S. Monge, J. Coudane, J. J. Robin, Synthesis and evaluation of triazole-linked poly(ε-caprolactone)-graft-poly(2-methyl-2-oxazoline) copolymers as potential drug carriers. Chem.Commun. 48 (2012) 2879-2881.

[7] H. senff, W. Richtering., Influence of cross-link density on rheological properties of temperature-sensitive microgel suspensions. Collioid polym sci 278 (2000) 830-840.

[8] H. Wei, S. X. Cheng, X. Z. Zhang, R. X. Zhuo, Thermo-sensitive polymeric micelles based on poly(*N*-isopropylacrylamide) as drug carriers. Prog. Polym. Sci. 34 (2009) 893-910.

[9] S. Q. Liu, N. Wiradharma, S. J. Gao, Y. W. Tong, Y. Y. Yang, Bio-functional micelles self-assembled from a folate-conjugated block copolymer for targeted intracellular delivery of anticancer drugs. Biomaterials 28 (2007) 1423-1433.

[10] B. Y. Du, A. X. Mei, Y. Yang, Q. F. Zhang, Q. Wang, J. T. Xu, Z. Q. Fan, Synthesis and micelle behavior of (PNIPAm-PtBA-PNIPAm)m amphiphilic multiblock copolymer. Polymer 51 (2010) 3497-3502.

[11] T. H. Qu, A. R. Wang, J. F. Yuan, J. H. Shi, Q. Y. Gao, Preparation and characterization of thermo-responsive amphiphilic triblock copolymer and its self-assembled micelle for controlled drug release. Colloids Surf. B: Biointerfaces 72 (2009) 94-100.

[12] S. M. Li, I. Rashkov, J. L. Espartero, N. Manolova, M. Vert, Synthesis, characterization, and hydrolytic degradation of PLA/PEO/PLA triblock copolymers with long poly(L-lactic acid) blocks. Macromolecules 29 (1996) 57-62.

[13] A. C. Albertsson, I. Varma, Degradable Aliphatic Polyesters, Vol. 157, Springer Berlin Heidelberg, 2002, pp. 1-40.

[14] G. S. He, L. L. Ma, J. Pan, S. Venkatraman, ABA and BAB type triblock copolymers of PEG and PLA: A comparative study of drug release properties and "stealth" particle characteristics. Int. J. Pharm. 334 (2007) 48-55.
[15] L. Yang, A. El Ghzaoui, S. M. Li, In vitro degradation behavior of poly(lactide)-poly(ethylene glycol) block copolymer micelles in aqueous solution. Int. J. Pharm. 400 (2010) 96-103.
[16] K. Fukashi, S. Kiyotaka, A. Takao, Y. Masayuki, S. Yasuhisa, O. Teruo, Preparation and characterization of thermally responsive block copolymer micelles comprising poly(*N*-isopropylacrylamide-*b*-DLlactide). J. Controlled Release 55 (1998) 87-98.
[17] S. Q. Liu, Y. Y. Yang, X. M. Liu, Y. W. Tong, Preparation and Characterization of Temperature-Sensitive Poly(*N*-isopropylacrylamide)-*b*-poly(d,l-lactide) Microspheres for Protein Delivery. Biomacromolecules 4 (2003) 1784-1793.
[18] J. Qin, Y. S. Jo, J. E. Ihm, D. K. Kim, M. Muhammed, Thermosensitive Nanospheres with a Gold Layer Revealed as Low-Cytotoxic Drug Vehicles. Langmuir 21 (2005) 9346-9351.
[19] E. Ayano, M. Karaki, T. Ishihara, H. Kanazawa, T. Okano, Poly(*N*-isopropylacrylamide)-PLA and PLA blend nanoparticles for temperature-controllable drug release and intracellular uptake. Colloids Surf. B: Biointerfaces 99 (2012) 67-73.
[20] H. Wei, X. Z. Zhang, C. Cheng, S. X. Cheng, R. X. Zhuo, Self-assembled, thermosensitive micelles of a star block copolymer based on PMMA and PNIPAAm for controlled drug delivery. Biomaterials 28 (2007) 99-107.
[21] K. Matyjaszewski, J. H. Xia, Atom Transfer Radical Polymerization. Chem. Rev. 101 (2001) 2921-2990.
[22] T. E. Patten, J. H. Xia, T. Abernathy, K. Matyjaszewski, Polymers with very low polydispersities from atom transfer radical polymerization. Science 272 (1996) 866-868.
[23] M. Hales, C. Barner-Kowollik, T. P. Davis, M. H. Stenzel, Shell-Cross-Linked Vesicles Synthesized from Block Copolymers of Poly(D,L-lactide) and Poly(*N*-isopropylacrylamide) as Thermoresponsive Nanocontainers. Langmuir 20 (2004) 10809-10817.
[24] Y. Z. You, C. Y. Hong, W. P. Wang, W. Q. Lu, C. Y. Pan, Preparation and Characterization of Thermally Responsive and Biodegradable Block Copolymer Comprised of PNIPAAM and PLA by Combination of ROP and RAFT Methods. Macromolecules 37 (2004) 9761-9767.
[25] J. Akimoto, M. Nakayama, K. Sakai, T. Okano, Molecular Design of Outermost Surface Functionalized Thermoresponsive Polymeric Micelles with Biodegradable Cores. J. Polym. Sci. Polym. Chem. 46 (2008) 7127-7137.
[26] J. Akimoto, M. Nakayama, K. Sakai, T. Okano, Temperature-Induced Intracellular Uptake of Thermoresponsive Polymeric Micelles. Biomacromolecules 10 (2009) 1331-1336.
[27] J. Akimoto, M. Nakayama, K. Sakai, T. Okano, Thermally Controlled Intracellular Uptake System of Polymeric Micelles Possessing Poly(*N*-isopropylacrylamide)-Based Outer Coronas. Mol. Pharm. 7 (2010) 926-935.
[28] Y. Bakkour, V. Darcos, F. Coumes, S. Li, J. Coudane, Brush-like amphiphilic copolymers based on polylactide and poly(ethylene glycol): Synthesis, self-assembly and evaluation as drug carrier. Polymer 54 (2013) 1746-1754.
[29] X. J. Loh, Y. L. Wu, W. T. J. Seow, M. N. I. Norimzan, Z. X. Zhang, F. Xu, E. T. Kang, K. G. Neoh, J. Li, Micellization and phase transition behavior of thermosensitive

poly(*N*-isopropylacrylamide)-poly(ε-caprolactone)-poly (*N*-isopropylacrylamide) triblock copolymers. Polymer 49 (2008) 5084-5094.
[30] G. Masci, L. Giacomelli, V. Crescenzi, Atom transfer radical polymerization of *N*-isopropylacrylamide. Macromol. Rapid Commun. 25 (2004) 559-564.
[31] J. D. Ye, R. Narain, Water-Assisted Atom Transfer Radical Polymerization of *N*-Isopropylacrylamide: Nature of Solvent and Temperature. J. Phys. Chem. B 113 (2009) 676-681.
[32] E. J. Lobb, I. Ma, N. C. Billingham, S. P. Armes, A. L. Lewis, Facile Synthesis of Well-Defined, Biocompatible Phosphorylcholine-Based Methacrylate Copolymers via Atom Transfer Radical Polymerization at 20 ^{O}C. J. Am. Chem. Soc. 123 (2001) 7913-7914.
[33] X. Lu, L. Zhang, L. Meng, Y. Liu, Synthesis of poly(*N*-isopropylacrylamide) by ATRP using a fluorescein-based initiator. Polym. Bull. 59 (2007) 195-206.
[34] H. Fischer, The Persistent Radical Effect In living Radical Polymerization. Macromolecules 30 (1997) 5666-5672.
[35] H. Fischer, The persistent radical effect in controlled radical polymerizations. J. Polym. Sci. Part A: Polym. Chem. 37 (1999) 1885-1901.
[36] K. Ohno, Y. Tsujii, T. Miyamoto, T. Fukuda, M. Goto, K. Kobayashi, T. Akaike, Synthesis of a Well-Defined Glycopolymer by Nitroxide-Controlled Free Radical Polymerization. Macromolecules 31 (1998) 1064-1069.
[37] T. Fukuda, A. Goto, K. Ohno, Mechanisms and kinetics of living radical polymerizations. Macromol. Rapid Commun. 21 (2000) 151-165.
[38] E. Berndt, M. Ulbricht, Synthesis of block copolymers for surface functionalization with stimuli-responsive macromolecules. Polymer 50 (2009) 5181-5191.
[39] H. Walderhaug, O. Soderman, NMR studies of block copolymer micelles. Curr. Opin. Colloid Interface Sci. 14 (2009) 171-177.
[40] X. J. Loh, Z. X. Zhang, Y. L. Wu, T. S. Lee, J. Li, Synthesis of Novel Biodegradable Thermoresponsive Triblock Copolymers Based on Poly[(R)-3-hydroxybutyrate] and Poly(*N*-isopropylacrylamide) and Their Formation of Thermoresponsive Micelles. Macromolecules 42 (2009) 194-202.
[41] S. Fujishige, K. Kubota, I. Ando, Phase-Transition of Aqueous-Solutions of Poly(*N*-isopropylacrylamide) and Poly(*N*-isopropylmethacrylamide). J. Phys. Chem. 93 (1989) 3311-3313.
[42] Y. Okada, F. Tanaka, Cooperative Hydration, Chain Collapse, and Flat LCST Behavior in Aqueous Poly(*N*-isopropylacrylamide) Solutions. Macromolecules 38 (2005) 4465-4471.
[43] C. Chang, H. Wei, C.Y. Quan, Y.Y. Li, J. Liu, Z.C. Wang, S.X. Cheng, X.Z. Zhang, R.X. Zhuo, Fabrication of thermosensitive PCL-PNIPAAm-PCL triblock copolymeric micelles for drug delivery. J. Polym. Sci. Pol. Chem. 46 (2008) 3048-3057.
[44] S. Cammas, K. Suzuki, C. Sone, Y. Sakurai, K. Kataoka, T. Okano, Thermo-responsive polymer nanoparticles with a core-shell micelle structure as site-specific drug carriers. J. Controlled Release 48 (1997) 157-164.

Chapter 3 Tunable thermo-responsive P(NIPAAm-*co*-DMAAm)-*b*-PLLA-*b*-P(NIPAAm-*co*-DMAAm) triblock copolymer micelles as drug carrier

Abstract: Thermo-responsive triblock copolymers were synthesized by atom transfer radical polymerization of *N*-isopropylacrylamide (NIPAAm) and *N,N*-dimethylacrylamide (DMAAm) using α,ω-bromopropionyl poly(L-lactide) as macroinitiator and a CuCl/tris(2-dimethylaminoethyl) amine (Me_6TREN) complex as catalyst. The polymerization was realized at 25 ^{o}C in a DMF/water mixture. DMAAm was incorporated in the copolymer as a hydrophilic comonomer in order to tune the lower critical solution temperature (LCST). The LCST increases linearly from 32.2 ^{o}C to 39.1 ^{o}C with increasing the DMAAm content from 0 to 24 %. The phase transition of polymeric micelles at the LCST occurs in a narrow temperature interval below 0.5 ^{o}C. Reversible size changes are observed when the temperature increases from 25 ^{o}C to 45 ^{o}C and then decreases down to 25 ^{o}C. Nano-size micelles (37 to 54 nm) with narrow distribution were obtained by self-assembly of amphiphilic copolymers in aqueous medium. The critical micelle concentration (CMC) ranges from 0.010 to 0.015 mg mL^{-1}. *In vitro* drug release studies show a much faster release at temperatures above the LCST. MTT assay was conducted to evaluate the cytotoxicity of copolymers. The nano-scale size, low CMC, rapid phase transition, LCST slightly above the body temperature and thermo-responsive drug release indicate that these copolymers could be potential candidates for applications in targeted delivery of drugs.

Keywords: thermo-responsive copolymer; poly(*N*-isopropylacrylamide); poly(L-lactide)

3.1 Introduction

Recently, “smart micelles” derived from stimuli-responsive polymers have drawn great attention as drug delivery systems (DDS) [1-3]. Among them, thermo-sensitive copolymers based on poly(*N*-isopropylacrylamide) (PNIPAAm) have been widely investigated, notably to build polymeric micelles for controlled delivery of anticancer drugs or DNA [4-10]. PNIPAAm could be considered as the “gold standard” thermo-responsive polymer with a lower critical solution temperature (LCST) around 32 ^{o}C, which is induced by a reversible hydration-dehydration transition [11, 12]. Variation of pH, concentration, chemical structure or biological environment only slightly affects the LCST. However, these copolymers are not degradable, which limits their potential applications as drug carrier.

As a biodegradable polymer, polylactide (PLA) has been extensively investigated for biomedical and pharmaceutical applications such as controlled drug release systems, medical implants and scaffolds in tissue engineering [13-16]. Block copolymers based on PNIPAAm and PLA combine both the thermo-sensitivity of PNIPAAm and the degradability of PLA [17-22]. Increasing the temperature above the LCST results in collapse of micelles and burst-like release of encapsulated drug [21]. Thus temporal drug delivery could be achieved by using thermo-sensitive and degradable polymeric micelles based on PLA and PNIPAAm.

The PNIPAAm moiety is supposed to be soluble in the blood stream, and becomes insoluble after accumulation in a locally heated tumor tissue. This property could be exploited for targeted delivery of drugs [23-26]. Therefore, polymeric micelles should be designed so as to exhibit a LCST slightly above the body temperature. Introduction of hydrophilic acrylamide comonomers such as dimethyl acrylamide (DMAAm) in PNIPAAm chains has been used to increase the LCST of the resulting copolymers. Most of the P(NIPAAm-*co*-DMAAm)-*b*-PLA diblock copolymers described in the literature were synthesized by combination of free radical polymerization and

ring-opening polymerization (ROP) [27-33]. The resulting copolymers exhibit poor compositions and large molecular weight distributions (dispersity $Đ$>2), which led to a broad phase transition at the LCST. Later on, Akimoto *et al.* synthesized well-defined P(NIPAAm-*co*-DMAAm)-*b*-PLA diblock copolymers by combination of reversible addition-fragmentation chain transfer polymerization (RAFT) and ROP [34-37]. The terminal dithiobenzoate (DTBz) groups were reduced to thiolgroups and reacted with maleimide (Mal). In aqueous media, the resulting copolymers formed surface-functionalized thermo-responsive micelles, hydrophobic DTBz-surface micelles demonstrating a significant lower LCST (30.7 °C) than Mal-surface micelles (40.0 °C). The LCST of micelle mixtures can be varied by changing the ratio of DTBz/Mal end-functional diblock copolymers [34]. The authors also studied thermally controlled intracellular uptake of copolymer micelle [35, 36]. Li *et al.* reported similar maleimide end-functional P(NIPAAm-*co*-DMAAm)-*b*-PLA and P(NIPAAm-*co*-DMAAm)-*b*-PCL copolymers with LCST of 39 °C and 40.5 °C, respectively [37]. Both the adriamycin release and the intracellular uptake were enhanced at 40 ° C as compared to 37 °C. However, precise tuning of the LCST could not be achieved by modification of end groups or mixing two copolymers with different end groups.

In the previous chapter, we reported the synthesis of thermo-sensitive PNIPAAm-*b*-PLA-*b*-PNIPAAm triblock copolymers by atom transfer radical polymerization (ATRP) using α, ω-bromopropionyl poly(L-lactide) (PLLA) as macroinitiator [38]. Excellent control over the molecular weights was achieved under mild conditions. The kinetics of polymerization and the self-assembly behavior of the resulting copolymers were investigated. However, the LCST of the copolymers ranges from 32.1 to 32.8 °C, *i.e.* much lower than the body temperature.

In this chapter, thermo-responsive and biodegradable P(NIPAAm-*co*-DMAAm)-*b*-PLLA-*b*-P(NIPAAm-*co*-DMAAm) triblock copolymers

were prepared *via* combination of ROP and ATRP. A DMAAm comonomer was introduced in order to tune the LCST slightly above body temperature for targeted drug delivery. The resulting copolymers were fully characterized by ^{1}H NMR, SEC and DOSY NMR. The physico-chemical properties of copolymer micelles were investigated in aqueous media. MTT assay was carried out to evaluate the cytotoxity of copolymers. The drug release behavior of micelles containing an antimicrobial agent, Amphotericin B, was investigated below and above the LCST.

3.2 Experimental Methods

3.2.1 Materials

L-lactide was purchased from Purac Biochem (Goerinchem, The Netherlands). Stannous 2-ethylhexanoate ($Sn(Oct)_2$), 1,4-benzene dimethanol, 2-bromopropionyl bromide, tris(2-dimethyl aminoethyl) amine (Me_6TREN), copper (I) chloride (CuCl), *N, N*-dimethyl formamide (DMF) and Amphotericin B were obtained from Sigma-Aldrich (St-Quentin Fallavier, France), and were used without further purification. Dichloromethane and toluene from Sigma-Aldrich were dried over calcium hydride for 24 h at room temperature and distilled under reduced pressure. NIPAAm and DMAAm were obtained from Sigma-Aldrich and purified through a basic aluminum oxide column. Triethylamine (Sigma-Aldrich) was dried over potassium hydroxyde for 24 h at room temperature and distilled. Ultrapure water with a conductivity of 18 MΩ was produced using a Millipore Milli-Q water system.

α,ω-bromopropionyl PLLA (Br-PLLA-Br) was prepared as previously reported [38].

3.2.2 Typical synthesis of P(NIPAAm-*co*-DMAAm)-*b*-PLLA-*b*-P(NIPAAm-*co*-DMAAm) *(Run T4, Table 3.2)*

Triblock copolymers were prepared using standard Schlenk technique. Typically, 100 mg Br-PLLA-Br (30.4×10^{-3} mmol, $M_{n,NMR}$=3300 g mol^{-1}), 572 mg NIPAAm (5.06 m mol), 1.07 mL DMAAm (1.03 mmol) and 6.0 mg CuCl (60.8×10^{-3} mmol) were dissolved in 3 mL DMF in a Schlenk tube. 0.6 mL H_2O was then added. After five freeze-pump-thaw cycles, 16 µL Me_6TREN (60.8×10^{-3} mmol) was added under argon atmosphere. The mixture was stirred at 25 ^oC for 1 h. The reaction was stopped by precipitation in diethyl ether, and the crude product was dissolved in 10 mL chloroform. The diluted polymer solution was allowed to pass through a basic aluminum oxide column to remove the catalyst complex, concentrated under reduced pressure, and precipitated again in diethyl ether. The final product was dried under vacuum at room temperature for 24 h.

^{1}H NMR (300 MHz, $CDCl_3$) (Figure 3.1): δ (ppm) = 7.28 (s, $4H_{Ar}$), 5.20 (m, $1H_a$), 4.00 (m, $1H_e$), 2.90 (d, $3H_g$), 2.09 (t, $1H_{d+d'}$), 1.78 (d, $2H_{c+c'}$), 1.58 (d, $3H_b$), 1.13 (d, $3H_f$)

$M_{n,NMR}$ =20000 g mol^{-1}, $M_{n,SEC}$ =24000 g mol^{-1}, $Đ$ =1.13.

3.2.3 Drug release studies

Amphotericin B (AmpB, 2.5 or 5 mg) and copolymer T4 (20 mg) were dissolved in 2 mL DMSO. The solution was then dropped into 40 mL ultrapure water. After 30 min stirring, the solution was introduced into a dialysis tube (molecular weight cut off, MWCO= 3500) and dialyzed against water for 48 hours. The dialyzed solution was filtered with 0.45 µm syringe filter to remove excess drug and then lyophilized. Blank copolymer micelles were prepared using the same procedure without AmpB.

The drug content and loading efficiency were determined by UV spectroscopy. 5 mg AmpB encapsulated polymeric micelles were dissolved in DMSO. UV measurements were realized at 388 nm. The concentration of AmpB was determined using a calibration curve obtained with a series of standard AmpB solutions in DMSO. The drug loading content and loading efficiency were calculated using the following equations:

$$Drug\ loading\ (wt\%) = \frac{weight\ of\ drug\ in\ micelles}{weight\ of\ drug\ loaded\ micelles} \times 100 \quad (1)$$

$$Loading\ efficiency\ (wt\%) = \frac{weight\ of\ drug\ in\ micelles}{weight\ of\ feeding\ drug} \times 100 \quad (2)$$

Drug release studies were carried out at two different temperatures. Briefly, 5 mg lyophilized polymeric micelle was reconstituted in 5 mL ultrapure water and then introduced into a dialysis tube (MWCO: 3500). The dialysis tube was placed in 20 mL ultrapure water in oven at 37 or 38 ^{o}C. At preset time interval, the release medium was recovered for analysis and renewed with fresh ultrapure water. The drug concentration was determined by UV spectroscopy at 388 nm.

3.2.4 Cytotoxicity

The cytotoxicity of polymers was evaluated by MTT assay. After sterilization by UV for 5 h, the copolymer T4 was dissolved in dulbecco's modified eagle's meduim (DMEM, Hyclone products) at a concentration of 6 mg mL^{-1}. Then the solution was transferred to 96-well plates (Corning costar, USA), 100 μL per well. The wells were placed in an incubator (NU-4850, NuAire, USA) at 37 ^{o}C under humidified atmosphere containing 5 % CO_2 for 24 h. After incubation, the copolymer in the form of a hydrogel was used as cell culture substrate.

Mouse cardiac myocytes (MCM) and mouse embryonic fibroblasts (MEF) in logarithmic growth phase were harvested and diluted with DMEM medium (10 % calf serum, 100 μg mL^{-1} Penicillin, 100 μg mL^{-1} streptomycin) to a concentration of 1×10^{5}

cells mL^{-1}. 100 μL cellular solution was added in hydrogel containing wells which were then placed in the same incubator at 37 ^{o}C under humidified atmosphere containing 5 % CO_2. 100 μL fresh medium was used as the negative control, and 100 μL solution of phenol in water as the positive control. After 2, 3 and 4 days culture, 20 μL 3-(4,5-dimethylthiazol-2-yl)-2,5-diphenyltetrazolium bromide (MTT) at 5 mg mL^{-1} were added. The medium was removed after 6 h incubation, and 150 μL dimethylsulfoxide (DMSO) was added. After 15 min shaking, the optical density (OD) was measured by using a microplate reader (Elx800, BioTek, USA) at 490 nm.

The relative growth ratio (RGR) was calculated by using the following equation:

$$RGR\ (\%) = (OD_{test\ sample}/OD_{negative\ Control}) \times 100 \qquad (3)$$

The cytotoxicity is generally noted in 0-5 levels according to the RGR value as shown in Table 3.1.

Table 3.1 Relationship between the RGR value and cytotoxicity level

RGR (%)	≥100	75-99	50-74	25-49	1-24	0
Level	0	1	2	3	4	5

The cellular morphology was observed using an Olympus CKX41 inverted microscope. After 3 days seeding, the test medium was replaced with 150 μL neutral red staining solution (NR) for 10 min at room temperature. The plates were rinsed 3 times with warm phosphate-buffered saline (PBS), and the morphology of cells adhered to the hydrogel surface was immediately observed under microscope.

3.2.5 Characterization

Nuclear magnetic resonance (^{1}H NMR) ^{1}H NMR spectra were recorded on a Bruker spectrometer (AMX300) operating at 300 MHz. Chemical shift was referenced to the peak of residual non-deuterated solvents.

Diffusion-ordered NMR spectroscopy (DOSY NMR) DOSY 2D NMR measurements were performed at 300 K on a BrukerAvance AQS600 NMR spectrometer operating at 600 MHz and equipped with a Bruker multinuclear z-gradient inverse probe head capable of producing gradients in the z direction with strength of 55 G cm^{-1}. The DOSY spectra were acquired with the ledbpgp2s pulse program from Bruker topspin software. All spectra were recorded with 32 K time domain data points in t_2 dimension and 32 t_1 increments. The gradient strength was logarithmically incremented in 32 steps from 2 % up to 95 % of the maximum gradient strength. All measurements were performed with a compromise diffusion delay Δ of 200 ms in order to keep the relaxation contribution to the signal attenuation constant for all samples. The gradient pulse length δ was 5 ms in order to ensure full signal attenuation. The diffusion dimension of the 2D DOSY spectra was processed by means of the Bruker topspin software (version 2.1).

Size exclusion chromatography (SEC) SEC measurements were performed on a Varian 390-LC equipped with a refractive index detector and two ResiPore columns (300×7.5 mm) at 60 °C at a flow rate of 1 mL min^{-1}. The eluent was DMF containing 0.1 *wt* % LiBr. Calibration was established with PMMA standards.

Fluorescence Spectroscopy The CMC of the copolymers was determined by fluorescence spectroscopy using pyrene as a hydrophobic fluorescent probe. Measurements were carried outon an RF 5302 Shimadzu spectrofluorometer (Japan) equipped with a Xenon light source (UXL-150S, Ushio, Japan). Briefly, an aliquot of pyrene solution (6×10^{-6} M in acetone, 1 mL) was added to different vials, and the solvent was evaporated. Then, 10 mL aqueous solutions at different concentrations were added to the vials. The final concentration of pyrene in each vial was 6×10^{-7} M. After equilibrating at room temperature overnight, the fluorescence excitation spectra of the solutions were recorded from 300 to 360 nm at an emission wavelength of 394 nm. The emission and excitation slit widths were 3 and 5 nm, respectively. The

excitation fluorescence values I_{337} and I_{333}, respectively at 337 and 333 nm, were used for subsequent calculations. The CMC was determined from the intersection of linear regression lines on the I_{337}/I_{333} ratio *versus* polymer concentration plots.

Cloud point The lower critical solution temperature (LCST) was estimated from the changes in the transmittance through copolymer solutions at a concentration of 3.0 mg mL^{-1} as a function of temperature. The measurements were carried out at a wavelength of 500 nm with a Perkin Elmer Lambda 35 UV-Visible spectrometer equipped with a Peltier temperature programmer PTP-1+1. The temperature ramp was 0.1 °C min^{-1}.

Dynamic light scattering (DLS) DLS measurements were carried out with a Malvern Instrument Nano-ZS equipped with a He-Ne laser (λ = 632.8 nm). Polymer solutions at a concentration of 1.0 mg mL^{-1} were filtered through a 0.45 μm PTFE microfilter before measurements. The correlation function was analyzed via the general purpose method (NNLS) to obtain the distribution of diffusion coefficients (D) of the solutes. The apparent equivalent hydrodynamic radius (R_H) was determined from the cumulant method using the Stokes-Einstein equation:

$$R_H = \frac{K_B T}{6\pi\eta\Gamma} \quad q^2 = \frac{K_B T}{6\pi\eta D_0} \qquad (4)$$

Where k_B is Boltzmann constant, T is the temperature, Γ is the relaxation frequency, q is the wave vector, η is the viscosity of the medium, and D_0 is the translational diffusion coefficient at finite dilution. Mean radius values were obtained from triplicate runs. Standard deviations were evaluated from hydrodynamic radius distribution.

Transmission electron microscopy (TEM) TEM experiments were carried out on a JEOL 1200 EXII instrument operating at an acceleration voltage 120 kV. The samples were prepared by dropping a polymer solution at a concentration of 1.0 mg mL^{-1} onto a carbon coated copper grid, followed by air drying.

Inductively Coupled plasma-mass spectrometry (ICP-MS) The residual copper content in the copolymers was quantified using ThemoFinnigan Element XR sector field ICP-MS previously calibrated using copper solutions in water. Typically, ICPMS samples were prepared by dissolution of the copolymers in nitric acid. The solution was then heated to fully decompose the polymer until no precipitate was visible. After that, the samples were dissolved in 10 mL deionized water before analysis to determine the copper concentration. Each sample was analyzed four times.

3.3 Results and discussion

3.3.1 Synthesis of P(NIPAAm-*co*-DMAAm)-*b*-PLLA-*b*-P(NIPAAm-*co*-DMAAm) triblock copolymer

Amphiphilic thermo-sensitive triblock copolymers, namely P(NIPAAm-*co*-DMAAm)-*b*-PLLA-*b*-P(NIPAAm-*co*-DMAAm), were synthesized by ATRP of NIPAAm and DMAAm using Br-PLLA-Br as macroinitiator (Scheme 3.1).
In the first step, ring opening polymerization of L-lactide was carried out using 1,4-benzyl methanol as initiator to yield α,ω-hydroxy PLLA (HO-PLLA-OH). The targeted degree of polymerization (*DP*) of PLLA was 40 which correspond to a theoretical M_n of 2900 g mol^{-1}. The M_n of HO-PLLA-OH determined by ^{1}H NMR was 3000 g mol^{-1}, *i.e.* very close to the targeted value. Moreover, the polymer exhibited a very low dispersity ($Đ$=1.03), in agreement with a good control of the reaction. In a second step, HO-PLLA-OH reacted with 2-bromopropionyl bromide in the presence of triethylamine, yielding α,ω-bromopropionyl PLLA (Br-PLLA-Br). The incorporation of bromopropionyl moiety was evidenced by ^{1}H NMR, and the anchoring proved to be quantitative. ^{1}H NMR and SEC analyses of Br-PLLA-Br ($M_{n,NMR}$= 3300 g mol^{-1}, $Đ$= 1.04) showed a slight increase of molecular weight and

unchanged dispersity compared to the starting HO-PLLA-OH, indicating that no chain cleavage occurred during the esterification reaction.

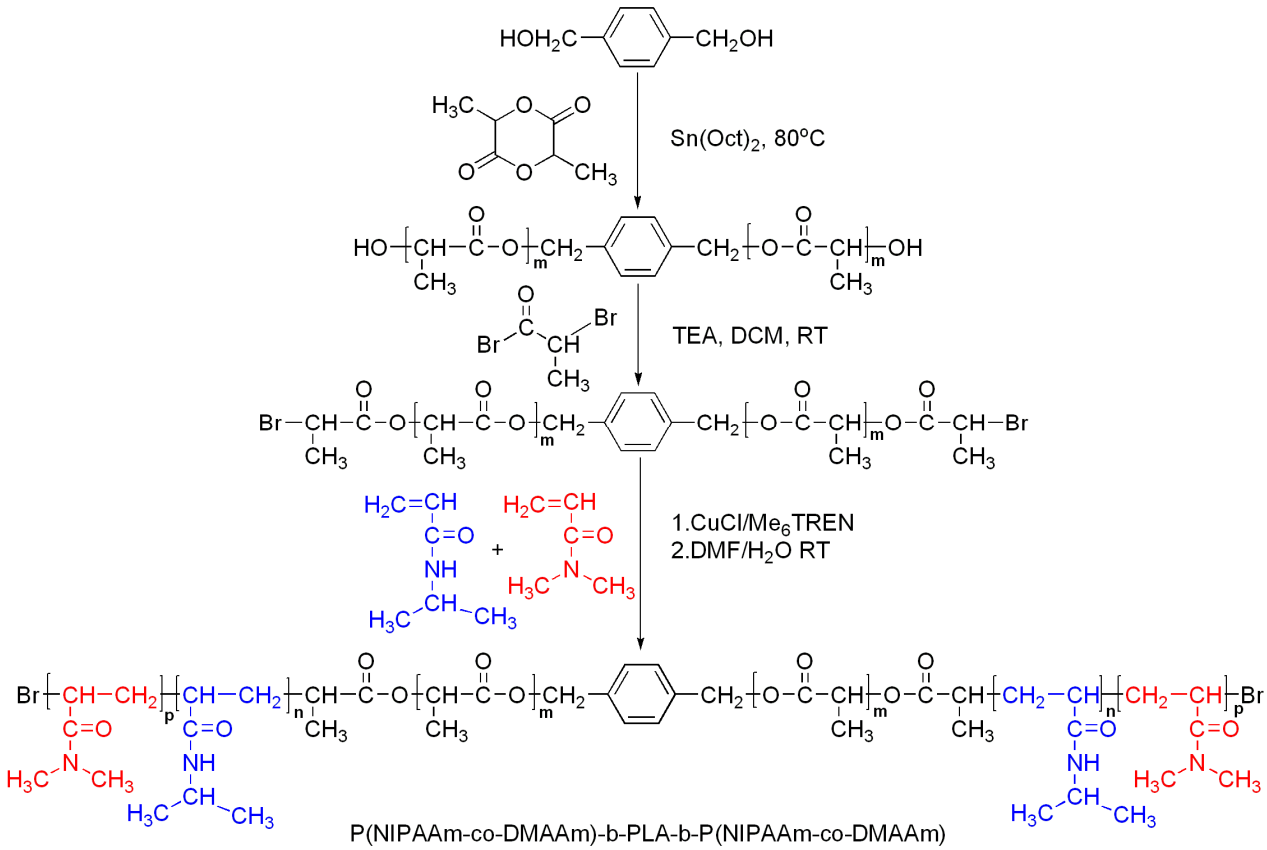

Scheme 3.1 Synthesis of P(NIPAAm-*co*-DMAAm)-*b*-PLLA-*b*-P(NIPAAm-*co*-DMAAm) triblock copolymers *via* combination of ROP and ATRP

Then, α, ω-bromopropionyl PLLA was used as macroinitiator for ATRP copolymerization of NIPAAm and DMAAm at 25 °C in a DMF/water mixture using CuCl/Me_6TREN complex as catalytic system (Scheme 3.1). A series of amphiphilic triblock copolymerswere prepared by varying the NIPAAm to DMAAm ratio, but using a constant ratio of monomers to PLLA (200 equivalents) to yield copolymers with similar molecular weights (Table 3.2). This should allow to elucidate the influence of NIPAAm to DMAAm ratio on the LCST since the effect of hydrophobic to hydrophiphilic ratio is discarded. The conversion of NIPAAm was found to be around 70 %, while the conversion of DMAAm is almost complete. This finding indicates that DMAAm exhibits higher reactivity than NIPAAm [39, 40].

Table 3.2 Characteristics of P(NIPAAm-*co*-DMAAm)-*b*-PLLA$_{40}$-*b*-P(NIPAAm-*co*-DMAAm) triblock copolymers

Run	[PLA$_{40}$]/NIPAAm /DMAAm[a]	DP$_{LA}$/DP$_{NIPAAm}$ /DP$_{DMAAm}$[b]	[NIPAAm] /[DMAAm][a]	$M_{n,NMR}$[b] g mol^{-1}	$M_{n,SEC}$[c] g mol^{-1}	$Đ$[c]
T1	1/200/0	40/172/0	100/0	22500	27000	1.10
T2	1/182.1/17.9	40/128/17	88.2/11.8	19500	25000	1.13
T3	1/172.6/27.4	40/116/25	82.8/17.2	19400	25700	1.15
T4	1/169.5/30.5	40/124/31	80.2/19.8	20000	24000	1.13
T5	1/164.6/35.4	40/112/34	76.9/23.1	19000	24000	1.18
T6	1/162.9/37.1	40/116/37	76.0/24.0	20000	23600	1.17

Conditions of ATRP: [M]$_0$=1.69 M, T=25^{o}C, [initiator]/[CuCl]/[Me$_6$TREN]=1/2/2, solvent mixture DMF/water=5/1.

[a] feed ratio. [b]calculated from ^{1}H NMR. [c]eetermined by SEC.

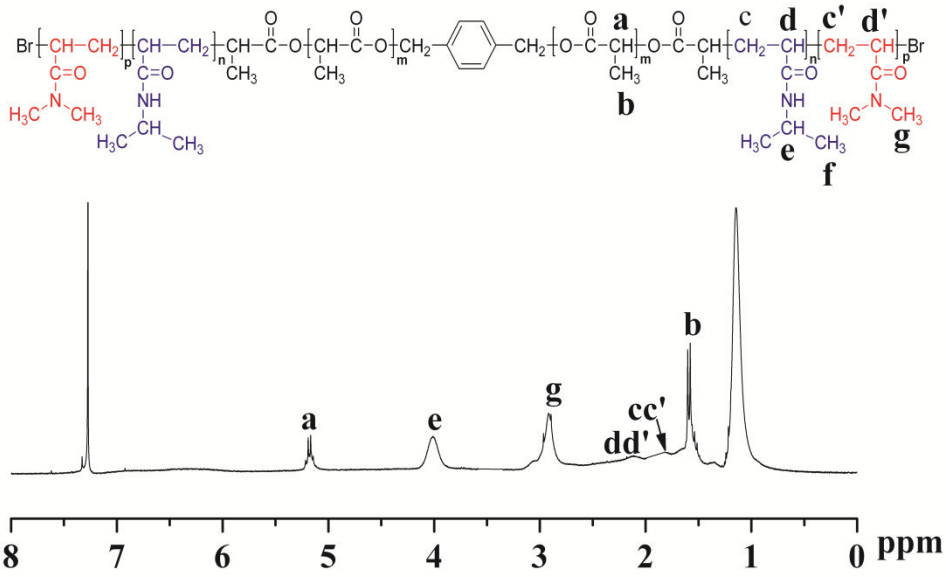

Figure 3.1 ^{1}H NMR spectrum of P(NIPAAm-*co*-DMAAm)-*b*-PLLA-*b*-(PNIPAAm-*co*-DMAAm) triblock copolymer in $CDCl_3$

The chemical structure of triblock copolymers was characterized by ^{1}H and DOSY NMR spectroscopy. Figure 3.1 shows the ^{1}H NMR spectrum of a copolymer in $CDCl_3$. The methyl (H_f, CH_3) and methine protons (H_e, CH) adjacent to the amine moiety of the NIPAAm units are observed at 1.1 and 4.0 ppm, respectively. The signal at 2.9

ppm is assigned to the methyl proton (H_g, CH_3) of DMAAm. The signals at 1.5 and 5.1 ppm are characteristic of the methyl (H_b) and methine protons (H_a, CH) of PLLA. The [LA]/[NIPAAm]/[DMAAm] ratio was calculated from the integrations of the methine protons (-C*H*(CH_3)-) of lactyl units at 5.1 ppm, methine protons (-NHC*H*(CH_3)$_2$-) of NIPAAm units at 4.0 ppm and methyl protons (-(C*H*$_3$)$_2$) of DMAAm at 2.9 ppm (equation 5). The DP of NIPAAm and DMAAm units, and the M_n of copolymers were then obtained using following equations:

$$[LA]/[NIPAAm]/[DMAAm] = I_a / I_e / (I_g/6) \quad (5)$$

$$DP_{NIPAAm} = DP_{LA} / ([LA]/[NIPAAm]) \quad (6)$$

$$DP_{DMAAm} = DP_{LA} / ([LA]/[DMAAm]) \quad (7)$$

$$M_{nNMR} = 72 \text{ x } DP_{LA} + 113 \text{ x } DP_{NIPAAm} + 98 \text{ x } DP_{DMAAm} \quad (8)$$

Where 72, 113 and 98 are the molecular weight of LA, NIPAAm and DMAAm units, respectively.

The efficiency of polymerization was also evaluated by DOSY NMR, one of the powerful tools to characterize block copolymers [41]. DOSY NMR is a two dimensional NMR technique in which the signal decays exponentially due to the self-diffusion behavior of individual molecules. This leads to two dimensions: the first dimension (F_2) accounts for the conventional chemical shift and the second one (F_1) for self-diffusion coefficients (D). Thus, each component in a mixture can be virtually separated, based on its own diffusion coefficient on the diffusion dimension. Figure 3.2 shows the DOSY pattern of copolymer T4 in dilute DMSO-d_6. The ^{1}H NMR spectrum exhibits signals corresponding to PLLA (δ=5.1 and 1.5 ppm), NIPAAm (δ=3.9 ppm) and DMAAm (δ=2.7, 2.8, 2.9 and 3.0 ppm). As shown on the DOSY pattern, the ^{1}H NMR signals of PLA and P(NIPAAm-*co*-DMAAm) present the same diffusion coefficient D=2.291 $\times$ 10^{-11} m^2s^2, in agreement with efficient copolymerization of NIPAAm and DMAAm on the Br-PLLA-Br macroinitiator. No free PNIPAAm was observed since the diffusion coefficient of PNIPAAm in dilute DMSO-d_6 was found to be D=5.248$\times$$10^{-11}$ m^2s^2.

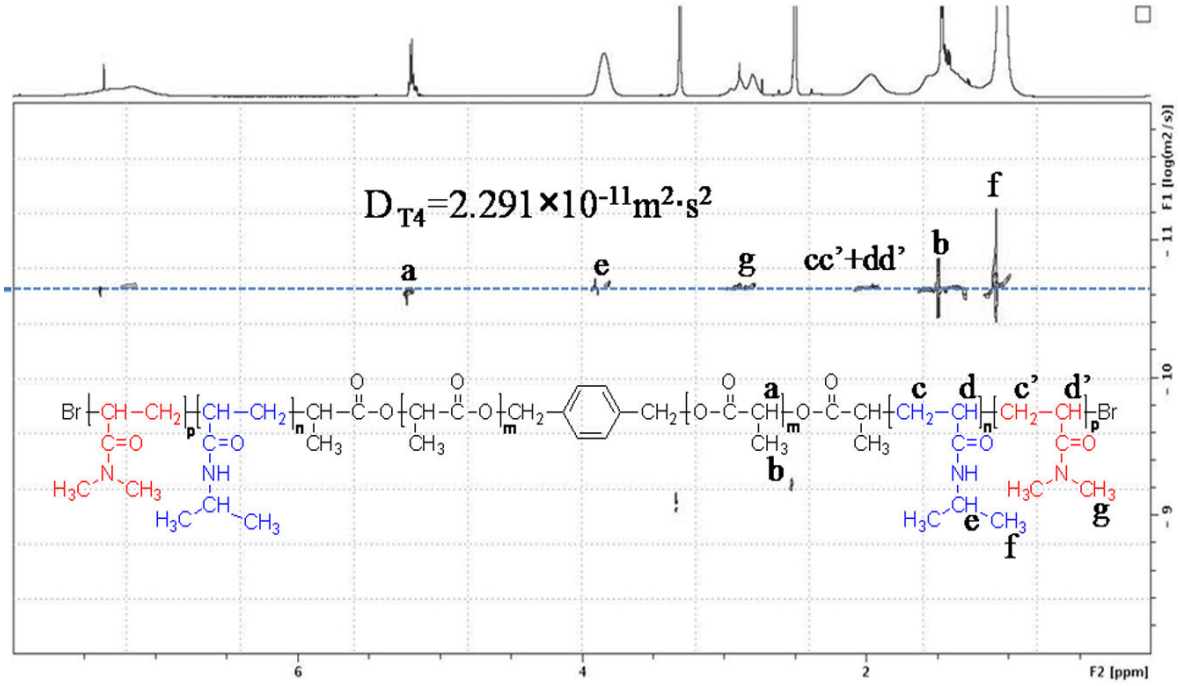

Figure 3.2 DOSY NMR spectrum of P(NIPAAm-*co*-DMAAm)-*b*-PLLA-P(NIPAAm-*co*-DMAAm) triblock copolymer in DMSO-d_6.

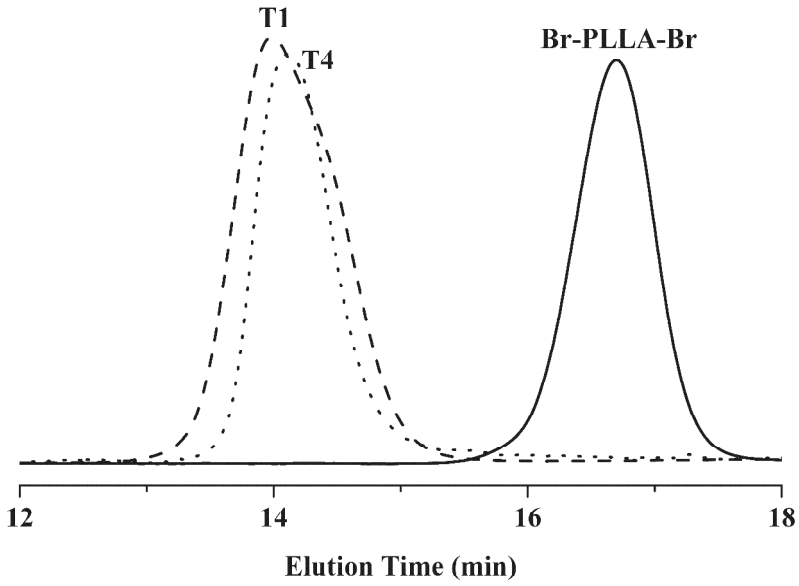

Figure 3.3 SEC chromatograms of Br-PLLA-Br macroinitiator and triblock copolymers (T1 and T4).

Figure 3.3 shows the SEC traces of the copolymers T1 and T4 in comparison with the Br-PLLA-Br macroinitiator. All the polymers exhibit narrow and unimodal molecular weight distributions. Furthermore, a shift of the copolymer traces towards higher

molecular weights is observed as compared to Br-PLLA-Br, indicating successful synthesis of block copolymers.

Table 3.2 summarizes the characteristics of the various copolymers. The [NIPAAm]/[DMAAm] molar ratio varies from 100/0 to 76/24 in the copolymers. DP_{NIPAAm} varies from 172 to 112, and DP_{DMAAm} varies from 0 to 37. The M_n obtained from SEC ranges from 23600 to 27000 g mol^{-1} with low dispersity ($Đ$=1.10-1.18). A good agreement was observed between the $M_{n,NMR}$ and $M_{n,SEC}$ values although the former is slightly lower than the latter.

After polymerization, the catalyst was removed by filtration through a basic alumina column. The copolymers recovered by precipitation in diethyl ether appeared almost colorless. ICP-MS measurements showed that the copper content in the copolymers was between 1 and 3 ppm.

3.3.2 Self-assembling of triblock copolymer micelles in aqueous medium

The physico-chemical properties of the amphiphilic copolymers in aqueous solution were determined in order to evaluate their potential as drug carrier. The different copolymers are water soluble and are able to form micellar aggregates by self-assembly in water using the direct dissolution method. The critical micelle concentration (CMC) was determined by fluorescence spectroscopy using pyrene as hydrophobic probe. Figure 3.4 shows the I_{337}/I_{333} ratio changes as a function of polymer concentration. The intensity ratio exhibits a substantial increase at a particular concentration, indicating the incorporation of pyrene into micelles. The *CMC* was obtained from the intersection of the two linear regression lines of the plots.

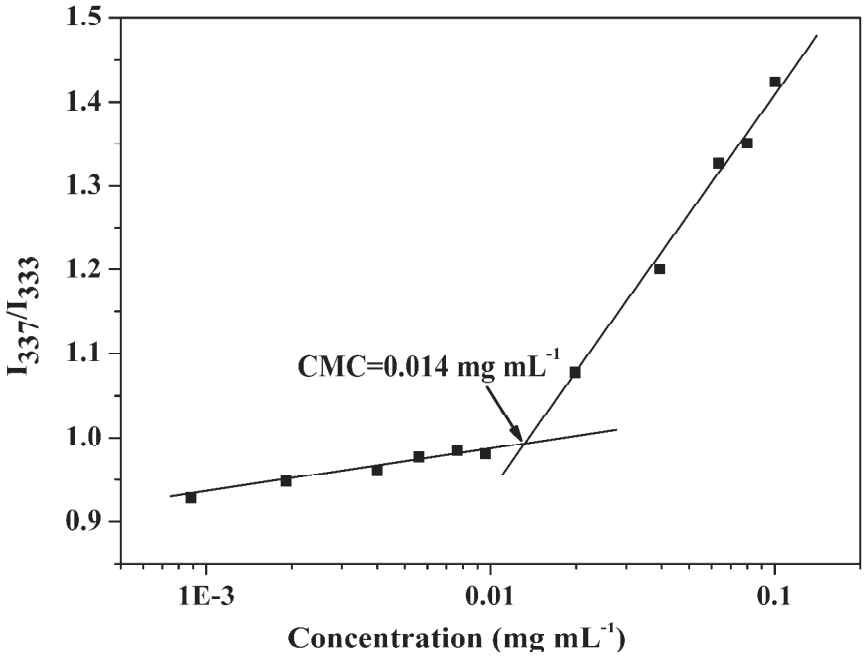

Figure 3.4 Plots of the I_{337}/I_{333} ratio changes from pyrene excitation spectra *versus* the concentration of P(NIPAAm-*co*-DMAAm)-*b*-PLLA-*b*-P(NIPAAm-*co*-DMAAm) (T4)

Table 3.3 Properties of P(NIPAAm-*co*-DMAAm)-*b*-PLLA-*b*-P(NIPAAm-*co*-DMAAm) micelles

Run	$DP_{LA}/DP_{NIPAAm}/DP_{DMAAm}$[a]	[NIPAAm]/[DMAAm][a]	LCST[b] °C	CMC[c] mg mL^{-1}	D_H[d] nm	PDI[d]
T1	40/172/0	100/0	32.3	0.010	40	0.12
T2	40/128/17	88.2/11.8	35.6	-	42	0.17
T3	40/116/25	82.8/17.2	37.1	0.013	42	0.21
T4	40/124/31	80.2/19.8	37.8	0.014	43	0.15
T5	40/112/34	76.9/23.1	38.8	-	55	0.22
T6	40/116/37	76.0:24.0	39.1	0.015	53	0.21

a) Calculated by NMR; b) Determined by UV spectroscopy; c) Determined by fluorescence spectroscopy; d) Determined by DLS.

As shown in Table 3.3, the CMC value of PNIPAAm-*b*-PLLA-*b*-PNIPAAm (T1) is 0.010 mg mL^{-1}, while those of P(NIPAAm-*co*-DMAAm)-*b*-PLLA-*b*-P(NIPAAm-*co*-DMAAm) are slightly higher. The CMC is dependent on different factors such as the composition, the hydrophilic to hydrophobic ratio, *etc*. The higher CMC value of P(NIPAAm-*co*-DMAAm)-*b*-PLLA-*b*-P(NIPAAm-*co*-DMAAm) as compared to PNIPAAm-*b*-PLLA-*b*-PNIPAAm is attributed to the presence of more hydrophilic

DMAAm units. It is also noted that the CMC values of the copolymers are lower that of the diblock copolymer with NIPAAm/DMAAm/LA ratio of 54/29/14 (0.022 mg mL^{-1}) reported by Akimoto *et al.*, but higher than those of the copolymers $P(NIPAAm/DMAAm)_{118}$-PLA_{59} and $P(NIPAAm/DMAAm)_{118}$-PCL_{60} reported by Li et al. (0.00184 and 0.00398 mg mL^{-1}, respectively) [34, 37]. These findings can be assigned to the fact that higher hydrophobic content leads to lower CMC. The very low CMC values demonstrate the strong tendency of copolymers toward formation of micelles, which is of major importance for the long circulation of micelles in the blood stream after injection induced dilution [42, 43].

3.3.3 Morphology and size distribution of micelles

TEM experiments were performed to examine the morphology of the self-assembling aggregates. As shown in Figure 3.5A, the micelles of copolymer T4 are spherical in shape with an average diameter of 32 nm. The size distribution of the copolymer micelles was determined by DLS (Figure 3.5B). The micelles exhibit a unimodal and narrow size distribution with an average hydrodynamic diameter of 43 nm and a dispersity of 0.15.

As frequently reported in the literature, the size obtained from DLS is larger than that from TEM. This difference could be attributed to the experimental conditions. In fact, DLS determines the hydrodynamic diameter of micelles in aqueous solution, whereas TEM shows the dehydrated solid state of micelles. Table 3.3 shows the DLS data of all copolymer micelles in water at 25 ^{o}C. The average diameter varies from 40 to 55 nm with narrow size distribution ($Đ$ = 0.15 to 0.22). The size of copolymer micelles increases with increasing the content of hydrophilic DMAAm units. The nano-size of micelles should allow them to escape from the reticuloendothelial system (RES) and preferentially accumulate in tumor tissues through the enhanced permeability and retention (EPR) effect [44, 45].

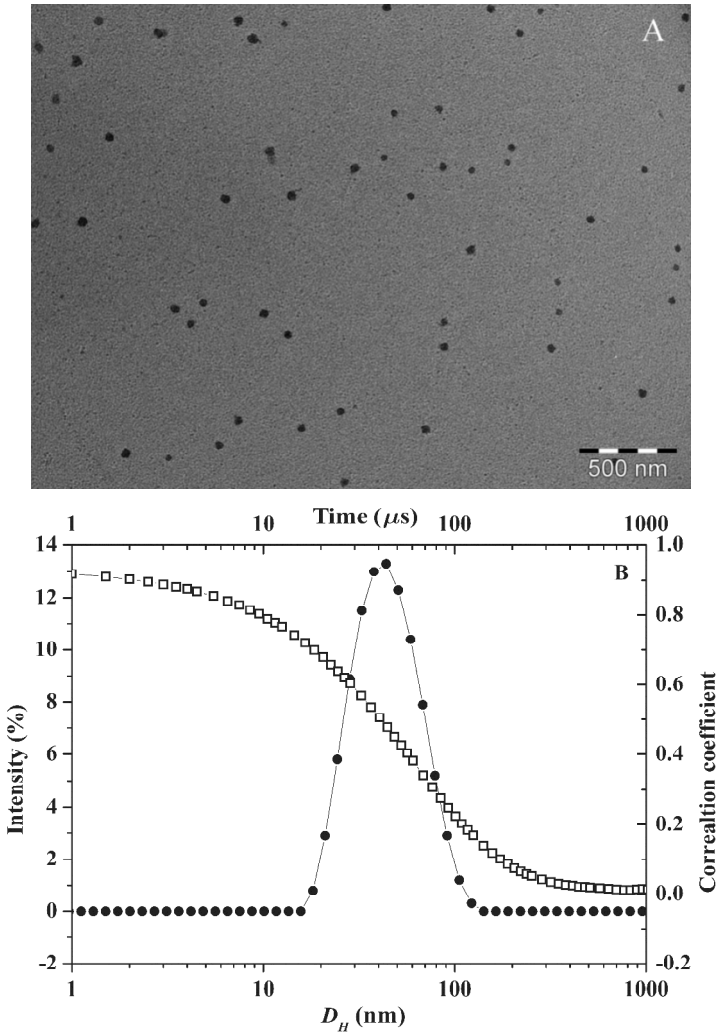

Figure 3.5 TEM (A) and DLS (B) results of the self-assembling micelles of copolymerT4 in aqueous medium.

It is noteworthy that the size of copolymer micelles is larger than that of the diblock copolymer (23 nm) reported by Akimoto *et al.*, but smaller than those of the copolymers P(NIPAAm/DMAAm)$_{118}$-PLA$_{59}$ and P(NIPAAm/DMAAm)$_{118}$-PCL$_{60}$ (170 and 87 nm, respectively) reported by Li *et al.* [34].

3.3.4 Thermo-responsive behavior of micelles

Our strategy for drug release is to use thermo-sensitive copolymers to target tumor tissue under hyperthermia. Therefore, the LCST should be slightly higher than the body temperature. Thermo-responsive polymers become insoluble when the temperature increases above the LCST due to coil-to-globule transition. This phase

transition can be evidenced by light transmission measurements of micellar solution as a function of temperature.

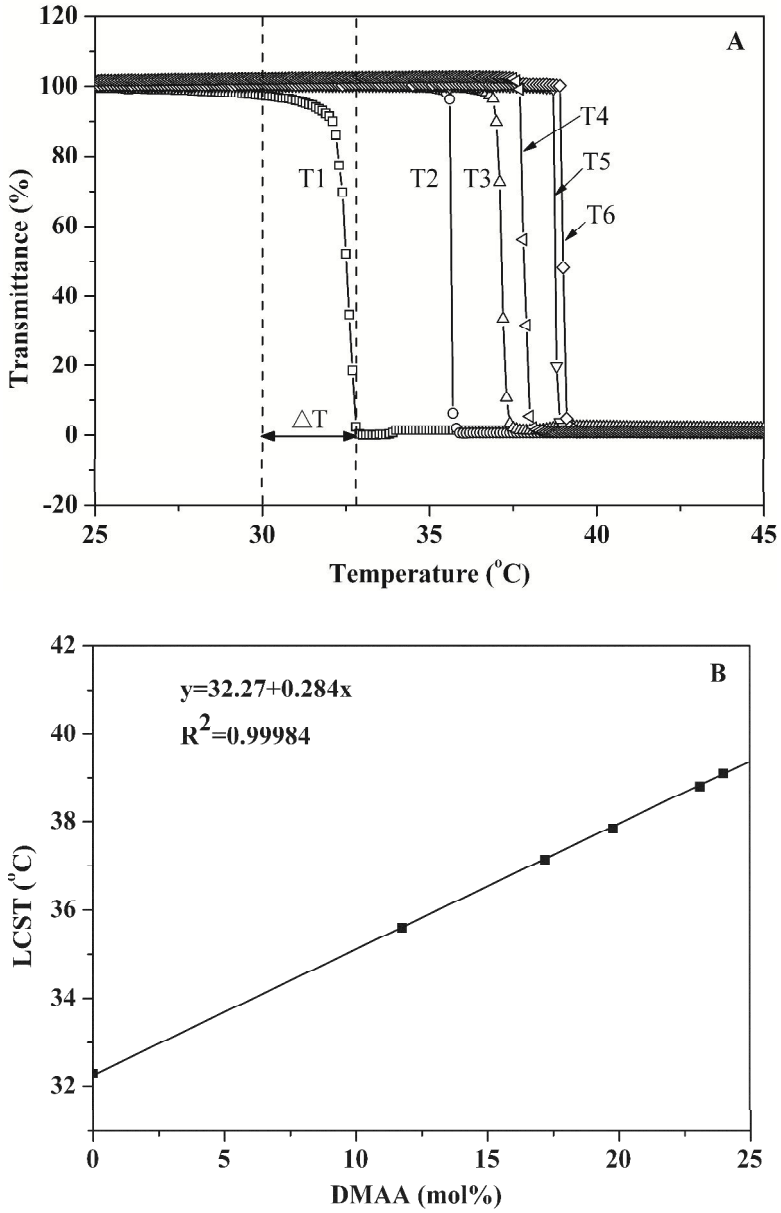

Figure 3.6 Plots of transmittance as a function of temperature (A) and plot of LCST values as a function (B) of DMAAm content for copolymer solutions at 3.0 mg mL^{-1}.

Figure 3.6 shows the transmission changes of different polymeric micelle solutions at 3.0 mg mL^{-1} with increasing temperature. A sharp transmittance decrease is detected around the LCST. The resulting LCST values are listed in Table 3.3. As expected, the LCST increases from 32.3 to 39.1 ^{o}C with the increase of DMAAm content in the

copolymers (Table 3.3). Moreover, a linear relationship is obtained between the LCST and the molar fraction of DMAAm up to 24 %, as shown in Figure 3.6B.

Therefore, the LCST can be tuned to temperatures inside tumor tissue by simply increasing the content of DMAAm units in the copolymers. This finding is consistent with literature data. In fact, Shen *et al.* reported that the LCST linearly increases with increasing the content of DMAAm in P(NIPAAm-*co*-DMAAm) copolymers [46]. The LCST of P(NIPAAm-*co*-DMAAm)-*b*-PLLA diblock copolymers with maleimide endgroup reported by Akimoto *et al.* and Li *et al.* is about 40 ^{o}C despite the different P(NIPAAm-*co*-DMAAm) to PLA ratios [34, 37]. In fact, diblock copolymers with maleimide endgroup lead to surface-functional thermo-responsive micelles, and the LCST of micelles can be tuned by mixing hydrophobic DTBz-surface micelles and Mal-surface ones [34]. In our case, the LCST of P(NIPAAm-*co*-DMAAm)-*b*-PLLA-*b*-P(NIPAAm-*co*-DMAAm) triblock copolymers can be precisely adjusted to above the body temperature by varying the NIPAAm to DMAAm ratio, which presents great interest for targeted delivery of anticancer drugs.

Moreover, introduction of DMAAm not only leads to LCST increase of copolymers, but also leads to an extremely narrow phase transition interval within 0.5 ^{o}C. As shown in Figure 3.6A, the optical transmittance of PNIPAAm-*b*-PLLA-*b*-PNIPAAm (T1) decreases from 100 % to 0 with increasing temperature between 30.0 to 32.8 ^{o}C (ΔT=2.8 ^{o}C). Similar behavior was reported in literature. Indeed, for PNIPAAm-*b*-PLLA diblock copolymer, a broad phase transition interval of ΔT=5 ^{o}C was observed [17, 18, 22]. In the case of DMAAm containing copolymer T4, the transmittance decrease from 100 % to 0 occurs in the temperature range of 37.6 to 38.0 ^{o}C, with a phase transition interval ΔT=0.4 ^{o}C. Narrow phase transition intervals below 0.5 ^{o}C were also observed for other DMAAm containing copolymers as shown in Figure 3.6A. Nakayama *et al.* reported phase transition intervals above 3 ^{o}C for P(NIPAAm-*co*-DMAAm)-*b*-PDLLA copolymers obtained by combination of radical

polymerization and ROP [32, 33]. On the contrary, Akimoto *et al.* reported narrow phase transition intervals within 0.5 ^{o}C of such copolymers by combination of RAFT and ROP, which is consistent with our work [34].

The phase transition of copolymers is illustrated by DLS. Figure 3.7 shows the reversible changes of the hydrodynamic diameter distribution depending on temperature. The size of the micelles increases from 35 to 640 nm when the temperature is raised from 25 to 45 ^{o}C. After quickly cooling down to 25 ^{o}C, the micelle size decreases to 38 nm. In fact, P(NIPAAm-*co*-DMAAm) chains are extended and coil-like in water under the LCST. When the temperature approaches the LCST, dehydration of P(NIPAAm-*co*-DMAAm) occurs, leading to precipitation of polymers and aggregation.

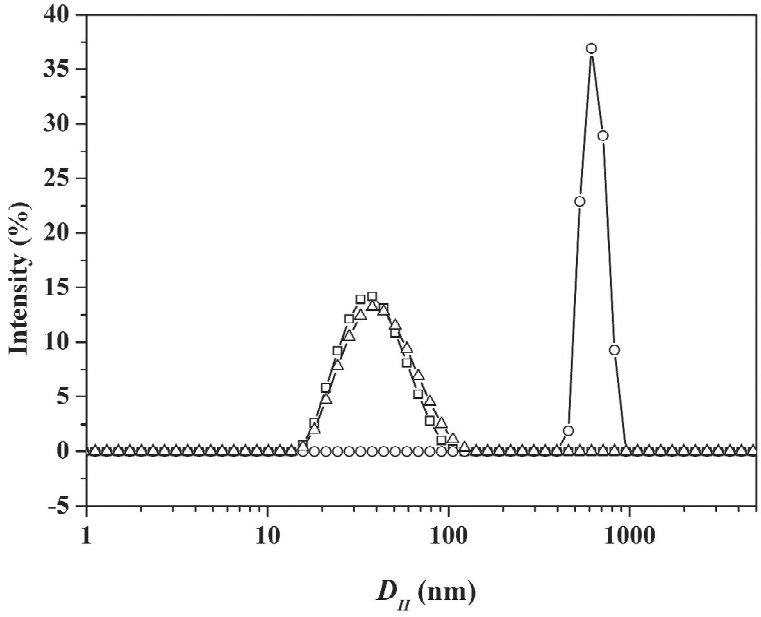

Figure 3.7 Reversible changes of the hydrodynamic diameter for T4 micelles at 3 mg mL^{-1} when the temperature is raised from 25 (□) to 45 ^{o}C (○), and cooled down to 25 ^{o}C (△).

The observed phase transition is due to a coil-to-globule transition governed by cooperative dehydration of hydrophilic chains. In the case of PNIPAAm, the hydrogen-bonding site (amide group) is blocked by a bulky hydrophobic group

(isopropyl group). The hydrophobic effect is very important in the LCST behavior of polymer solutions. In fact, a "water cage" is formed around the isopropyl and amide groups in the PNIPAAm blocks. Phase transition occurs upon increasing temperature due to complex dehydration of PNIPAAm at the LCST, excluding water molecules from the water cage [47-49].The micelles aggregate into large size particles. When randomly distributed DMAAm is introduced, the P(NIPAAm-*co*-DMAAm) chains become more hydrophilic as compared to PNIPAAm, and the LCST transition shifts to higher temperature and becomes sharper. Sharp transition makes the micelles more sensitive to temperature changes and favors quick release of drug above the LCST.

3.3.5 *In vitro* drug release

When used as drug carrier, polymeric micelles are capable of encapsulating hydrophobic drugs. Amphotericin B (AmpB), a poorly water-soluble drug for the treatment of systemic mycosis, was used as a model drug [43, 50, 51]. 2.5 or 5 mg AmpB was loaded in 20 mg polymeric micelles by dialysis. The drug loading content and loading efficiency of AmpB into polymeric micelles are given in Table 3.4. When the initial drug amount increases from 2.5 to 5 mg, drug content increases from 8.2 to 11.8 %, but the loading efficiency decreases from 83 % to 59 %, which is consistent with literature [50].

Table 3.4 Drug loading and loading efficiency of Amp B in polymeric micelles

Sample	Polymer	LCST (^{o}C)	Drug/polymer (mg/mg)	Drug loading (%)	Loading efficiency (%)
1	T4	37.8	2.5/20	8.2	83
2	T4	37.8	5/20	11.8	59

As shown in Figure 8A, a linear calibration curve was previously established between the UV absorbance and curcumin concentration with a correlation coefficient of 0.99986. An initial burst release of the drug absorbed on the surface of micelles is

observed in all cases. Sample 2 with higher drug content exhibits slower drug release, which could be attributed to the poor solubility of AmpB (Figure 3.8B).

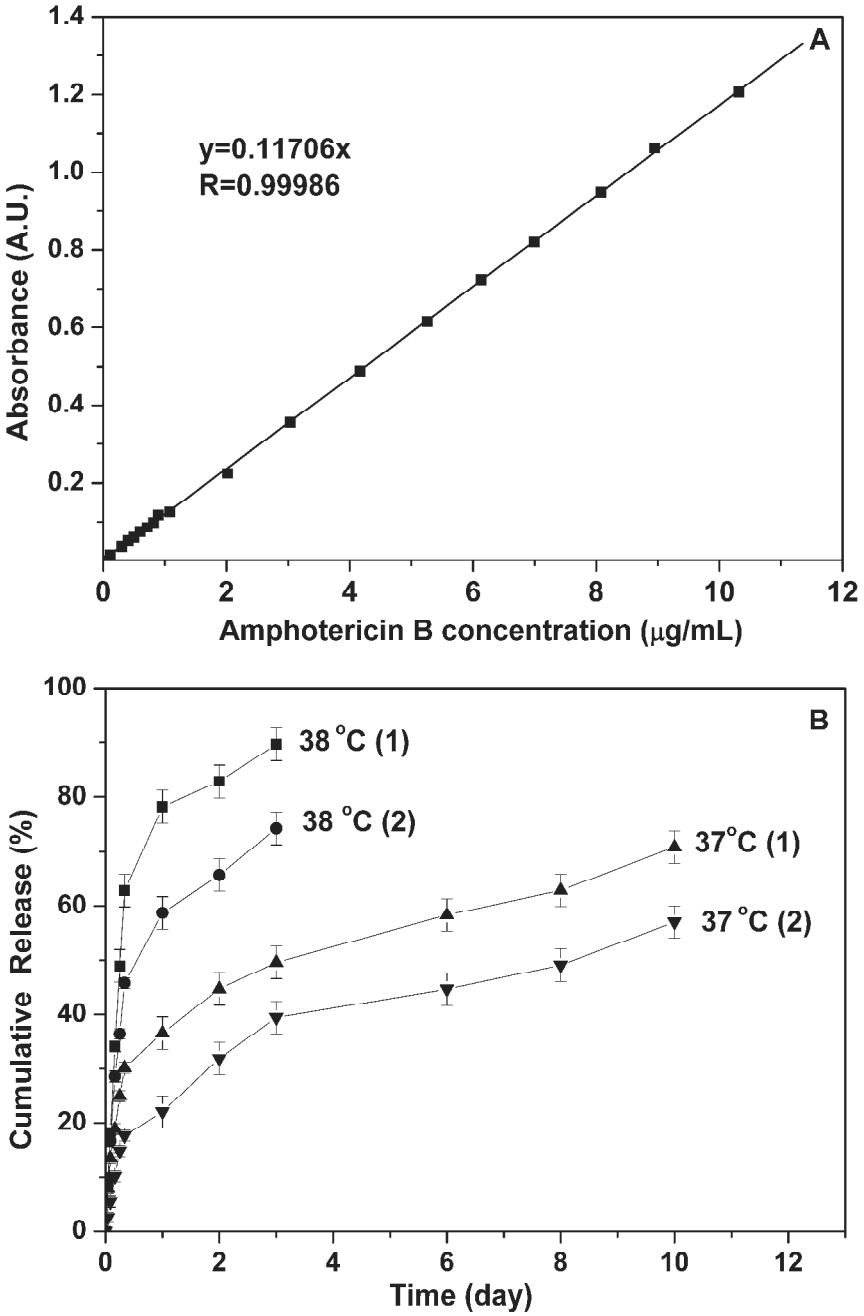

Figure 3.8 Drug release profiles of AmpB loaded polymeric micelles (Samples 1 and 2) at 37 and 38 ^{o}C in water.

On the other hand, the *in vitro* drug release from polymer micelles presents a thermo-sensitive behavior. At temperature below the LCST (37 °C), the release of AmpB is relatively slow. After 3 days, nearly 50 % and 32 % of drug are released for

sample 1 and sample 2, respectively. In contrast, at 38 °C which is above the LCST, the release rate is much faster with 90 and 75 % of released drug in both samples. These preliminary results suggest that drug loaded micelles could be injected to a human body and achieve quick drug release at the tumor site where the temperature is higher than the LCST. Thus, the drug release behavior indicates that these copolymers could be potential candidates for applications in targeted delivery of drugs.

Li *et al*. comparatively studied the release of adriamycin from maleimide end-functional P(NIPAAm-*co*-DMAAm)-*b*-PLA and P(NIPAAm-*co*-DMAAm)-*b*-PCL copolymer micelles under physiological conditions (37 °C and pH = 7.3) and in simulated tumor environment (40 °C and pH = 5.3) [37]. The authors observed that only half of entrapped adriamycin was released out within one week under physiological conditions, while about 90 % adriamycin was released within 10 h in simulated tumor environment. Nevertheless, faster degradation of micelles at 40 °C and pH = 5.3 could have contributed to the faster drug release together with the LCST effect. Nakayama *et al.* studied the release of doxorubicin from P(NIPAAm-*co*-DMAAm)-*b*-PCL and P(NIPAAm-*co*-DMAAm)-*b*-P(LA-*co*-CL) copolymer micelles below and above the LCST [32]. No difference was detected in the case of P(NIPAAm-*co*-DMAAm)-*b*-PCL at 42.5 °C and 37 °C. In contrast, the release of doxorubicin is much faster at 41°C than that at 35 °C in the case of P(NIPAAm-*co*-DMAAm)-*b*-P(LA-*co*-CL). Again, degradation of micelles plays a key role in drug release because P(LA-*co*-CL) degrades much faster than PCL [52]. In our case, the faster release of AmpB can be assigned to the destabilization of micelles above the LCST since little difference of degradation could be expected at 38 °C and 37 °C.

3.3.6 Cytocompatibility

In vitro cytotoxicity is generally evaluated by MTT assay for the screening of biomaterials [53]. MTT assay is based on the reaction between MTT and

mitochondrial succinate dehydrogenases in living cells to form a purple formazan which is soluble in DMSO but insoluble in water. The OD value of formazan-DMSO solution is considered to be proportional to the number of living cells.

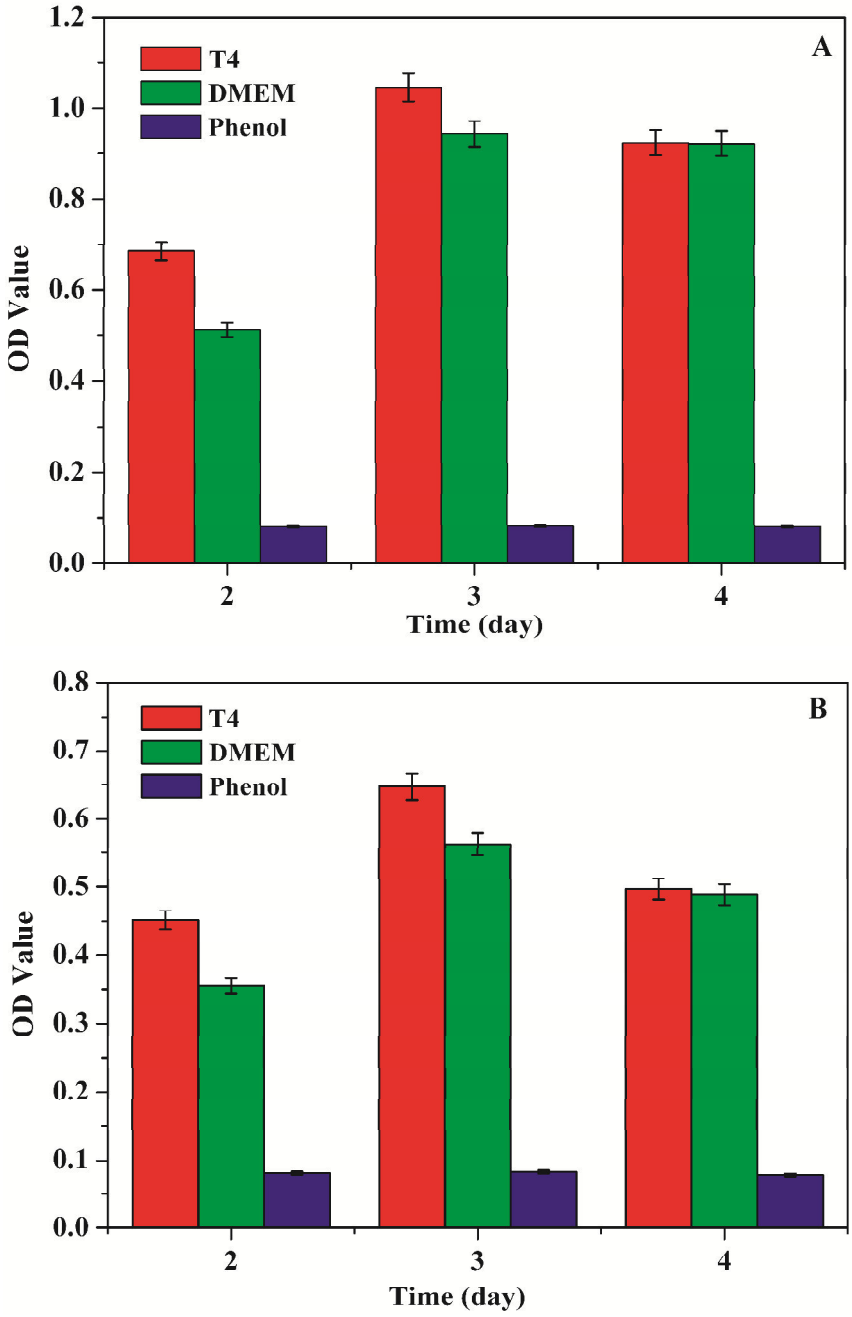

Figure 3.9 Optical density values of MCM (A) and MEF(B) solutions after 2, 3 and 4 days culture in DMEM with copolymer substrate (T4), and controls (DMEM and 5 % phenol

The effect of copolymer T4 on the growth of MCM and MEF cells is shown in Figure 3.9, in comparison with controls (DMEM medium and 5 % phenol). The OD values on polymer substrate are slightly higher than those in the culture solution, and much higher than those in phenol. The RGR values of copolymer T4 are well above 100 % during 4 days incubation with MCF and MEF cells, corresponding to a cytotoxicity level of 0 (Table 3.5).

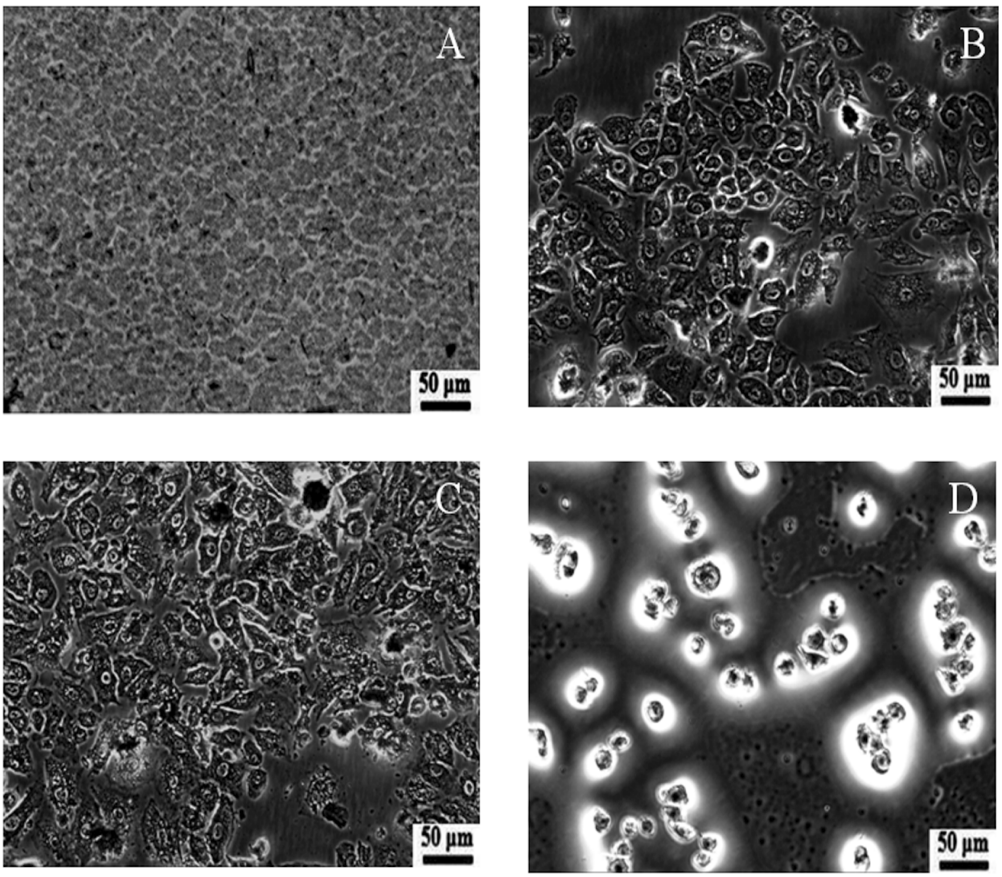

Figure 3.10 Microscopic images of cells stained by NR after 3 days culture in different media: (A) Copolymer T4 substrate without cell; (B) MCM cells on polymer substrate in DMEM; (C) MEF cells on polymer substrate in DMEM; (D) MEF cells in 5 % phenol medium

Table 3.5 RGR values of copolymers T4 with MCM and MEF cells during 4 days incubation

Cell	RGR (%)		
	2 days	3 days	4 days
MCM	133.8±1.1	110.8±3.0	100.2±1.2
MEF	127.3±1.6	114.9±2.0	101.6±1.0

Figure 3.10 shows the morphology of cells after 3 days culture. Large number of cells died in the toxic phenol medium (Figure 3.10D). On the contrary, cell adhesion and proliferation are observed on the copolymer substrate (Figure 3.10B and Figure 3.10C). Cells exhibit spindle, polygon or oval shapes, and the pseudopodium of cells stretches out. Therefore, MTT assay and cell morphology observation indicate that P(NIPAAm-*co*-DMAAm)-*b*-PLLA-*b*-P(NIPAAm-*co*-DMAAm) copolymers presents outstanding cytocompatibility and could be used for biomedical applications.

3.4 Conclusion

P(NIPAAm-*co*-DMAAm)-*b*-PLLA-*b*-P(NIPAAm-*co*-DMAAm) triblock copolymers were prepared by ATRP using Br-PLLA-Br as macroinitiator. The resulting copolymers present well defined molecular weights and narrow dispersities. The LCST of the copolymers linearly increases from 32.3 to 39.1 °C with increasing the DMAAm content. Self-assembling micelles were prepared by dissolving the copolymers in aqueous medium. The copolymers have very low CMC (10 to 15 μg mL^{-1}) and nano-size (40 to 55 nm). The presence of DMAAm units in the copolymers leads to an extremely sharp phase transition, as compared to PNIPAAm-*b*-PLLA-*b*-PNIPAAm copolymers. Moreover, reversible size changes were observed when the micelle solutions was heated from 25 to 45 ^{o}C and then cooled down to 25 ^{o}C. Much faster drug release is detected at temperatures above the LCST in *in vitro* studies. The MTT assay and cell morphology observation confirm the good biocompatibility of these thermo-sensitive copolymers.

Therefore, the small size and low CMC, the LCST slightly above the body temperature, the rapid phase transition at LCST, the thermo-responsive drug release behavior above LCST, and the good cytocompatilibity indicate that P(NIPAAm-*co*-DMAAm)-*b*-PLLA-*b*-P(NIPAAm-*co*-DMAAm) copolymers are promising candidates for applications in targeted delivery of anticancer drugs.

In this chapter, the preliminary study of drug release has been performed in water. However, the properties of micelles in physiological conditions (pH=7.4, PBS) should be investigated to determine the effects of salt and drug loading on the LCST, the size and morphology of micelles. In the next chapter, an anticancer drug, curcumin, has been used as drug model for a systemic study on the drug release properties of P(NIPAAm-*co*-DMAAm)-*b*-PLLA-*b*-P(NIPAAm-*co*-DMAAm) copolymers.

3.5 References

[1] A. K. Bajpai, S. K. Shukla, S. Bhanu, S. Kankane, Responsive polymers in controlled drug delivery. Prog. Polym. Sci. 33 (2008) 1088-1118.

[2] A. Kumar, A. Srivastava, I. Y. Galaev, B. Mattiasson, Smart polymers: Physical forms and bioengineering applications. Prog. Polym. Sci. 32 (2007) 1205-1237.

[3] B. Guillerm, V. Darcos, V. Lapinte, S. Monge, J. Coudane, J. J. Robin, Synthesis and evaluation of triazole-linked poly(ε-caprolactone)-graft-poly(2-methyl-2-oxazoline) copolymers as potential drug carriers. Chemical Communications 48 (2012) 2879-2881.

[4] W. Y. Ooi, M. Fujita, P. J. Pan, H. Y. Tang, K. Sudesh, K. Ito, N. Kanayama, T. Takarada, M. Maeda, Structural characterization of nanoparticles from thermoresponsive poly(*N*-isopropylacrylamide)-DNA conjugate. J. Colloid Interface Sci. 374 (2012) 315-320.

[5] A. Wang, C. Tao, Y. Cui, L. Duan, Y. Yang, J. Li, Assembly of environmental sensitive microcapsules of PNIPAAm and alginate acid and their application in drug release. J. Colloid Interface Sci. 332 (2009) 271-279.

[6] C. H. Hu, X. Z. Zhang, L. Zhang, X. D. Xu, R. X. Zhuo, Temperature- and pH-sensitive hydrogels to immobilize heparin-modified PEI/DNA complexes for sustained gene delivery. J. Mater. Chem. 19 (2009) 8982-8989.

[7] Y. Liu, X. Cao, M. Luo, Z. Le, W. Xu, Self-assembled micellar nanoparticles of a novel star copolymer for thermo and pH dual-responsive drug release. J. Colloid Interface Sci. 329 (2009) 244-252.

[8] P. VanRijn, H. Park, K. O. Nazli, N. C. Mougin, A. Boker, Self-Assembly Process of Soft Ferritin-PNIPAAm Conjugate Bionanoparticles at Polar-Apolar Interfaces. Langmuir 29 (2013) 276-284.

[9] N. M. Matsumoto, P. Prabhakaran, L. H. Rome, H. D. Maynard, Smart Vaults: Thermally-Responsive Protein Nanocapsules. ACS Nano 7 (2013) 867-874.

[10] H. Wei, S. X. Cheng, X. Z. Zhang, R. X. Zhuo, Thermo-sensitive polymeric micelles based on poly(*N*-isopropylacrylamide) as drug carriers. Prog. Polym. Sci. 34 (2009) 893-910.

[11] H. G. Schild, Poly (*N*-isopropylacrymide)-experiment, theory and application. Prog. Polym. Sci. 17 (1992) 163-249.

[12] W. R. H senff, Influence of cross-link density on rheological properties of temperature-sensitive microgel suspensions. collioid polym sci 278 (2000) 830-840.

[13] A. C. Albertsson, I. Varma, Degradable Aliphatic Polyesters, Vol. 157, Springer Berlin

Heidelberg, 2002, pp. 1-40.
[14] G. S. He, L. L. Ma, J. Pan, S. Venkatraman, ABA and BAB type triblock copolymers of PEG and PLA: A comparative study of drug release properties and"stealth" particle characteristics. Int. J. Pharm. 334 (2007) 48-55.
[15] L. Yang, A. E. Ghzaoui, S. M. Li, In vitro degradation behavior of poly(lactide)-poly(ethylene glycol) block copolymer micelles in aqueous solution. Int. J. Pharm. 400 (2010) 96-103.
[16] I. Barwal, A. Sood, M. Sharma, B. Singh, S. C. Yadav, Development of stevioside Pluronic-F-68 copolymer based PLA-nanoparticles as an antidiabetic nanomedicine. Colloid Surf. B-Biointerfaces 101 (2007) 510-516.
[17] K. Fukashi, S. Kiyotaka, A. Takao, Y. Masayuki, S. Yasuhisa, O. Teruo, Preparation and characterization of thermally responsive block copolymer micelles comprising poly(*N*-isopropylacrylamide-*b*-DLlactide). J. Controlled Release 55 (1998) 87-98.
[18] J. Qin, Y. S. Jo, J. E. Ihm, D. K. Kim, M. Muhammed, Thermosensitive Nanospheres with a Gold Layer Revealed as Low-Cytotoxic Drug Vehicles. Langmuir 21 (2005) 9346-9351.
[19] E. Ayano, M. Karaki, T. Ishihara, H. Kanazawa, T. Okano, Poly (*N*-isopropylacrylamide)-PLA and PLA blend nanoparticles for temperature-controllable drug release and intracellular uptake. Colloids Surf. B: Biointerfaces 99 (2012) 67-73.
[20] Y. Z. You, C. Y. Hong, W. P. Wang, W. Q. Lu, C. Y. Pan, Preparation and Characterization of Thermally Responsive and Biodegradable Block Copolymer Comprised of PNIPAAM and PLA by Combination of ROP and RAFT Methods. Macromolecules 37 (2004) 9761-9767.
[21] M. Hales, C. Barner-Kowollik, T. P. Davis, M. H. Stenzel, Shell-Cross-Linked Vesicles Synthesized from Block Copolymers of Poly(D,L-lactide) and Poly(*N*-isopropylacrylamide) as Thermoresponsive Nanocontainers. Langmuir 20 (2004) 10809-10817.
[22] H. Wei, X. Z. Zhang, C. Cheng, S. X. Cheng, R. X. Zhuo, Self-assembled, thermosensitive micelles of a star block copolymer based on PMMA and PNIPAAm for controlled drug delivery. Biomaterials 28 (2007) 99-107.
[23] S. J. T. Rezaei, M. R. Nabid, H. Niknejad, A. A. Entezami, Folate-decorated thermoresponsive micelles based on star-shaped amphiphilic block copolymers for efficient intracellular release of anticancer drugs. Int. J. Pharm. 437 (2012) 70-79.
[24] S. J. T. Rezaei, M. R. Nabid, H. Niknejad, A. A. Entezami, Multifunctional and thermoresponsive unimolecular micelles for tumor-targeted delivery and site-specifically release of anticancer drugs. Polymer 53 (2012) 3485-3497.
[25] F. N. Chearuil, O. I. Corrigan, Thermosensitivity and release from poly *N*-isopropylacrylamide-polylactide copolymers. Int. J. Pharm. 366 (2009) 21-30.
[26] J. Zhang, R. D. K. Misra, Magnetic drug-targeting carrier encapsulated with thermosensitive smart polymer: Core-shell nanoparticle carrier and drug release response. Acta Biomater. 3 (2007) 838-850.
[27] F. Kohori, K. Sakai, T. Aoyagi, M. Yokoyama, M. Yamato, Y. Sakurai, T. Okano, Control of adriamycin cytotoxic activity using thermally responsive polymeric micelles composed of poly(*N*-isopropylacrylamide-*co*-*N,N*-dimethylacrylamide)-*b*-poly(d,l-lactide). Colloids and Surfaces B: Biointerfaces 16 (1999) 195-205.
[28] S. Q. Liu, Y. Y. Yang, X. M. Liu, Y. W. Tong, Preparation and Characterization of Temperature-Sensitive Poly(*N*-isopropylacrylamide)-*b*-poly(d,l-lactide) Microspheres for Protein

Delivery. Biomacromolecules 4 (2003) 1784-1793.
[29] S. Q. Liu, Y. W. Tong, Y. Y. Yang, Incorporation and in vitro release of doxorubicin in thermally sensitive micelles made from poly(*N*-isopropylacrylamide-*co*-*N,N*-dimethylacrylamide)-*b*-poly(d,l-lactide-*co*-glycolide) with varying compositions. Biomaterials 26 (2005) 5064-5074.
[30] S. Q. Liu, Y. W. Tong, Y. Y. Yang, Thermally sensitive micelles self-assembled from poly(N-isopropylacrylamide-co-N,N-dimethylacrylamide)-*b*-poly(D,L-lactide -co-glycolide) for controlled delivers of paclitaxel. Mol. Biosyst. 1 (2005) 158-165.
[31] S. Q. Liu, N. Wiradharma, S. J. Gao, Y. W. Tong, Y. Y. Yang, Bio-functional micelles self-assembled from a folate-conjugated block copolymer for targeted intracellular delivery of anticancer drugs. Biomaterials 28 (2007) 1423-1433.
[32] M. Nakayama, T. Okano, T. Miyazaki, F. Kohori, K. Sakai, M. Yokoyama, Molecular design of biodegradable polymeric micelles for temperature-responsive drug release. J. Controlled Release 115 (2006) 46-56.
[33] M. Nakayama, J. E. Chung, T. Miyazaki, M. Yokoyama, K. Sakai, T. Okano, Thermal modulation of intracellular drug distribution using thermoresponsive polymeric micelles. React. Funct. Polym. 67 (2007) 1398-1407.
[34] J. Akimoto, M. Nakayama, K. Sakai, T. Okano, Molecular Design of Outermost Surface Functionalized Thermoresponsive Polymeric Micelles with Biodegradable Cores. J. Polym. Sci. Part A: Polym. Chem. 46 (2008) 7127-7137.
[35] J. Akimoto, M. Nakayama, K. Sakai, T. Okano, Temperature-Induced Intracellular Uptake of Thermoresponsive Polymeric Micelles. Biomacromolecules 10 (2009) 1331-1336.
[36] J. Akimoto, M. Nakayama, K. Sakai, T. Okano, Thermally Controlled Intracellular Uptake System of Polymeric Micelles Possessing Poly(N-isopropylacrylamide)-Based Outer Coronas. Mol. Pharm. 7 (2010) 926-935.
[37] W. Li, J. F. Li, J. Gao, B. H. Li, Y. Xia, Y. C. Meng, Y. S. Yu, H. W. Chen, J. X. Dai, H. Wang, Y. J. Guo, The fine-tuning of thermosensitive and degradable polymer micelles for enhancing intracellular uptake and drug release in tumors. Biomaterials 32 (2011) 3832-3844.
[38] Y. F Hu, V. Darcos, S. Monge, S. M. Li, Synthesis and self-assembling of poly(N-isopropylacrylamide-block-poly(L-lactide)-block-poly(N-isopropylacrylamide) triblock copolymers prepared by combination of ring-opening polymerization and atom transfer radical polymerization. J. Polym. Sci. Part A: Polym. Chem. 51 (2013) 3274-3283..
[39] G. Masci, L. Giacomelli, V. Crescenzi, Atom transfer radical polymerization of N-isopropylacrylamide. Macromol. Rapid Commun. 25 (2004) 559-564.
[40] K. Bauri, S. Roy, S. Arora, R. Dey, A. Goswami, G. Madras, P. De, Thermal degradation kinetics of thermo-responsive poly(N-isopropylacrylamide-co-N,N-dimethylacrylamide) copolymers prepared via RAFT polymerization. J.Therm. Anal. Calorim. 111 (2013) 753-761.
[41] Y. Bakkour, V. Darcos, S. M. Li, J. Coudane, Diffusion ordered spectroscopy (DOSY) as a powerful tool for amphiphilic block copolymer characterization and for critical micelle concentration (CMC) determination. Polym. Chem. 3 (2012) 2006-2010.
[42] M. Yokoyama, T. Okano, Y. Sakurai, H. Ekimoto, C. Shibazaki, K. Kataoka, Toxicity and Antitumor Activity against Solid Tumors of Micelle-forming Polymeric Anticancer Drug and Its Extremely Long Circulation in Blood. Cancer Res.51 (1991) 3229-3236.
[43] M. L. Adams, A. Lavasanifar, G. S. Kwon, Amphiphilic Block Copolymers for Drug Delivery.

J. Pharm. Sci. 92 (2003) 1343-1355.
[44] Y. Yan, G. K. Such, A. P. R. Johnston, J. P. Best, F. Caruso, Engineering Particles for Therapeutic Delivery: Prospects and Challenges. ACS Nano 6 (2012) 3663-3669.
[45] C. Oerlemans, W. Bult, M. Bos, G. Storm, J. F. Nijsen, W. Hennink, Polymeric Micelles in Anticancer Therapy: Targeting, Imaging and Triggered Release. Pharm. Res. 27 (2010) 2569-2589.
[46] Z. Shen, K. Terao, Y. Maki, T. Dobashi, G. Ma, T. Yamamoto, Synthesis and phase behavior of aqueous poly(N-isopropylacrylamide-co-acrylamide), poly(N-isopropylacrylamide-co-N,N-dimethylacrylamide) and poly(N-isopropylacrylamide-co-2-hydroxyethyl methacrylate). Colloid Polym. Sci. 284 (2006) 1001-1007.
[47] E. C. Cho, J. Lee, K. Cho, Role of Bound Water and Hydrophobic Interaction in Phase Transition of Poly(N-isopropylacrylamide) Aqueous Solution. Macromolecules 36 (2003) 9929-9934.
[48] Y. Okada, F. Tanaka, Cooperative Hydration, Chain Collapse, and Flat LCST Behavior in Aqueous Poly(N-isopropylacrylamide) Solutions. Macromolecules 38 (2005) 4465-4471.
[49] Y. Ono, T. Shikata, Hydration and Dynamic Behavior of Poly(N-isopropylacrylamide)s in Aqueous Solution:A Sharp Phase Transition at the Lower Critical Solution Temperature. J. Am. Chem. Soc. 128 (2006) 10030-10031.
[50] K. C. Choi, J. Y. Bang, P. I. Kim, C. Kim, C. E. Song, Amphotericin B-incorporated polymeric micelles composed of poly(d,l-lactide-co-glycolide)/dextran graft copolymer. Int. J. Pharm. 355 (2008) 224-230.
[51] T. A. Diezi, J. K. Takemoto, N. M. Davies, G. S. Kwon, Pharmacokinetics and nephrotoxicity of amphotericin B-incorporated poly(ethylene glycol)-block-poly(N-hexyl stearate l-aspartamide) micelles. J. Pharm. Sci. 100 (2011) 2064-2070.
[52] S. M. Li, J. L. Espartero, P. Foch, M. Vert, Structural characterization and hydrolytic degradation of a Zn metal initiated copolymer of L-lactide and epsilon-caprolactone. J. Biomater. Sci. Polym. Ed. 8 (1996) 165-187.
[53] Y. L. Luo, C. H. Zhang, F. Xu, Y. S. Chen, Novel THTPBA/PEG-derived highly branched polyurethane scaffolds with improved mechanical property and biocompatibility. Polym. Adv. Technol. 23 (2012) 551-557.

Chapter 4 Thermo-responsive release of curcumin from P(NIPAAm-*co*-DMAAm)-*b*-PLLA-*b*-P(NIPAAm-*co*-DMAAm) triblock copolymers micelles

Abstract Thermo-responsive micelles are prepared by self-assembly of amphiphilic P(NIPAAm-*co*-DMAAm)-*b*-PLLA-*b*-P(NIPAAm-*co*-DMAAm) triblock copolymer using solvent evaporation/film hydration method. The resulting micelles exhibit very low critical micelle concentration (CMC) which slightly increases from 0.0113 to 0.0144 mg mL^{-1} while the DMAAm content increases from 31.8 to 39.4 % in the hydrophilic P(NIPAAm-*co*-DMAAm) blocks. The lower critical solution temperatures (LCST) of copolymers varies from 44.7 °C to 49.4 °C in water as determined by UV spectroscopy, and decreases by *ca.* 3.5 °C in phosphate buffered saline (PBS). Curcumin was encapsulated in the core of micelles. High drug loading up to 20 % is obtained with high loading efficiency (>94 %). The LCST of drug loaded micelles ranges from 37.5 to 38.0 ^{o}C with drug loading increasing from 6.0 to 20 %. The micelles with diameters ranging from 48 to 88 nm remain stable over one month due to the negative surface charge as determined by zeta potential (-12.4 to -18.7 mV). Drug release studies were performed under *in vitro* conditions at 37 °C and 40 °C, *i.e*. below and above the LCST, respectively. Initial burst release is observed in all cases, followed by a slower release. The release rate is higher at 40 °C than that at 37 °C due to thermo-responsive release across the LCST. Micelles with lower drug loading exhibit higher release rate than those with higher drug loading, which is assigned to the solubility effect. Peppas' theory was applied to describe the release behaviors. Moreover, the *in vitro* cytotoxicity of copolymers was evaluated using MTT assay. The results show that the copolymers present good cytocompatibility.

Keywords: thermo-responsive; micelle; self-assembly; block copolymer; poly(L-lactide); poly(*N*-isopropylacrylamide); curcumin

4.1 Introduction

Self-assembled micelles from amphiphilic block copolymers have been widely investigated as nanocarrier for controlled release of drugs [1-4]. Nano-size polymeric micelles exhibit outstanding properties such as reduced side effects, improved therapeutic efficacy, selective targeting, stable storage, and prolonged blood circulation time. Furthermore, polymeric micelles can achieve higher accumulation at the target site through the enhanced permeability and retention (EPR) effect [5-7].

Curcumin, a natural polyphenol derived from curcuma longa, exhibits a wide spectrum of pharmacological activities including anti-oxidant, anti-inflammatory, anti-microbial, anti-amyloid and anti-tumor properties due to its diverse range of molecular targets [8]. In the past decades, it was regarded as a prominent drug for treating inflammation, cystic fibrosis, Alzheimer's and malarial diseases and cancer [9-12]. However, the therapeutic efficacy of curcumin is limited by its extremely low solubility (11 ng mL^{-1}) in water [13]. Moreover, rapid metabolism and elimination lead to poor bioactivity of curcumin [14].

Recently, polymer micelles have been used to encapsulate curcumin so as to enhance the solubility, cellular uptake and anti-tumor bioactivity [15-19]. Micelles prepared from poly(ethylene glycol)-*b*-poly(ε-caprolactone) (mPEG-*b*-PCL) diblock copolymers have been largely studied for controlled delivery of curcumin. However, mPEG-*b*-PCL micelles with drug loading of 9.9 % were unstable as aggregates were observed in 72 hours [15]. Song *et al.* reported the preparation, pharmacokinetics and distribution of curcumin loaded micelles using poly(D,L-lactide-*co*-glycolide)-*b*-poly(ethylene glycol)-*b*-poly(D,L-lactide-*co*-glycolide) (PLGA-*b*-PEG-*b*-PLGA) triblock copolymers [19]. The prolongation of half-life, enhanced residence time and decreased total clearance indicate that the micelles could prolong the acting time of curcumin *in vivo*. Nevertheless, both the drug loading (6.4 %) and encapsulation efficiency (70 %) need to be improved.

Polymer-conjugate micelles were prepared to enhance the curcumin loading, but only 7.5 % cumulative drug release were obtained after 60 hours as drug release is controlled by degradation of micelles [20].

Among the polymeric micelles described in literature, none is sensitive to environmental changes. It is well known that different from normal tissues, tumor has a particularly high temperature (~42 ^{o}C) [21]. Therefore, thermo-sensitive polymeric micelles based on poly(*N*-isopropylacrylamide) (PNIPAAm) with a lower critical solution temperature (LCST) at 32 ^{o}C attracted much attention for targeted stimuli-responsive drug release [22-26]. The hydrophilic PNIPAAm outer shell becomes hydrophobic by increasing the temperature above the LCST. The selective accumulation of micelles at a specific site could be enhanced as a result of enhanced micelle adsorption to cells by hydrophobic interactions between the polymeric micelles. Therefore, thermo-responsive micelles could deliver the drugs *via* a stimuli-responsive targeting process at tumor sites. In addition, nano-scaled thermo-responsive polymeric micelles could combine the passive targeting by EPR effect and active targeting by stimuli response, thus leading to accelerated release of the encapsulated drug at desired sites.

To the best of our knowledge, no thermo-responsive curcumin encapsulated polymeric micelles have been reported, so far. In this work, thermo-responsive micelles were prepared from copolymers composed of a poly(L-lactide) (PLLA) central block and two poly(*N*-isopropylacrylamide-*co*-*N*,*N*-dimethylacrylamide) (P(NIPAAm-*co*-DMAAm)) lateral blocks, using solvent evaporation/film hydration method. Curcumin was loaded in the core of micelles during the fabrication procedure. Drug release studies were realized under *in vitro* conditions in a pH=7.4 phosphate buffer saline at 37 and 40 ^{o}C. The cytotoxicity of micelles was evaluated using MTT assay. The results are reported herein in comparison with literature data.

4.2 Materials and methods

4.2.1 Materials

α, ω-Bromopropionyl PLLA (Br-PLLA-Br) with degree of polymerization (DP) of 40 was prepared as previously reported [27]. Tris(2-dimethyl aminoethyl) amine (Me_6TREN), copper (I) chloride (CuCl), *N*-isopropylacrylamide (NIPAAm), *N*, *N*-dimethyl formamide (DMF), chloroform, dicholoromethane, diethyl ether, basic aluminum oxide, Tween 80, ethylenediaminetetraacetic acid tetrasodiumsalt hydrate (EDTA-Na_4 •H_2O) and curcumin were obtained from Sigma-Aldrich and used without further purification. DMAAm was obtained from Sigma-Aldrich and purified through a basic aluminum oxide column. Ultrapure water with a conductivity of 18 MΩ was produced using a Millipore Milli-Q water system.

4.2.2 Synthesis of P(NIPAAm-*co*-DMAAm)-*b*-PLA-*b*-P(NIPAAm-*co*-DMAAm) triblock copolymer (T2, Table 2)

Triblock copolymers were prepared by atom transfer radical polymerization (ATRP) at 25 ^{o}C using a DMF/water mixture solvent as reported previously [28]. Typically, 100 mg Br-PLLA-Br (30.4×10^{-3} mmol, $M_{n,NMR}$= 3300 g mol^{-1}), 511.4 mg NIPAAm (4.52 mmol), 159.4 mg DMAAm (1.61 mmol) and 6.0 mg CuCl (60.8×10^{-3} mmol) were dissolved in 3 mL DMF in a Schlenk tube. 0.5 mL H_2O was then added. After five freeze-pump-thaw cycles, 16μL Me_6TREN (60.8×10^{-3} mmol) was added under argon atmosphere. The mixture was stirred at 25 ^{o}C for 1 h. The reaction was stopped by precipitation in diethyl ether. The crude product was dissolved in 10 mL chloroform and passed through a basic aluminum oxide column for 3 times to remove the catalyst complex. After concentration under reduced pressure, the solution was precipitated again in diethyl ether. The product was dissolved in DMF and then

dialyzed for 3 days in a dialysis bag (MWCO: 3500) to remove the monomer and trace copper against Mill-Q water adding ethylenediaminetetraacetic acid tetrasodium salt hydrate. The product was then collected by lyophilization.

4.2.3 Preparation of curcumin-loaded polymeric micelles

Typically, 2.51mg curcumin and 17.53 mg copolymer T2 (Sample 2, Table 4.3) were dissolved in 20 mL acetone. The solvent was evaporated in rotary evaporator at room temperature to yield a membrane on the wall of the flask. After vacuum drying for 24 hours, 20 mL Milli-Q water was added to the flask. Drug loaded micelles were obtained under stirring at room temperature. The micelle solution was then centrifuged at 5000 rpm for 10 min to remove unload curcumin, and the supernatant was lyophilized and stored at 4 ^{o}C before use.

4.2.4 *In vitro* drug release

The drug loading (DL) and encapsulation efficiency (EE) were determined as follows. 5 mg lyophilized micelles were dissolved in 5 mL acetonitrile/ammonium acetate (10 mM) mixture solution (pH= 4.0). Then the solution was diluted 100 times. The concentration of curcumin was determined by UV-Vis spectroscopy at 424 nm, using a previously established standard calibration curve. The drug loading and encapsulation efficiency were calculated according to the following equations:

$$Drug\ loading\ (\%) = \frac{weight\ of\ loaded\ drug}{weight\ of\ polymeric\ micelles} \times 100 \qquad (1)$$

$$Encapsulation\ efficiency\ (\%) = \frac{weight\ of\ drug\ in\ micelles}{theoretical\ drug\ loading} \times 100 \qquad (2)$$

Drug loaded micelles (2 mg) were dispersed in 2 mL PBS solution (pH=7.4), and then introduced into a dialysis bag (MWCO: 3500). The bag was placed in 10 mL PBS containing 0.5 *wt*% Tween80 in an incubator (Heidolph 1000) with gentle shaking (150 rpm) at 37 or 40 ^{o}C. At specific time intervals, the release medium was removed

and replaced by pre-warmed (37 ^{o}C) fresh medium. The withdrawn solution was then diluted 10 times with pH=4.0 acetonitrile/ammonium acetate (10 mM) mixture solution for UV measurement.

4.2.5 *In vitro* cytotoxicity

The cytotoxicity of copolymers was evaluated by MTT assay. After UV sterilization for 5 hours, the copolymer T2 was dissolved in dulbecco's modified eagle's meduim (DMEM, Hyclone products) at a concentration of 6 mg mL^{-1}. Then the solution was transferred to 96-well plates (Corning costar, USA), 100 μL per well. The wells were placed in an incubator (NU-4850, NuAire, USA) at 37 ^{o}C under humidified atmosphere containing 5 % CO_2 for 24 hours. After incubation, the copolymer in the form of a hydrogel was used as cell culture substrate.

Murine fibrosarcoma (L929) and human lungcarcinoma cell (A549) in logarithmic growth phase were harvested and diluted with DMEM medium (10 % calf serum, 100 μg mL^{-1} Penicillin, 100 μg mL^{-1} streptomycin) to a concentration of 1×10^{5} cells mL^{-1}. 100 μL cellular solution was added in each hydrogel containing well which was then placed in the same incubator under humidified atmosphere containing 5 % CO_2 at 37 ^{o}C. 100 μL fresh medium was used as the negative control, and 100 μL of 5 % phenol solution as the positive control. After 2, 3 and 4 days, 20 μL 3-(4,5-dimethylthiazol-2-yl)-2,5-diphenyltetrazolium bromide (MTT) at 5 mg mL^{-1} were added. The medium was removed after 6 hours incubation, and 150 μL dimethylsulfoxide (DMSO) was added. After 15 min shaking, the optical density (OD) was measured by using a microplate reader (Elx800, BioTek, USA) at 490 nm. The relative growth ratio (RGR) was calculated by using the following equation:

$$RGR\,(\%) = (OD_{test\ sample}/OD_{negative\ control}) \times 100 \qquad (3)$$

The cytotoxicity is generally noted in 0-5 levels according to the RGR value as shown in Table 4.1.

Table 4.1 Relationship between the RGR value and cytotoxicity level

RGR (%)	≥100	75-99	50-74	25-49	1-24	0
Level	0	1	2	3	4	5

The cellular morphology was observed using an Olympus CKX41 inverted microscope. After 3 days seeding, the test medium was replaced with 150 μL neutral red staining solution (NR) for 10 minutes at room temperature. The plates were rinsed 3 times with warm PBS, and the morphology of cells adhered to the hydrogel surface was immediately observed under microscope.

4. 2.6 Characterization

Nuclear magnetic resonance (^{1}H NMR) ^{1}H NMR spectra were recorded on a Bruker spectrometer (AMX300) operating at 300 MHz.Chemical shift was referenced to the peak of residual non-deuterated solvents.

Size exclusion chromatography (SEC) SEC measurements were performed on a Varian 390-LC equipped with a refractive index detector and two ResiPore columns (300×7.5 mm) at 60 °C at a flow rate of 1 mL min^{-1}. The eluent was DMF containing 0.1 *wt* % LiBr. Calibration was established with PMMA standards.

Fluorescence Spectroscopy The critical micellar concentration (CMC) of copolymers was determined by fluorescence spectroscopy using pyrene as a hydrophobic fluorescent probe. Measurements were carried outon an RF 5302 Shimadzu spectrofluorometer (Japan) equipped with Xenon light source (UXL-150S, Ushio, Japan). The fluorescence excitation spectra of copolymer solutions containing 6×10^{-7} M pyrene were recorded from 300 to 360 nm at an emission wavelength of 394 nm. The emission and excitation slit widths were 3 and 5 nm, respectively. The excitation fluorescence values I_{337} and I_{333}, respectively at 337 and 333 nm, were used for subsequent calculations.

Cloud point The LCST was estimated from the changes in the transmittance through copolymer solutions at 1.0 mg mL^{-1} as a function of temperature. The measurements were carried out at a wavelength of 500 nm with a Perkin ElmerLambda 35 UV-Visible spectrometer equipped with a Peltier temperature programmer PTP-1+1. The temperature ramp was 0.1 °C min^{-1}.

Dynamic light scattering (DLS) and Zeta-Potential (ZP) The size and zeta-potential of micelles were determined by using Zetasizer Nano-ZS (Malvern Instrument Ltd. UK) equipped with a He-Ne laser (λ = 632.8 nm). Polymer solutions at 1.0 mg mL^{-1} were filtered through a 0.45 μm PTFE microfilter before measurements.

Transmission electron microscopy (TEM) TEM experiments were carried out on a JEOL 1200 EXII instrument operating at an acceleration voltage of 120 kV. The samples were prepared by dropping a polymer solution at 1.0 mg mL^{-1} onto a carbon coated copper grid, followed by air drying.

Inductively Coupled plasma-mass spectrometry (ICP-MS) The residual copper content in the copolymers was quantified using ThemoFinnigan Element XR sector field ICP-MS previously calibrated using copper solutions in water. Typically, samples were prepared by dissolution of the copolymers in nitric acid. The solution was then heated to fully decompose the polymer until no precipitate was visible. After that, the samples were dissolved in 10 mL deionized water before analysis to determine the copper concentration. Each sample was analyzed four times.

4.3 Results and discussion

4.3.1 Synthesis of triblock copolymers

A series of P(NIPAAm-*co*-DMAAm)-*b*-PLA-*b*-P(NIPAAm-*co*-DMAAm) triblock copolymers were successfully synthesized by ATRP as described in a previous work [28]. The DP of PLLA macroinitiator is 40, while that of NIPAAm and DMAAm ranges from 63 to 74, and from 32 to 41, respectively (Table 4.2).

Table 4.2 Characteristics of P(NIPAAm-*co*-DMAAm)-*b*-PLA-*b*-P(NIPAAm-*co*-DMAAm) triblock copolymers

Run	PLA/NIPAAm /DMAAm [a]	[LA]/[NIPAAm] /[DMAAm][b]	NIPAAm/ DMAAm[b]	$M_{n,\,NMR}$[b] g mol^{-1}	$M_{n,\,SEC}$[c] gmol^{-1}	$Đ$[c]
T1	1/148.8/51.2	40/74/34	68.2/31.8	18300	26000	1.1
T2	1/147.5/52.5	40/65/32	65.8/34.2	19700	25000	1.1
T3	1/142.6/57.4	40/66/36	64.8/35.2	14300	21000	1.1
T4	1/136.2/63.8	40/63/41	61.6/39.4	14500	18000	1.1

a) feed ratio (in equivalents); b) calculated by NMR; c) determined by SEC

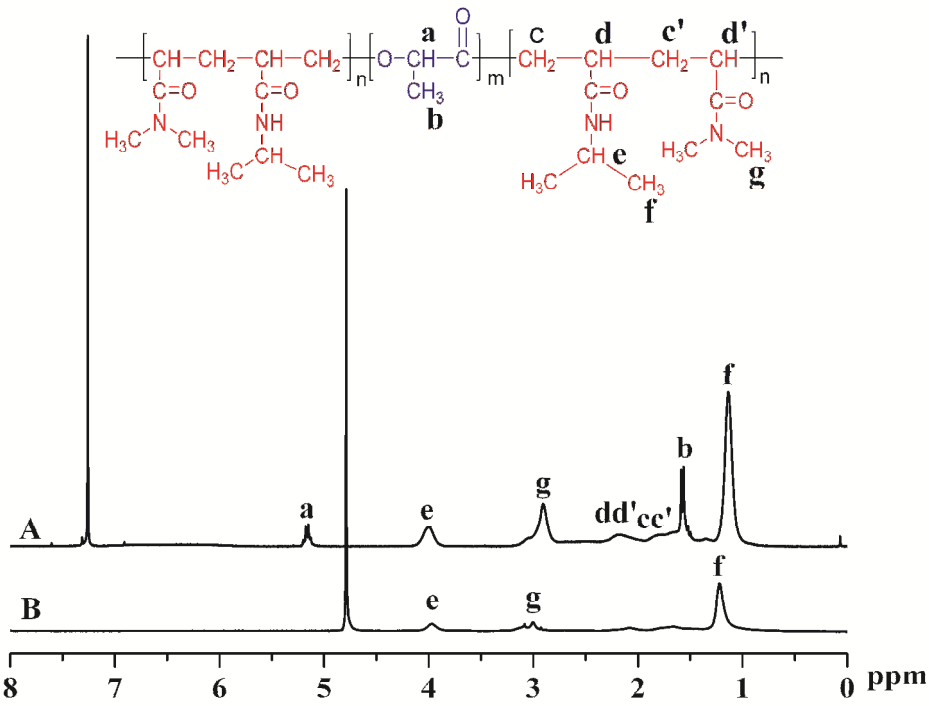

Figure 4.1 ^{1}H NMR spectra of triblock copolymer T2 in (A) $CDCl_3$, and (B) D_2O.

Various NIPAAm/DMAAm ratios were used to tailor the properties of the resulting copolymers. The molecular weights determined by SEC ($M_{n,SEC}$) range from 18,000 to 26,000 g $mol^{-1}$with narrow dispersity ($Đ$= 1.1), whereas the molecular weights determined by ^{1}H NMR ($M_{n,NMR}$) are lower. $M_{n,SEC}$ values are obtained with respect to poly(methyl methacrylate) standards, and are generally higher than absolute molecular weights.

The chemical structure of triblock copolymers was characterized by ^{1}H NMR spectroscopy. As shown in Figure 4.1A, the peaks at 1.1 and 4.0 ppm were attributed respectively to the methyl (H_f, CH_3) and the methine protons (H_e, CH) adjacent to the amine moiety of the NIPAAm units. The signal at 2.9 ppm is assigned to the methyl proton (H_g, CH_3) of the DMAAm units. The signals at 1.6 and 5.2 ppm are characteristic of the methyl (H_b) and methine protons (H_a, CH) of PLLA. The composition of copolymers, the DP of NIPAAm and DMAAm in the hydrophilic block, and the molecular weight (M_n) of copolymers were calculated from the integrations o f the methine protons of lactyl units at 5.1 ppm, the methine protons of NIPAAm units at 4.0 ppm, and the methyl protons of DMAAm at 2.9 ppm.

After polymerization, the catalyst was removed by filtration through a basic alumina column. The copolymers recovered by precipitation in diethyl ether appeared almost colorless. ICP-MS measurements showed that the copper content in the copolymers was between 1 and 3 ppm.

4.3.2 Characterization of polymer micelles

It is well-known that amphiphilic copolymers can form polymeric micelles by self-assembly in aqueous medium. Figure 4.1B shows the ^{1}H NMR spectrum of copolymer T2 obtained in D_2O. Compared with the ^{1}H NMR spectrum in $CDCl_3$ (Figure 4.2A), the peaks belonging to PLLA moieties at 5.2 and 1.6 ppm totally

disappear in D_2O. This finding evidences the aggregation of copolymers into micelles with the PLLA block in the core and P(NIPAAm-*co*-DMAAm) blocks at the corona.

Table 4.3 Characterization of triblock copolymer micelles

Copolymer	CMC[a] g mL^{-1}	D[b] (nm)	PDI[b]	LCST[c] (^oC)	LCST[d] (^oC)	ZP[e] (mV)
T1	11.3	37	0.11	44.7	41.4	-18.7
T2	13.1	39	0.11	45.6	42.1	-12.4
T3	13.7	41	0.14	45.9	42.5	-15.3
T4	14.4	44	0.17	49.4	46.2	-16.4

a) by fluorescence spectroscopy; b) by DLS; c) by UV spectroscopy in deionzed water; d) by UV spectroscopy in PBS; e) by Zetasizer Nano-ZS

The CMC is an important parameter which reflects the stability of micelles upon dilution. The lower the CMC, the higher the stability of micelle. In this work, the CMC was determined by fluorescence spectroscopy using pyrene as the probe. As shown in Table 4.3, the CMC of copolymers slightly increases from 0.0113 to 0.0144 mg mL^{-1} while the content of DMAAm increases from 31.8 % for T1 to 39.4 % for T4 in the hydrophilic part. In fact, the CMC is dependent on different factors such as the composition, the hydrophilic to hydrophobic ratio, the molecular weight, *etc.* The DMAAm units are more hydrophilic than NIPAAm ones. Thus, higher DMAAm contents lead to higher CMC. The very low CMC values indicate the strong tendency of copolymers toward formation of micelles, which is of major importance for the stability of micelles in the bloodstream after injection induced dilution [29].

The LCST of copolymers was determined by light transmission measurements using UV spectroscopy. As shown in Table 4.3, the LCST value in distilled water increases from 44.7 to 49.4 °C with increasing DMAAm content in the hydrophilic blocks. LCST measurements were also performed in a pH 7.4 phosphate buffered saline (PBS) to mimic the *in vivo* conditions. A decrease of *ca*. 3.5 degrees in LCST values is observed in PBS as compared to those in distilled water.

The size and size distribution of copolymer micelles were determined by dynamic light scattering (DLS). The average diameter varies from 37 to 44 nm, and the dispersity (PDI) from 0.11 to 0.17 with increasing DMAAm content in the hydrophilic blocks. The zeta-potential of copolymer micelles varies in the -12.4 to -18.7 mV range. The zeta potential value decreases with the increase of hydrophilic content. This finding well agrees with the structure of micelles having PLLA block in the core and P(NIPAAm-*co*-DMAAm) blocks at the corona.

4.3.3 Preparation and characterization of drug loaded micelles

Curcumin is a natural anticancer drug, but its application is limited due to poor solubility. Copolymer T2 with a LCST of 42.1 °C in PBS was selected for drug release studies. Different ratios of curcumin and copolymer T2 were used to prepare drug loaded micelles by solvent evaporation/membrane rehydration method (Table 4.4). After lyophilization, the micelles were dispersed in PBS solution for drug release studies.

Table 4.4 Properties of curcumin-loaded micelles prepared from copolymer T2

Sample	Drug/Polymer (mg/mg)	DL (%)	EE (%)	LCST[a] (^{o}C)	D[b] (nm)	PDI[b]	Zeta-potential (mV)	
							In water	In PBS
1	1.2/18.9	6.0	97.2	38.0	48	0.19	-13.9	-7.51
2	2.5/17.5	12.1	96.6	37.8	54	0.21	-15.5	-7.68
3	4.5/16.3	20.4	94.1	37.5	88	0.25	-18.1	-2.39

a) by UV in PBS; b) by DLS in water

The drug loading (DL) and encapsulation efficiency (EE) of micelles were obtained by light transmission measurements using UV spectroscopy. When the initial drug amount increases from 1.2 to 4.50 mg with approximately the same amount of polymer, drug loading increases from 6.0 to 20.4 %. The loading efficiency is above 94 % in all cases.

The curcumin-loaded micelle samples in PBS at 1 mg mL^{-1} are shown in Figure 4.2, in comparison with a 6.0 % curcumin aqueous solution. In water, curcumin remains as a sediment at the bottom due to the poor solubility (Figure 4.2A). On the contrary, a homogenous and transparent yellow solution is obtained in the case of curcumin-loaded micelles (Figure 2B, C and D), showing that hydrophobic curcumin was successfully loaded inside the polymeric micelles.

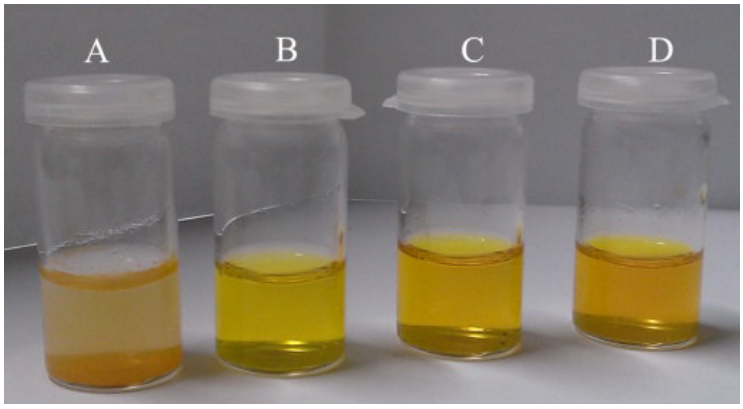

Figure 4.2 Image of (A) 6.0 % curcumin in H_2O; (B) 6.0 % curcumin-loaded micelles in PBS; (C) 12.1 % curcumin-loaded micelles in PBS; (D) 20.4 % curcumin-loaded micelles in PBS.

The effect of drug loading on the micelle properties was investigated in detail (Table 4.4). Figure 4.3 shows the DLS and TEM results of samples 1, 2 and 3. With increase of drug load from 6.0 to 20.4 %, the average size of micelles increases from 48 to 88 nm with corresponding PDI increasing from 0.19 to 0.25. This finding well agrees with literature data. In fact, Gong *et al.* reported an increase of size (from 21.7 to 36.2 nm) and PDI (from 0.098 to 0.259) of curcumin loaded mPEG-*b*-PCL micelles [15]. The size of our micelles is larger than that of mPEG-*b*-PCL (22 to 36 nm) or PLGA-PEG-PLGA micelles (29 nm), probably due to higher hydrophobic to hydrophilic ratios [15, 19].

TEM experiments were performed to examine the morphology of the self-assembled aggregates. As shown in Figure 4.3, the curcumin-loaded micelles with DL=6.0 %, 12.1 % and 20.4 % are spherical in shape with an average diameter of 33, 42 and 75

nm, respectively. The size obtained from DLS is larger than that from TEM due to different experimental conditions. In fact, DLS allows determining the hydrodynamic diameter of micelles in aqueous solution, whereas TEM shows the dehydrated solid state of micelles.

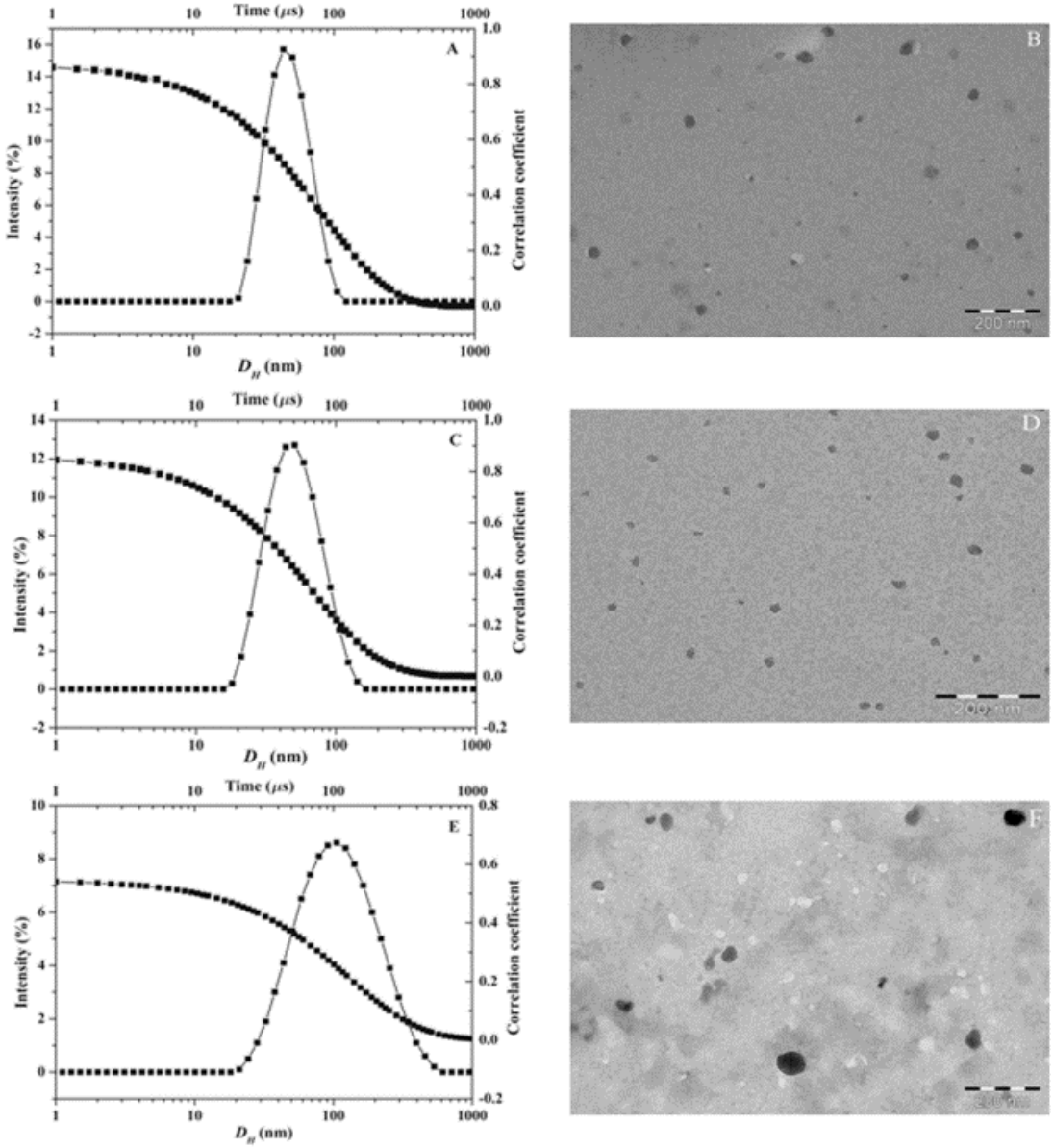

Figure 4.3 DLS spectra and TEM micrographs of curcumin loaded micelles. (A) and (B): sample 1 (DL=6.0 %); (C) and (D): sample 2 (DL=12.1 %); (E) and (F): sample 3 (DL=20.4 %).

The zeta potential of curcumin-loaded micelles in water ranges from -13.9 mV for Sample 1 to -18.1 mV for Sample 3, indicating good micellar stability. Compared to blank polymer micelles, curcumin-loaded micelles present higher charge due to larger surface area, resulting from the increase of micelle size. The ZP of sample 1, sample 2 and sample 3 decreases to -7.51, -7.68 and -2.39 mV in PBS, respectively. This significant decrease can be attributed to the ionic screening effect and clustered aggregate [23]. All the samples remained homogeneously transparent over 1 month. It is known that more pronounced zeta potential absolute values tend to stabilize particles in suspension. The electrostatic repulsion between micelles with the same electrical charge prevents aggregation of micelles [30, 31]. Thus, the negatively charged surface of micelles could help to stabilize the micelles via both the steric and electrostatic mechanisms. It is of interest to note that mPEG-PCL micelles with 9.9 % curcumin loading remained stable for 72 h [15]. On the other hand, Liu *et al.* reported stable mPEG-PCL micelles with small size (28.2 nm) with low zeta potential (0.41 mV) [17]. The stability was attributed to the stereospecific blockade of micelles although the authors did not mention the duration of micelle stability.

Both the size and zeta potential are important physicochemical properties of micelles because they determine the physical stability as well as the biopharmaceutical properties. The nano-size (48-88 nm) of curcumin-loaded micelles allows them to escape from the reticuloendothelial system (RES) and preferentially accumulate in tumor tissues through the EPR effect [32-35]. The charge of nanomaterials is also an important factor to affect the biocompatibility [35]. Generally, positive charges are considered as harmful to the plasma exposure of nanomaterials since they could induce the formation of primary platelet clots [36-38]. On the contrary, negative charges of micelles are beneficial to negatively charged human blood as they could enhance the binding of micelles to proteins, reduce undesirable clearance by the reticuloendothelial system such as liver, improve the blood compatibility, and thus deliver the anti-cancer drugs more efficiently to the tumor sites [37, 39].

4.3.4 Phase transition of curcumin loaded polymeric micelles

It is well known that the drug release of thermo-responsive polymeric micelles is controlled by the phase transition (Figure 4.4). Generally, the P(NIPAAm-*co*-DMAAm) block is hydrophilic and the solution is transparent below the LCST. When the temperature increases above the LCST, dehydration of P(NIPAAm-*co*-DMAAm) occurs due to coil-to-globule transition, leading to precipitation of polymers and the release of drug from polymer matrix.

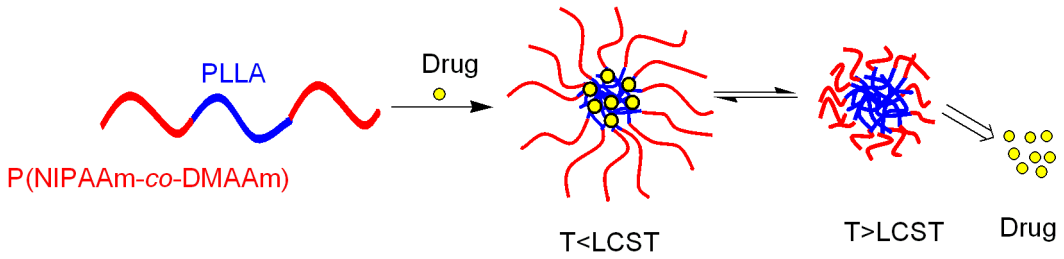

Figure 4.4 Illustration of drug release from thermo-responsive polymeric micelles controlled by phase transition.

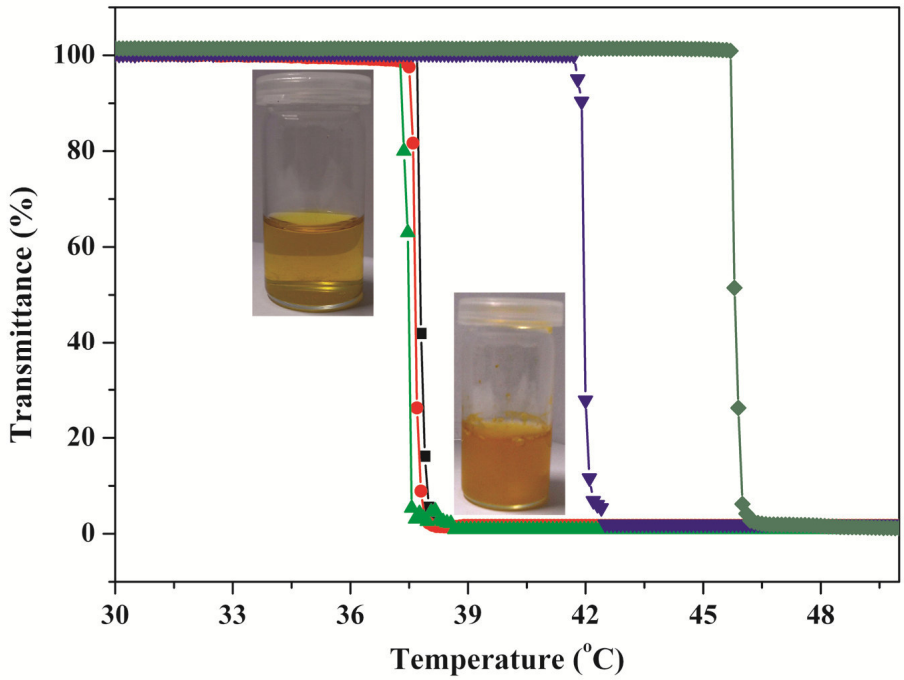

Figure 4.5 Phase transition of curcumin-loaded micelles at 1 mg mL^{-1} determined by UV-Vis spectroscopy. (◆) DL=0 in water; (▼) DL=0 in PBS; (■) DL=6.0 % in PBS; (●) DL=12.1 % in PBS; (▲) DL=20.4 % in PBS.

Figure 4.5 shows the phase transition of various curcumin-loaded micelles in water or in PBS. The initially transparent solution of curcumin-loaded micelles becomes turbid when the temperature increases above the LCST. In the meantime, the transmittance of the solution rapidly decreases from 100 % to 0.

The presence of salt greatly affects the behavior of thermo-responsive polymers. As shown in Figure 4.5, the LCST of blank micelles decreases from 45.6 ^{o}C in water to 42.1 ^{o}C in PBS due to the high ionic strength in PBS and screening effect from counter-ions. The presence of phosphate leads to partial dehydration of the macromolecules and consequently to a decrease of the LCST. The influence of drug loading on the LCST was also considered in PBS. The LCST of curcumin-loaded micelles with 6.0 % drug load is 38.0 ^{o}C in PBS, which is lower by 4.1 ^{o}C than that of drug free micelles (Figure 4.5, Table 3). This finding is assigned to the enhanced core hydrophobicity due to encapsulated drug. Higher drug load leads to lower LCST, but the decrease is very limited. In fact, the LCST only slightly decreases from 38.0 to 37.5 ^{o}C when the drug load increases from 6.0 % to 20.4 %. In addition, the phase transition intervals are very sharp (<0.5 ^{o}C) in all cases, as reported in our previous work [28]. The fast phase transition favors rapid response of drug release when the micelles were delivered to the tumor site.

4.3.5 *In vitro* drug release

Drug release was performed under physiological conditions (PBS, pH=7.4) at 37 °C (below the LCST) and 40 ^{o}C (above the LCST), respectively. The amount of curcumin was determined from the UV-visible absorbance at 424 nm. A linear calibration curve was previously established between the UV absorbance and curcumin concentration with a correlation coefficient of 0.99991 (Figure 4.6A).

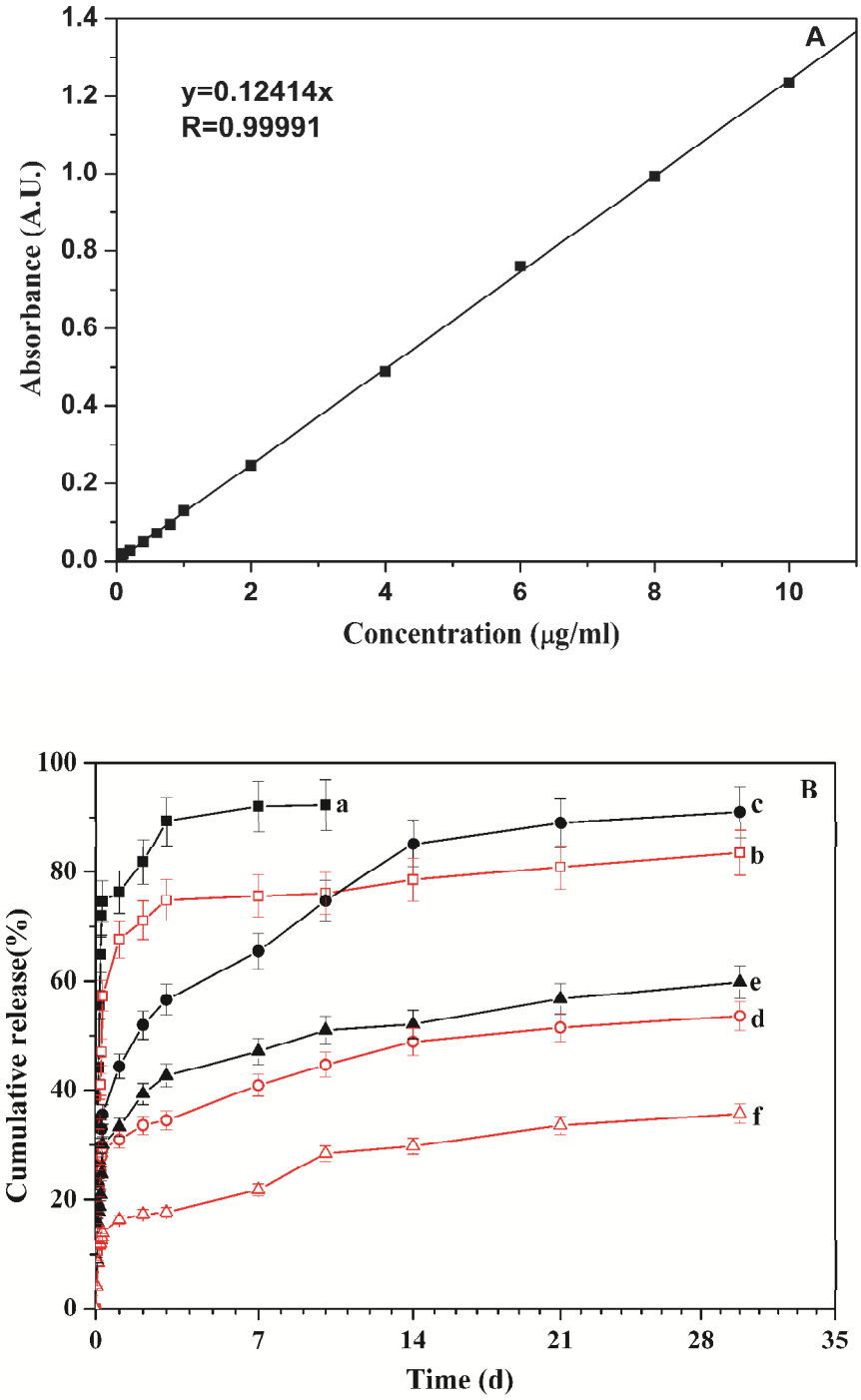

Figure 4.6 Calibration curve (A) and drug release profiles (B) of curcumin-loaded micelles at 37 ^{o}C (red) and 40 ^{o}C (black): a and b - sample 1 (DL=6.0 %); c and d - sample 2 (DL=12.1 %); e and f - sample 3 (DL=20.4 %).

The *in vitro* release profiles are shown in Figure 4.6B. The release rate of curcumin from micelles is strongly influenced by the phase transition at the LCST. The cumulative drug release at 40 ^{o}C (above LCST) is much higher than that at 37 ^{o}C

(below LCST). In all cases, burst-like release is observed. The cumulative release for samples 1, 2 and 3 after 1 hour at 40 °C is 23.6 %, 14.7 % and 9.0 %, respectively, while it is 16.3 %, 10.4 % and 4.1 % at 37 °C. The burst-like release at 37 ^{o}C can be attributed to the release of drug located at the interface between the core and corona of micelles. The larger burst-like release at 40 ^{o}C is attributed not only to the fast release because of phase transition above the LCST, but also to the release of drug located at the interface.

Sample 1 with 6.0 % drug loading shows the fastest drug release. After the first 3 days, 89.3 % and 74.9 % of the loaded curcumin are released at 40 °C and 37 °C, respectively. Beyond, the release rate slows down. The cumulative release of curcumin reaches 84 % at 37 °C after 30 days and 92.3 % at 40 ^{o}C after 10 days. The release rate is slower for sample 2 with initial drug loading of 12.1 %. The cumulative release is 85.2 % and 48.9 % after 14 days, and 91.1 % and 53.6 % after 30 days at 40 ^{o}C and 37 ^{o}C, respectively. Sample 3 with initial drug loading of 20.4 % shows the slowest drug release. After 30 days, curcumin release reaches 59.8 % and 35.7 % at 40 °C and 37 °C, respectively. Therefore, drug release is not only dependent on the phase transition across the LCST, but also on the drug loading. In fact, the solubility of curcumin in the release medium is a limiting factor. Samples with higher drug loading exhibits lower release rate because of the solubility effect. It should also be noted that the LCST of cur-micelles is dynamically changing with the release of curcumin. Theoretically, the LCST will increase up to 42.1 ^{o}C when the drug release reaches 100 % for all the samples as shown in Figure 4.5.

Peppas *et al.* proposed the following semi-empirical equation to describe the drug release mechanism from a polymeric matrix [40-42]:

$$\frac{M_t}{M_0} = kt^n \qquad (4)$$

$$\log(M_t/M_0) = n\log t + \log k \qquad (5)$$

Where M_t and M_0 are the cumulative amount of released drug at time t and the drug loading, respectively, k is a constant incorporating structural and geometric characteristic of the device and n is the release exponent indicating the drug release mechanism. For spherical particles, the value of n is equal to 0.43 for Fickian diffusion, and equal to 0.85 for swelling-controlled mechanism. In contrast, n<0.43 means combination of diffusion and erosion controlled release, and 0.43<n<0.85 is assigned to anomalous transport mechanism.

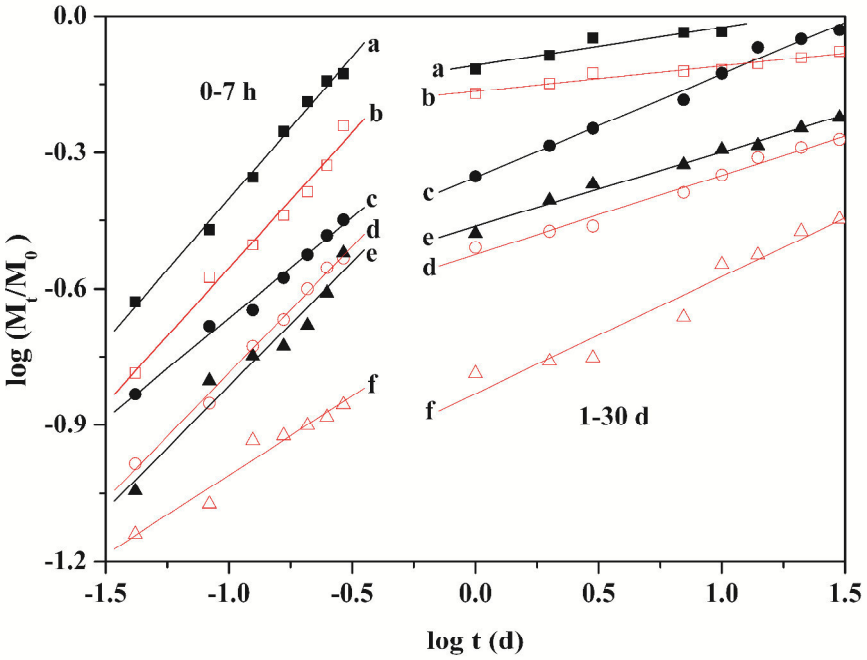

Figure 4.7 Plots of theoretical fitting to Peppas model for curcumin release from curcumin-loaded micelles (the symbols are the same as in Figure 4.6).

Figure 4.7 presents the theoretical fitting plots. The various release curves are divided in two stages: from 0 to 7 hours and from 1 to 30 days. The fitting parameters n, k and the correlation coefficient R^2 are summarized in Table 5. For the first stage, the n values at 40 ^{o}C are in the range of 0.43 to 0.85, suggesting that the release of curcumin involves anomalous transport probably due to phase transition across the LCST. The n values of sample 1 and 2 at 37 ^{o}C are also in the range of 0.43 to 0.85, which could be assigned to the initial burst release. The n value of sample 3 at 37 ^{o}C is 0.349, indicating diffusion and degradation controlled release according to Peppas'

theory. It might also be attributed to the highest drug loading and compact micelle structure. For the second stage, the *n* values in all cases are well below 0.43, suggesting a combination of diffusion and degradation controlled release. For both stages, the *k* values at 40 ^{o}C are higher than those at 37 ^{o}C, which confirms a faster drug release above the LCST due to collapse of micelles.

Table 4.5 Release exponent (*n*), rate constant (*k*) and correlation coefficient (R^2) for drug release from drug loaded polymer micelles.

Sample	Time interval	40^{o}C			37 ^{o}C		
		n	*k*	R^2	*n*	*k*	R^2
Sample 1	0-7h	0.6238	1.6667	0.997	0.5969	1.1033	0.992
	1-30d	0.0843	0.7780	0.943	0.0552	0.6834	0.974
Sample 2	0-7h	0.4430	0.6002	0.995	0.5563	0.5904	0.997
	1-30d	0.22693	0.4421	0.994	0.17396	0.2990	0.991
Sample 3	0-7h	0.5444	0.5376	0.975	0.3490	0.2187	0.974
	1-30d	0.1638	0.3448	0.994	0.2576	0.1477	0.972

Therefore, the release of curcumin from thermo-responsive curcumin-loaded micelles is strongly affected by the phase transition across the LCST. Such release would favor drug accumulation at a specific tumor site where the temperature is above the LCST. Thus the micelles could combine the passive targeting by EPR effect due to the small size ranging from 47.5 to 88.2 nm, and the active targeting by thermo-responsive phase transition.

4.3.6 *In vitro* cytocompatibility

Curcumin is a natural polyphenolic compound with low intrinsic toxicity. The *in vitro* cytotoxicity of copolymers is evaluated by MTT assay, a widely used method for the screening of biomaterials. MTT assay is based on the reaction between MTT and mitochondrial succinate dehydrogenases in living cells to form a purple formazan which is soluble in DMSO but insoluble in water. The OD value of formazan-DMSO solution is considered to be proportional to the number of living cells.

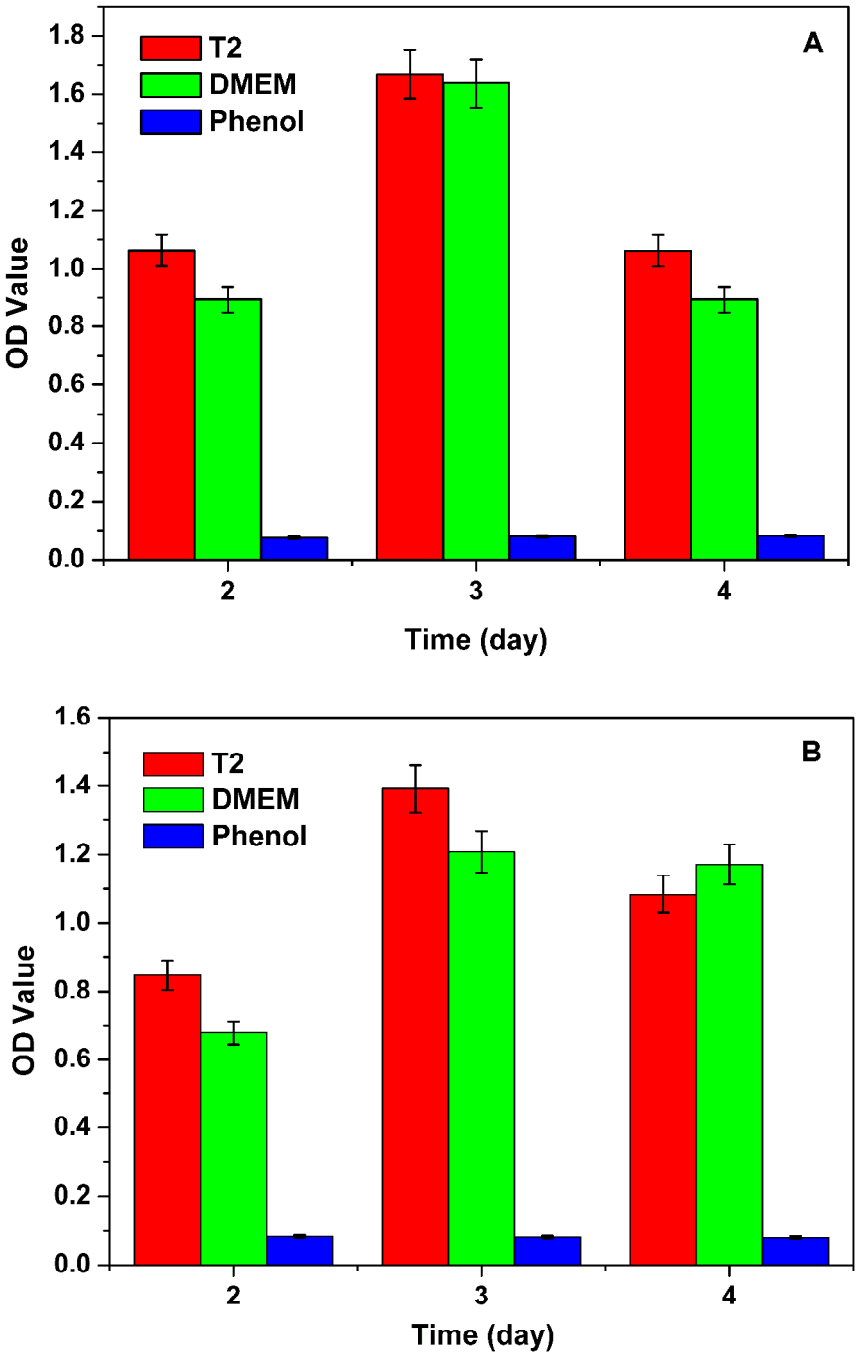

Figure 4.8 Optical density values of L929 (A) and A549 (B) solutions after 2, 3 and 4 days culture in DMEM with copolymer substrate (T2), and controls (DMEM and 5 % phenol).

The effects of copolymer T2 on the proliferation of L929 and A549 cells are shown in Figure 4.8. In comparison with controls (DMEM medium and 5 % phenol), the OD values on polymer substrate are close to those in the culture medium, and much higher than those in phenol. The RGR values (Table 4.6) of copolymer T2 are well

above 92.6 % during 4 days incubation with L929 and A549 cells, corresponding to a cytotoxicity level of 0 and 1 as defined in Table 1, thus indicating that the copolymers present no cytotoxicity.

Table 4.6 RGR values of copolymers T2 with A549 and L929 cells during 4 days incubation.

Cell type	RGR (%)		
	2 days	3 days	4 days
L929	118.9	102.0	118.8
A549	124.9	115.2	92.6

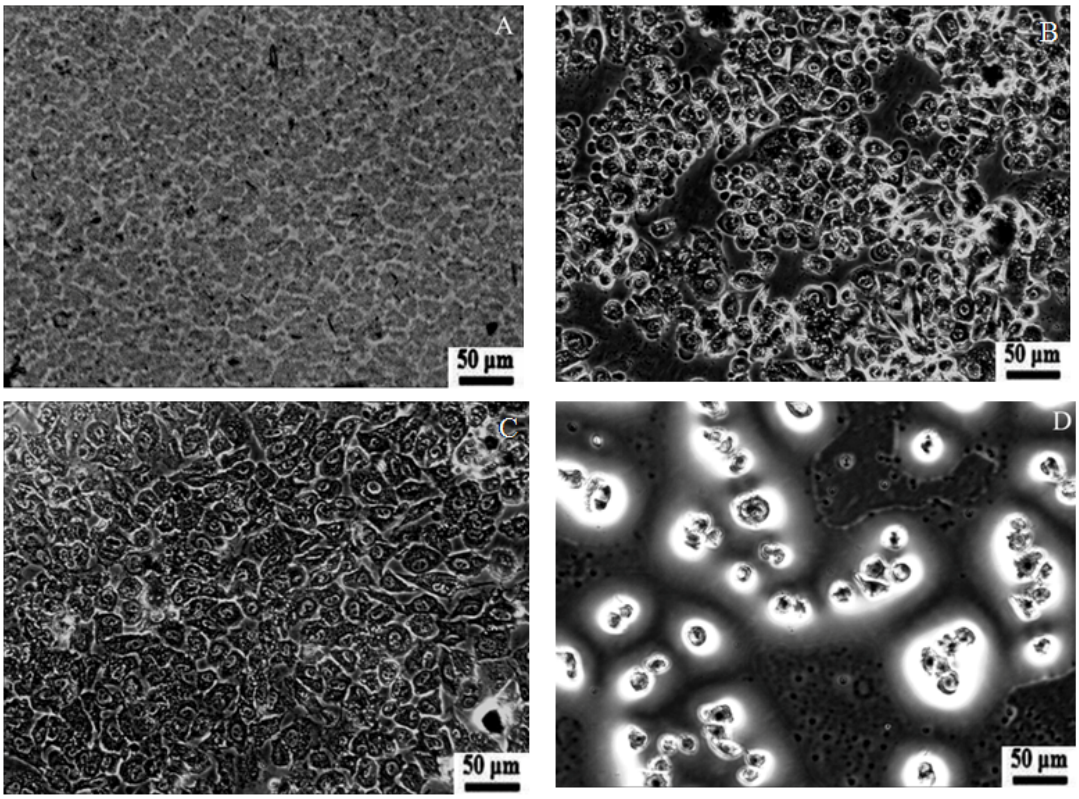

Figure 4.9 Microscopic images of cells stained by NR after 3 days culture in different media: (A) Copolymer T2 substrate without cells; (B) L929 cells on polymer substrate in DMEM; (C) A549 cells on polymer substrate in DMEM; (D) A549 cells in 5 % phenol medium.

Figure 4.9 shows the morphology of cells after 3 days culture. Large number of cells died in the toxic phenol medium (Figure 4.9). On the contrary, cell adhesion and proliferation are observed on the copolymer substrate (Figure 4.9B and Figure 4.9C). Cells exhibit spindle, polygon or oval shapes, and the pseudopodium of cells stretches

out. Therefore, MTT assay and cell morphology results indicate that P(NIPAAm-*co*-DMAAm)-*b*-PLLA-*b*-P(NIPAAm-*co*-DMAAm) copolymers present outstanding cytocompatibility and could be used for biomedical applications.

4.4 Conclusions

In this work, thermo-responsive micelles are prepared by self-assembly of P(NIPAAm-*co*-DMAAm)-*b*-PLLA-*b*-P(NIPAAm-*co*-DMAAm) triblock copolymers as drug carrier, where curcumin was used as a model drug. Compared to mPEG-*b*-PCL or PLGA-*b*-PEG-*b*-PLGA micelles, the thermo-responsive micelles described in this manuscript present several advantages. First, lower CMC values ranging from 0.0113 to 0.0144 mg mL^{-1} are obtained, which should enhance the stability of micelles during long circulation in the bloodstream after injection induced dilution. Second, high curcumin loading up to 20.4 % was achieved. Meanwhile, the micelles remain stable over 1 month due to the negative surface charge as shown by zeta potential measurements. Last, the micelles with sizes ranging from 47.5 to 88.2 nm could combine the passive targeting by EPR effect and thermo-responsive targeted release. Such responsive behavior will favor the release at a specific tumor site (~42 ^{o}C). Therefore, all these properties show that the thermo-responsive micelles described in this work are promising as a functional drug carrier.

Recently, due to the possible concerns on the toxicity of *N*-isopropylacrylamide monomer, Lutz *et al.* reported new thermo-responsive and biocompatible copolymer from ATRP of two PEG Analogues: 2-(2-methoxyethoxy) ethyl methacrylate (MEO_2MA) and oligo(ethylene glycol) methacrylate (OEGMA) [43-47]. Thus, in order to make a comparison, following work will focus on the synthesis and self-assembly of PLA/PEG analogues as drug carrier.

4.5 Reference

[1] L. Yang, A. El Ghzaoui, S. M. Li, In vitro degradation behavior of poly(lactide)-poly(ethylene glycol) block copolymer micelles in aqueous solution. Int. J. Pharm. 400 (2010) 96-103.

[2] L. Yang, X. Qi, P. Liu, A. El Ghzaoui, S. M. Li, Aggregation behavior of self-assembling polylactide/poly(ethylene glycol) micelles for sustained drug delivery. Int. J. Pharm.394 (2010) 43-49.

[3] H. Z. Zhao, L. Y. L. Yung, Selectivity of folate conjugated polymer micelles against different tumor cells. Inter. J. Pharm. 349 (2008) 256-268.

[4] M. Watanabe, K. Kawano, M. Yokoyama, P. Opanasopit, T. Okano, Y. Maitani, Preparation of camptothecin-loaded polymeric micelles and evaluation of their incorporation and circulation stability. Inte. J. Pharm. 308 (2006) 183-189.

[5] G. Gaucher, M. H. Dufresne, V. P. Sant, N. Kang, D. Maysinger, J. C. Leroux, Block copolymer micelles: preparation, characterization and application in drug delivery. J. Control. Release 109 (2005) 169-188.

[6] K. Kataoka, A. Harada, Y. Nagasaki, Block copolymer micelles for drug delivery: design, characterization and biological significance. Adv. Drug Deliv. Rev. 47 (2001) 113-131.

[7] V. P. Torchilin, Structure and design of polymeric surfactant-based drug delivery systems. J. Control. Release 73 (2001) 137-172.

[8] R. K. Maheshwari, A. K. Singh, J. Gaddipati, R. C. Srimal, Multiple biological activities of curcumin: A short review. Life Sci. 78 (2006) 2081-2087.

[9] B. B. Aggarwal, A. Kumar, A. C. Bharti, Anticancer potential of curcumin: Preclinical and clinical studies. Anticancer Res. 23 (2003) 363-398.

[10] D. K. Agrawal, P. K. Mishra, Curcumin and its analogues: Potential anticancer agents. Med. Res. Rev. 30 (2009) 818-860.

[11] P. Anand, C. Sundaram, S. Jhurani, A .B. Kunnumakkara, B. B. Aggarwal, Curcumin and cancer: An "old-age" disease with an "age-old" solution. Cancer Lett. 267 (2008) 133-164.

[12] A. B. Kunnumakkara, P. Anand, B. B. Aggarwal, Curcumin inhibits proliferation, invasion, angiogenesis and metastasis of different cancers through interaction with multiple cell signaling proteins. Cancer Lett. 269 (2008) 199-225.

[13] H. H. Tonnesen, Solubility, chemical and photochemical stability of curcumin in surfactant solutions - Studies of curcumin and curcuminolds, XXVIII. Pharmazie 57 (2002) 820-824.

[14] P. Anand, A. B. Kunnumakkara, R. A. Newman, B. B. Aggarwal, Bioavailability of curcumin: Problems and promises. Mol. Pharm. 4 (2007) 807-818.

[15] C. Gong, S. Deng, Q. Wu, M. Xiang, X. Wei, L. Li, X. Gao, B. Wang, L. Sun, Y. Chen, Y. Li, L. Liu, Z. Qian, Y. Wei, Improving antiangiogenesis and anti-tumor activity of curcumin by biodegradable polymeric micelles. Biomaterials 34 (2013) 1413-1432.

[16] M. L. Gou, K. Men, H. S. Shi, M. L. Xiang, J. A. Zhang, J. Song, J. L. Long, Y. Wan, F. Luo, X. Zhao, Z. Y. Qian, Curcumin-loaded biodegradable polymeric micelles for colon cancer therapy in vitro and in vivo. Nanoscale 3 (2011) 1558-1567.

[17] L. Liu, L. Sun, Q. Wu, W. Guo, L. Li, Y. Chen, Y. Li, C. Gong, Z. Qian, Y. Wei, Curcumin

loaded polymeric micelles inhibit breast tumor growth and spontaneous pulmonary metastasis. Inter. J. Pharm. 443 (2013) 175-182.
[18] L. Song, Y. Shen, J. Hou, L. Lei, S. Guo, C. Qian, Polymeric micelles for parenteral delivery of curcumin: Preparation, characterization and in vitro evaluation. Colloids Surf. A: Physicochem. Eng. Aspects 390 (2011) 25-32.
[19] Z. M. Song, R. L. Feng, M. Sun, C. Y. Guo, Y. Gao, L. B. Li, G.. X. Zhai, Curcumin-loaded PLGA-PEG-PLGA triblock copolymeric micelles: Preparation, pharmacokinetics and distribution in vivo. J. Colloid Inter. Sci. 354 (2011) 116-123.
[20] R. L. Yang, S. A. Zhang, D. L. Kong, X. L. Gao, Y. J. Zhao, Z. Wang, Biodegradable Polymer-Curcumin Conjugate Micelles Enhance the Loading and Delivery of Low-Potency Curcumin. Pharm. Res. 29 (2012) 3512-3525.
[21] A. Chilkoti, M. R. Dreher, D. E. Meyer, D. Raucher, Targeted drug delivery by thermally responsive polymers. Adv. Drug Deliv. Rev. 54 (2002) 613-630.
[22] H. Wei, S. X. Cheng, X. Z. Zhang, R. X. Zhuo, Thermo-sensitive polymeric micelles based on poly(N-isopropylacrylamide) as drug carriers. Prog. Polym. Sci. 34 (2009) 893-910.
[23] F. Xu, S. Z. Zheng, Y. L. Luo, Thermosensitive *t*-PLA-*b*-PNIPAAm tri-armed star block copolymer nanoscale micelles for camptothecin drug release. J. Polym. Sci. Part A: Polym. Chem. 51 (2013) 4429-4439.
[24] C. Chang, H. Wei, D. Q. Wu, B. Yang, N. Chen, S. X. Cheng, X. Z. Zhang, R. X. Zhuo, Thermo-responsive shell cross-linked PMMA-*b*-P(NIPAAm-*co*-NAS) micelles for drug delivery. Inter. J. Pharm. 420 (2011) 333-340.
[25] I. S. Kim, Y. I. Jeong, C. S. Cho, S. H. Kim, Thermo-responsive self-assembled polymeric micelles for drug delivery *in vitro*. Int. J. Pharm. 205 (2000) 165-172.
[26] S. J. T. Rezaei, M. R. Nabid, H. Niknejad, A. A. Entezami, Folate-decorated thermoresponsive micelles based on star-shaped amphiphilic block copolymers for efficient intracellular release of anticancer drugs. Inter. J. Pharm. 437 (2012) 70-79.
[27] Y. F Hu, V. Darcos, S. Monge, S. M. Li, Synthesis and self-assembling of poly(N-isopropylacrylamide-block-poly(L-lactide)-block-poly(N-isopropylacrylamide) triblock copolymers prepared by combination of ring-opening polymerization and atom transfer radical polymerization. J. Polym. Sci. Part A: Polym. Chem. 51 (2013) 3274-3283.
[28] Y. F Hu, V. Darcos, S. Monge, S. M Li, Y. Zhou, F. Su, Tunable thermo-responsive P(NIPAAm-*co*-DMAAm)-*b*-PLLA-*b*-P(NIPAAm-*co*-DMAAm) triblock copolymer micelles as drug carriers. J. Mater. Chem. B 2 (2014) 2738-2748.
[29] M. Yokoyama, T. Okano, Y. Sakurai, H. Ekimoto, C. Shibazaki, K. Kataoka, Toxicity and Antitumor Activity against Solid Tumors of Micelle-forming Polymeric Anticancer Drug and Its Extremely Long Circulation in Blood. Cancer Res. 51 (1991) 3229-3236.
[30] S. S. Feng, G. F. Huang, Effects of emulsifiers on the controlled release of paclitaxel (Taxol (R)) from nanospheres of biodegradable polymers. J. Control. Release 71 (2001) 53-69.
[31] H. Ding, F. Wu, Y. Huang, Z.R. Zhang, Y. Nie, Synthesis and characterization of temperature-responsive copolymer of PELGA modified poly(*N*-isopropylacrylamide). Polymer 47 (2006) 1575-1583.
[32] Y. Yan, G. K. Such, A. P. R. Johnston, J. P. Best, F. Caruso, Engineering Particles for Therapeutic Delivery: Prospects and Challenges. ACS Nano 6 (2012) 3663-3669.
[33] C. Oerlemans, W. Bult, M. Bos, G. Storm, J. F. Nijsen, W. Hennink, Polymeric Micelles in

Anticancer Therapy: Targeting, Imaging and Triggered Release. Pharm. Res. 27 (2010) 2569-2589.
[34] H. Maeda, J. Wu, T. Sawa, Y. Matsumura, K. Hori, Tumor vascular permeability and the EPR effect in macromolecular therapeutics: a review. J. Control. Release 65 (2000) 271-284.
[35] N. Bertrand, J. Wu, X. Y. Xu, N. Kamaly, O. C. Farokhzad, Cancer nanotechnology: The impact of passive and active targeting in the era of modern cancer biology. Adv. Drug Deliv. Rev. 66 (2014) 2-25.
[36] Y. Yamamoto, Y. Nagasaki, Y. Kato, Y. Sugiyama, K. Kataoka, Long-circulating poly(ethylene glycol)-*b*-poly(D,L-lactide) block copolymer micelles with modulated surface charge. J. Control. Release 77 (2001) 27-38.
[37] C. B. He, Y. P. Hu, L. C. Yin, C. Tang, C. H. Yin, Effects of particle size and surface charge on cellular uptake and biodistribution of polymeric nanoparticles. Biomaterials 31 (2010) 3657-3666.
[38] R. B. Campbell, D. Fukumura, E. B. Brown, L. M. Mazzola, Y. Izumi, R. K. Jain, V. P. Torchilin, L. L. Munn, Cationic charge determines the distribution of liposomes between the vascular and extravascular compartments of tumors. Cancer Res. 62 (2002) 6831-6836.
[39] K. Xiao, Y. P. Li, J. T. Luo, J. S. Lee, W. W. Xiao, A. M. Gonik, R. G. Agarwal, K. S. Lam, The effect of surface charge on in vivo biodistribution of PEG-oligocholic acid based micellar nanoparticles. Biomaterials 32 (2011) 3435-3446.
[40] P. L. Ritger, N. A. Peppas, A simple equation for description of solute release I. Fickian and non-fickian release from non-swellable devices in the form of slabs, spheres, cylinders or discs. J. Control. Release 5 (1987) 23-36.
[41] P. L. Ritger, N. A. Peppas, A simple equation for description of solute release II. Fickian and anomalous release from swellable devices. J. Control. Release 5 (1987) 37-42.
[42] J. Siepmann, N. A. Peppas, Modeling of drug release from delivery systems based on hydroxypropyl methylcellulose (HPMC). Adv. Drug Deliv. Rev. 64 (2012) 163-174.
[43] J. F. Lutz, A. Hoth, Preparation of Ideal PEG Analogues with a Tunable Thermosensitivity by Controlled Radical Copolymerization of 2-(2-Methoxyethoxy)ethyl Methacrylate and Oligo(ethylene glycol) Methacrylate. Macromolecules 39 (2006) 893-896.
[44] J. F. Lutz, K. Weichenhan, O. Akdemir, A. Hoth, About the Phase Transitions in Aqueous Solutions of Thermoresponsive Copolymers and Hydrogels Based on 2-(2-methoxyethoxy)ethyl Methacrylate and Oligo(ethylene glycol) Methacrylate. Macromolecules 40 (2007) 2503-2508.
[45] J. F. Lutz, J. Andrieu, S. uzgun, C. Rudolph, S. Agarwal, Biocompatible, Thermoresponsive, and Biodegradable: Simple Preparation of "All-in-One" Biorelevant Polymers. Macromolecules 40 (2007) 8540-8543.
[46] J. F. Lutz, Polymerization of oligo(ethylene glycol) (meth)acrylates: Toward new generations of smart biocompatible materials. J. Polym. Sci. Part A: Polym. Chem. 46 (2008) 3459-3470.
[47] J. F. Lutz, Thermo-Switchable Materials Prepared Using the OEGMA-Platform. Adv. Mater. 23 (2011) 2237-2243.

Chapter 5 Thermo-responsive micelles from comb-like block copolymers of polylactide and poly(ethylene glycol) analogues: Synthesis, Micellization and *In vitro* drug release

Abstract: Thermo-responsive comb-like P(MEO_2MA-*co*-OEGMA)-*b*-PLLA-*b*-P(MEO_2MA-*co*-OEGMA) triblock copolymers were synthesized by atom transfer radical polymerization of MEO_2MA and OEGMA co-monomers using a Br-PLLA-Br macroinitiator. The resulting copolymers with MEO_2MA/OEGMA molar ratio ranging from 79/21 to 42/58 were characterized by ^1H NMR and SEC. Thermo-responsive micelles were obtained by self-assembly of copolymers in aqueous medium. The properties of micelles were determined by CMC, DLS, TEM and LCST measurements. The micelles are spherical in shape with sizes varying from 21 to 103 nm. A hydrophobic anticancer drug, curcumin, was encapsulated in micelles by using membrane hydration method. The micelles size decreases from 103 to 38 nm with 10.8 % drug loading, suggesting that drug loading strongly affects the self-assembly procedure. The LCST decreases from 45.1 °C for blank micelles to 40.6 and 38.3 ^oC with 5.9 % and 10.8 % drug loading. *In vitro* drug release was performed in pH=7.4 PBS at different temperatures. Data show that the release rate significantly increased above the LCST. The burst-like release was depressed by the enhanced interaction between drug and comb-like copolymer chains.

Keywords: Polylactide; PEG analogues; Comb-like copolymer; Micellization; Curcumin; Thermo-responsive; Drug release

5.1 Introduction

Cancer is nowadays a leading cause of death in the world. The World Health Organization reported the approximately 14 million new cases and 8.2 million cancer related deaths in 2012. For cancer therapy, the ideal drug delivery system should be stimuli responsive to the local environment of tumor [1-3]. In fact, the tumor issue is very different from normal tissues with higher temperature (~42 ^{o}C), lower pH (<5.3) and anomalous vessel (intercellular gap junction of 300-700 nm) [4-6]. Therefore, thermo-responsive polymeric micelles have been increasingly investigated for targeted delivery of anticancer drugs [7-11]. So far, poly(*N*-isopropylacylamide) (PNIPAAm), which displays a lower critical solution temperature (LCST) at 32 ^{o}C, is the most studied thermo-responsive polymer in biomedical applications [5, 12-15]. Slight variation of pH, concentration, or chemical environment only slightly affects the LCST of PNIPAAm, which is considered as the "Golden standard" of thermo-responsive polymers. Nevertheless, the presence of residual N-isopropylacrylamide monomer in PNIPAAm based polymers has raised concerns on the toxicity.

Recently, Lutz *et al.* reported novel thermo-responsive copolymers of 2-(2-methoxyethoxy) ethyl methacrylate (MEO_2MA) and oligo(ethylene glycol) methacrylate (OEGMA), and hydrogels of both monomers using ethylene glycol dimethacrylate as cross-linker by atom transfer radical polymerization (ATRP) [16-23]. These PEG analogues exhibit a LCST between 26 and 90 ^{o}C which can be precisely adjusted by varying the co-monomers ratio. They are thus attractive for targeted drug delivery due to combination of thermo-responsive properties and good biocompatibility as linear PEG [21].

However, PEG analogues generally adopt a compact coil conformation in aqueous medium [20]. Introduction of hydrophobic block is thus required in order to obtain thermo-responsive polymeric micelles as potential carrier of targeted drug delivery.

Saeed *et al.* synthesized poly(lactide-*co*-glycolide)-*b*-poly(oligo(ethyleneglycol) methacrylate) (PLGA-*b*-POEGMA) diblock copolymers by combining ring opening polymerization (ROP) and reversible addition fragmentation chain transfer (RAFT) polymerization, and studied the self-assembly, drug release and cytotoxicity of the copolymer micelles [24]. Later on, Luzon *et al.* obtained POEGMA-*b*-PCL-*b*-POEGMA triblock copolymers by ATRP, using α,ω-bromopropionyl poly(ε-caprolactone) (Br-PCL-Br) as macroinitiator [25]. The critical micelle concentration (CMC) and critical micelle temperature (CMT) were determined. The same synthetic route was adopted by Bakkour *et al.* for the synthesis of POEGMA-*b*-PLLA-*b*-POEGMA triblock copolymers [26]. The self-assembly and drug encapsulation potential of the copolymers were reported. Most recently, Fenyves *et al.* synthesized amphiphilic bottlecomb block copolymers containing PLA and PEG side chains using a grafting-from method, and studied their self-assembly in aqueous medium. Spherical, cylindrical micelles as well as bilayer structures were observed [27]. However, the LCST of these copolymers was in the range of 75 to 85 °C, *i.e.* much higher than the body temperature.

In our previous work, well defined thermo-responsive poly(*N*-isopropylacrymine-*co*-*N,N*-dimethylacrylamine)-*b*-poly(L-lactide)-*b*-poly(*N*-isopropylacrymine-*co*-*N,N*-dimethylacrylamine) P(NIPAAm-*co*-DMAAm)-*b*-PLLA-*b*-P(NIPAAm-*co*-DMAAm) micelles has been investigated as drug carrier [28, 29]. The cytotoxicity evaluated by MTT assay showed that unreacted NIPAAm was eliminated by dialysis. *In vitro* drug release studies present a much faster release at temperatures above the LCST than below, suggesting that the copolymer micelles could be promising for targeted delivery of antitumor drugs.

In this work, for the first time, we report a series of amphiphilic comb-like triblock polymers composed of a biodegradable PLLA central block and two lateral thermo-responsive P(MEO_2MA-*co*-OEGMA) blocks prepared by combination of

ROP and ATRP. The self-assembly and thermo-responsive properties of the copolymers were determined by CMC, DLS, TEM and LCST measurements. The LCST was adjusted precisely by varying MEO_2MA/OEGMA ratio. Thermo-responsive drug release from copolymer micelles was investigated below or above the LCST, and compared with that from P(NIPAAm-*co*-DMAAm)-*b*-PLLA-*b*-P(NIPAAm-*co*-DMAAm) micelles.

5.2 Experimental Section

5.2.1 Materials

L-lactide was purchased from PuracBiochem (Goerinchem, The Netherlands). Stannous 2-ethylhexanoate ($Sn(Oct)_2$), 1,4-benzene dimethanol, 2-bromopropionyl bromide, tris(2-dimethyl aminoethyl) amine (Me_6TREN), copper (I) chloride (CuCl), *N,N*-dimethyl formamide (DMF) and curcumin were obtained from Sigma-Aldrich (St-Quentin Fallavier, France), and were used without further purification. Dichloromethane and toluene from Sigma-Aldrich were dried over calcium hydride for 24 h at room temperature and distilled under reduced pressure. MEO_2MA and OEGMA (M_n=300 g mol^{-1}) were obtained from Sigma-Aldrich and purified through a basic aluminum oxide column. Triethylamine (Sigma-Aldrich) was dried over potassium hydroxide for 24 h at room temperature and distilled. Ultrapure water with a conductivity of 18 MΩ was produced using a Millipore Milli-Q water system. α,ω-Bromopropionyl PLLA (Br-PLLA-Br) with degree of polymerization (DP) of 40 was prepared as previously reported [30].

5.2.2 Synthesis of P(MEO_2MA-*co*-OEGMA)-*b*-PLLA-*b*-P(MEO_2MA-*co*-OEGMA) copolymer (copolymer T5, Table 5.1)

Triblock copolymers were prepared using standard Schlenk technique. Typically, 100 mg Br-PLLA-Br (30.4×10^{-3} mmol, $M_{n,NMR}$= 3300 g mol^{-1}), 461 mg MEO_2MA (2.451

mmol), 1.1 g OEGMA (3.676 mmol) and 6 mg CuCl (60.6×10^{-3} mmol) were dissolved in 2 mL DMF. After five freeze-pump-thaw cycles, 16 μL Me_6TREN (60.8×10^{-3} mmol) was added under argon atmosphere. The mixture was stirred at 80 ^{o}C for 6 h. The reaction was stopped by exposition to air for 2 h at room temperature. A dialysis was then carried out for 3 days in a dialysis tube (MWCO: 3500 D) to remove residual monomers and copper against Mill-Q water containing ethylenediaminetetraacetic acid tetrasodium salt hydrate. The product was finally collected by lyophilization.

^{1}H NMR (300 MHz, CDCL3) (Figure 5.1) δ (ppm)=7.26 (*s*, $4H_{Ar}$); 5.14 (*m*, $1H_a$); 4.08 (*t*, $2H_c$); 3.63+3.55(*t*, $2H_d$); 3.37 (*s*, $3H_e$); 1.56 (*d*, $3H_b$)

5.2.3 Preparation of curcumin loaded micelles

The micelles were prepared by solvent evaporation/membrane hydration method. Typically, 1.2 mg curcumin and 18.8 mg copolymer T5 (Sample 1, Table 5.2) were dissolved in 10 mL acetone, and then the solvent was evaporated in rotary evaporator at room temperature to yield a membrane at the wall of the round flask. After vacuum drying for 24 h, 20 mL Mill-Q water was added to the flask, yielding self-assembled micelles at room temperature. The resulting micellar solution was then centrifuged at 5000 rpm for 10 min to remove unloaded curcumin. The supernatant was lyophilized, and dispersed in deionized water or PBS to yield a drug loaded micellar solution at a concentration of 1 mg mL^{-1} for physiochemical characterization and drug release studies.

5.2.4 *In vitro* drug release

The drug loading (DL) and encapsulation efficiency (EE) of micelles were determined as follows. 0.1 mL drug loaded micellar solution (1 mg mL^{-1}) was dissolved in 2.4 mL 60/40 acetonitrile/ammonium acetate (pH=4.0, 10 mM) mixture solution. The concentration of curcumin was determined by UV-Vis spectroscopy at λ=424 nm,

using a calibration curve previously established from a series of standard curcumin solutions with concentrations from 0.008 to 10 μg mL^{-1}. The DL and EE were calculated from following formulae:

$$Drug\ loading\ (\%) = \frac{weight\ of\ loaded\ drug}{weight\ of\ \ polymeric\ micelles} \times 100 \qquad (1)$$

$$Encapsulation\ efficiency\ (\%) = \frac{weight\ of\ \ drug\ in\ micelles}{theoretical\ drug\ loading} \times 100 \qquad (2)$$

3 mL drug loaded micelles in PBS (pH= 7.4, 1 mg mL^{-1}) were introduced into a dialysis tube (MWCO: 3500 D). The tube was incubated in 10 mL PBS containing 0.5 % Tween80 in an incubator (Heidolph 1000) with gentle shaking (150 rpm) at 37 or 41 ^{o}C. At specific time intervals, the release medium was totally removed and replaced by pre-warmed fresh PBS. The solution was then diluted 5-10 times with 60/40 acetonitrile/ammonium acetate (pH=4.0, 10 mM) mixture, and the amount of released curcumin was determined from UV measurements using a calibration curve.

5.2.5 Characterization

Nuclear magnetic resonance (NMR) ^{1}H NMR spectra were recorded on a Bruker spectrometer (AMX300) operating at 300 MHz. Chemical shift was referenced to the peak of residual non-deuterated solvents.

Size exclusion chromatography (SEC) SEC measurements were performed on a Varian 390-LC equipped with a refractive index detector and two ResiPore columns (300×7.5 mm) at 60 °C at a flow rate of 1 $mLmin^{-1}$. The eluent was DMF containing 0.1 *wt* % LiBr. Calibration was established with PMMA standards.

Fluorescence spectroscopy The CMC of the copolymers was determined by fluorescence spectroscopy using pyrene as a hydrophobic fluorescent probe. Measurements were carried out on an RF 5302 Shimadzu spectrofluorometer (Japan) equipped with a Xenon light source (UXL-150S, Ushio, Japan). Briefly, 1 mL pyrene

solution (6×10^{-6} M) in acetone was added to different vials, and the solvent was evaporated. Then, 10 mL aqueous solutions of different copolymer concentrations were added to the vials. After equilibrating at room temperature overnight, the fluorescence excitation spectra of the solutions were recorded from 300 to 360 nm at an emission wavelength of 394 nm. The emission and excitation slit widths were 3 and 5 nm, respectively. The excitation fluorescence values I_{337} and I_{333}, respectively at 337 and 333 nm, were used for subsequent calculations. The CMC was determined from the intersection of linear regression lines on the I_{337}/I_{333} ratio *versus* polymer concentration plots.

Phase transition The LCST of copolymers was estimated from the transmittance changes of 1.0 mg mL^{-1} solutions as a function of temperature. The measurements were carried out at a wavelength of 500 nm with a Perkin Elmer Lambda 35 UV-Visible spectrometer equipped with a Peltier temperature programmer PTP-1+1. The temperature ramp was 0.1 °C min^{-1}.

Dynamic light scattering (DLS) The size and zeta-potential of micelles in aqueous medium were measured by Zetasizer Nano-ZS (Malvern Instrument Ltd. UK) equipped with a He-Ne laser (λ= 632.8 nm). The correlation function of DLS was analyzed via the general purpose method (NNLS) to obtain the distribution of diffusion coefficients (D) of the solutes. The apparent equivalent hydrodynamic radius (R_H) was determined from the cumulant method using the Stokes-Einstein equation. Mean radius values were obtained from triplicate runs. Standard deviations were evaluated from hydrodynamic radius distribution.

Transmission electron microscopy (TEM) TEM experiments were carried out on a JEOL 1200 EXII instrument operating at an acceleration voltage 120 kV. The samples were prepared by dropping a polymer solution at 1.0 mg mL^{-1} onto a carbon coated copper grid, followed by air drying.

Inductively coupled plasma-mass spectrometry (ICP-MS) The residual copper content in the copolymers was quantified using ThemoFinnigan Element XR sector field ICP-MS previously calibrated using copper solutions in water. Typically, ICP-MS samples were prepared by dissolving copolymers in nitric acid. The solution was then heated to fully decompose the polymers. After that, the samples were dissolved in 10 mL deionized water before analysis to determine the copper concentration. Each sample was analyzed four times.

5.3 Results and discussion

5.3.1 Synthesis of copolymers by ATRP

P(MEO_2MA-*co*-OEGMA)-*b*-PLLA-*b*-P(MEO_2MA-*co*-OEGMA) triblock copolymers were successfully synthesized by ATRP of MEO_2MA and OEGMA, using a α,ω-telechelic Br-PLLA-Br as macroinitiator (Scheme 5.1). The reaction was performed in DMF at 80 °C for 6 h using a CuCl/Me_6TREN catalytic system. The conversion of monomers is *ca.* 58 % as determined by ^{1}HNMR.

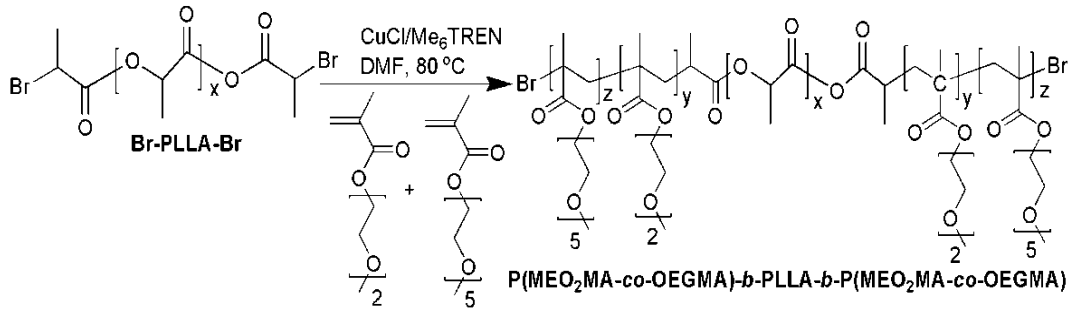

Scheme 5.1 Synthesis of P(MEO_2MA-*co*-OEGMA)-*b*-PLLA-*b*-P(MEO_2MA-*co*-OEGMA) triblock copolymers

Figure 5.1 shows a typical ^{1}H NMR spectrum of triblock copolymers. The signals at 5.2 and 1.6 ppm are characteristic of methine (H_a, CH) and the methyl (H_b) protons of PLLA, respectively. The signal at 4.0 ppm is assigned to the methylene protons (H_c) adjacent to the ester bond of both MEO_2MA and OEGMA. Other methylene protons (H_d) of MEO_2MA and OEGMA are observed at 3.6 ppm. The signal at 3.4 ppm is

assigned to the methyl end group of MEO_2MA and OEGMA. The *DP* of MEO_2MA and OEGMA and the $M_{n,\,NMR}$ of copolymers were calculated from the integrations of the methine protons of LA units at 5.2 ppm, methylene protons adjacent to ester bond at 4.0 ppm and other methylene protons at 3.6 ppm of both MEO_2MA and OEGMA moieties according to the following equations:

$$x/(y+z) = I_a/(I_c/2)$$

$$(2y+2z)/(6y+18z) = I_c/I_d$$

$$M_{n,NMR} = 72x + 188y + 300z$$

Where *x*, *y* and *z* are the *DP* of PLLA, MEO_2MA and OEGMA, and 72, 188 and 300 are the molecular weight of LA, MEO_2MA and OEGMA repeat units, respectively.

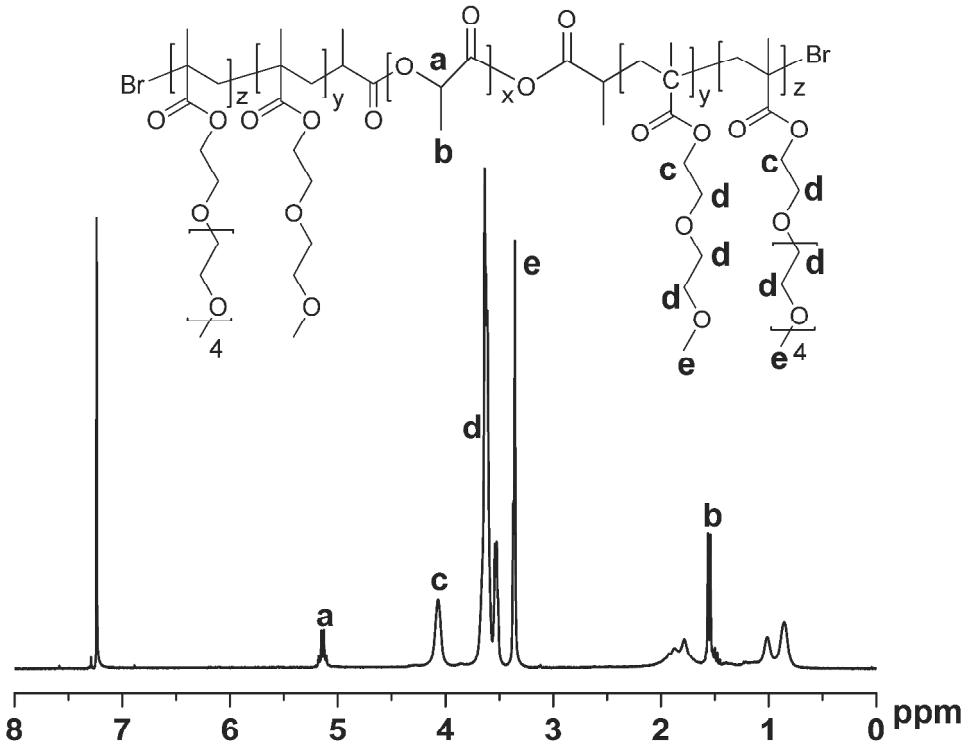

Figure 5.1 ^1H NMR of P(MEO_2MA-*co*-OEGMA)-*b*-PLLA-*b*-P(MEO_2MA-*co*-OEGMA) triblock copolymers.

Table 5.1 shows the molecular characteristics of P(MEO_2MA-*co*-OEGMA)-*b*-PLLA-*b*-P(MEO_2MA-*co*-OEGMA) triblock polymers with MEO_2MA to OEGMA molar ratios from 79/21 to 42/58. The composition

determined by ^{1}H NMR is close to the feed ratio, which indicated the successful polymerization of both monomers initiated by Br-PLA-Br macroinitiator. The *DP* of PLLA is 40, and that of OEGMA and MEO_2MA moieties varies from 22 to 66, and from 85 to 48, respectively.

Table 5.1 Molecular characteristics of P(MEO_2MA-*co*-OEGMA)-*b*-PLLA-*b*-P(MEO_2MA-*co*-OEGMA) triblock copolymers.

Copolymer [a]	$[MEO_2MA]_0$/ $[OEGMA]_0$	$[MEO_2MA]$/ $[OEGMA]$ [b]	x/y/z [b]	M_n [b]	M_n [c]	$Đ$ [c]
T1	80/20	79/21	40/85/22	25900	25700	1.42
T2	70/30	68/32	40/86/33	28900	27100	1.37
T3	60/40	57/43	40/67/49	30600	18000	1.39
T4	50/50	49/51	40/65/53	31400	11700	1.37
T5	40/60	42/58	40/48/66	32100	9800	1.38

a) *ATRP* conditions: [PLLA]/[monomers]/[CuCl]/[Me_6TREN]=1/200/2/2, *[M]*=1.74 M, *T*= 80 ^oC, Reaction time=6 h,

b) Calculated from *NMR*

c) Obtained from *SEC*.

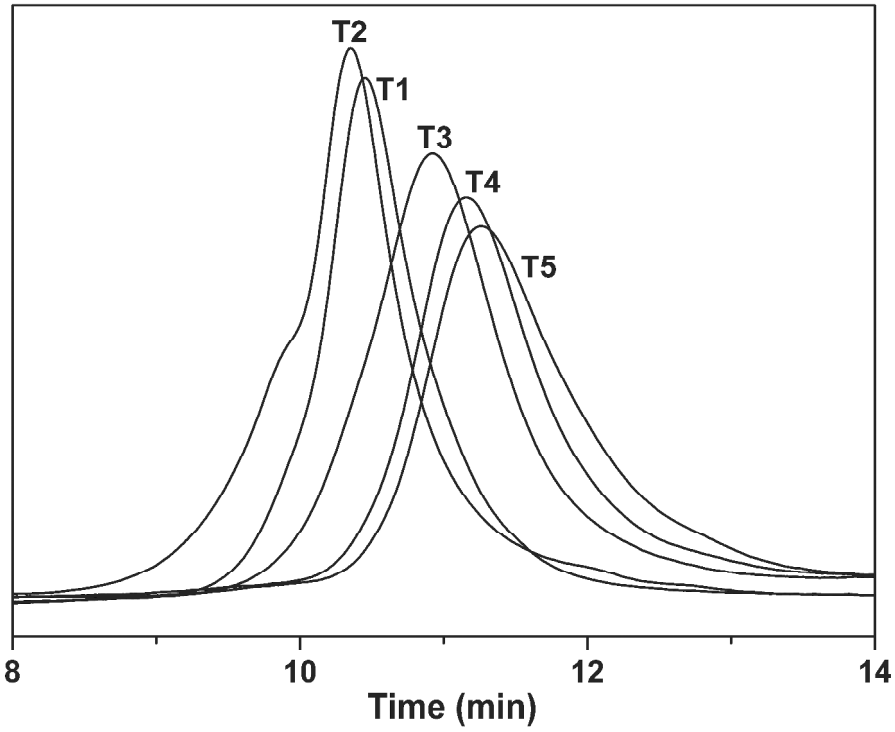

Figure 5.2 SEC chromatograms of triblock copolymers.

The molecular weight of copolymers obtained from ^{1}H NMR varies from 25, 900 to 32, 100 with increasing OEGMA content since OEGMA has higher M_n than MEO_2MA. Figure 5.2 presents the SEC curves of the copolymers. A monomodal molecular weight distribution is observed in all cases with dispersity ($Đ$) of about 1.40. The M_n obtained by SEC varies from 27, 100 to 9, 800 g mol^{-1}. A difference is observed between the M_n values obtained by NMR and by SEC, in particular for copolymers T3, T4 and T5 with high OEGMA contents.

The fact that the M_n obtained by *SEC* was lower than that determined by NMR could be illustrated by the unusual behavior of POEGMA macromolecular combes in solution [31]. Similar findings have been reported by Lutz *et al*. [19]. In our work, the copolymers have the same central PLLA block (*DP*=40) and various terminal PEG analogues. As the *DP* of POEGMA increases, the main chain becomes longer than the side chain and the PEG analogues exhibit a cylindrical comb structure [25]. Experimental molecular weights measured for triblock copolymers are much lower than those calculated from NMR, indicating that such copolymers most likely adopt a random coil conformation in DMF solution. Comb-like polymers have different relationship of retention volume *vs*. molecular weight compared to the PMMA standards in SEC calibration [31, 32]. Moreover, anomalous elution was also demonstrated for other comb-like polymers [33].

ICP-MS measurements showed that the copper content in the copolymers is between 1 and 3 ppm, which is acceptable for biomedical or pharmaceutical applications.

5.3.2 Self-assembly polymer micelles in aqueous medium

The amphiphilic copolymers are water soluble and are able to form micellar aggregates by self-assembly in water using the direct dissolution method. The critical micellar concentration (CMC) is an important parameter to evaluate the stability of micelles. Figure 5.3 shows the I_{337}/I_{333} ratio changes as a function of copolymer T5

concentration. The intensity ratio exhibits a substantial increase at a particular concentration, indicating the incorporation of pyrene inside micelles. The CMC was obtained from the intersection of the two linear regression lines of the plots.

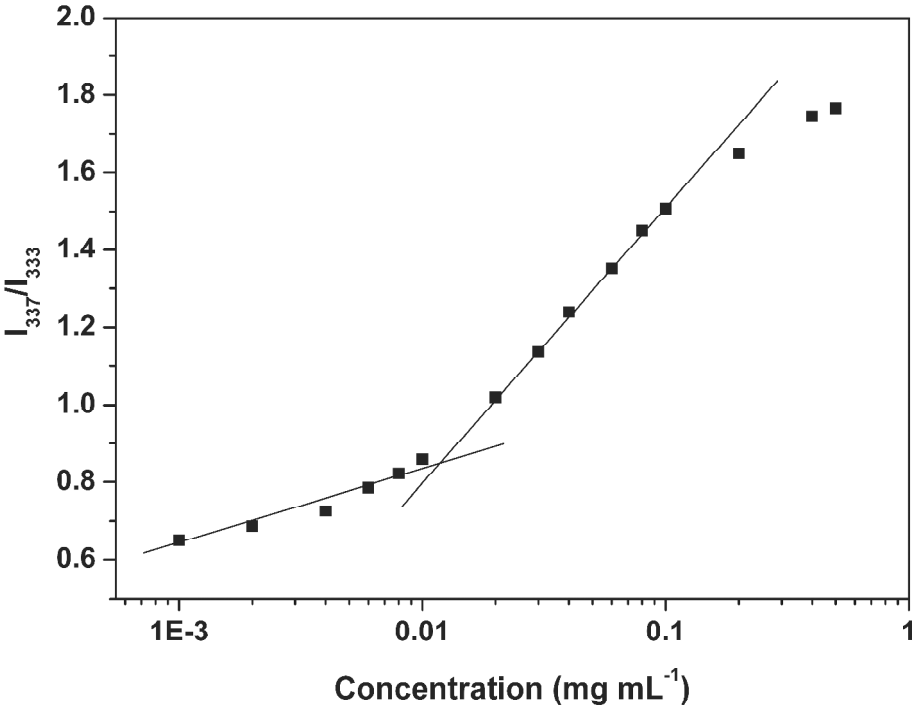

Figure 5.3 Plots of the I_{337}/I_{333} ratio changes from pyrene excitation spectra *versus* the concentration of copolymer T5.

As summarized in Table 5.2, the CMC value of triblock copolymers increases from 0.0113 to 0.0130 mg mL^{-1} as the content of OEGMA increasing from 21 to 58 % due to the higher hydrophilicity of OEGMA units [26]. The CMC is 10 times lower than that of POEGMA-PLLA-POEGMA copolymers (0.08-0.12 mg mL^{-1}) reported by Bakkour *et al.* and 2 times lower than that of POEGMA-PCL-POEGMA micelles (0.0254-0.0372 mg mL^{-1}) reported by Mario *et al.* [25, 26]. In this work, the lower CMC of copolymers could be assigned to the presence of MEO_2MA moieties which are less hydrophilic than OEGMA ones. The very low CMC demonstrates the strong tendency of copolymers toward formation of micelles, which is of major importance for the stability of micelles in long circulation in the bloodstream after injection induced dilution [34].

5.3.3 Phase transition of polymeric micelles

The LCST of micelles in water increases from 36.4 to 56.7 ^{o}C with the content of OEGMA increasing from 21 % to 43 %. Data are not available for copolymers with higher OEGMA contents due to fast evaporation of water above 60 ^{o}C. The LCST of micelles in PBS increases from 24.8 to 45.1 ^{o}C as the content of OEGMA increases from 32 % to 58 %. The salt has significant influence on the thermal behavior of copolymers. A decrease of nearly 17 ^{o}C was observed when comparing the LCST values in PBS and in water in the case of copolymers T2 and T3. Interestingly, Lutz *et al.* reported that the LCST of P(MEO_2MA-*co*-OEGMA) in NaCl solution was 3 ^{o}C lower than that in deionized water at a concentration of 3 mg mL^{-1} [16]. However, the LCST of copolymers based on PEG analogues in PBS has not been reported, so far. The difference can be assigned to the fact that phosphate has stronger dehydration effect than NaCl.

Table 5.2 Properties of P(MEO_2MA-*co*-OEGMA)-*b*-PLLA-*b*-P(MEO_2MA-*co*-OEGMA) triblock copolymer micelles

Polymer	[MEO_2MA]/ [OEGMA] [a]	CMC [b] (mg mL^{-1})	D_H [c] (nm)	PDI [c]	LCST [d] (^{o}C)	LCST [e] (^{o}C)	ZP [f]
T1	79/21	0.0113	21	0.384	36.4	-	-0.77
T2	68/32	0.0120	39	0.274	41.0	24.8	-1.06
T3	57/43	0.0123	69	0.261	56.7	39.8	-1.22
T4	49/51	0.0125	90	0.259	-	42.2	-1.58
T5	42/58	0.0130	103	0.392	-	45.1	-1.99

a) determined by ^{1}H NMR; b) determined by fluorometry; c) by DLS in water; d) by UV in water; e) by UV in PBS; f) by DLS in water

5.3.4 Size distribution of polymeric micelles

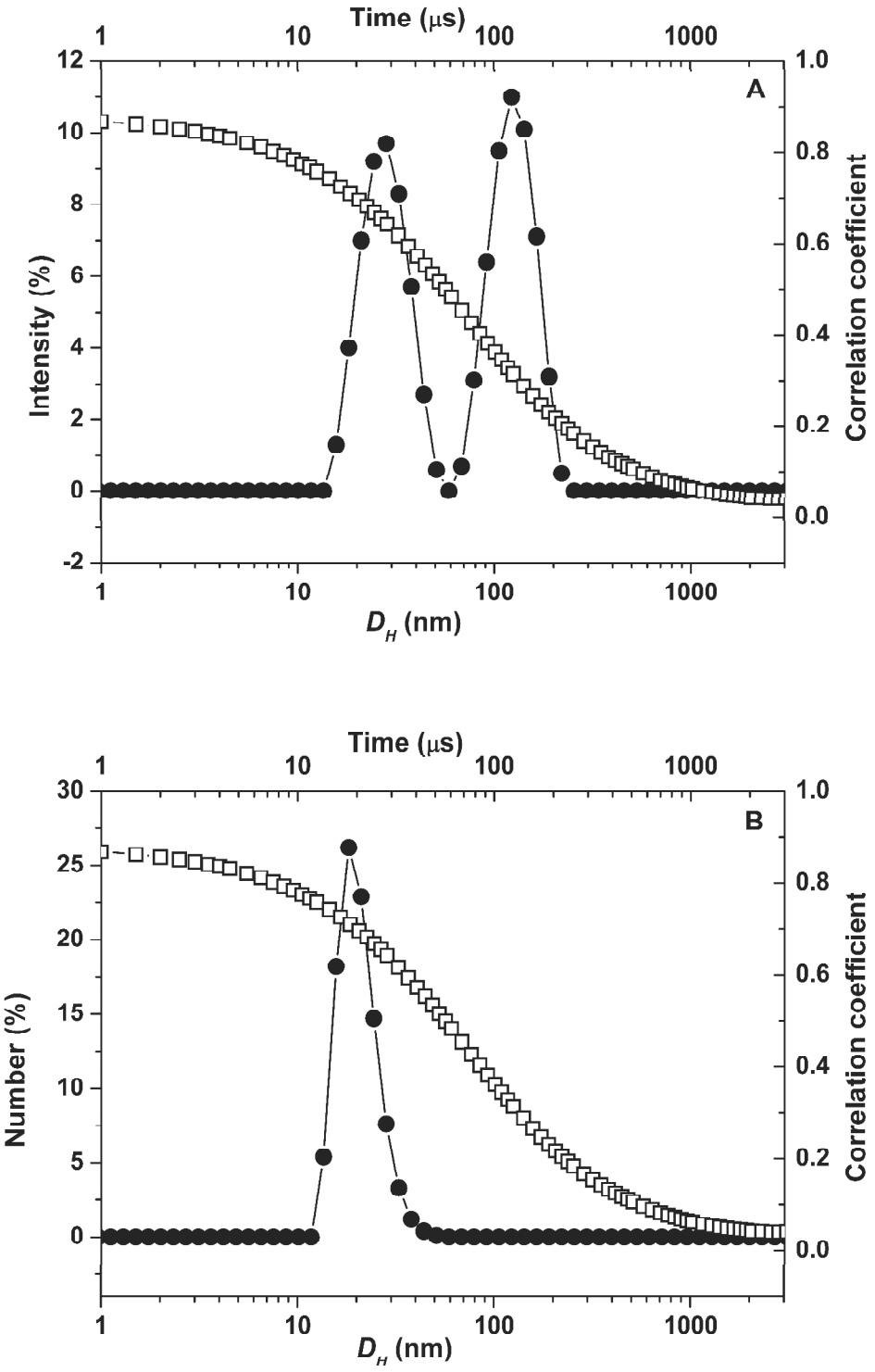

Figure 5.4 Intensity size distribution (A) and number size distribution (B) of triblock copolymer T1 measured by DLS at room temperature.

DLS was used to determine the size distribution of polymeric micelles. Figure 5.4 shows the typical size distributions of copolymer T1 at 1 mg mL^{-1}. Two populations of micelles are observed on intensity size distribution: one population with average size of 21 nm and another one around 197 nm (Figure 5.4A). Nevertheless, the latter is indeed a negligible minority, as evidenced by the number size distribution shown in Figure 5.4B. The larger aggregates represent less than 0.2 % of the overall number distribution. Similar findings have been reported in literature in the case of P(MEO_2MA-*co*-OEGMA) copolymers [20]. Hence, the copolymers adopt mostly micellar conformation with sizes of *c.a* 20 nm at room temperature.

Indeed, all the size distributions of micelles observed by DLS exhibit bimodal distribution with intensity distribution and mostly unimodal distribution with number distribution. The average diameter of micelles increases from 21 to 103 nm with the content of OEGMA increasing from 21 % to 58 %, which is consistent with the CMC results (Table 5.2).

Zeta potential denotes the charge difference between the layer of ions adsorbed onto the micelle surface and the bulk of the dispersing medium. The ZP value of copolymer micelles ranges from -0.77 to -1.99 mV, which implies a nearly neutral surface charge.

5.3.5 Preparation and characterization of drug loaded micelles

Curcumin is a natural anticancer drug, but its application is limited by the poor water solubility (11 ng mL^{-1}). Nanotechnology was used to encapsulate curcumin into the hydrophobic core of polymeric micelles [29, 35-38]. In the present work, curcumin loaded micelles were prepared with theoretical drug loading of 6.0 and 12.0 % using solvent evaporation/membrane hydration method, in comparison with blank micelles.

The drug loading and encapsulation efficiency of micelles were obtained by light transmission measurements using UV spectroscopy. As shown in Table 5.3, when the initial drug amount increases from 1.2 to 2.4 mg, drug content increases from 5.9 % to 10.8 %. The encapsulation efficiency was above 90.2 % in both cases, which is higher than the value of 70 % obtained for linear poly(lactide-*co*-glycolide)-*b*-poly(ethylene glycol)-*b*-poly (lactide-*co*-glycolide) (PLGA-PEG-PLGA) reported by Song *et al.* [38]. The improved loading efficiency may be attributed to the enhanced drug-polymer interaction between curcumin with both PLA segments and polymethacrylate (PMA) backbone [39].

Table 5.3 Properties of curcumin-loaded polymer (T5) micelles

Sample	Drug/polymer [a)] (mg/mg)	DL[b)] (wt %)	E [b)] (wt %)	LCST [c)] (^{o}C)	D_H[d)] (nm)	PDI[d)]	ZP[e)]
1	0/20	-	-	45.1	103	0.392	-1.99
2	1.2/18.8	5.9	98.3	40.6	57	0.364	-29.8
3	2.4/17.6	10.8	90.2	38.3	38	0.295	-44.9

a) in feed; b) determined by UV absorbance; c) by UV transmittance in PBS; d) by DLS; e) by DLS in water

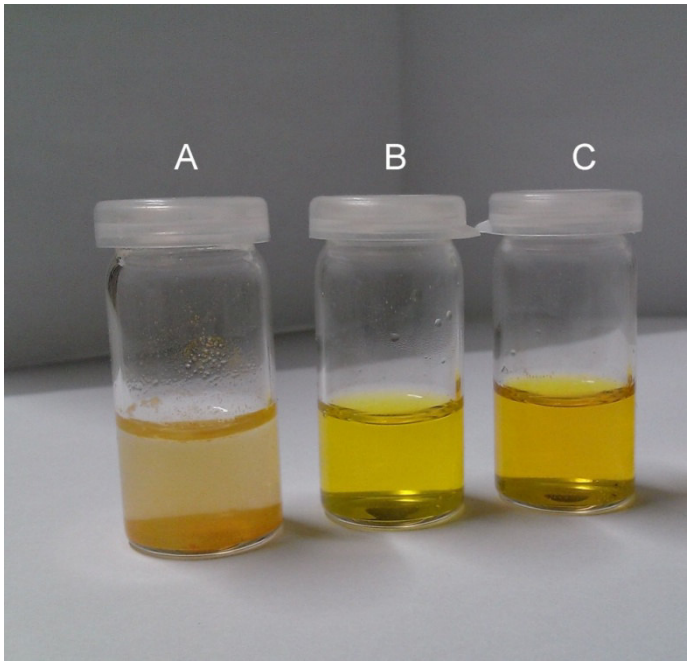

Figure 5.5 Images of curcuminin solution: (A) 6.0 % curcumin in PBS; (B) Sample 2 (DL=5.9 %); (C) Sample 3 (DL=10.8 %).

The images of curcumin-loaded micelles in PBS at 1 mg mL^{-1} are shown in Figure 5.5. In water, curcumin remains as a sediment at the bottom due to the poor solubility (Figure 5.5A). On the contrary, a homogenous and transparent yellow solution is obtained in the case of curcumin-loaded micelles (Figure 5.5B and 5.5C), showing that hydrophobic curcumin was successfully loaded inside polymeric micelles.

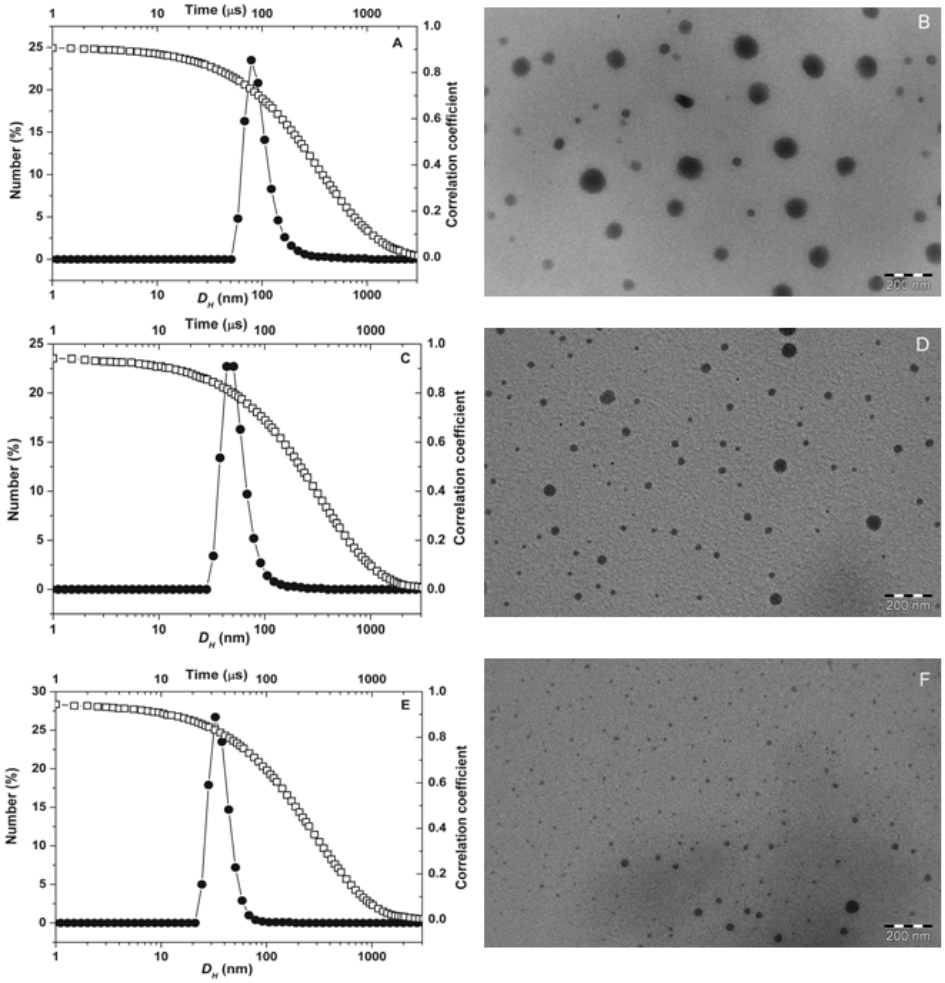

Figure 5.6 DLS spectra and TEM micrographs of curcumin loaded micelles. (A) and (B): Sample 1 (DL=0); (C) and (D): Sample 2 (DL=5.9 %); (E) and (F): Sample 3 (DL=10.8 %).

The size and the morphology of micelles were obtained by DLS and TEM measurements. The average size of micelles loaded with 5.9 and 10.8 % curcumin was 57 and 38 nm (Figure 5.6 and Table 5.3), respectively, which is much smaller than the size of blank micelles (103 nm). TEM shows that the micelles are spherical in shape with average size apparently smaller than that obtained by DLS. In fact, the

difference between DLS and TEM results is usually attributed to the experimental conditions. DLS allows determining the hydrodynamic diameter of micelles in aqueous solution, whereas TEM shows the dehydrated solid state of micelles.

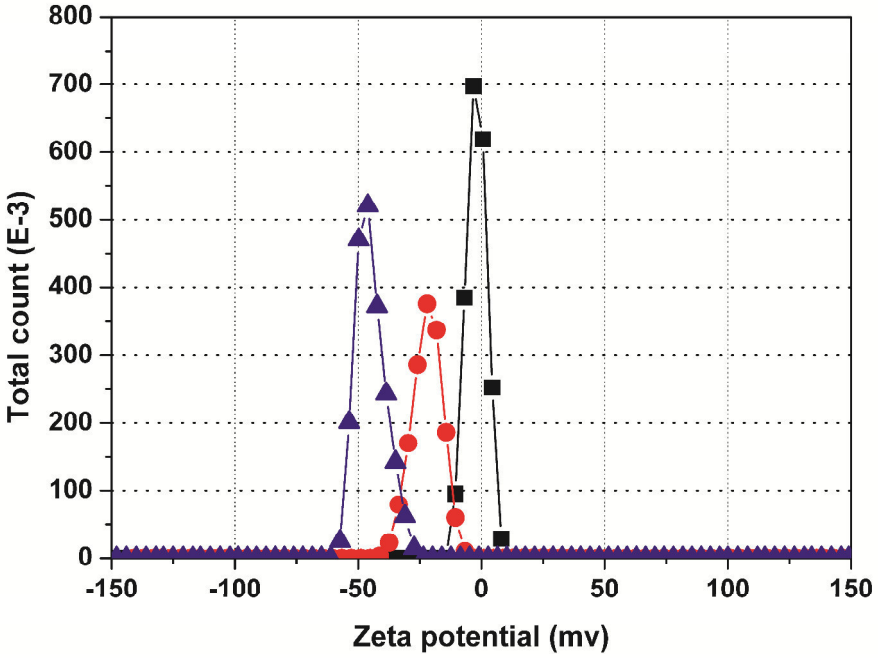

Figure 5.7 Zeta potential of curcumin-loaded micelles: (■) sample 1 (DL=0); (●) sample 2 (DL=5.9 %); (▲) sample 3 (DL=10.8 %).

Figure 5.7 shows the zeta potential of blank and curcumin-loaded micelles. The blank micelles present a zeta potential at -1.99 mV, which implies a nearly neutral surface charge. Interestingly, the absolute zeta potential value increases to -29.8 and -44.9 mV with 5.9 % and 10.8 % drug loading, respectively. The significant increase of surface charge could be assigned to the encapsulation of curcumin, which offers multiple carboxyl groups [38, 39]. It is also noteworthy that the size decreases from 102.2 nm for blank micelles to 56.6 and 37.6 nm for drug loaded micelles with DL = 5.9 or 10.8 %, suggesting the existence of mesophase in micelles.

In fact, the structure of self-assembled micelles is similar to that of POEGMA-*b*-PCL-*b*-POEGMA triblock copolymer micelles proposed by Luzon *et al.* [25]. As shown in Scheme 5.2, there exist three different chemically different blocks (two hydrophobic and one thermo-responsive). Premicelles are composed of a PLA

core, a PMA shell and an oligoPEG corona. PMA blocks exhibit a relatively strong affinity to water due to surface active ester groups. As the concentration increases above the CMC, copolymer chains aggregate to form spherical micelles, which can be regarded as soft matter dispersions with ordered inner structure stabilized by hydrophilic corona. It could be assumed that triblock copolymers achieve steric stabilization by having PLA blocks absorbed at interface of PMA, whereas hydrophilic comb blocks extend into the external aqueous phase. Consequently, copolymer micelles have an internal mesophase.

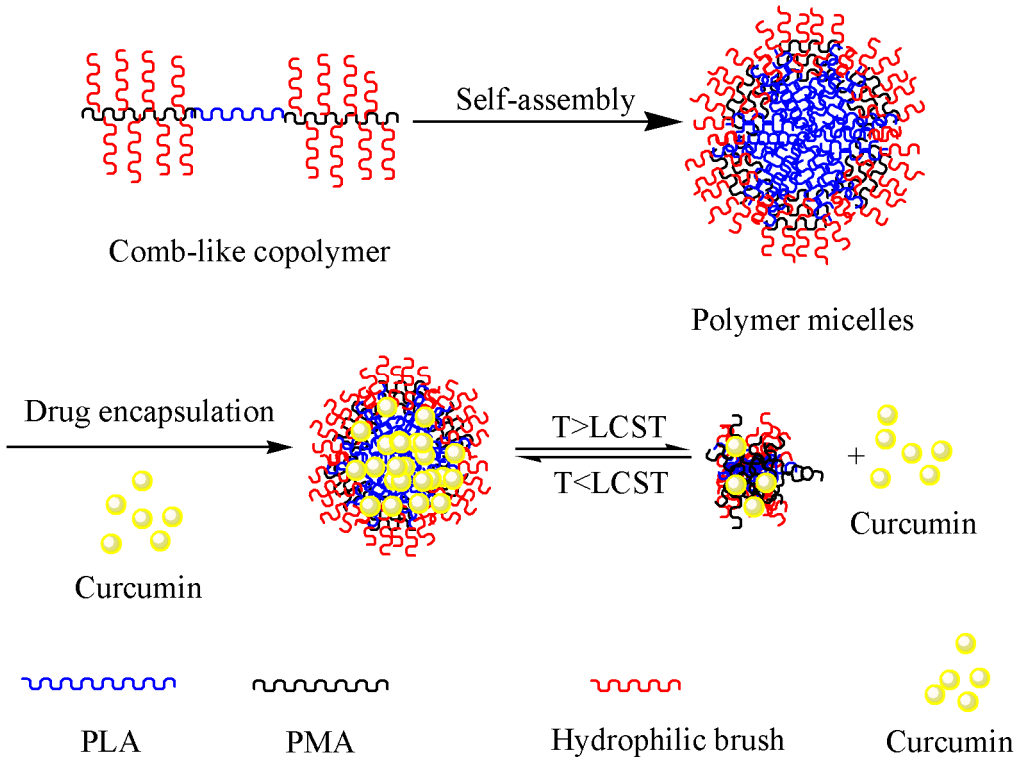

Scheme 5.2 Illustration of micellar structures during drug loading

In the present work, curcumin loaded micelles were prepared by solvent evaporation/membrane rehydration method. Thus, curcumin could play an important role in the micellization procedure. In fact, curcumin was encapsulated in the core and in the mesophase, leading to decrease of micelle size and increase of zeta potential. Therefore, curcumin loaded micelles exhibit more compacted core structure than blank micelles. Similarly findings have been reported by Zhang *et al.* in the case of amphotericin B loaded micelles prepared from comb-like block copolymers [42].

5.3.6 Phase transition of curcumin loaded micelles

The encapsulation of curcumin not only decreases the sizes of micelles, but also diminishes the LCST as determined by UV spectroscopy. Figure 5.8 shows that the transmittance of aqueous polymer solutions rapidly decreases from 100 % to 10 % around the LCST. Blank micelles exhibit a LCST at 45.1 ^{o}C, whereas the LCST of sample 2 and sample 3 with 5.9 % and 10.8 % drug loading is detected at 40.6 ^{o}C and 38.3 °C. The effect of hydrophobic drug on the LCST could be attributed to the increase of the core hydrophobicity, in agreement with DLS and TEM data. The higher the drug loading, the lower the LCST.

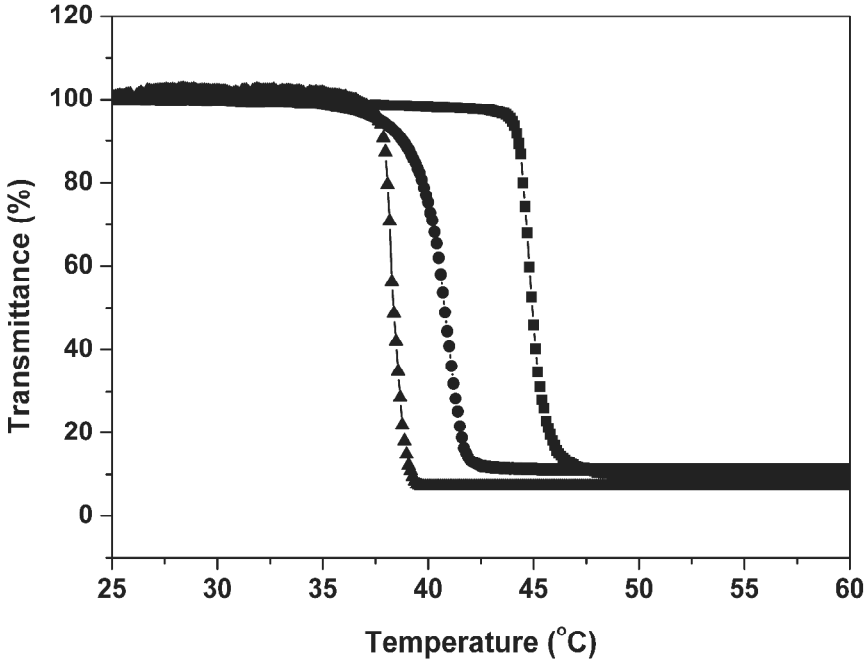

Figure 5.8 Phase transition of blank and curcumin-loaded micelles determined by UV-Vis spectroscopy at 1mg mL^{-1} in PBS. (■) blank micelles; (●) DL=5.9 %; (▲) DL=10.8 %.

Moreover, as shown in Figure 5.8, phase transition interval of *c.a* 1.5 ^{o}C was observed, which is slightly broader than that of P(NIPAAm-*co*-DMAAm)-*b*-PLLA-*b*-P(NIPAAm-*co*-DMAAm) micelles previously reported [28, 29]. In fact, PNIPAAm chains become dehydrated globules above the LCST with formation of intramolecular and intermolecular NH···O=C hydrogen

bonding. However, in the case of PEG analogues, the polymer-polymer interactions in the globules are Van Der Waals forces which are weaker than H-bonding, thus leading to a broader phase transition [16, 20].

5.3.7 *In vitro* drug release

Drug release was performed under physiological conditions (PBS, pH=7.4) at 37 °C (below the LCST) and 41 ^{o}C (above the LCST), respectively. The amount of curcumin was determined from UV-visible absorbance at 424 nm. As shown in Figure 9A, a linear calibration curve was previously established between the UV absorbance and curcumin concentration with a correlation coefficient of 0.99991.

The drug release profiles are shown in Fig. 9B. An initial fast release from micelles was observed in all cases, followed by slower release. 7.7 % and 6.2 % of curcumin were released from sample 2 and sample 3 at 1 h at 41°C, in contrast to 5.9 % and 3.5 % of curcumin released at 37 ^{o}C. Release of curcumin from sample 2 and sample 3 reached 80.3 % and 58.2 % after 4 day at 41 °C, in contrast to 66.1 and 45.5 % at 37 °C. Beyond, the release from sample 2 at 41 ^{o}C reached 89.5 % and 92.6 % at 7 and 14 days. For sample 3, 74.2 % and 75.9 % release were detected after 10 and 14 days at 41 °C. On the other hand, sample 2 and sample 3 showed a cumulative release of 81.8 % and 59.5 % after 14 days at 37 ^{o}C, respectively.

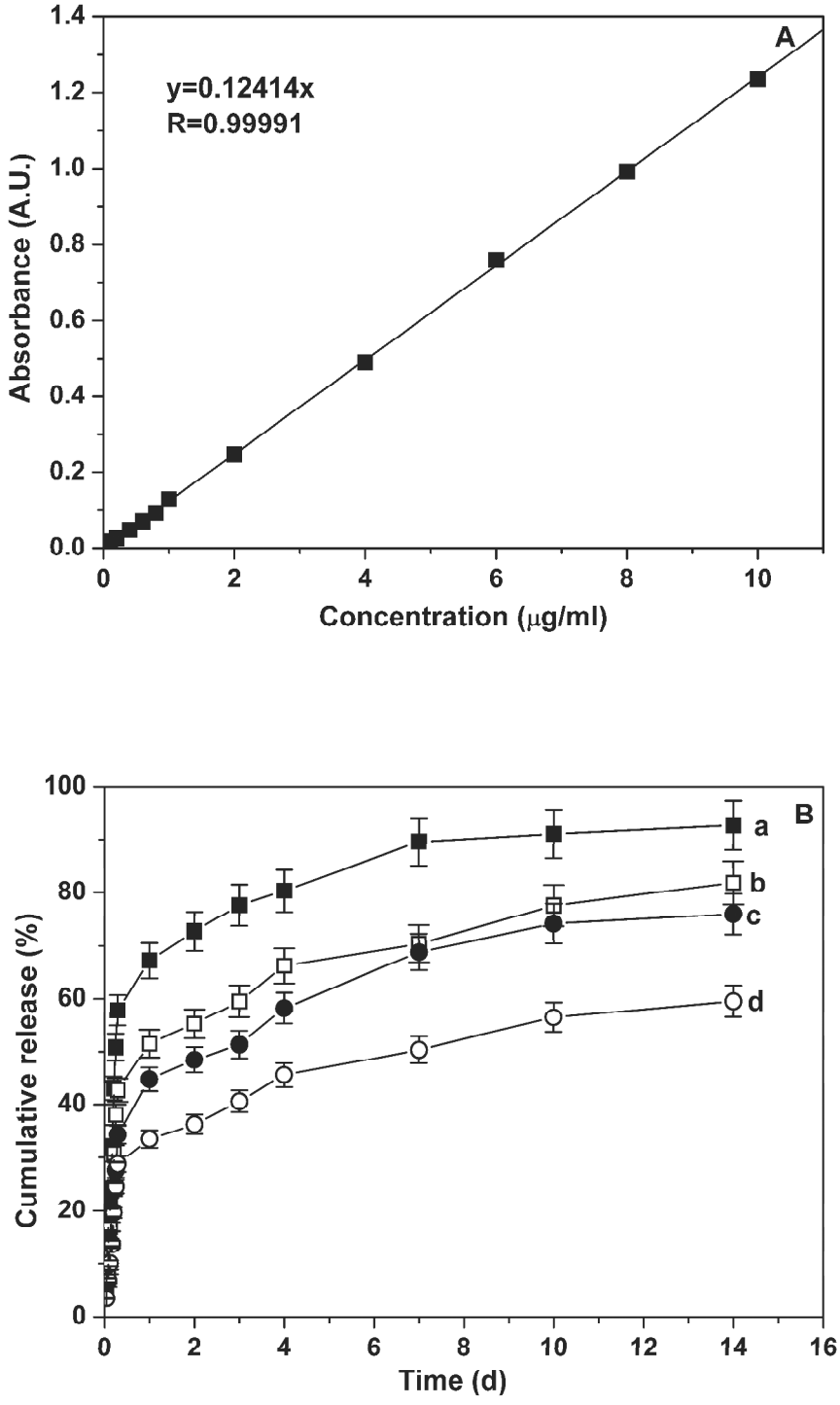

Figure 5.9 Calibration curve (A) and drug release profiles (B) of curcumin-loaded micelles: a) sample 2 (DL=5.9 %) at 41 ^{o}C; b) sample 2 (DL=5.9 %) at 37 ^{o}C; c) sample 3 (DL=10.8 %) at 41 ^{o}C; d) sample 3 (DL=10.8 %) at 37 ^{o}C.

Therefore, drug release is not only dependent on the phase transition across the LCST, but also on the drug loading. In fact, the solubility of curcumin in the release medium is a limiting factor. Samples with higher drug loading exhibit lower release rate because of the solubility effect. Besides, the micelles of sample 3 with higher drug loading have a more compacted core as compared to sample 2 due to stronger interactions between drug and hydrophobic blocks. It should also be noted that the LCST of drug loaded micelles is dynamically changing with the release of curcumin. Theoretically, the LCST should increase up to 45.1 ^{o}C when drug release reaches 100 % for all the samples.

It is of interest to compare the drug release behaviors from P(NIPAAm-*co*-DMAAm)-*b*-PLLA-*b*-P(NIPAAm-*co*-DMAAm) and PLA/PEG analogues micelles [29, 30]. Faster drug release is observed above the LCST than below the LCST in both cases. However, the drug release rate from the former is faster than that from the latter. In fact, P(NIPAAm-*co*-DMAAm)-*b*-PLLA-*b*-P(NIPAAm-*co*-DMAAm) micelles exhibit initially a larger burst-like release and then a slower release. In contrast, PLA/PEG analogues micelles present smaller burst-like release, and then drug release gradually increases. The depressed burst release and slower drug release may be related to the enhanced interaction between the drug and hydrophobic blocks. In fact, as shown in Scheme 2, both the inner PLA segment and intramolecular PMA blocks may contribute to the enhanced interaction [39].

Therefore, curcumin loaded micelles with thermo-responsive P(OEGMA-co-MEO_2MA) corona, PMA interface and PLLA core exhibit low CMC and nano size. The micelles could be easily administrated by intravenous injection. The thermo-responsive drug release behavior shows that these polymeric micelles are very promising as carrier of hydrophobic drugs.

5.4 Conclusion

Thermo-responsive comb-like P(MEO_2MA-*co*-OEGMA)-*b*-PLLA-*b*-P(MEO_2MA-*co*-OEGMA) triblock copolymers were synthesized by ATRP using a Br-PLLA-Br macroinitiator, and characterized by ^{1}H NMR and SEC. The physico-chemical properties of copolymers are dependent on the composition, namely the ratio of MEO_2MA/OEGMA ranging from 79/21 to 42/58 (mol/mol). The LCST increases from 24.8 ^{o}C to 45.1 ^{o}C in PBS with increasing the content of OEGMA. Micellization of copolymers was investigated by CMC, TEM and DLS measurements. The CMC of copolymers increases from 0.0109 to 0.0137 mg mL^{-1}, and the size of micelles increases from 20.7 to 102.5 nm with increasing the content of OEGMA. A hydrophobic anticancer drug, curcumin, was successfully encapsulated in micelles. The drug loading was 5.9 % and 10.8 % with loading efficiency higher than 90 %. The LCST of drug loaded micelles was 40.6 ^{o}C and 38.3 ^{o}C, respectively, which is lower than blank micelles by 4.5 and 6.8 °C. TEM and DLS results show a strong decrease of micellar size, suggesting that the hydrophobic drug plays a major role in the self-assembly procedure of drug loaded micelles. In *vitro* drug release exhibits thermo-responsive dependence across the LCST. Micelles with low drug loading show fast release than micelles with high drug loading. The higher drug loading and depressed burst-like release could be assigned to the enhanced interaction between drug and comb-like copolymers with two hydrophobic blocks, i.e. PLLA and PMA. Therefore, the nanosize, low CMC and thermo-responsive drug release indicate that P(MEO_2MA-*co*-OEGMA)-*b*-PLLA-*b*-P(MEO_2MA-*co*-OEGMA) triblock copolymers are promising candidate for targeted delivery of anti-tumor drugs.

5.5 Reference

1. R. Savic, L. B. Luo, A. Eisenberg and D. Maysinger, Micellar nanocontainers distribute to defined cytoplasmic organelles. Science 300 (2003) 615-618.
2. J. A. Hubbell, Enhancing drug function. Science 300 (2003) 595-596.
3. N. Bertrand, J. Wu, X. Y. Xu, N. Kamaly and O. C. Farokhzad, Cancer nanotechnology: The

impact of passive and active targeting in the era of modern cancer biology. Adv. Drug Deliv. Rev. 66 (2014) 2-25.
4. T. Yahara, T. Koga, S. Yoshida, S. Nakagawa, H. Deguchi, K. Shirouzu, Relationship Between Microvessel Density and Thermographic Hot Areas in Breast Cancer. Surg. Today 33 (2003) 243-248.
5. A. Chilkoti, M. R. Dreher, D. E. Meyer, D. Raucher, Targeted drug delivery by thermally responsive polymers. Adv. Drug Deliv. Rev. 54 (2002) 613-630.
6. F. Danhier, O. Feron, V. Prat, To exploit the tumor microenvironment: Passive and active tumor targeting of nanocarriers for anti-cancer drug delivery. J. Controlled Release 148 (2010) 135-146.
7. S. Hocine and M. H. Li, Thermoresponsive self-assembled polymer colloids in water. Soft Matter 9 (2013) 5839-5861.
8. J. Du and R. K. O'Reilly, Advances and challenges in smart and functional polymer vesicles. Soft Matter 5 (2009) 3544-3561.
9. A. K. Bajpai, S. K. Shukla, S. Bhanu and S. Kankane, Responsive polymers in controlled drug delivery. Prog. Polym. Sci. 33 (2008) 1088-1118.
10. S. Ganta, H. Devalapally, A. Shahiwala and M. Amiji, A review of stimuli-responsive nanocarriers for drug and gene delivery. J. Controlled Release 126 (2008) 187-204.
11. D. Schmaljohann, Thermo- and pH-responsive polymers in drug delivery. Adv. Drug Deliv. Rev. 58 (2006) 1655-1670.
12. H. Ding, F. Wu, Y. Huang, Z. R. Zhang, Y. Nie, Synthesis and characterization of temperature-responsive copolymer of PELGA modified poly(N-isopropylacrylamide). Polymer 47 (2006) 1575-1583.
13. H. Wei, S. X. Cheng, X. Z. Zhang, R. X. Zhuo, Thermo-sensitive polymeric micelles based on poly(N-isopropylacrylamide) as drug carriers. Prog. Polym. Sci.34 (2009) 893-910.
14. W. Li, J. F. Li, J. Gao, B. H. Li, Y. Xia, Y. C. Meng, Y. S. Yu, H. W. Chen, J. X. Dai, H. Wang, Y. J. Guo, The fine-tuning of thermosensitive and degradable polymer micelles for enhancing intracellular uptake and drug release in tumors. Biomaterials 32 (2011) 3832-3844.
15. F. Xu, S. Z. Zheng, Y. L. Luo, Thermosensitive *t*-PLA-*b*-PNIPAAm tri-armed star block copolymer nanoscale micelles for camptothecin drug release. J. Polym. Sci. Part A: Polym. Chem. 51 (2013) 4429-4439.
16. J. F. Lutz, O. Akdemir, A. Hoth, Point by Point Comparison of Two Thermosensitive Polymers Exhibiting a Similar LCST: Is the Age of Poly(NIPAM) Over? J. Am. Chem. Soc. 128 (2006) 13046-13047.
17. J. F. Lutz, J. Andrieu, S. uzgun, C. Rudolph, S. Agarwal, Biocompatible, Thermoresponsive, and Biodegradable:Simple Preparation of "All-in-One" Biorelevant Polymers. Macromolecules 40 (2007) 8540-8543.
18. J. F. Lutz, H. G. Borner, Modern trends in polymer bioconjugates design. Prog. Polym.Sci. 33 (2008) 1-39.
19. J. F. Lutz, A. Hoth, Preparation of Ideal PEG Analogues with a Tunable Thermosensitivity by Controlled Radical Copolymerization of 2-(2-Methoxyethoxy) ethyl Methacrylate and Oligo(ethylene glycol) Methacrylate. Macromolecules 39 (2006) 893-896.
20. J. F. Lutz, K. Weichenhan, O. Akdemir, A. Hoth, About the Phase Transitions in Aqueous Solutions of Thermoresponsive Copolymers and Hydrogels Based on 2-(2-methoxyethoxy) ethyl Methacrylate and Oligo(ethylene glycol) Methacrylate. Macromolecules 40 (2007) 2503-2508.

21. J. F. Lutz, Polymerization of oligo(ethylene glycol) (meth)acrylates: Toward new generations of smart biocompatible materials. J. Polym. Sci. Part A: Polym. Chem. 46 (2008) 3459-3470.
22. N. Fechler, N. Badi, K. Schade, S. Pfeifer, J. F. Lutz, Thermogelation of PEG-Based Macromolecules of Controlled Architecture. Macromolecules 42 (2008) 33-36.
23. J. F. Lutz, Thermo-Switchable Materials Prepared Using the OEGMA-Platform. Adv. Mater. 23 (2011) 2237-2243.
24. A. O. Saeed, S. Dey, S. M. Howdle, K. J. Thurecht and C. Alexander, One-pot controlled synthesis of biodegradable and biocompatible co-polymer micelles. J. Mater. Chem. 19 (2009) 4529-4535.
25. M. Luzón, T. Corrales, F. Catalina, V. San Miguel, C. Ballesteros and C. Peinado, Hierarchically organized micellization of thermoresponsive rod-coil copolymers based on poly[oligo(ethylene glycol) methacrylate] and poly(ε-caprolactone). J. Polym. Sci. Part A: Polym. Chem. 48 (2010) 4909-4921.
26. Y. Bakkour, V. Darcos, F. Coumes, S. M. Li and J. Coudane, Comb-like amphiphilic copolymers based on polylactide and poly(ethylene glycol): Synthesis, self-assembly and evaluation as drug carrier. Polymer 54 (2013) 1746-1754.
27. R. Fenyves, M. Schmutz, I. J. Horner, F. V. Bright and J. Rzayev, Aqueous Self-Assembly of Giant Bottlecomb Block Copolymer Surfactants as Shape-Tunable Building Blocks. J. Am. Chem. Soc. 136 (2014) 7762-7770.
28. Y. F. Hu, V. Darcos, S. Monge, S. M. Li, Y. Zhou, F. Su, Tunable thermo-responsive P(NIPAAm-co-DMAAm)-*b*-PLLA-*b*-P(NIPAAm-*co*-DMAAm) triblock copolymer micelles as drug carriers. J. Mater. Chem. B 2 (2014) 2738-2748.
29. Y. F. Hu, V. Darcos, S. Monge, S. M. Li, Y. Zhou, F. Su, Thermo-responsive release of curcumin from micelles prepared by self-assembly of amphiphilic P(NIPAAm-*co*-DMAAm)-*b*-PLLA-*b*-P (NIPAAm-*co*-DMAAm) triblock copolymers. Inter. J. Pharm. 476 (2014) 31-40.
30. Y. F. Hu, V. Darcos, S. Monge and S. M. Li, Synthesis and self-assembling of poly(N-isopropylacrylamide-block-poly(L-lactide)-block-poly(N-isopropylacrylamide) triblock copolymers prepared by combination of ring-opening polymerization and atom transfer radical polymerization. J. Polym. Sci. Part A: Polym. Chem. 51 (2013) 3274-3283.
31. M. Zhang and A. H. E. Müller, Cylindrical polymer combes. J. Polym. Sci. Part A: Polym. Chem. 43 (2005) 3461-3481.
32. L. Gu, Z. Shen, S. Zhang, G. Lu, X. Zhang and X. Huang, Novel Amphiphilic Centipede-Like Copolymer Bearing Polyacrylate Backbone and Poly(ethylene glycol) and Polystyrene Side Chains. Macromolecules 40 (2007) 4486-4493
33. M. Gerle, K. Fischer, S. Roos, A. H. E. Muller, M. Schmidt, S. S. Sheiko, S. Prokhorova and M. Muller, Main Chain Conformation and Anomalous Elution Behavior of Cylindrical Combes As Revealed by GPC/MALLS, Light Scattering, and SFM. Macromolecules 32 (1999) 2629-2637.
34. M. Nakayama, J. E. Chung, T. Miyazaki, M. Yokoyama, K. Sakai and T. Okano, Thermal modulation of intracellular drug distribution using thermoresponsive polymeric micelles. React. Funct. Polym. 67 (2007) 1398-1407.
35. M. L. Gou, K. Men, H. S. Shi, M. L. Xiang, J. A. Zhang, J. Song, J. L. Long, Y. Wan, F. Luo, X. Zhao and Z. Y. Qian, Curcumin-loaded biodegradable polymeric micelles for colon cancer therapy *in vitro* and *in vivo*. Nanoscale 3 (2011) 1558-1567.

36. C. Mohanty, S. Acharya, A. K. Mohanty, F. Dilnawaz, S. K. Sahoo, Curcumin-encapsulated MePEG/PCL diblock copolymeric micelles: a novel controlled delivery vehicle for cancer therapy. Nanomed. 5 (2010) 433-449.
37. O. Naksuriya, S. Okonogi, R. M. Schiffelers, W. E. Hennink, Curcumin nanoformulations: A review of pharmaceutical properties and preclinical studies and clinical data related to cancer treatment. Biomaterials 35 (2014) 3365-3383.
38. Z. M. Song, R. L. Feng, M. Sun, C. Y. Guo, Y. Gao, L. B. Li, G. X. Zhai, Curcumin-loaded PLGA-PEG-PLGA triblock copolymeric micelles: Preparation, pharmacokinetics and distribution *in vivo*. J.Colloid Interface Sci.354 (2011) 116-123.
39. J. Z. Du, L. Y. Tang, W. J. Song, Y. Shi and J. Wang, Evaluation of Polymeric Micelles from Comb Polymer with Poly(epsilon-caprolactone)-*b*-Poly(ethylene glycol) Side Chains as Drug Carrier. Biomacromolecules 10 (2009) 2169-2174.
40. R. L. Yang, S. A. Zhang, D. L. Kong, X. L. Gao, Y. J. Zhao, Z. Wang, Biodegradable Polymer-Curcumin Conjugate Micelles Enhance the Loading and Delivery of Low-Potency Curcumin. Pharm. Res. 29 (2012) 3512-3525.
41. H. D. Tang, C. J. Murphy, B. Zhang, Y. Q. Shen, M. H. Sui, E. A. Van Kirk, X. W. Feng, W. J. Murdoch, Amphiphilic curcumin conjugate-forming nanoparticles as anticancer prodrug and drug carriers: *in vitro* and *in vivo* effects. Nanomed. 5 (2015) 855-865.
42. X. W. Zhang, X. Q. Zhu, F. Y. Ke, L. Ye, E. Q. Chen, A. Y. Zhang, Z. G. Feng, Preparation and self-assembly of amphiphilic triblock copolymers with polyrotaxane as a middle block and their application as carrier for the controlled release of Amphotericin B. Polymer 50 (2009) 4343-4351.

Conclusions and perspectives

In this thesis, two families of amphiphilic and thermo-responsive block copolymers based on poly(L-lactide) (PLLA) and polyacrylamide or poly(oligo(ethylene glycol) methacrylate) are successfully synthesized by ATRP using the same Br-PLLA-Br (DP=40) macroinitiator. The self-assembly, phase transition, drug release and cytotoxicity of the various copolymers are studied to evaluate their potential as nanocarrier for thermo targeted delivery of antitumor drugs. The following conclusions are drawn from this work:

1) PNIPAAm-*b*-PLLA-*b*-PNIPAAm triblock copolymers are obtained by ATRP of NIPAAm using a α, ω-Br-PLLA-Br macroinitiator. The latter is prepared by ring opening polymerization of L-lactide followed by reaction with 2-bromopropionyl bromide. The ATRP of NIPAAm is performed in a DMF/water (5/1) mixture using CuCl/Me_6TREN catalyst system at room temperature, yielding copolymers with well controlled molecular weights and narrow dispersities. PNIPAAm-*b*-PLLA-*b*-PNIPAAm copolymers with NIPAAm/LA ratios from 2.4 to 6.9 are susceptible to self-assemble in aqueous medium to yields spherical micelles of sizes from 31 to 83 nm. The CMC of copolymers is in the range of 0.0077-0.016 mg mL^{-1} and the LCST in the range of 32.1-32.8 ^{o}C. The micelles exhibit different thermo-responsive behaviors at high or low concentrations. At 3.0 mg mL^{-1}, aggregation of micelles occurs when the temperature is raised above the LCST, leading to micelle size increase. In contrast, at 0.2 mg mL^{-1}, a decrease of micelle size is detected because of the collapse of PNIPAAm blocks above the LCST. The original micelle size is recovered when the temperature is decreased below the LCST in both cases, indicating that the system is thermo-reversible.

2) P(NIPAAm-*co*-DMAAm)-*b*-PLLA-*b*-P(NIPAAm-*co*-DMAAm) triblock copolymers can be obtained under the same conditions. With the ratio of NIPAAm to

DMAAm ranging from 100/0 to 76/24 in the hydrophilic blocks, the LCST of copolymers linearly increases the LCST to the range of 32.3 to 39.1. Moreover, introduction of DMAAm leads to very narrow phase transition across LCST within 0.5 ^{o}C, in contrast to a phase transition interval of 2.8 °C for PNIPAAm-*b*-PLLA-*b*-PNIPAAm. Increasing the DMAAm content also leads to larger micelle size from 40 to 55 nm, and higher CMC from 0.010 to 0.015 mg mL^{-1} due to the more hydrophilic nature of DMAAm as compared to NIPAAm. Copolymer micelles are able to encapsulate hydrophobic drugs by using dialysis method with loading efficiency above 59 %. *In vitro* drug release performed at 37 or 38 °C in water exhibits an initial burst release. The release rate at 38 °C is much faster than that at 37 °C, suggesting that these copolymer micelles could achieve thermo-responsive release after *in vivo* administration. Moreover, MTT assay and cell morphology observation indicate that the copolymers present outstanding cytocompatibility.

3) The drug release properties of P(NIPAAm-*co*-DMAAm)-*b*-PLLA-*b*-P(NIPAAm-*co*-DMAAm) are further studied with higher DMAAm content from 31.8 to 39.4 % in the hydrophilic P(NIPAAm-*co*-DMAAm) blocks. The LCST of copolymers varies from 44.7 °C to 49.4 °C in water and decreases by *ca.* 3.5 °C in PBS. Increase of DMAAm content also leads to slight CMC increase from 0.0113 to 0.0144 mg mL^{-1}, and slight micelle size increase from 37 to 44 nm. The zeta-potential of micelles varies in the -12.4 to -18.7 mV range, in agreement with the structure of micelles having PLLA block in the core and P(NIPAAm-*co*-DMAAm) blocks at the corona. A hydrophobic anticancer drug, curcumin, is encapsulated by using film hydration method with drug loading increases from 6.0 to 20.4 % and loading efficiency above 94 %. The LCST of blank micelles decreases from 45.6 ^{o}C in water to 42.1 ^{o}C in PBS. When with 6.0 % drug, the LCST further decreases from 42.1 to 38.0 ^{o}C in PBS. Higher drug loading leads to lower LCST, but the decrease is very limited as the LCST only lightly decreases to 37.5 ^{o}C with 20.4 % drug loading. On the other hand, the micelle size increases from

39 nm for blank micelles to 88 nm with drug loading of 20.4 %, indicating that curcumin incorporation leads to larger micelles. All micelles remain homogeneously transparent over 1 month due to the negative surface charge.

In vitro drug release presents an initial burst release in all cases, followed by a slower release. Thermo-responsive release is observed as the release rate is higher at 40 °C than that at 37 °C. Application of Peppas' theory indicates a combination of diffusion and degradation controlled release.

4) Triblock comb-like copolymers of PLA/PEG analogues with MEO_2MA/OEGMA molar ratio ranging from 79/21 to 42/58 are synthesized by ATRP in DMF at 80 ^oC using the same α, ω-Br-PLLA-Br macroinitiator and CuCl/Me_6TREN catalyst system. The LCST in PBS increases from 24.8 to 45.1 ^oC with the increase of OEGMA content from 32 % to 58 %. Spherical micelles with size from 20.7 to 102.5 nm are obtained by self-assembly of copolymers in aqueous medium with a CMC from 0.0109 to 0.0137 mg mL^{-1}. Curcumin is encapsulated by using film hydration method with drug loading of 5.9 % and 10.8 % and loading efficiency higher than 90 %.The LCST of drug loaded micelles was 40.6 ^oC and 38.3 ^oC, which is lower than blank micelles by 4.5 and 6.8 °C, respectively. The size of curcumin loaded micelles decreases from 103 to 38 nm while the zeta potential decreases from -1.99 mV to -44.9 mV, which indicates that the hydrophobic drug plays an important role in the self-assembly procedure of drug loaded micelles.

In *vitro* drug release exhibits thermo-responsive dependence across the LCST. Micelles with low drug loading show fast release than micelles with high drug loading. The higher drug loading and depressed burst-like release could be assigned to the enhanced interaction between drug and comb-like copolymers with two hydrophobic blocks, i.e. PLLA and PMA.

Therefore, an innovative work has been accomplished on thermo-responsive micelles as nanocarrier for anticancer applications. The copolymers obtained by ATRP exhibit well-defined chain structures. Self-assembled copolymer micelles exhibit nano-size, very low CMC and thermo-responsive drug release behavior, which present great potential in antitumor applications. Further investigations can be envisaged in future: 1) Synthesis and self-assembly of PLA-PNIPAAm (and PLA-PEG analogues) diblock copolymers; 2) Preparation of other aggregate architectures including polymersomes, worm-like micelles, nanotubes as well as hydrogels; 3) Synthesis of block copolymers with PLLA or PDLA macroinitiator so as to obtain stereocomplex micelles; 4) synthesis of thermo-responsive copolymers with targeting molecules by click chemistry.

Publications

1 **Y. F. Hu**, V. Darcos, S. Monge, S. M. Li, Thermoresponse micelles from comb-like copolymers of polylactide and PEG Analogues: Synthesis, Micellization and *In vitro* drug release, *Internal Journal of Pharmaceutics,* submitted.

2 **Y. F. Hu**, V. Darcos, S. Monge, S. M. Li, Y. Zhou, F. Su, Thermo-responsive release of curcumin from micelles prepared by self-assembly of amphiphilic P(NIPAAm-*co*-DMAAm)-*b*-PLA-*b*-P(NIPAAm-*co*-DMAAm) triblock copolymers, *Internal Journal of Pharmaceutics*, 476 (2014) 31-40

3 **Y. F. Hu**, V. Darcos, S. Monge, S. M. Li, Y. Zhou, F. Su, Tunable thermo-responsive P(NIPAAm-*co*-DMAAm)-*b*-PLLA-*b*-P(NIPAAm-*co*-DMAAm) triblock copolymer micelles as drug carriers. *Journal of Materials Chemistry B*, 2 (2014) 2738-2748.

4 **Y. F. Hu**, V. Darcos, S. Monge, S. M. Li, Synthesis and self-assembling of poly(*N*-isopropylacrylamide-block-poly(L-lactide)-block-poly(*N*-isopropylacrylamide) triblock copolymers prepared by combination of ring-opening polymerization and atom transfer radical polymerization. *Journal of Polymer Science part A*: *Polymer Chemistry*, 51 (2013) 3274-3283.

Acknowlegdements

After 3 and half years PH.D study, finally I could have my defense and have a delighted time. I am a shy person and not so good at express myself. Herein, I write this final part with cheerful and complicated mood. I have taken an interesting experience in Montpellier. I was lost and stand in the cold wind in Montpellier due to the delay of plane and train at 21th, November 2011. I asked a passenger with my poor French to call my supervisor Suming Li to pick me. Then I found Montpellier is really nice city with nice people.

First, I would like to express my appreciation to my supervisor, Suming Li. We have met and knew with each other for 10 years. I still remember the first time we met at Fudan University, China when I was 22 years old and a fresh noob mater student. Suming not only advised my thesis work but also took care of my daily life. I have nice experience under his advising and I learn a lot of stuff from him, including how to start a scientific project, write papers as well as interact with people.

I also want to thank Dr Vincent, my co-supervisor for his excellent direction on my polymer synthesis. The valuable suggestion from him improved the thesis and my profession skills, although we have different opinions at some times. I am want to thank Dr sophie Monge for her support of my test. Perhaps I did most of the test in her lab. She is a really nice person to teach me how to use the machine and book the time for me. I am also grateful to Dr Jean Coudane for his full support as the director of the laboratory and Dr Boustta Mahfoud for his favor as my seat adjacent to endure my messy desk. I should send many thanks to Xiaohan Wu. He helped me everything in my early life in France. Many thanks to the couple of Adrien Leroy and Fanny Coumes for their help familiar with lab and solve the problems I asked with stunning patience. Many thanks present to Marc-Alexandre with whom I really enjoy the talk. Many thanks also should present to Dominique Arama who always say hello to me in

Chinese. Appreciation also should be presented to Benjamin Nottelet, Sylvie Hunger, Xavier Dumont and Cedric paniagua for their support, to Frank Godiard for TEM measurements, to all the members in our laboratory for providing a enjoyable work environment.

A part of this thesis work was carried out in the College of Chemical Engineering, Qingdao University of Science and Technology, China. Thanks Yang Zhou and Feng Su for their excellent work.

At last, I wish to express my sincere gratitude to my wife. She accompanies me for 3 years in France. It is not easy for her especially she is always homesick and takes care of my baby daughter alone for most of time. Finally, I finished my job and could have a nice time with my family.

When I recall the past years, there are a lots of emotion, freshness, curiousness, understanding, cheerfulness for my work, moved tears for the birth of my daughter. It is interesting life in France as a foreigner for these 3 years. It will affect me for the whole life. It is time to say goodbye to friends and people in the lab. I will miss you all.

RESUME
Deux séries de copolymères tribloc thermo-sensibles et amphiphiles, à savoir poly(L-lactide)/poly(*N*-isopropylacrylamide-*co*-*N,N*-diméthylacrylamide) et poly(L-lactide)/poly(2-(2-méthoxyéthoxy) éthyl méthacrylate-*co*-oligo(éthylène glycol) méthacrylate) ont été synthétisées par polymérisation radicalaire par transfert d'atomes en utilisant le Br-PLLA-Br comme macroamorceur dans des conditions douces. Les copolymères obtenus présentent une structure de chaînes bien définie avec une dispersité étroite, et sont capable de s'auto-assembler dans un milieu aqueux pour donner des micelles sphériques de taille en dessous de 100 nm et de faible concentration micellaire critique (<0.016 mg mL^{-1}). La température critique inférieure de solution peut être ajustée avec précision en faisant varier le rapport NIPAAm/DMAAm ou MEO_2MA/OEGMA. Un principe actif hydrophobe, curcumine, a été choisi comme modèle pour déterminer les propriétés de libération des micelles à différentes températures. Une libération thermo-sensible de curcumine a été observée, indiquant que ces copolymères sont prometteurs pour la libération ciblée de principes actifs anti-tumoraux.

Mots-clés: thermo-sensible, polymérisation radicalaire par transfert d'atomes, poly(L-lactide), poly(*N*-isopropylacrylamide), oligo(éthyl glycol) méthacrylate, auto-assemblage, libération ciblée de principes actifs.

Synthesis, self-assembly and controlled drug delivery of novel thermo-responsive and amphiphilic block copolymers based on polylactide, polyacrylamide and Poly[oligo(ethylene glycol) methacrylate]

ABSTRACT
Two series of thermo-responsive and amphiphilic triblock copolymers, *i.e.* poly(L-lactide)/poly(*N*-isopropylacrylamide-*co*-*N,N*-dimethylacrylamide) and poly(L-lactide)/poly(2-(2-methoxyethoxy) ethyl methacrylate-*co*-oligo(ethylene glycol) methacrylate) were synthesized by atom transfer radical polymerization using Br-PLLA-Br as macroinitiator under mild conditions. The obtained copolymers present well defined chain structures with narrow dispersity, and are able to self-assemble in aqueous medium yielding spherical micelles with size below 100 nm and low critical micellization concentration (<0.016 mg mL^{-1}). The lower critical solution temperature is precisely adjusted by changing the NIPAAm/DMAAm or MEO_2MA/OEGMA ratio. A hydrophobic drug, curcumin, is taken as a model to evaluate the drug release properties of micelles at different temperatures. Thermo-responsive drug release behavior is observed, indicating that these copolymers are promising candidate for targeted delivery of anticancer drugs.

Keywords: thermo-responsive, atom transfer radical polymerization, poly(L-lactide), poly(*N*-isopropylacrylamide), oligo(ethylene glycol) methacrylate, self-assembly, targeted drug delivery.

Intitulé et addresse de l'unité ou laboratoire
Equipe Biopolymères Artificiels, Institut des Biomolécules Max Mousseron, UMR CNRS 5247, Faculté de Pharmacie -Université de Montpellier- 15 avenue Charles Flahaut, 34093 Montpellier, France